

Universität Potsdam

Arbeitsgruppe Prof. Dr. André Laschewsky

**New hydrogel forming thermo-responsive block copolymers
of increasing structural complexity**

Dissertation zur Erlangung des akademischen Grades

"doctor rerum naturalium" (Dr. rer. nat.)

in der Wissenschaftsdisziplin "Kolloid- und Polymerchemie"

eingereicht an der

Mathematisch-Naturwissenschaftlichen Fakultät

der Universität Potsdam

von

Anna Miasnikova

Potsdam, im Februar 2012

This work is licensed under a Creative Commons License:
Attribution - Noncommercial - Share Alike 3.0 Germany
To view a copy of this license visit
<http://creativecommons.org/licenses/by-nc-sa/3.0/de/>

Published online at the
Institutional Repository of the University of Potsdam:
URL <http://opus.kobv.de/ubp/volltexte/2012/5995/>
URN <urn:nbn:de:kobv:517-opus-59953>
<http://nbn-resolving.de/urn:nbn:de:kobv:517-opus-59953>

Acknowledgments

At first I would like to acknowledge the significant contribution of my advisor, Professor André Laschewsky, both regarding this work, which he steadily helped improving, and the global experience of these years. I am certain to keep the many lessons learned from him for the rest of my scientific career.

The support and guidance of other scientists from the Fraunhofer Institute for Applied Polymer Research was much appreciated. I sincerely thank Dr. Michael Päch, for sharing his knowledge of laboratory work with me. His little tricks and big ideas helped me out of dead-ends many times. Also, the support of Dr. Erik Wischerhoff is gratefully acknowledged: I always found his door open for help and discussions. Finally, Dr. Eckhard Görnitz is acknowledged for his help with the rheometer.

In addition, I gratefully acknowledge Professors Christine M. Papadakis and Peter Müller-Buschbaum, of the Technische Universität München, and their respective students Joseph Adelsberger and Qi Zhong for the fruitful collaboration and interesting discussions.

I was very pleased to work with my internship students Anne-Christin Stötzer and Carlos Adrián Benítez-Montoya, their collaboration was always very stimulating. In particular, Adrián is acknowledged for his experimental work on azobenzene containing polymers.

Special thank goes to my present and past officemates, for many productive and equally many unproductive, but very pleasant, hours: Jens Buller, Martin Sütterlin, Sandor Dippel and Dr. Christoph Wieland. I also thank my colleagues Dr. Katja Skrabania and Christoph Herfurth for successful collaboration on common projects, as well as the “French community”: Dr. Nezha Badi, Olivia Mauger, Dr. Jean-Noël Marsat and Marie-Claire Despinasse for their friendship.

I much appreciated to work side by side with many other wonderful PhD students and technicians of the Universität Potsdam and the Fraunhofer Institute: Laura Vogel, Verena Jentzen, Kristina Blümel, Nicole Stahlberg, Kristin Schade, Dr. Falko Pippig, Oscar Rojas, Zoya Zarafshani, Frank Stahlhut, Jarosław Tomczyk, Dr. Jan Weiß, Dr. Sebastian Pfeifer, Jonas Koelsch, Anne Enzenberg and Robert Bernin.

I thank the Deutsche Forschungsgemeinschaft DFG, priority program SPP1259 “Intelligente Hydrogele” for the financial support.

At last, my gratitude goes to all those who were with me in deeds and thoughts during those exciting but challenging years.

List of Publications

Manuscripts peer-reviewed

1. **A. Miasnikova** and A. Laschewsky, "Influencing the phase transition temperature of poly(methoxy diethylene glycol acrylate) by molar mass, end groups, and polymer architecture", *J. Polym. Sci. Part A: Polym. Chem.*, **2012**, published on line
2. **A. Miasnikova**, A. Laschewsky, G. De Paoli, C. M. Papadakis, P. Müller-Buschbaum, S. S. Funari, "Thermoresponsive hydrogels from symmetrical triblock copolymers poly(styrene-block-(methoxy diethylene glycol acrylate)-block-styrene)", *Langmuir*, **2012**, 28, 4479
3. K. Skrabania, **A. Miasnikova**, A. M. Bivigou-Koumba, D. Zehm, A. Laschewsky, "Examining the UV-vis absorption of RAFT chain transfer agents and their use for polymer analysis", *Polym. Chem.*, **2011**, 2, 2074

Manuscripts to be published

1. **A. Miasnikova** and A. Laschewsky, "Thermo-responsive hydrogels from amphiphilic block copolymers, effect of topology and hydrophobe length", *in preparation*.
2. **A. Miasnikova**, C. A. Benitez-Montoya, A. Laschewsky, "Temperature and Light responsive polymers containing azobenzene groups", *in preparation*.

Awards

1. **2nd oral presentation prize**, Interdisziplinäres Doktorandensymposium, **2010**, Potsdam
2. **1st poster prize, (joined with Christoph Herfurth)** 6th European Detergents Conference, **2010**, Fulda (Germany)
3. **Best oral presentation award**, Meeting on Controlled Radical Polymerizations, **2009**, Houffalize, (Belgium)

Oral Presentations at International Conferences (Speaker A.M.)

- “New gel forming thermosensitive polymers of increasing structural complexity” **A. Miasnikova**, G. De Paoli, A. Laschewsky, C.M. Papadakis, P. Müller-Buschbaum, Intelligente Hydrogele, Cologne, July **2011**
- “Thermoresponsive polymers: on the way to injectable hydrogels” **A. Miasnikova**, A. Laschewsky, 3. Interdisziplinäres Doktorandensymposium, Potsdam, October **2010**
- “The self-assembly of triblock copolymers into smart hydrogels” **A. Miasnikova**, A. Laschewsky, C. M. Papadakis, P. Müller-Buschbaum, Polysolvat-8, Strasbourg (France), July **2010**
- “The transition from smart micelles to hydrogels from thermoresponsive block copolymers” **A. Miasnikova**, A. M. Bivigou-Koumba, A. Laschewsky, C.M. Papadakis, P. Müller-Buschbaum, Meeting on Controlled Radical Polymerizations, Houffalize (Belgium), September **2009**
- “Synthesis and characterization of thermoresponsive hydrogels from amphiphilic block copolymers ” **A. Miasnikova**, A. M. Bivigou-Koumba, A. Laschewsky, C.M. Papadakis, P. Müller-Buschbaum, Intelligente Hydrogele, Aachen, March **2009**

Poster Presentations

- “Self-assembly and functionalization of amphiphilic block copolymers”, **A. Miasnikova**, C. A. Benitez Montoya, S. Dippel, A. Laschewsky, PolyOr2011 "Polymers on the Odra River", Opole (Poland), July **2011**
- “Cononsolvency in thermoresponsive PNIPAM-based block copolymers” G. De Paoli, S. Jaksch, **A. Miasnikova**, A. Laschewsky, P. Müller-Buschbaum, C. M. Papadakis, DPG spring Meeting 2011, Dresden, March **2011**
- “Hydrogels made of polymeric surfactants” A. Laschewsky, C. Herfurth, **A. Miasnikova**, C. Wieland, SEPAWA 57. Congress & 6th European Detergency Conference, Fulda, October **2010**
- “Hydrogels made of polymeric surfactants” A. Laschewsky, C. Herfurth, **A. Miasnikova**, C. Wieland, Polydays, Berlin, October **2010**

- “The self-assembly of triblock copolymers into smart hydrogels. Comparing polyNIPAM with polyMDEGA as responsive hydrophilic block” **A. Miasnikova**, A. M. Bivigou-Koumba, A. Laschewsky, C. M. Papadakis, P. Müller-Buschbaum, Golm International Symposium on Bioactive Surfaces, Potsdam, Mai **2010**
- “The self-assembly of triblock copolymers into smart hydrogels. Comparing polyNIPAM with polyMDEGA as responsive hydrophilic block” **A. Miasnikova**, A. M. Bivigou-Koumba, A. Laschewsky, C. M. Papadakis, P. Müller-Buschbaum, DPG Spring Meeting 2010, Regensburg, March **2010**
- “The Transition From Smart Micelles to Hydrogels of Block Copolymer Surfactants” A. M. Bivigou-Koumba , E. Görnitz, J. Kristen, A. Laschewsky, **A. Miasnikova**, P. Müller-Buschbaum, C. M. Papadakis, 5th European Detergency Conference, Würzburg, October **2009**

Summary

This work describes the synthesis and characterization of stimuli-responsive polymers made by reversible addition-fragmentation chain transfer (RAFT) polymerization and the investigation of their self-assembly into “smart” hydrogels. In particular the hydrogels were designed to swell at low temperature and could be reversibly switched to a collapsed hydrophobic state by rising the temperature. Starting from two constituents, a short permanently hydrophobic polystyrene (PS) block and a thermo-responsive poly(methoxy diethylene glycol acrylate) (PMDEGA) block, various gelation behaviors and switching temperatures were achieved.

New RAFT agents bearing *tert*-butyl benzoate or benzoic acid groups, were developed for the synthesis of diblock, symmetrical triblock and 3-arm star block copolymers. Thus, specific end groups were attached to the polymers that facilitate efficient macromolecular characterization, e.g by routine ¹H-NMR spectroscopy. Further, the carboxyl end-groups allowed functionalizing the various polymers by a fluorophore.

Because reports on PMDEGA have been extremely rare, at first, the thermo-responsive behavior of the polymer was investigated and the influence of factors such as molar mass, nature of the end-groups, and architecture, was studied. The use of special RAFT agents enabled the design of polymer with specific hydrophobic and hydrophilic end-groups. Cloud points (CP) of the polymers proved to be sensitive to all molecular variables studied, namely molar mass, nature and number of the end-groups, up to relatively high molar masses. Thus, by changing molecular parameters, CPs of the PMDEGA could be easily adjusted within the physiological interesting range of 20 to 40°C.

A second responsivity, namely to light, was added to the PMDEGA system via random copolymerization of MDEGA with a specifically designed photo-switchable azobenzene acrylate. The composition of the copolymers was varied in order to determine the optimal conditions for an isothermal cloud point variation triggered by light. Though reversible light-induced solubility changes were achieved, the differences between the cloud points before and after the irradiation were small. Remarkably, the response to light differed from common observations for azobenzene-based systems, as CPs decreased after UV-irradiation, i.e with increasing content of *cis*-azobenzene units.

The viscosifying and gelling abilities of the various block copolymers made from PS and PMDEGA blocks were studied by rheology. Important differences were observed between diblock

copolymers, containing one hydrophobic PS block only, the telechelic symmetrical triblock copolymers made of two associating PS termini, and the star block copolymers having three associating end blocks. Regardless of their hydrophilic block length, diblock copolymers PS11-PMDEGA_n were freely flowing even at concentrations as high as 40 wt. %. In contrast, all studied symmetrical triblock copolymers PS8-PMDEGA_n-PS8 formed gels at low temperatures and at concentrations as low as 3.5 wt. % at best. When heated, these gels underwent a gel-sol transition at intermediate temperatures, well below the cloud point where phase separation occurs. The gel-sol transition shifted to markedly higher transition temperatures with increasing length of the hydrophilic inner block. This effect increased also with the number of arms, and with the length of the hydrophobic end blocks. The mechanical properties of the gels were significantly altered at the cloud point and liquid-like dispersions were formed. These could be reversibly transformed into hydrogels by cooling.

This thesis demonstrates that high molar mass PMDEGA is an easily accessible, presumably also biocompatible and at ambient temperature well water-soluble, non-ionic thermo-responsive polymer. PMDEGA can be easily molecularly engineered via the RAFT method, implementing defined end-groups, and producing different, also complex, architectures, such as amphiphilic triblock and star block copolymers, having an analogous structure to associative telechelics. With appropriate design, such amphiphilic copolymers give way to efficient, “smart” viscosifiers and gelators displaying tunable gelling and mechanical properties.

Zusammenfassung

Diese Arbeit befasst sich mit der RAFT-vermittelten Synthese und Charakterisierung von stimuliempfindlichen Polymeren und ihrer Selbstorganisation zu „intelligenten“ Hydrogelen. Die Hydrogele wurden so entwickelt, dass sie bei niedrigen Temperaturen stark quellen, bei Temperaturerhöhung jedoch reversibel in einem hydrophoben, kollabierten Zustand umgewandelt werden. Mit dem permanent hydrophoben Polystyrol (PS) und dem hydrophilen, thermisch schaltbaren Poly(methoxy-diethylenglycol-acrylat) (PMDEGA) als Bausteine, wurden unterschiedliche Gelierungsverhalten und thermische Übergangstemperaturen erreicht.

Zur Synthese von Diblock-, symmetrischen Triblock- und dreiarmligen Sternblock-Copolymeren wurden neue funktionelle Kettenüberträger entwickelt. Diese gestatteten es, *tert*-butyl Benzoeester und Benzoesäure Endgruppen in die Polymere einzubauen, die einerseits eine effiziente Analyse mittels Routine $^1\text{H-NMR}$ und darüber hinaus eine spätere Funktionalisierung der Endgruppen mit einer Fluoreszenzsonde ermöglichten.

Da über PMDEGA kaum Daten vorlagen, wurde der Einfluss von Molekulargewicht, Endgruppen und Architektur auf das thermo-responsive Verhalten untersucht. Die speziellen Kettenüberträger ermöglichten es, gezielt hydrophobe wie hydrophile Endgruppen in die Polymere einzuführen. Die Trübungspunkte der wässrigen Lösungen von PMDEGA zeigten sich bis zu relativ hohen molaren Massen abhängig gegenüber allen untersuchten Variablen, nämlich dem Molekulargewicht, der Art und Zahl von Endgruppen. Durch Variation der diversen Parameter ließ sich die Schalttemperatur von PMDEGA in physiologisch relevanten Temperaturbereich von 20 bis 40 °C einstellen.

Um die Polymere für einen zweiten Stimulus, nämlich Licht, empfindlich zu machen, wurden Azobenzol-funktionalisierte Acrylate synthetisiert und statistisch mit MDEGA copolymerisiert. Die Zusammensetzung der Polymeren wurde variiert und das isotherme Schalten der Löslichkeit durch Licht untersucht. Obwohl ein reversibles Schalten erreicht wurde, waren die Unterschiede zwischen den Trübungstemperaturen von UV-Licht bestrahlten und unbestrahlten Proben nur gering. Interessanterweise senkte die UV-Bestrahlung, d.h. ein erhöhter Gehalt von *cis*-Azobenzol-Gruppen, die Trübungstemperaturen herab. Dies ist genau umgekehrt als für azobenzolbasierten Systeme klassisch beschrieben.

Die Gelbildung der verschiedenen Blockcopolymeren von PS und PMDEGA wurde mittels Rheologie untersucht. Dabei traten deutliche Unterschiede auf, zwischen dem

Gelierungsverhalten der Diblockcopolymeren, die nur einen PS Block enthalten, dem der symmetrischen Triblockcopolymeren, die zwei assoziative PS Endblöcken besitzen, und dem der Sternpolymeren, die drei assoziative PS Blöcke aufweisen. Unabhängig von der Länge des hydrophilen Blockes, bilden Diblockcopolymeren des Typs PS11-PMDEGAN keine Gele, sondern selbst bei hohen Konzentrationen von 40 Gew. % Lösungen. Im Gegensatz dazu bildeten die Triblockcopolymeren des Typs PS8-PMDEGAN-PS8 Gele bei niedrigen Temperaturen, vereinzelt schon ab 3.5 wt. %. Mit steigender Temperatur, tritt bereits unterhalb des Trübungspunktes für diese Systeme ein Gel-Sol Übergang auf. Der Gel-Sol Übergang bewegt sich zu höheren Temperaturen mit steigender Länge des hydrophilen inneren Blocks. Dieser Trend verstärkt sich mit zunehmender Anzahl von Endblöcken und deren Länge. An der Trübungstemperatur veränderten sich die mechanischen Eigenschaften aller Gele signifikant und die gebildeten flüssigen Dispersionen ließen sich reversibel beim Abkühlen wieder zu Gel schalten.

Diese Arbeit, zeigt dass PMDEGA ein bei niedrigen Temperaturen gut wasserlösliches, nicht-ionisches, thermisch-schaltbares und wahrscheinlich biokompatibles Polymer ist. PMDEGA liest sich einfach mittels den RAFT-Verfahren molekular maßschneiden, mit spezifischen Endgruppen und komplexen Polymerarchitekturen. Solche amphiphilen Triblock- und Sternblock-Copolymeren hoher Molmasse, wirken als assoziative Telechele. Daher eignen sich bei entsprechendem Design diese amphiphilen Blockcopolymeren als effiziente Verdicker und Gelbildner mit einstellbaren mechanischen und thermischen Eigenschaften.

List of Abbreviations

AA	Acrylic acid
AIBN	2,2'-Azobis(isobutyronitrile)
ATRP	Atom transfer radical polymerization
azoMDEGA	6-[4-(4-methoxyphenylazo)phenyl]diethylene glycol acrylate
CP	Cloud point
CRP	Controlled/"living" radical polymerization
CTA	Chain transfer agent
δ	Chemical shift (NMR)
DLS	Dynamic light scattering
DMF	<i>N,N</i> -Dimethylformamide
DMSO	Dimethyl sulfoxide
DP _n	Number average degree of polymerization
DSC	Differential scanning calorimetry
EDC	Ethyl (dimethylaminopropyl) carbodiimide
EG	Ethylene glycol
EO	Ethylene oxide
FCS	Fluorescence correlation spectroscopy
FRP	Free radical polymerization
GPC	Gel permeation chromatography
G'	Storage modulus
G''	Loss modulus
LCST	Lower critical solution temperature
M _n	Number average molecular weight
M _w	Weight average molecular weight
MA	Methyl acrylate
MDEGA	Methoxy diethylene glycol acrylate
MMA	Methyl methacrylate
NHS	<i>N</i> -Hydroxysuccinimide
NIPAM	<i>N</i> -Isopropylacrylamide
NMP	Nitroxide mediated polymerization
NMR	Nuclear magnetic resonance
PDI	Polydispersity index (M _w /M _n)

PEG	Poly(ethylene glycol)
PEO	Poly(ethylene oxide)
PMDEGA	Poly(methoxy diethylene glycol acrylate)
ppm	Parts per million (NMR)
PS	Polystyrene
RAFT	Reversible addition-fragmentation chain transfer
R_H	Hydrodynamic radius
R_f	Retention factor (thin layer chromatography)
RI	Refractive index
S	Styrene
SAXS	Small-angle X-ray scattering
SEC	Size exclusion chromatography
TFA	Trifluoroacetic acid
TLC	Thin layer chromatography
UV-vis	Ultraviolet–visible

Contents

ACKNOWLEDGEMENTS	ii
LIST OF PUBLICATIONS	iii
SUMMARY	vi
ZUSAMMENFASSUNG	viii
LIST OF ABBREVIATIONS	x
I. Introduction	1
1.1. Controlled polymerization	2
1.2. Stimuli-responsive polymers	5
1.2.1. Thermo-responsive polymers	5
1.2.2. The structural effect: examples of thermo-responsive polymers	7
1.3. Self-assembly of block copolymers	9
1.3.1. Gels, general definitions	9
1.3.2. Hydrogels made of amphiphilic block copolymers	11
1.3.3. Thermo-responsive hydrogels	13
1.4. Outlook of the thesis	14
1.5. References	17
II. Synthesis, characterization and modification of telechelic polymers	23
2.1. Design of chain transfer agents	23
2.2. Multifunctional CTAs with COOH functionalities	25
2.3. Characterization by ¹ H-NMR spectroscopy	26
2.4. Characterization by UV-vis spectroscopy	29
2.4.1. Factors influencing the absorption	29
2.4.2. Analysis of homopolymers	32
2.4.3. Analysis of block copolymers	35
2.5. Deprotection of <i>tert</i> -butyl end-groups	37
2.6. Functionalization of block copolymers with a rhodamine fluorophore	39
2.7. Conclusion	43
2.8. Acknowledgements	43
2.9. References	44

III. Thermoresponsive behavior of PMDEGA polymers	47
3.1. Thermoresponsive behavior of PMDEGA homopolymers	47
3.1.1. Synthetical strategy	47
3.1.2. Behavior of the homopolymers in aqueous solutions	49
3.1.3. Thermoresponsive behavior of PMDEGA series C in pH = 7 buffered solution	52
3.2. Thermoresponsive behavior of PMDEGA block copolymers	53
3.2.1. Synthesis of poly(S-block-MDEGA) with different architectures	53
3.2.2. Behavior of the block copolymers in aqueous solution	54
3.3. Conclusion	58
3.4. References	59
IV. Photoswitchable copolymers containing azobenzene moieties	61
4.1. Synthesis of copolymers of MDEGA and azoMDEGA	62
4.1.1. Synthetical strategy	62
4.1.2. Retardation in copolymerization reaction	63
4.2. Characterization of the copolymers	66
4.2.1. Structural determination	66
4.2.2. Photochromism of P(MDEGA-co-azoMDEGA) in aqueous solution	67
4.3. Thermo-responsive behavior of P(MDEGA-co-azoMDEGA)	69
4.3.1. Solubility of the copolymers in water	69
4.3.2. Photocontrol of the cloud point temperatures	70
4.4. Conclusion	73
4.5. Acknowledgements	74
4.6. References	75
V. Thermoresponsive hydrogels from symmetrical triblock copolymers	77
5.1. Concentration dependent thermoresponsive behavior	78
5.1.1. Synthesis and analysis of PS-PMDEGA-PS	78
5.1.2. Collapse transition at various concentrations	79
5.1.3. Gel formation: a visual test	81
5.2. Rheological analysis of PS-PMDEGA-PS polymers	82
5.2.1. Frequency sweep experiments	82
5.2.2 Temperature sweep experiments	84
5.3. Structural characterization of the association as studied on PS8-PMDEGA452-PS8	87
5.3.1. Phase boundaries as determined by rheology	87

5.3.2. Dynamic light scattering in diluted solution	88
5.3.3. Temperature-resolved small-angle x-ray scattering (SAXS)	89
5.4. Conclusion	91
5.5. Acknowledgments	92
5.6. References	93
VI. Making gels stronger: influence of the length and the number of end-blocks	95
6.1. Influence of polymer topology on gelation	97
6.1.1. Comparison of triblock and diblock copolymers	97
6.1.2. Comparison of triblock and 3-arm star copolymers	99
6.2. Influence of the hydrophobic block length	102
6.2.1. Triblock copolymers design	102
6.2.2. Frequency sweep experiments	102
6.2.3. Investigation in concentrated solution	104
6.3. Conclusion	106
6.4. References	108
VII. Conclusion	110
VIII. Experimental part	113
8.1. Analytical instruments	113
8.2. Synthesis of chain transfer agents	113
8.3. Synthesis of monomers	123
8.4. Synthesis of rhodamine B piperazine amide	127
8.5. Synthesis of polymers	128
8.6. Polymers functionalization	130
8.7. Methods	131
8.8. References	132
IX. Annex	133
9.1. Supplementary information to Chapter 5	133
9.2. Supplementary information to Chapter 6	136
9.3. Supplementary information to Chapter 8	139

I Introduction

Nearly 50 % of all commercial synthetic polymers are made via free the radical polymerization (FRP) process,¹ which belongs to the class of chain-growth addition polymerization.² The fields of application are numerous and these polymers are present in industries as various as construction, cosmetic or pharmacy, and used as rheological modifiers, suspension stabilizers, surfaces' coating or scaffolds.³⁻⁹

The success of FRP is largely due to the tolerance of the technique to various functionalities and impurities, as well as to the possibility to access high molar mass polymers in short reaction times.² An extensive range of monomers can thus be polymerized, in most cases without the removal of inhibitor or oxygen, and bearing functionalities such as carboxylic acid, hydroxyl or amine. Additionally, radical polymerization is tolerant to water and can therefore be easily carried out in a variety of heterogeneous media.¹⁰

However, FRP does have some serious limitations. For example, transfer and termination reactions are unavoidable, in particular through radical coupling and disproportionation, and occur at high rate. This reduces the lifetime of propagating radicals to often less than a few seconds. As a consequence, at any given time during the reaction, most of the macromolecular chains are dead, i.e. they lost the active radical end that allows them to grow further. Thus, because of slow rate of initiation compared to the rate of propagation, and because of the randomly occurring termination reactions, the resulting polymers are produced with a broad molar mass distribution. Therefore, it is not possible to prepare through FRP, polymers with precise molar mass, well-defined end-groups or architecture, such as block copolymers and gradient copolymers.¹¹

As a consequence, the options for macromolecular engineering are limited, and new, more efficient materials are still needed. A first solution to improve the existing polymers may be the design of materials with greater control over molar mass, polydispersity, functionality, and architecture. Second, the possibility to produce and study such well-defined polymeric samples will subsequently improve our understanding of the relationship between polymers' structure and properties. As discussed above, these defined architectural parameters cannot be achieved by standard FRP. Yet, since its discovery by Szwarc in 1956, well-defined polymers with uniform molar mass, desired functionality and various architectures could be produced by living ionic polymerization.¹² However, ionic polymerizations typically require stringent reaction conditions and have a limited range of polymerizable monomers.¹³ The emergence of reversible

deactivation radical polymerization RDRP (formally often referred to as controlled/living radical polymerization: CRP)¹⁴ in the 1980ies, allowed to combine most of the advantages of FRP with a control close to the one achieved par ionic polymerizations.^{15, 16} Since then, the promising field on the controlled polymerization is constantly growing.

1.1. Controlled polymerization

Mechanistically, CRPs take from both ionic and radical polymerizations: As in the case of ionic polymerizations, CRP implies initiation of most polymer chains at low conversion and the presence of two polymeric species of different reactivity. Whereas in ionic polymerization the two species are ions pairs and free ions, CRP results from the equilibrium between active and dormant polymer chains.^{17, 18} In CRP, this equilibrium allows to reduce, at any given moment, the concentration of propagating radical chains in the reaction media, which consequently lowers the probability of termination reactions to occur. Thus, even if terminations cannot be entirely avoided, as it can be done a priori in ionic polymerization, the degree of control is often sufficient to keep the amount of dead chains below 10 %.

Apart from this fundamental kinetics analogous to ionic polymerizations, CRP is very similar to FRP and proceeds through the same intermediates. Therefore, both radical polymerizations exhibit similar chemo-, regio- and stereo-selectivities, and can be applied to similar range of monomers. Retaining most advantages of FRP, and gaining the control over polymerization process, CRP extends the range of polymeric materials that can be made by radical polymerization.

Three main methods of controlled radical polymerization are currently used. Two techniques are based on the reversible activation/deactivation process of the active radicals, namely the catalyzed atom transfer, in Atom Transfer Radical Polymerization (ATRP)¹⁹⁻²² and the dissociation-combination, in Nitroxide Mediated Polymerization (NMP).^{23, 24} The technique used in this thesis, Reversible Addition-Fragmentation chain Transfer (RAFT) polymerization, proceeds with a different mechanism, the degenerative chain transfer.²⁵⁻²⁹

In ATRP mechanism, the transition metal complex $Mt^0/Ligand$ is responsible for the homolytic cleavage of the alkyl bond P_n-X which generates the corresponding higher oxidation state metal halide complex $X-Mt^{n+1}/Ligand$ (with a rate constant k_{act}) and the propagating radical P_n^\bullet (Figure 1.1). P_n^\bullet can then react with vinyl monomer (k_p), terminate as in conventional free radical polymerization by either coupling or disproportionation (k_t), or be reversibly deactivated (k_{deact})

by $X-M_t^{n+1}/\text{Ligand}$ to form the halide-capped dormant polymer chain. The latter process must be made kinetically dominant in order to achieve a good control over the polymerization.⁵

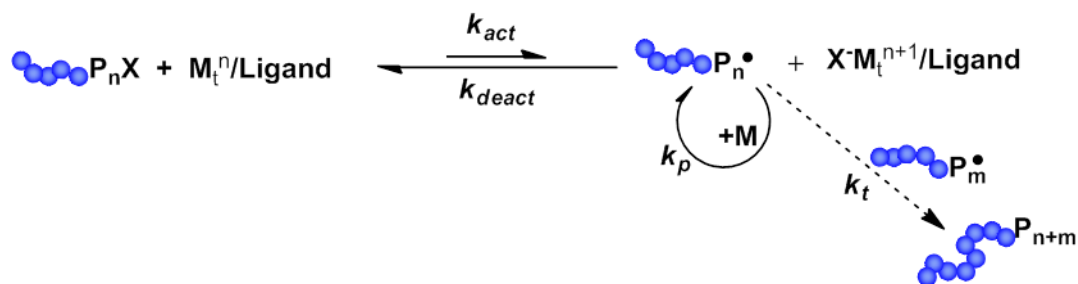


Figure 1.1: General scheme of ATRP

Similarly in the NMP process, the dormant species is cleaved by a thermal or photochemical stimulus to produce the stable free radical and the active propagating radical. (Figure 1.2)

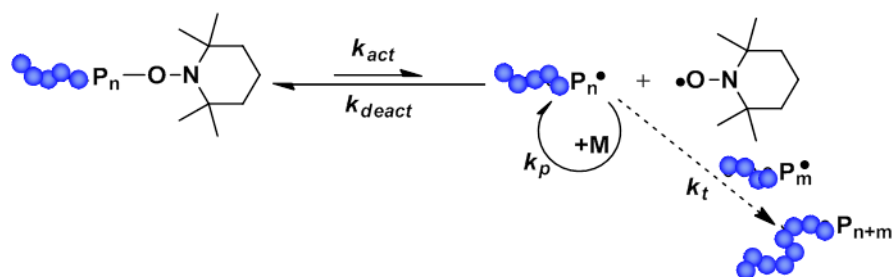


Figure 1.2: General scheme of NMP, here with TEMPO as regulating nitroxide

Both NMP and ATRP are controlled by the persistent radical effect (PRE) first described by Fischer:^{30, 31} when a propagating radical undergoes a termination reaction, the concentration of the deactivating species increases. This in turn renders the deactivation reaction more favorable than the termination reaction, and allows a self-regulation of the active radical concentration.

In the RAFT process the control is generally achieved through thiocarbonylthio compounds, known as RAFT agents or chain transfer agents (CTAs). After a conventional initiation period, the propagating chain P_m^\bullet adds to the $C=S$ double bond of the CTA or the macroCTA to produce an intermediate carbon-centered radical. This carbon-centered radical can then undergo β -scission, to generate a dormant macroCTA and either to re-form the initial propagating radical P_m^\bullet or to liberate a new propagating radical P_n^\bullet . This process establishes a symmetrical equilibrium between the propagating radical and dormant macroCTA (Figure 1.3).³²

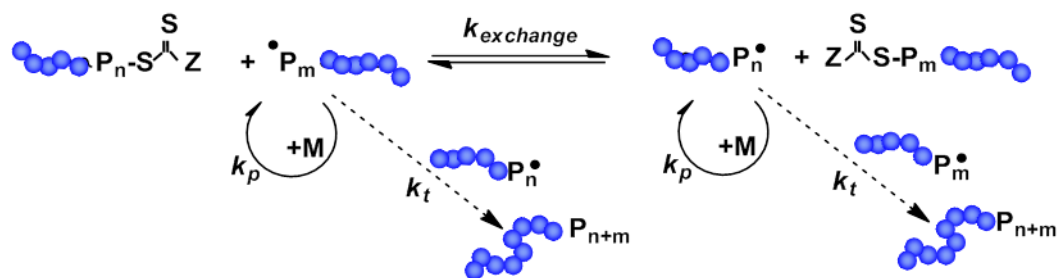


Figure 1.3: General scheme of RAFT polymerization

The RAFT process does not use the persistent radical effect, because the activation and deactivation reactions occur at the same time. As a consequence, the process is kinetically different from NMR or ATRP, and follows typical free radical polymerization kinetics.³² Moreover, and most important in the context of this thesis, the RAFT process is particularly suited to confer 2 functional end-groups to a polymer, with a very large choice of functionalization.^{28, 33, 34}

As the concentration of CTA is experimentally set to be much larger than the one of propagating radical, the growing chains are constantly deactivated and stay mostly in the dormant state. Therefore, and as in the other CRP techniques, the overall lifetime of growing chains is extended from about 1 s in FRP to more than 1 h. The increased reaction time has several experimental advantages, such as the possibility to stop the polymerization at a desired conversion to yield pre-defined molar masses. Even more interesting, one can use the knowledge of the polymerization kinetics to inject a second monomer during the polymerization and introduce an additional block or as in the work of Lutz et al.^{35, 36} an additional functionality to the polymer chain.^{35, 36}

In conclusion, CRP is a powerful technique to create new interesting materials from well-known monomers, which is still strongly developing and improving. As an example, one can cite the recent efforts to conduct CRP in aqueous “green” media,³⁷⁻⁴⁰ or combine the different CRP technique together for the production of controlled giant macromolecules.⁴¹⁻⁴³ As the overall goal of this thesis is to study the self-assembly and the thermo-responsive behavior of complex polymers, RAFT polymerization was employed to design materials with great control over molar mass, architecture, and end-group functionality.

1.2. Stimuli-responsive polymers

Stimuli-responsive polymers are polymers that undergo abrupt physical changes in response to a trigger or small variations in the environmental conditions. The response mechanism is for instance based on a change of solvent quality to the polymer, i.e. a fast and reversible transition of the polymer chains from a dissolved, highly swollen state to a collapsed state. The reversible solubility makes these polymers attractive building blocks for smart systems, as for instance reversible physical gels,^{44, 45} responsive micellar carriers,^{46, 47} switchable surfaces,^{48, 49} or capsules with controlled release.⁵⁰ Up to date, polymers responding to either physical, chemical or biochemical triggers have been designed.⁵¹ Biochemical triggers can be broadly defined as molecules used in living systems such as enzymes, ligands, or antigens.^{52, 53} Typical chemical stimuli are the presence of oxidants.⁵⁴ Finally and most relevant in the context of this thesis, physical stimuli are temperature change, light irradiation or variation of pH, ionic strength, magnetic and electric field.⁵⁵⁻⁵⁷ The different stimuli can be used as integrated orthogonal triggers or in combination. Also, a thermo-responsive behavior can be used to amplify the effect of the second stimulus.

1.2.1. Thermo-responsive polymers

Thermo-responsive polymers undergo abrupt physical changes triggered by small variation of temperature. In few cases, they are hydrophobic at low temperature and become hydrophilic upon heating; the transition type is then characterized by an Upper Critical Solution Temperature (UCST).^{58, 59} However, the majority of non-ionic thermo-responsive polymers experience the opposite change; i.e. from hydrophilic and swollen they abruptly become hydrophobic and collapsed. The latter transition type is characterized by a Lower Critical Solution Temperature (LCST).⁶⁰ The transformation can be generally observed with bare eye, as the clear polymer solution becomes cloudy at the transition temperature. The temperature at which the transformation is observed is thus called the “cloud point” CP and can be monitored by turbidimetry.

Such thermo-responsive polymers, which undergo a transition from hydrophilic to hydrophobic upon heating, have received much attention in recent years.^{6, 51, 61, 62} As the purpose of this thesis is to build thermo-responsive self-assembling hydrogels from block-copolymers of the LCST transition type, the discussion will be focused on the LCST phenomenon in water.

The building segments of the LCST type polymers are made from both hydrophobic and hydrophilic moieties. Clearly, polymers built exclusively from hydrophilic segments are soluble in

water at any temperatures, whereas those predominantly constituted of hydrophobic segments are always insoluble. The intermediate structure of the thermo-responsive polymers is thus at the source of their intermediate solubility. The delicate balance between the segment-water interactions and the segments-segments interactions determines their transition temperature. Structural factors that increase the segment-water interaction will increase polymer solubility and thus the LCST. On the opposite, LCST will be lowered by factors that favor the segment-segment interaction or disfavor polymer-water interaction.⁶

The thermodynamics behind thermo-responsive behavior of the polymers were outlined in two excellent recent reviews by Dimitrov et al.⁶³ and Aseyev et al.,⁶⁴ and are summarized in the following. From a thermodynamical point of view, a polymer is solubilized in water as long as the free energy of dissolution $\Delta G = \Delta H - T\Delta S$, i.e., the difference between the enthalpic and the entropic components is negative. At low temperature, the dissolution is driven by a strong negative enthalpic component ΔH , resulting from the hydrogen bonding between water and appropriate polar moieties of the polymer. The entropic ΔS term is however unfavorable to dissolution, because hydrogen bonding between the polymer's hydrophilic moieties and water, as well as the hydrophobic moieties of the polymer require an organization of water molecules. At higher temperature, the water molecules become more mobile and as a consequence the hydrogen bonding weakens. The predominant contribution to the equation shifts from favorable enthalpic to unfavorable entropic and the free energy of dissolution ΔG becomes positive. Practically, with temperature increase, polymer bound water molecules are released in the bulk and the segment-segment associations in the polymer become stronger, forcing the system to undergo phase separation (See Figure 1.4).

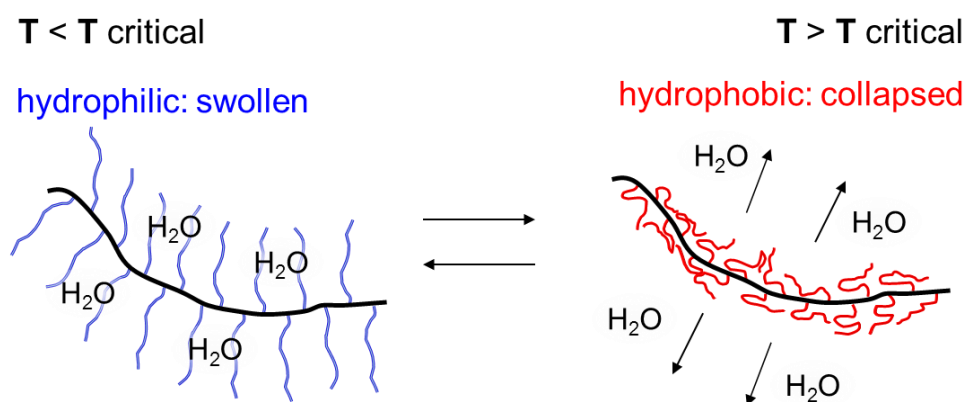


Figure 1.4: General scheme of the reversible conformational changes in a thermo-responsive hydrophilic polymer.

1.2.2. The structural effect: examples of thermo-responsive homopolymers

Acrylamides

The currently most studied thermo-responsive polymers are the poly((meth)acrylamide)s and in particular poly(*N*-isopropylacrylamide) **PNIPAM**.⁶⁵⁻⁷¹ Other examples for thermo-responsive poly(acrylamide)s are poly(*N*-ethylacrylamide),^{72, 73} poly(*N,N*-diethylacrylamide)^{72, 74} or poly(*N*-propylacrylamide),⁷⁵ as well as poly(*N*-isopropylmethacrylamide)⁷⁶ and poly(*N*-ethylmethacrylamide) as examples for poly(methacrylamide)s. Following the previous discussion, one can see that the thermo-responsive behavior of these polymers is due to the combination of hydrophobic alkyl groups, and hydrophilic amide moieties, strongly interacting with water below the LCST.⁷⁷ The structure of some polyacrylamides along with their cloud points (CP) is represented in Figure 1.5. Note that the values of CP increase with decreasing hydrophobicity of the polymer alkyl substituent, from 23°C for the *n*-propyl to 72°C to the less hydrophobic ethyl.

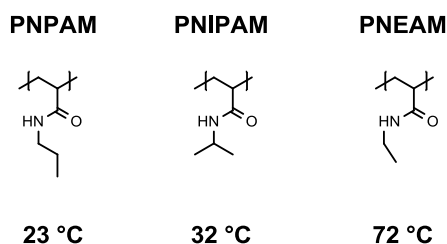


Figure 1.5: Chemical structure and cloud points of some acrylamide homopolymers.

Generally, this class of polymers has simultaneous H-bonding donor and acceptor qualities, through the hydrogen atom of the amide moiety. Thus, when the cloud points are measured in a heating to cooling cycle, polyacrylamides exhibit a sharp transition when heated, but a hysteresis when the solution is subsequently cooled down.^{69, 78} The latter phenomenon is explained by the strong intra- and inter-polymer attractive interactions, since when the polymer collapses, H-bonds are formed between the polymer units, requiring conformational rearrangements before redissolution of the resulting aggregates.

As other thermo-responsive polymers, one can cite poly(*N*-vinylcaprolactam),⁷⁹ from the class of poly(*N*-vinylamide)s, substituted poly(oxazoline)s,⁸⁰ poly(ethylene oxide) PEO,⁸¹ the PEO analogous (meth)acrylates,⁸²⁻⁸⁴ as well as polyvinyl alcohol, produced by hydrolysis of polyvinyl acetate, whose LCST in water is modulated by the number of residual polyvinyl acetate units still

present.⁸⁵ It is obvious that the choice of thermo-responsive polymer is extremely large, and most of them have never been fully studied. For the synthesis of amphiphilic, thermo-responsive block copolymers, it was important to choose a polymer with a convenient transition temperature window, and interesting to choose one which has been nearly overlooked in the past. Thus, poly(methoxy diethylene glycol acrylate) (PMDEGA) was selected as it fully corresponds to the above mentioned criteria. Indeed PMDEGA, that bears two ethylene glycol units in the side chain, presents a LCST in the range of 37 °C⁸⁶ to 45 °C.⁸⁷ Though its LCST is accordingly close to body temperature range, PMDEGA has found surprisingly little interest so far, in contrast to the much studied PNIPAM with an LCST of 32 °C. Additional advantages of PMDEGA are described below in details.

PEG (meth)acrylates

Among the non-ionic water-soluble polymers, poly(ethylene oxide) PEO, also often synonymously called poly(ethylene glycol) PEG, is arguably the most popular one. By virtue of its good biocompatibility, it is also frequently employed for biological and pharmaceutical applications.^{88, 89} Typically, PEG is produced by ring opening anionic polymerization of oxirane, i.e., by a demanding process with little tolerance to most functional groups. Recent years have seen an effort to combine the attractive properties of linear PEG and the advantages of free radical polymerization, by end-capping PEG oligomers with vinyl moieties and polymerizing the resulting functional monomers via a free radical process. Such PEG-vinyl polymer hybrids may belong to various vinyl polymer families, so far mostly to the polyacrylates^{86, 90} and polymethacrylates,^{82, 83, 91, 92} and to a lesser extent to the polystyrenes.⁸⁶ Whereas underivatized PEG is fully water-soluble up to high temperatures, many oligomers that are end-capped with hydrophobic moieties exhibit a volume phase transition of the lower critical solution temperature (LCST) type,⁹³ and the PEG derived vinyl polymers do the same. Characteristically, PEO derived vinyl polymers display sharp transition temperatures with only a small hysteresis between the heating and cooling cycles. Their LCSTs can be easily adjusted by several molecular parameters, including the number of ethylene glycol units in the side chains,⁸⁴ the nature of terminal group of the side chains,⁸⁴ or by copolymerizing PEG monomers of different hydrophilicities.^{90, 94} Also, the chemical nature of the polymer backbone chosen has a primordial influence on the collapse temperature. For example, the LCST of poly(oligoethylene glycol acrylates) is always higher than the LCST of the corresponding poly(methacrylate)s,⁹⁵ an effect that can be easily explained by the missing hydrophobic α -methyl group on the polymer backbone. Indeed, using infrared spectroscopy, the group of Yasushi Maeda, observed that the

H-bonding to the carbonyl group was much reduced in PMDEGMA as compared to PMDEGA, because of this steric effect.⁸⁷

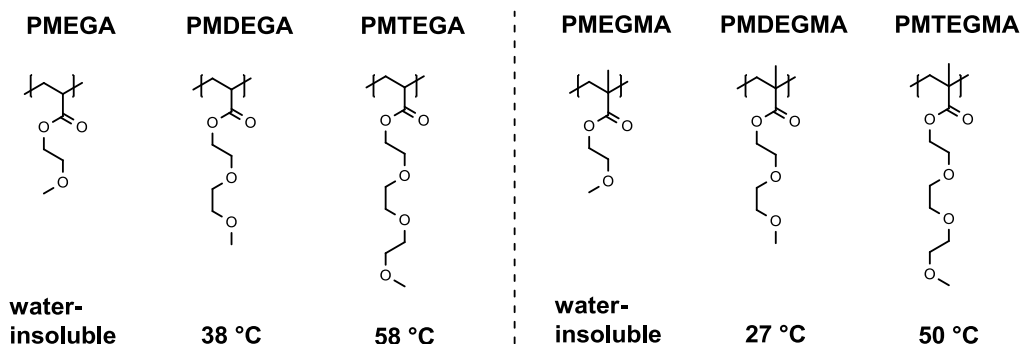


Figure 1.6: Chemical structure and cloud points of several PEG (meth)acrylate homopolymers.

Thus, poly(methoxy diethylene glycol methacrylate) (PMDEGMA), bearing the shortest possible PEG side chain to achieve water-solubility, presents a LCST in the range of 24-28 °C.⁸²⁻⁸⁴ This is about 15 °C lower than the LCST range of the polyacrylate analog PMDEGA, which has been reported between 37 °C⁸⁶ to 45 °C.⁸⁷ Since the first reporting in 1949,⁹⁶ the scientific studies of this polymer have been extremely rare.^{47, 86, 87, 90, 97} In particular, systematic studies are virtually missing. Keeping the potential usefulness of PMDEGA in the biomedical context in mind, and considering the discrepancy of the reported phase transition temperatures, this work focus on the effect of various molecular parameters on the thermo-responsiveness of this polymer.

1.3. Self-assembly of block copolymers

1.3.1. Gel, general definitions

Gels are commonly used for the formulation of everyday life products, such as personal care and cosmetic applications, and can be found in specialized fields, such as optical aids or bioengineering.^{7, 9, 98} Noteworthy, despite their great industrial importance, a clear definition of the notion “gel” is still missing. Considering the variety of structures that allow gelation, it is not surprising. Gels can be defined as three-dimensional networks made of low molar mass molecules,⁹⁹ polymers, particles, colloids, or fibers, interconnected with each other.^{100, 101} The interstitial pores of these networks are characteristically filled with large amounts of solvent. Thus, the wet and soft gels have the advantage to be similar to a large degree to biological tissues, when the solvent is water. In this case the gels are called hydrogels.⁹⁸

As gels are composed of liquid stabilized by a solid network matrix, they exhibit characteristics of both elastic solid and viscous fluid.¹⁰² For this reason, gels are often said to be viscoelastic. Sometimes the distinction is made between the term viscoelastic, used primarily for solid gels, and the term rheologic applied for rather liquid gels.¹⁰³ The connecting groups, holding the network, are called cross-links and can be either of chemical or of physical nature. Chemical gels have covalent, permanent bounds as cross-links. Thus they truly consist of one “infinite” macromolecule and cannot be broken by the thermal movements of their constituents. As examples, one can cite gels prepared by radical copolymerization of monomer and cross-linker,¹⁰⁴ gels obtained by vulcanization or UV-irradiation of polymers containing active groups.^{105, 106} From the rheological point of view, the permanent structure of the chemical gels is reflected by strong moduli, largely independent of temperature or frequency variations (see Chapter 5). Despite their good mechanical properties prior rupture, those systems lack the possibility of melting, reprocessing, or redissolving.

Differently, physical gels are hold by non-permanent physical cross-links. Because the energy of the connection is of the order of the thermal energy, the cross-links can be reversibly formed and destroyed by the thermal motion of the gel constituents.¹⁰⁷ Thus, the equilibrium between connected and disconnected states is only reached if the average lifetime τ of the cross-links is shorter than the time of observation.¹⁰⁸ Rheologically, physical gels are therefore usually dependent of both temperature and frequency and their moduli are weaker than those of chemically cross-linked gels. However, the dynamic nature of the physical gels provides several advantages, such as convenient processing, as physical gels can be made free flowing by dilution, or the ability to self-heal, as the non-covalent connections will naturally rebuild after fracture.^{109, 110} Figure 1.7 gives an example of the self-healing ability of a physical hydrogel, build by hydrophobic interactions.



Figure 1.7: Hydrogels of copolymers of stearyl methacrylate and acrylamide at concentration of 5 wt. % in 0.5 M NaCl solution. One of the gel samples is colored with methylene blue for clarity. After cutting into the gels in two pieces and pressing the fractured surfaces together, they merge into once single piece.¹⁰⁹

The existing physical cross-links are numerous and are for instance made by hydrogen bonding,^{111, 112} hydrophobic,^{44, 113} crystalline or electrostatic interactions,^{114, 115} or the formation of complexes¹¹⁶⁻¹¹⁸ (see Figure 1.8). Finally, it should be added, that the cross-links could be real, as in a covalent network, or apparent, as in colloidal or microgel suspensions,¹¹⁹ or in the case of solutions of long rigid fibrillar molecules.¹²⁰ In the first case, the gel-like rheological behavior is due to the hindered motion of the individual structures because of aggregation (flocculation or coagulation), in the latter case because of entanglements. In such materials, not the direct cross-links, but geometrical or topological constraints lead to gel-like rheology.

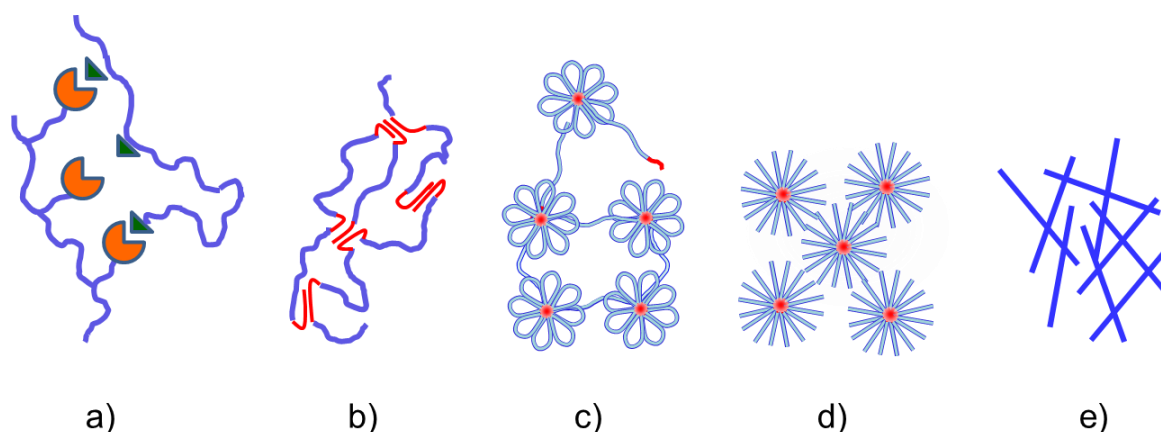


Figure 1.8: Schematical representation of various types of physical cross-links: a) ions association or complex formation; b) association by microcrystalline junctions; c) hydrophobic association; d) micelles jamming; e) entanglements of long rigid polymers.

1.3.2. Hydrogels made of amphiphilic block copolymers

Water soluble polymers carrying hydrophobic blocks or hydrophobic groups, such as short alkyl or fluorocarbon chains are widely used as rheological modifiers by hydrophobic interactions.¹²¹⁻¹²³ Apart from their chemical nature, the position of the hydrophobic segments can be varied from randomly distributed along the polymer chain to specifically positioned at the chain-ends.^{121, 124, 125}

Because the field of gelling polymer is vast, the discussion will be restricted to only amphiphilic block copolymers with hydrophobic outer blocks, as they represent the main interest of this work. At low concentration, these block copolymers self-assemble in micelles with the hydrophobic, insoluble block forming the core and the soluble hydrophilic block the swollen stabilizing corona.¹²⁶ With increased concentration, block copolymers can form physical gels, in which micelles serve as cross-links that dissociate and associate by temperature, external force, or added agents.^{124, 127, 128} Interestingly, molecular characteristics, such as architecture,

chemical composition or block length, are all parameters of influence on the micellization and gelation of block copolymers.¹²¹ Thus, the relatively recent development of controlled polymerization, revived and extended fundamental investigations of these gels, by offering a convenient synthetic possibility to make well defined block copolymers of different architectures and block lengths. Subsequently, the understanding of the role played by the molecular parameters offers a great opportunity to design various materials with specific properties.

The most simple amphiphilic block copolymer is a diblock, with one hydrophobic block B and one hydrophilic block A. With this rather simple architecture already, the polymer will self-assemble in different morphologies depending on the block -lengths and -composition.¹²⁴ However, in the case of polymers bearing short hydrophobic end-block, spherical micelles are usually formed, with a small hydrophobic core and a swollen hydrophilic corona.

The rheology of these polymers is determined by the interaction of the coronas. When the concentration is sufficiently high, the solution of micelles may stop flowing because of the repulsion between the swollen polymer chains.^{121, 129} The phenomenon is called “jamming” and functions by the same repulsive mechanisms as the ones used to stabilize dispersions by protective colloids.² Generally, concentrations of about 30 wt. % are needed to occupy all the volume available,^{129 130} but much lower gelation threshold can be achieved with worm-like micelles, or with micelles decorated with hydrophobic, interacting groups. In the first case the critical gelation concentration can be as low as 10 wt. %, ¹³¹ in the second, as low as 1.5 wt %.¹³²

The self-assembly of amphiphilic block copolymers with more than one hydrophobic outer block B, such as symmetrical triblock copolymers BAB, or multi arm star block copolymers, is different.^{44, 121} The specific architecture with two or more hydrophobic outer “stickers”, induces two possibilities of chains arrangement in micelles. On the one hand, the inner block can form loops with the hydrophobic extremities placed in the same micelle core, which at high concentration leads to gels of densely packed micelles, similar to gels of amphiphilic diblock copolymers.¹³³ On the other hand, the outer blocks can be placed in different micelle cores, while the inner block adopts a bridge conformation. Thus above a critical concentration, which is much lower than in the case of diblock copolymers, a gel of bridged micelles is formed.^{116, 134} Whereas both types of organization coexist in a polymer solution, the mechanical properties result mainly from the proportion of active bridges.¹²¹ This proportion depends on several molecular parameters such as the lengths of the inner and the outer blocks,¹³⁵⁻¹³⁸ and their respective chemical compositions.^{133, 139} However, little is known about the influence of the latter parameter, and this adds to the difficulties to foresee, how a given polymer will behave in solution.

Reports on new amphiphilic copolymers synthesized by controlled radical polymerization techniques are increasingly evolving.^{34, 43, 140, 141} Among these polymers, two classes can be distinguished, namely the permanent amphiphiles and the (mostly thermo-) responsive ones.

1.3.3. Thermo-responsive hydrogels

Polymeric hydrogels, can be made intelligent or responsive, and in this aspect imitate, to a certain degree, living materials.¹⁴² For example, their swelling can be controlled by temperature, pH, light, and specific solutes such as glucose.^{58, 143} This property was applied to demonstrate the uptake and release of solutes, including drugs,^{144, 145} proteins, and surfactants.^{8, 98, 146, 147}

In the context of block copolymers hydrogels, thermo-responsivity can be achieved by two distinct manners. Whereas the characters of the blocks A and B remain unchanged in the permanent systems, in the thermo-responsive systems the character of the block A or B can be switched from hydrophilic to hydrophobic by temperature (Figure 1.9).^{4, 44, 63, 148} Up to now, in the field of symmetrical BAB block copolymers, most of the research was focused on polymers with a permanently hydrophilic inner block A and thermo-responsive outer blocks B exhibiting a LCST. At low temperatures, these polymers are fully hydrophilic and dissolved in water as single molecules. When the temperature crosses the phase transition temperature of the B block, the outer blocks become hydrophobic and thus, trigger the formation of micelles or gels. The association of such BAB blocks copolymers has been investigated employing various thermo-responsive B blocks, such as poly(2-hydroxypropyl methacrylate),¹²⁷ poly(N-isopropyl acrylamide) PNIPAM,^{45, 149-152} poly(ethoxy diethylene glycol acrylate)⁴⁵ or related copolymers with acrylic acid.¹⁵³

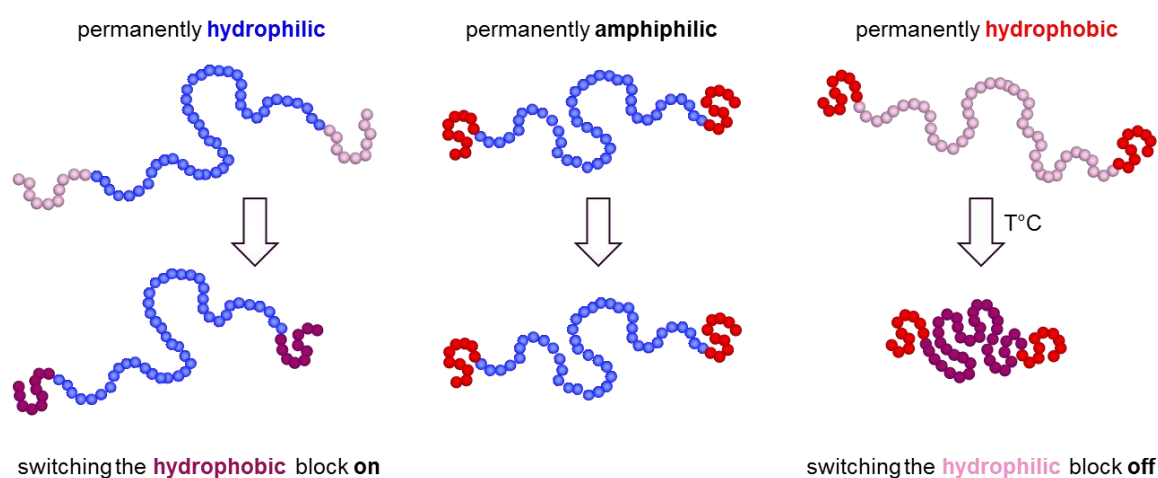


Figure 1.9: Structural changes triggered by temperature in permanent and thermo-responsive triblock copolymers.

Studies on BAB triblock with permanently hydrophobic outer blocks B and switchable hydrophilic inner block A are, however, rare. Some reports can be found on the presumably related associating telechelics made of a switchable A block functionalized with low molecular weight hydrophobic end caps, as in the work of F. Winnik et al. using PNIPAM.^{123, 154} For analogous BAB triblock copolymers, however, most reports are confined to the micellization of such polymers in dilute solutions.¹⁵⁵⁻¹⁵⁷ Reports on the gelation behavior of thermo-responsive BAB block copolymers with switchable inner A block have been generally restricted to poly(ethylene oxide)¹⁵⁸⁻¹⁶² and PNIPAM.^{163, 164} The latter A-block was for instance end-capped with permanently hydrophobic polystyrene,^{163, 165, 166} poly(2-ethylhexyl acrylate),¹⁶³ or poly(octadecyl acrylate)¹⁶³ outer B blocks.

Yet, their particular architecture confers very interesting properties to these systems. Different from permanent hydrogels or thermo-responsive hydrogels made by heat, the permanently hydrophobic outer blocks B and switchable hydrophilic inner block A allow the structure to be swollen below the cloud point, and renders it biphasic and collapsed, above. Thus, if well-understood and controlled, this responsive behavior can be successfully used in various applications. Because hydrogels made by such block copolymers can be made highly liquid in the collapse state, it was suggested by Jeong et al. to use them as injectable drug delivery system.¹⁶⁷ If the LCST of the inner block is above the body temperature, the collapsed dispersion is fluid when hot and can be injected. Once in the patient body, the polymer is cooled below its LCST, quickly swells and recovers its mechanical stability.

Such systems can also be used as thermo-responsive membranes with controlled permeability, regulated by the opening and closing of pores by temperature,¹⁶⁵ or as actuators in microfluidic and lab-on-a-chip devices, where the ability of the materials to expand their volume in wet cold environment and reversible shrink by heat, can be used.¹⁶⁸

Using well-defined block copolymers, made by controlled radical polymerization, this work has for objective to further study these interesting systems, in regard of their self-assembly and their response to temperature.

1.4. Outlook of the thesis

The following work describes the study of stimuli responsive polymers based on the so far hardly utilized thermo-responsive monomer methoxy diethylene glycol acrylate **MDEGA**, and the self-assembly of these polymers to “smart” hydrogels. The polymers were all synthesized by RAFT, one of the techniques of controlled radical polymerization. The thesis starts with the synthesis and characterization of the homo- and block- (co)polymers, continues with the analysis of their

responsive behavior and finishes with the study of the temperature-dependent rheological properties of the resulting hydrogels. The manuscript is organized in the following parts:

Chapter 1 gives an introduction to the 3 topics of importance in the context of this thesis, namely controlled radical polymerization, thermo-responsive behavior of synthetic polymers and self-assembly of block copolymers into hydrogels.

Chapter 2 describes the synthesis by RAFT of well-defined **PMDEGA** homopolymers and block copolymers of **MDEGA** and styrene **S**, in 3 different architectures: diblock, symmetrical triblock and 3-arm star block copolymers. A synthetical strategy is also given to produce polymers with reactive carboxylic acid termini. The reactivity is further demonstrated by a functionalization of the polymer with a rhodamine fluorophore. The first chapter also discusses the current challenges in the analysis of amphiphilic block copolymers with complex architecture and presents two convenient analytical solutions based on the improved use of $^1\text{H-NMR}$ and UV-vis spectroscopies.

Chapter 3 presents the study of the thermo-responsive behavior of **PMDEGA** homo- and copolymers, with a broad parameters variation. 3 series of **PMDEGA** homopolymers with hydrophobic and hydrophilic end-groups are systematically tested and the influence of molar mass and end-groups on cloud point analysed. The influence of block architecture is also described with 3 additional series of diblock, triblock and star block copolymers of **PMDEGA** and polystyrene **PS**.

Chapter 4 discusses the introduction in the thermo-responsive **PMDEGA** system of a secondary response to light. For this purpose the synthesis of an azobenzene containing acrylate, **azoMDEGA**, and its copolymerization with **MDEGA** is described. Further, the response to light and to temperature is analyzed, on a series of **MDEGA/azoMDEGA** copolymers with various contents of **azoMDEGA**.

Chapter 5 deals with the self-assembly of symmetrical triblock **PS-PMDEGA-PS** into smart hydrogels. Critical gelation concentrations as well as mechanical changes induced by temperature are reported. In particular, the influence of the inner block length on the gelation behavior is tested on polymer samples of concentration from 5 to 30 wt. %. Temperature dependent DLS and SAXS analysis are used to correlate structural information to the observed rheological properties.

Chapter 6 reports the influence of topology on the gelation behavior of **PS/PMDEGA** block copolymers of similar composition but 3 different architectures, namely diblock, triblock and 3-

arm star block copolymers. Additionally, in an effort to make the gel more resistant to temperature variations below the cloud point, the effect of hydrophobic block length is studied on a triblock copolymer of **PS-PMDEGA-PS**.

Chapter 8 gives an overview of the experimental set-ups used in this work.

1.5. References

1. Braunecker, W. A.; Matyjaszewski, K. *Prog. Polym. Sci.* 2007, 32, 93-146.
2. Odian, G. G., *Principles of polymerization*. 4th Edition ed.; John Wiley and Sons: Hoboken (USA), 2004; p 812.
3. Wischerhoff, E.; Badi, N.; Laschewsky, A.; Lutz, J.-F. *Adv. Polym. Sci.* 2011, 204, 1-33.
4. Huynh, C. T.; Nguyen, M. K.; Lee, D. S. *Macromolecules* 2011, 44, 6629-6636.
5. Matyjaszewski, K.; Müller, A. H. E.; eds., *Controlled and Living Polymerizations. From Mechanisms to Applications*. Wiley-VCH: Weinheim, 2009.
6. Liu, R.; Fraylich, M.; Saunders, B. *Colloid. Polym. Sci.* 2009, 287, 627-643.
7. Jagur-Grodzinski, J. *Polym. Adv. Techn.* 2010, 21, 27-47.
8. Stuart, M. A. C.; Huck, W. T. S.; Genzer, J.; Müller, M.; Ober, C.; Stamm, M.; Sukhorukov, G. B.; Szleifer, I.; Tsukruk, V. V.; Urban, M.; Winnik, F.; Zauscher, S.; Luzinov, I.; Minko, S. *Nature Mater.* 2010, 9, 101-113.
9. Kopeček, J. *J. Polym. Sci. Part A: Polym. Chem.* 2009, 47, 5929-5946.
10. Asua, J. M. *J. Polym. Sci., Part A: Polym. Chem.* 2004, 42, 1025-1041.
11. Matyjaszewski, K.; Davis, T. P., *Handbook of Radical Polymerization*. John Wiley and Sons: Hoboken (USA), 2002.
12. Szwarc, M. *Nature* 1956, 178, 1168-1169.
13. Matyjaszewski, K., *Advances in Controlled/Living Radical Polymerization*. ACS: 2003; Vol. 854, p 704.
14. Jenkins, A. D.; Jones, R. G.; Moad, G. *Pure Appl. Chem.* 2010, 82, 483-491.
15. Otsu, T.; Yoshida, M. *Makromol. Chem., Rapid Commun.* 1982, 3, 127-132.
16. Otsu, T.; Yoshida, M.; Kuriyama, A. *Polym. Bull.* 1982, 7, 45-50.
17. Greszta, D.; Mardare, D.; Matyjaszewski, K. *Macromolecules* 1994, 27, 638-644.
18. Goto, A.; Fukuda, T. *Prog. Polym. Sci.* 2004, 29, 329-385.
19. Wang, J.-S.; Matyjaszewski, K. *J. Am. Chem. Soc.* 1995, 117, 5614-5615.
20. Kato, M.; Kamigaito, M.; Sawamoto, M.; Higashimura, T. *Macromolecules* 1995, 28, 1721-1723.
21. Matyjaszewski, K.; Xia, J. *Chem. Rev.* 2001, 101, 2921-2990.
22. Tsarevsky, N. V.; Matyjaszewski, K. *Chem. Rev.* 2007, 107, 2270-2299.
23. Georges, M. K.; Veregin, R. P. N.; Kazmaier, P. M.; Hamer, G. K. *Macromolecules* 1993, 26, 2987-2988.
24. Hawker, C. J.; Bosman, A. W.; Harth, E. *Chem. Rev.* 2001, 101, 3661-3688.
25. Chiefari, J.; Chong, Y. K.; Ercole, F.; Krstina, J.; Jeffery, J.; Le, T. P. T.; Mayadunne, R. T. A.; Meijs, G. F.; Moad, C. L.; Moad, G.; Rizzardo, E.; Thang, S. H. *Macromolecules* 1998, 31, 5559-5562.
26. Moad, G.; Rizzardo, E.; Thang, S. H. *Aust. J. Chem.* 2006, 59, 669-692.
27. Theato, P. *J. Polym. Sci. Part A: Polym. Chem.* 2008, 46, 6677-6687.

28. Barner-Kowollik, C.; ed., *Handbook of RAFT Polymerization*. Wiley-VCH: Weinheim (Germany), 2008.
29. Moad, G.; Rizzardo, E.; Thang, S. H. *Polym. Int.* 2011, 60, 9-25.
30. Fischer, H. *Chem. Rev.* 2001, 101, 3581-3610.
31. Tang, W.; Tsarevsky, N. V.; Matyjaszewski, K. *J. Am. Chem. Soc.* 2006, 128, 1598-1604.
32. Barner-Kowollik, C., In *Handbook of RAFT Polymerization*, Wiley-VCH Verlag GmbH & Co. KGaA: 2008.
33. Tasdelen, M. A.; Kahveci, M. U.; Yagci, Y. *Prog. Polym. Sci.* 2011, 36, 455-567.
34. Gregory, A.; Stenzel, M. H. *Prog. Polym. Sci.* 2012, 37, 38-105.
35. Schmidt, B. V. K. J.; Fechler, N.; Falkenhagen, J.; Lutz, J.-F. *Nature Chemistry* 2011, 3, 234-238.
36. Lutz, J.-F.; Schmidt, B. V. K. J.; Pfeifer, S. *Macromol. Rapid Commun.* 2011, 32, 127-135.
37. Burguière, C.; Pascual, S.; Coutin, B.; Polton, A.; Tardi, M.; Charleux, B.; Matyjaszewski, K.; Vairon, J.-P. *Macromol. Symp.* 2000, 150, 39-44.
38. Manguian, M.; Save, M.; Charleux, B. *Macromol. Rapid Commun.* 2006, 27, 399-404.
39. Min, K.; Gao, H.; Matyjaszewski, K. *J. Am. Chem. Soc.* 2005, 127, 3825-3830.
40. Semsarilar, M.; Perrier, S. *Nat Chem* 2010, 2, 811-820.
41. Yagci, Y.; Atilla Tasdelen, M. *Prog. Polym. Sci.* 2006, 31, 1133-1170.
42. Zehm, D.; Laschewsky, A.; Heunemann, P.; Gradzielski, M.; Prévost, S.; Liang, H.; Rabe, J. P.; Lutz, J.-F. *Polym. Chem.* 2011, 2, 137-147.
43. Zehm, D.; Laschewsky, A.; Gradzielski, M.; Prévost, S.; Liang, H.; Rabe, J. P.; Schweins, R.; Gummel, J. *Langmuir* 2010, 26, 3145-3155.
44. Tsitsilianis, C. *Soft Matter* 2010, 6, 2372-2388.
45. Vogt, A. P.; Sumerlin, B. S. *Soft Matter* 2009, 5, 2347-2351.
46. Ganta, S.; Devalapally, H.; Shahiwala, A.; Amiji, M. *J. Controlled Release* 2008, 126, 187-204.
47. Weiss, J.; Laschewsky, A. *Langmuir* 2011, 27, 4465-4473.
48. Uchida, K.; Sakai, K.; Ito, E.; Hyeong Kwon, O.; Kikuchi, A.; Yamato, M.; Okano, T. *Biomaterials* 2000, 21, 923-929.
49. Wischerhoff, E.; Uhlig, K.; Lankenau, A.; Börner, H. G.; Laschewsky, A.; Duschl, C.; Lutz, J.-F. *Angew. Chem. Int. Ed.* 2008, 47, 5666-5668.
50. Esser-Kahn, A. P.; Odom, S. A.; Sottos, N. R.; White, S. R.; Moore, J. S. *Macromolecules* 2011, 44, 5539-5553.
51. Lee, H.-i.; Pietrasik, J.; Sheiko, S. S.; Matyjaszewski, K. *Prog. Polym. Sci.* 2010, 35, 24-44.
52. Miyata, T.; Asami, N.; Uragami, T. *J. Polym. Sci., Part B: Polym. Phys.* 2009, 47, 2144-2157.
53. Woodcock, J. W.; Jiang, X.; Wright, R. A. E.; Zhao, B. *Macromolecules* 2011, 44, 5764-5775.
54. Yamamoto, S.-i.; Pietrasik, J.; Matyjaszewski, K. *Macromolecules* 2008, 41, 7013-7020.
55. Jiang, J.; Tong, X.; Morris, D.; Zhao, Y. *Macromolecules* 2006, 39, 4633-4640.
56. Tao, X.; Gao, Z.; Satoh, T.; Cui, Y.; Kakuchi, T.; Duan, Q. *Polym. Chem.* 2011, 2, 2068-2073.
57. Schattling, P.; Jochum, F. D.; Theato, P. *Chem. Commun.* 2011, 47, 8859-8861.

58. Reinicke, S.; Schmalz, H. *Colloid Polym. Sci.* 2011, 289, 497-512.
59. Tian, H.-Y.; Yan, J.-J.; Wang, D.; Gu, C.; You, Y.-Z.; Chen, X.-S. *Macromol. Rapid Commun.* 2011, 32, 660-664.
60. Somcynsky, T. *Polym. Eng. Sci.* 1982, 22, 58-63.
61. Mano, J. F. *Adv. Eng. Mater.* 2008, 10, 515-527.
62. Hu, J.; Liu, S. *Macromolecules* 2010, 43, 8315-8330.
63. Dimitrov, I.; Trzebicka, B.; Müller, A. H. E.; Dworak, A.; Tsvetanov, C. B. *Prog. Polym. Sci.* 2007, 32, 1275-1343.
64. Aseyev, V.; Tenhu, H.; Winnik, F. *Adv. Polym. Sci.* 2011, 242, 29-89.
65. Xue, W.; Huglin, M. B.; Jones, T. G. J. *Eur. Polym. J.* 2005, 41, 239-248.
66. Liu, H. Y.; Zhu, X. X. *Polymer* 1999, 40, 6985-6990.
67. Ding, Y.; Ye, X.; Zhang, G. *Macromolecules* 2005, 38, 904-908.
68. Kujawa, P.; Aseyev, V.; Tenhu, H.; Winnik, F. M. *Macromolecules* 2006, 39, 7686-7693.
69. Cheng, H.; Shen, L.; Wu, C. *Macromolecules* 2006, 39, 2325-2329.
70. Berber, M. R.; Mori, H.; Hafez, I. H.; Minagawa, K.; Tanaka, M.; Niidome, T.; Katayama, Y.; Maruyama, A.; Hirano, T.; Maeda, Y.; Mori, T. *J. Phys. Chem. B* 2010, 114, 7784-7790.
71. Adelsberger, J.; Meier-Koll, A.; Bivigou-Koumba, A. M.; Busch, P.; Holderer, O.; Hellweg, T.; Laschewsky, A.; Müller-Buschbaum, P.; Papadakis, C. M. *Colloid Polym. Sci.* 2011, 289, 711-720.
72. Taylor, L. D.; Cerankowski, L. D. *J. Polym. Sci., Part A: Polym. Chem.* 1975, 13, 2551-2570.
73. Xue, W.; Huglin, M. B.; Jones, T. G. J. *Macromol. Chem. Phys.* 2003, 204, 1956-1965.
74. Idziak, I.; Avoce, D.; Lessard, D.; Gravel, D.; Zhu, X. X. *Macromolecules* 1999, 32, 1260-1263.
75. Ito, D.; Kubota, K. *Macromolecules* 1997, 30, 7828-7834.
76. Starovoytova, L.; Spěváček, J. *Polymer* 2006, 47, 7329-7334.
77. Tiktopulo, E. I.; Uversky, V. N.; Lushchik, V. B.; Klenin, S. I.; Bychkova, V. E.; Ptitsyn, O. B. *Macromolecules* 1995, 28, 7519-7524.
78. Sun, S.; Wu, P. *J. Phys. Chem. B* 2011, 115, 11609-11618.
79. Vihola, H.; Laukkanen, A.; Hirvonen, J.; Tenhu, H. *Eur. J. Pharm. Sci.* 2002, 16, 69-74.
80. Hoogenboom, R.; Thijs, H. M. L.; Jochems, M. J. H. C.; van Lankvelt, B. M.; Fijten, M. W. M.; Schubert, U. S. *Chem. Commun.* 2008, 5758-5760.
81. Durme, K. V.; Verbrugghe, S.; Du Prez, F. E.; Van Mele, B. *Macromolecules* 2004, 37, 1054-1061.
82. Lutz, J.-F.; Hoth, A. *Macromolecules* 2006, 39, 893-896.
83. Yamamoto, S.-I.; Pietrasik, J.; Matyjaszewski, K. *J. Polym. Sci., Part A: Polym. Chem.* 2008, 46, 194-202.
84. Han, S.; Hagiwara, M.; Ishizone, T. *Macromolecules* 2003, 36, 8312-8319.
85. Eagland, D.; Crowther, N. J. *Eur. Polym. J.* 1991, 27, 299-301.
86. Hua, F.; Jiang, X.; Li, D.; Zhao, B. *J. Polym. Sci., Part A: Polym. Chem.* 2006, 44, 2454-2467.
87. Maeda, Y.; Yamauchi, H.; Kubota, T. *Langmuir* 2009, 25, 479-482.

88. Barz, M.; Luxenhofer, R.; Zentel, R.; Vicent, M. J. *Polym. Chem.* 2011, 2, 1900-1918.
89. Dormidontova, E. E. *Macromolecules* 2001, 35, 987-1001.
90. Lavigueur, C.; Garcia, J. G.; Hendriks, L.; Hoogenboom, R.; Cornelissen, J. J. L. M.; Nolte, R. J. M. *Polym. Chem.* 2011, 2, 333-340.
91. Lutz, J.-F.; Akdemir, Ö.; Hoth, A. *J. Am. Chem. Soc.* 2006, 128, 13046-13047.
92. Roth, P. J.; Jochum, F. D.; Forst, F. R.; Zentel, R.; Theato, P. *Macromolecules* 2010, 43, 4638-4645.
93. Dormidontova, E. E. *Macromolecules* 2004, 37, 7747-7761.
94. Lutz, J.-F. *J. Polym. Sci. Part A: Polym. Chem.* 2008, 46, 3459-3470.
95. Maeda, Y.; Kubota, T.; Yamauchi, H.; Nakaji, T.; Kitano, H. *Langmuir* 2007, 23, 11259-11265.
96. Rehberg, C. E.; Faucette, W. A. *J. Org. Chem.* 1949, 14, 1094-1098.
97. Zhong, Q.; Wang, W.; Adelsberger, J.; Golosova, A.; Koumba, A. M. B.; Laschewsky, A.; Funari, S. S.; Perlich, J.; Roth, S. V.; Papadakis, C. M.; Müller-Buschbaum, P. *Colloid Polymer Sci.* 2011, 289, 569-581.
98. Chaterji, S.; Kwon, I. K.; Park, K. *Prog. Polym. Sci.* 2007, 32, 1083-1122.
99. Tanaka, M.; Ikeda, T.; Mack, J.; Kobayashi, N.; Haino, T. *J. Org. Chem.* 2011, 76, 5082-5091.
100. Nishinari, K., Some Thoughts on The Definition of a Gel. Gels: Structures, Properties, and Functions. In Tokita, M.; Nishinari, K., Eds. Springer Berlin / Heidelberg: 2009; Vol. 136, pp 87-94.
101. Rogovina, L.; Vasil'ev, V.; Braudo, E. *Polym. Sci. Ser. C* 2008, 50, 85-92.
102. Tanaka, F., *Polymer Physics: Applications to Molecular Association and Thermoreversible Gelation*. Cambridge University Press: Cambridge (UK), 2011; p 404.
103. Brinson, H. F.; Brinson, L. C., *Polymer engineering science and viscoelasticity: an introduction*. Springer: Houston (USA), 2008.
104. Gao, H.; Miasnikova, A.; Matyjaszewski, K. *Macromolecules* 2008, 41, 7843-7849.
105. Ghosh, B.; Urban, M. W. *Science* 2009, 323, 1458-1460.
106. Urban, M. W. *Nat Chem* 2012, 4, 80-82.
107. Zhang, S.; Lee, K. H.; Frisbie, C. D.; Lodge, T. P. *Macromolecules* 2011, 44, 940-949.
108. Tadros, F. T., *Rheology of Dispersions: Principles and Applications*. Wiley-VCH Verlag Weinheim (Germany), 2010.
109. Tuncaboylu, D. C.; Sari, M.; Oppermann, W.; Okay, O. *Macromolecules* 2011, 44, 4997-5005.
110. Cordier, P.; Tournilhac, F.; Soulie-Ziakovic, C.; Leibler, L. *Nature* 2008, 451, 977-980.
111. Lei, Y.; Lodge, T. P. *Soft Matter* 2012, 8.
112. Sijbesma, R. P.; Beijer, F. H.; Brunsveld, L.; Folmer, B. J. B.; Hirschberg, J. H. K. K.; Lange, R. F. M.; Lowe, J. K. L.; Meijer, E. W. *Science* 1997, 278, 1601-1604.
113. Lodge, T. P. *Macromol. Chem. Phys.* 2003, 204, 265-273.
114. Rehm, T.; Schmuck, C. *Chem. Commun.* 2008, 801-813.

115. Agrawal, S. K.; Sanabria-DeLong, N.; N. Tew, G.; Bhatia, S. R. *J. Mater. Res.* 2006, 21, 2118-2125.
116. Liu, J.; Chen, G.; Guo, M.; Jiang, M. *Macromolecules* 2010, 43, 8086-8093.
117. Tamesue, S.; Takashima, Y.; Yamaguchi, H.; Shinkai, S.; Harada, A. *Angew. Chem. Int. Ed.* 2010, 49, 7461-7464.
118. Zhao, Y.-L.; Stoddart, J. F. *Langmuir* 2009, 25, 8442-8446.
119. Kegel, W. K.; Lekkerkerker, H. N. W. *Nat Mater* 2011, 10, 5-6.
120. Qiao, Y.; Lin, Y.; Yang, Z.; Chen, H.; Zhang, S.; Yan, Y.; Huang, J. *J. Phys. Chem. B* 2010, 114, 11725-11730.
121. Chassenieux, C.; Nicolai, T.; Benyahia, L. *Curr. Opin. Colloid Interface Sci.* 2011, 16, 18-26.
122. Pham, Q. T.; Russel, W. B.; Thibault, J. C.; Lau, W. *Macromolecules* 1999, 32, 5139-5146.
123. Kujawa, P.; Watanabe, H.; Tanaka, F.; Winnik, F. M. *Eur. Phys. J. E Soft Matter.* 2005, 17, 129-137.
124. Hamley, I. W., *Block Copolymers in Solution: Fundamentals and Applications*. John Wiley & Sons Chichester (UK), 2005.
125. Krieg, E.; Rybtchinski, B. *Chem. Eur. J.* 2011, 17, 9016-9026.
126. Riess, G. *Prog. Polym. Sci.* 2003, 28, 1107-1170.
127. Madsen, J.; Armes, S. P.; Lewis, A. L. *Macromolecules* 2006, 39, 7455-7457.
128. Ge, Z.; Xie, D.; Chen, D.; Jiang, X.; Zhang, Y.; Liu, H.; Liu, S. *Macromolecules* 2007, 40, 3538-3546.
129. Bhatia, S. R.; Mourchid, A.; Joanicot, M. *Curr. Opin. Colloid Interface Sci.* 2001, 6, 471-478.
130. Chen, C. F.; Lin, C. T. Y.; Chu, I. M. *Polym. Int.* 2010, 59, 1428-1435.
131. Mortensen, K.; Brown, W.; Almdal, K.; Alami, E.; Jada, A. *Langmuir* 1997, 13, 3635-3645.
132. Kimerling, A. S.; Rochefort, W. E.; Bhatia, S. R. *Ind. Eng. Chem. Res.* 2006, 45, 6885-6889.
133. Giacomelli, F. C.; Riegel, I. C.; Petzhold, C. L.; da Silveira, N. P.; Stepanek, P. *Langmuir* 2008, 25, 731-738.
134. Bae, S. J.; Suh, J. M.; Sohn, Y. S.; Bae, Y. H.; Kim, S. W.; Jeong, B. *Macromolecules* 2005, 38, 5260-5265.
135. Semenov, A. N.; Joanny, J. F.; Khokhlov, A. R. *Macromolecules* 1995, 28, 1066-1075.
136. Balsara, N. P.; Tirrell, M.; Lodge, T. P. *Macromolecules* 1991, 24, 1975-1986.
137. Nguyen-Misra, M.; Mattice, W. L. *Macromolecules* 1995, 28, 1444-1457.
138. Calucci, L.; Forte, C.; Buwalda, S. J.; Dijkstra, P. J.; Feijen, J. *Langmuir* 2010, 26, 12890-12896.
139. Buwalda, S. J.; Dijkstra, P. J.; Calucci, L.; Forte, C.; Feijen, J. *Biomacromolecules* 2009, 11, 224-232.
140. Hayward, R. C.; Pochan, D. J. *Macromolecules* 2010, 43, 3577-3584.
141. Holder, S. J.; Sommerdijk, N. A. J. M. *Polym. Chem.* 2011, 2, 1018-1028.
142. Roya, D.; Cambrea, J. N.; Sumerlin, B. S. *Prog. Polym. Sci.* 2010, 35, 278-301.
143. Alexeev, V. L.; Das, S.; Finegold, D. N.; Ashe, S. A. *Clin. Chem.* 2004, 50, 2353-2360.

144. Qiu, Y.; Park, K. *Adv. Drug Delivery Rev.* 2001, 53, 321-339.
145. Bajpai, A. K.; Shukla, S. K.; Bhanu, S.; Kankane, S. *Prog. Polym. Sci.* 2008, 33, 1088-1118.
146. Park, M. H.; Joo, M. K.; Choi, B. G.; Jeong, B. *Acc. Chem. Res.* 2012, ASAP.
147. Pasparakis, G.; Vamvakaki, M. *Polym. Chem.* 2011, 2, 1234-1248.
148. McCormick, C. L.; Sumerlin, B. S.; Lokitz, B. S.; Stempka, J. E. *Soft Matter* 2008, 4, 1760-1773.
149. Zhao, X.; Liu, W.; Chen, D.; Lin, X.; Lu, W. W. *Macromol. Chem. Phys.* 2007, 208, 1773-1781.
150. Skrabania, K.; Li, W.; Laschewsky, A. *Macromol. Chem. Phys.* 2008, 209, 1389-1403.
151. Kirkland, S. E.; Hensarling, R. M.; McConaughy, S. D.; Guo, Y.; Jarrett, W. L.; McCormick, C. L. *Biomacromolecules* 2007, 9, 481-486.
152. Ge, Z.; Zhou, Y.; Tong, Z.; Liu, S. *Langmuir* 2011, 27, 1143-1151.
153. O'Lenick, T. G.; Jin, N.; Woodcock, J. W.; Zhao, B. *J. Phys. Chem. B* 2011, 115, 2870-2881.
154. Koga, T.; Tanaka, F.; Motokawa, R.; Koizumi, S.; Winnik, F. M. *Macromolecules* 2008, 41, 9413-9422.
155. Ge, Z.; Chen, D.; Zhang, J.; Rao, J.; Yin, J.; Wang, D.; Wan, X.; Shi, W.; Liu, S. *J. Polym. Sci., Part A: Polym. Chem.* 2007, 45, 1432-1445.
156. Dai, F.; Wang, P.; Wang, Y.; Tang, L.; Yang, J.; Liu, W.; Li, H.; Wang, G. *Polymer* 2008, 49, 5322-5328.
157. Zhou, J.; Wang, L.; Yang, Q.; Liu, Q.; Yu, H.; Zhao, Z. *J. Phys. Chem. B* 2007, 111, 5573-5580.
158. Castelletto, V.; Hamley, I. W.; Yuan, X. F.; Kelarakis, A.; Booth, C. *Soft Matter* 2005, 1, 138-145.
159. Kelarakis, A.; Havredaki, V.; Yuan, X.-F.; Yang, Y.-W.; Booth, C. *J. Mater. Chem.* 2003, 13, 2779-2784.
160. Kelarakis, A.; Havredaki, V.; Yuan, X.-F.; Chaibundit, C.; Booth, C. *Macromol. Chem. Phys.* 2006, 207, 903-909.
161. He, Y.; Boswell, P. G.; Bühlmann, P.; Lodge, T. P. *J. Phys. Chem. B* 2006, 111, 4645-4652.
162. He, Y.; Lodge, T. P. *Macromolecules* 2007, 41, 167-174.
163. Bivigou-Koumba, A.; Görnitz, E.; Laschewsky, A.; Müller-Buschbaum, P.; Papadakis, C. *Colloid. Polym. Sci.* 2010, 288, 499-517.
164. Zhou, Y.; Jiang, K.; Song, Q.; Liu, S. *Langmuir* 2007, 23, 13076-13084.
165. Nykänen, A.; Nuopponen, M.; Laukkanen, A.; Hirvonen, S.-P.; Rytelä, M.; Turunen, O.; Tenhu, H.; Mezzenga, R.; Ikkala, O.; Ruokolainen, J. *Macromolecules* 2007, 40, 5827-5834.
166. Nykänen, A.; Nuopponen, M.; Hiekkataipale, P.; Hirvonen, S.-P.; Soininen, A.; Tenhu, H.; Ikkala, O.; Mezzenga, R.; Ruokolainen, J. *Macromolecules* 2008, 41, 3243-3249.
167. Jeong, B.; Bae, Y. H.; Lee, D. S.; Kim, S. W. *Nature* 1997, 388, 860-862.
168. Harmon, M. E.; Tang, M.; Frank, C. W. *Polymer* 2003, 44, 4547-4556

II Synthesis, characterization and modification of telechelic polymers

An important feature of the RAFT process is the possibility to attach diverse functional end-groups to polymers in a nearly quantitative and optionally symmetrical or non-symmetrical manner, by appropriate design of the so-called R and Z groups of the initially engaged degenerative chain transfer agent (CTA).¹⁻³ The resulting polymers are functionalized with the R and Z groups from the initial CTA, which e.g. can be exploited for characterization, or used for further modification of the polymer.⁴⁻⁷

This work is focused on the synthesis of homopolymers as well as of block copolymers of methoxy diethylene glycol acrylate MDEGA, with precise molar masses, low polymer dispersity, and with defined end-groups, or defined end blocks, respectively. In particular were targeted block copolymers bearing a short hydrophobic polystyrene end-blocks (B blocks) of three different architectures, namely diblock AB, symmetrical triblock BAB, and 3-arm star (BA)₃.

2.1. Design of chain transfer agents

The targeted architectures can be synthesized by RAFT polymerization in two steps using, respectively, mono-, bi- and tri-functional CTAs.^{7, 8} Importantly for the synthesis of complex architectures, the RAFT technique allows to place the active chain end, here the carbonyl thio Z-group, either at the extremities or in the middle of the growing polymer chain. Therefore, as in the case of symmetrical block copolymers, two types of RAFT agents can be considered.^{7, 9, 10} In type 1, the active groups of the polymer chain are placed at the outer ends of the polymer (Z-C(=S)-S-R-S-C(=S)-Z, see Figure 2.1). The polymer is then growing inside out, and the first block to be polymerized is placed in the middle of the macromolecule.⁹ In type 2, the active groups are positioned in the middle of the polymer chain (R-S-C(=S)-Z-C(=S)-S-R, see Figure 2.1). In this case, the polymer is growing outside in and the first block is placed at the outer ends.¹⁰

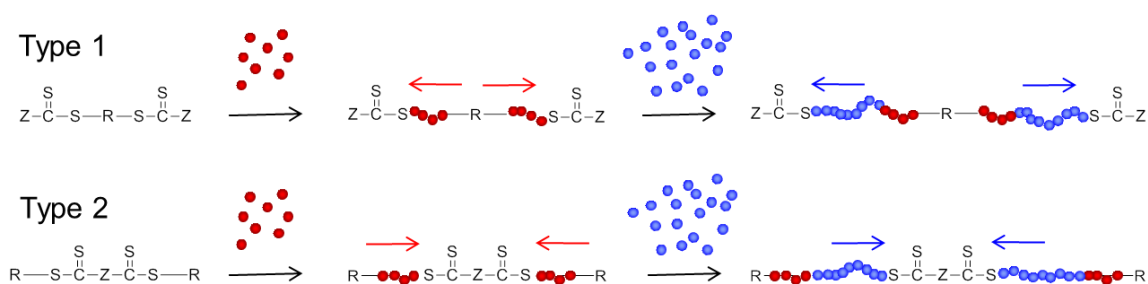


Figure 2.1: Symmetrical triblock copolymers synthesis using CTAs of type 1 or type 2.

In this work, bifunctional and trifunctional CTAs of type 2 were chosen, to afford respectively symmetrical BAB triblock and 3-arm star copolymers. By using these CTAs, styrene (S) can be polymerized first, followed by MDEGA in a second step. The approach allowed to keep an identical hydrophobic polystyrene block while varying the length of the inner hydrophilic PMDEGA block.

A further objective was to introduce functional groups at the chain-ends to facilitate polymer characterization by ^1H -NMR spectroscopy and for the modification of the macromolecules by a post-polymerization step. As starting base for the CTAs synthesis, trithiocarbonate moieties as Z groups and para substituted benzylic R-groups were chosen. Similar RAFT agents were found suitable for the polymerization of styrene, acrylamides and acrylates.¹⁰ Because in the case of simple benzylic R-groups, the overlapping of the ^1H signals prevent end-group analysis of polystyrenes, appropriate substitution of the aryl moieties is necessary to induce a strong signal shift of aromatic protons and resolve the R group from the polystyrene signals. It was therefore interesting to choose a substitution of the R group that will at the same time induce a shift of the ^1H signals and be chemically active. The recent development of click chemistry provides a large number of efficient reactions for polymer modification.^{6, 11, 12} Within the tool box, the copper catalyzed Huisgen 1,3-dipolar cycloaddition of azides and alkynes, the Diels-Alder, Hetero Diels-Alder Cycloaddition or the activated ester reactions were all successfully applied to polymers synthesis and modification.^{1, 13} Because many benzoic acid derivatives are commercially available and show ^1H signals in the high ppm region, the activated ester chemistry was chosen as an effective way to couple polymers bearing benzoic acid moieties to amine containing molecules. Additionally, when catalyzed by the combination of *N*-hydroxysuccinimide (NHS) and ethyl(dimethylaminopropyl)carbodiimide (EDC), the reaction can be performed with high yield.^{1, 11, 14, 15}

Figure 2.2 presents the targeted chain transfer agents bearing a chemically active carboxylic acid moiety, an aromatic ring for improved polymer characterization by ^1H -NMR and multiple functionalities for the synthesis of diblock (**CTA1**), triblock (**CTA2** and **CTA7**) and 3-arm star (**CTA8**) block copolymers.

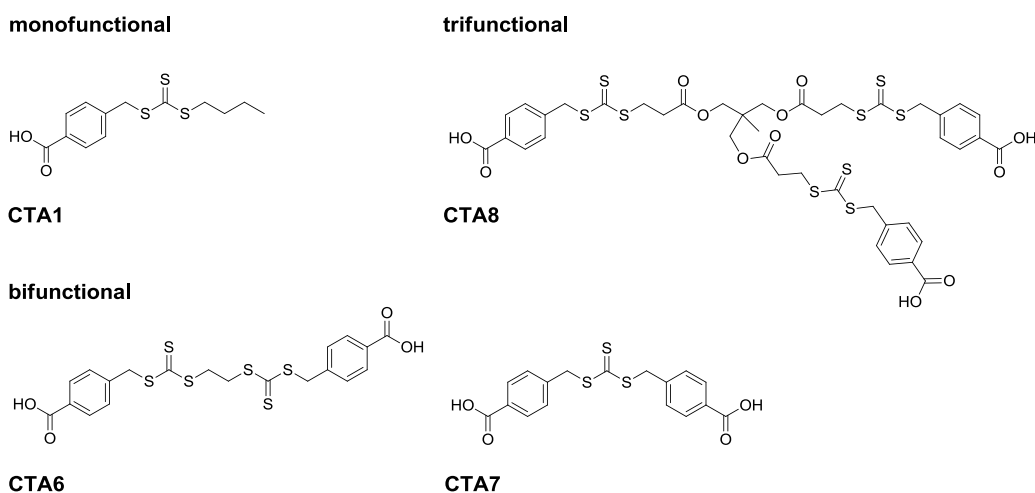


Figure 2.2: Chemical formula of the envisaged multifunctional RAFT agents (CTAs).

2.2. Multifunctional CTAs with COOH functionalities

The monofunctional **CTA1** was synthesized by conventional procedures¹⁰ and was readily soluble in both benzene and styrene, chosen as polymerization media for respectively MDEGA and styrene.

Next, the bifunctional **CTA6** bearing two benzoic acid moieties and a central ethylene moiety between the two trithiocarbonate functions was synthesized. During the synthesis of **CTA6** in benzene, a dull yellow product precipitated. Although it was found reasonably pure by ¹H-NMR analysis, the product could not be dissolved in any organic solvent with the exception of DMSO, and therein only to 2 g·L⁻¹. An attempt to dissolve **CTA6** in styrene at 110°C for the synthesis of telechelic polystyrene failed. A similar RAFT agent **CTA7**, lacking this time the inner ethylene moiety, was alternatively synthesized. Again as for **CTA6**, **CTA7** could only be dissolved in DMSO. The synthesis of the trifunctional **CTA8** was therefore not attempted, as it seemed highly probable to produce again an insoluble product.

While α -functional and an α,ω -functional CTA bearing propionic acid moieties were readily soluble in toluene or methyl ethyl ketone,^{16, 17} in the case of **CTA6** and **CTA7** the combination of rigid aromatic rings and carboxylic acid moieties, both H-bond donor and acceptor, probably lead to the formation of strand-like supramolecular complexes, stable enough to withstand dissolution and high temperatures.¹⁸ Although the polymerization could be attempted in DMSO, it did not appear as an ideal procedure, as the synthesis of short polystyrene requires large

amounts of CTA, which need to be dissolved in large volume of solvent. At high dilution, the polymerization of styrene risks to be too slow to be well controlled.

To keep the idea of a telechelic polymer with two benzoic acid end-groups, the carboxylic acid moieties were therefore masked in the primary CTAs by a protective group, which could be removed in a post-polymerization step. The classic *tert*-butyl ester group^{19, 20} was chosen as protective group, as it:

- Is resistant to basic and nucleophilic attack, thus can withstand the synthesis of CTAs
- Improves the solubility of the final product.
- is removed by acidolysis, to which trithiocarbonates are resistant in water free conditions.

The synthesis of the multifunctional **CTA2** and **CTA3** (Figure 2.3), bearing respectively 2 and 3 *tert*-butyl benzoate moieties, was successful and the resulting CTAs were readily soluble in variety of organic solvents, such as acetone, chloroform, dichloromethane, benzene, or tetrahydrofuran. Thus, the polymers in this work were all made using **CTA1**, **CTA2** or **CTA3**.

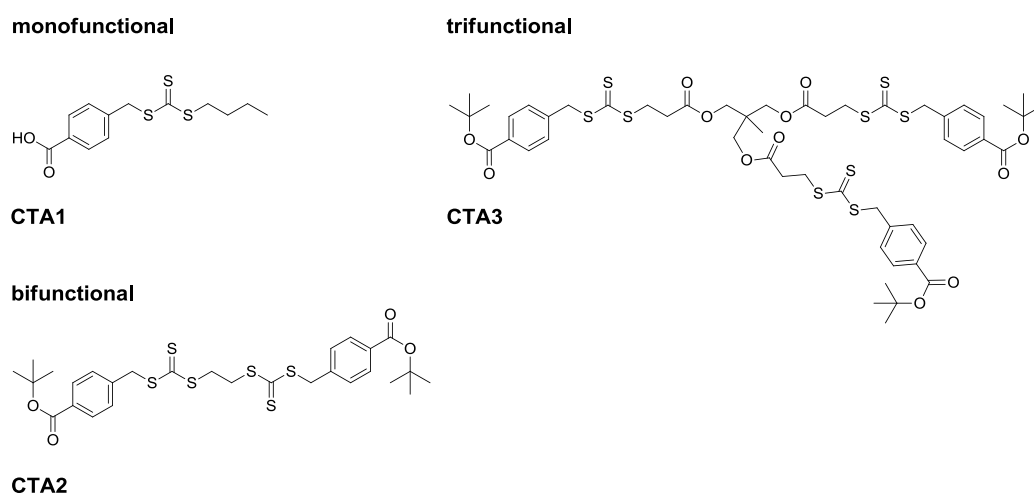


Figure 2.3: Chemical formula of multifunctional RAFT agents (CTAs) employed for polymer synthesis.

2.3. Characterization by ¹H-NMR spectroscopy

¹H-NMR analysis of polymers made with **CTA2** is described below, to exemplify the efficiency of the new CTAs as polymers' characterization tool.

The series of homopolymers, PMDEGA-a, synthesized with **CTA2** was made in one step, by varying the monomer to CTA ratio. The same **CTA2** was used to synthesize the series of symmetrical triblock copolymers. As mentioned above, triblock copolymers were made in 2 steps, polymerizing first styrene (i) followed by MDEGA (ii).

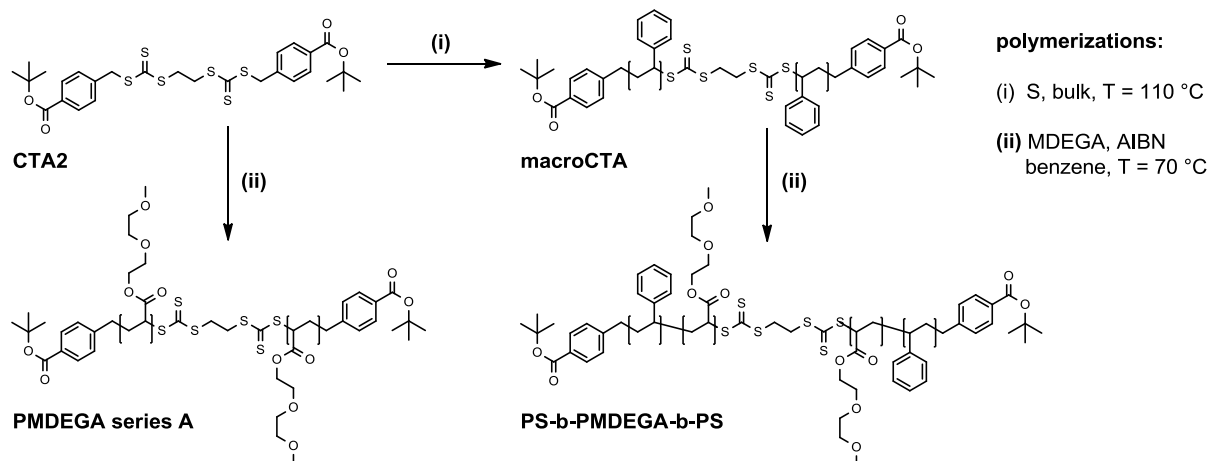


Figure 2.4: Synthesis of PMDEGA homopolymers of series A and of symmetrical triblock copolymers using the bifunctional RAFT agent **CTA2**.

In the case of polystyrene, the incorporation of functional moieties into the R and the Z groups of the primary **CTA2**, gave rise to two distinct, well-resolved signals in the $^1\text{H-NMR}$ spectra (Figure 2.5.a): a doublet at 7.80 ppm for the ortho aryl protons of the benzoate moiety in the R group (signal 1), and a singlet at 3.61 ppm of the central ethylene moiety of the Z group between the two trithiocarbonate functions (signal 5). These enable the determination of number average molar masses M_n by comparing the intensity of the R or the Z groups signals with the intensity of the characteristic PS aryl signals. Moreover, in the particular case of polystyrene, $^1\text{H-NMR}$ spectroscopy could also provide the extent of end-group functionalization, since the Z and R signals could be integrated separately. This verification is important for the block extension step, since a lack of active end-group would prevent some of the macroCTA to polymerize further and lead to mixture of triblock and primary polystyrene block in the final product. Within the experimental precision, a virtually complete preservation of end groups (ratio Z/R=1) was found for the synthesized polystyrenes.

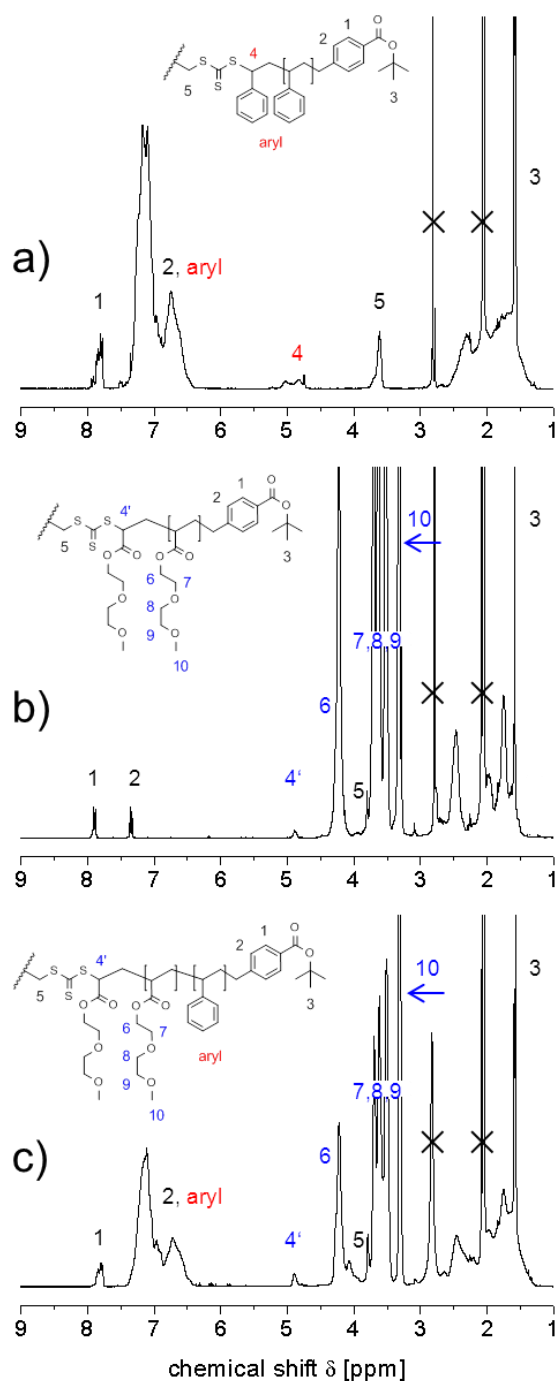


Figure 2.5: ^1H -NMR spectra of a) PS_{16} , b) PMDEGA-53a and c) PS8-PMDEGA53-PS8 in acetone- d_6 . Signals marked by “x” originate from the solvent and water.

The characterization of PMDEGA containing homo- and co-polymers proceeded in a similar way. As seen in Figure 2.5.b and c, the aromatic signal of the benzoate moieties (signal 1) is also well-resolved from the typical signals of the PMDEGA repeat units (signals 6-10). By integration of the signal 1 and the signal 10, the number average molar mass M_n was derived. Noteworthy, signal 5 resulting from the central ethylene moiety is still visible in ^1H spectra of both homo- and co-

polymers, but is partially overlapped by signals coming from PMDEGA repeating units. Thus in the case of homo- and co-polymers made with PMDEGA, the conservation of the RAFT active end-groups cannot be quantified by $^1\text{H-NMR}$. This cross-check could be extremely informative, as it allows the detection of a possible loss of the central trithiocarbonates, which is difficult by other methods. In fact, any disappearance of the absorption signal may indicate a cleavage of the triblock or the star copolymer into two or three diblock copolymers with presumably different properties. Although such a cleavage is considered rather improbable, it was recently reported to occur in cyclic ether solvents, such as the commonly used tetrahydrofuran.^{4, 21} In an attempt to verify the conservation of the trithiocarbonate and thus of the Z group, a complementary characterization method was therefore developed, based on the strong absorbance of the thiocarbonylthio moiety in the UV-vis range.

2.4. Characterization by UV-vis spectroscopy

2.4.1. Factors influencing the absorption

The thiocarbonylthio moiety is naturally present in all polymers made by RAFT. Due to an allowed $\pi\text{-}\pi^*$ transition, the group is a strong chromophore, with a molar absorptivity ϵ well above $10\,000\text{ L}\cdot\text{mol}^{-1}\cdot\text{cm}^{-1}$ at about 300 nm in the UV region.⁵ It was therefore interesting to utilize the group as a natural label for polymer characterization. Indeed, if the molar absorptivity ϵ of the chromophore is known, and if it is assumed that exactly one trithiocarbonate moiety is present in every polymer chain, the number average molar mass of polymer can be derived. The concentration of the trithiocarbonate chromophore in a solution, and thus the polymer concentration, can be calculated using the Lambert-Beer's law:

$$c = A / (l \times \epsilon) \quad (\text{eq. 1})$$

$$\text{with } c \text{ defined as: } c = m / (M_n \times V) \quad (\text{eq.2})$$

Here, c is the molar concentration of the polymer, A is the experimentally determined absorbance of the sample, l is the path length of the cell in cm, ϵ is the molar absorptivity in $\text{L}\cdot\text{mol}^{-1}\cdot\text{cm}^{-1}$, m is mass of the polymer, M_n is the number average molar mass, and V is the volume of the solvent. The calculated value of c is directly converted into the value of M_n of the polymer sample by combining eqs. 1 and 2 into eq.3 with the experimental values of m and V .

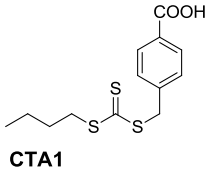
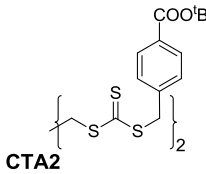
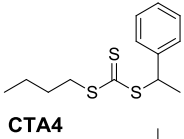
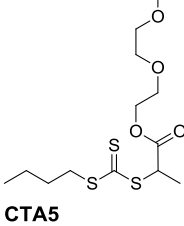
$$M_n = (m \times l \times \epsilon) / (A \times V) \quad (\text{eq. 3})$$

Therefore, if the trithiocarbonate Z-group is fully preserved in the polymer, the molar mass calculated by UV-vis, based on the Z-group as internal standard should match the one determined by $^1\text{H-NMR}$, based on the R-group as internal standard. In contrast, a higher value of

M_n derived from UV-vis compared to the one derived from $^1\text{H-NMR}$ will be a strong indicator of trithiocarbonate loss. The method is simple and does not require elaborated equipment; yet the obvious problem consists in the determination of the polymer absorption coefficient ϵ . In the rare publications employing UV-vis as characterization method,²²⁻²⁴ the coefficient of the primary CTA was taken as polymer coefficient in the Lambert-Beer's equation. However, it is questionable if the two coefficients are indeed equal, since the substitution pattern of the thiocarbonylthio moiety can notably change in the course of the polymerization when the R-group is replaced by the growing polymer chain.²⁵

In her PhD thesis, Katja Skrabania addressed the problem, by carrying out an extensive spectral analysis of a large set of dithioester and trithiocarbonate RAFT agents.²⁶ The goal was to determine the influence of the trithiocarbonate substitution on the values of λ_{max} and ϵ . She found that the values were affected by both the substitution pattern and the solvent in which the coefficient was measured. As a continuation, in this work spectral data of 4 supplementary CTAs (**CTA1**, **CTA2**, **CTA4** and **CTA5**) are reported. The 4 CTAs were all functionalized with alkylsulfanyl motifs as Z-group but had different R groups. **CTA1** and **CTA2** were designed for polymer synthesis, and functionalized with benzyl R groups, while the R groups of **CTA4** and **CTA5** were specifically designed to imitate the substitution pattern of respectively polystyrene and **PMDEGA** (Table 2.1). The substituents were thus ethylbenzyl for the **PS** model **CTA4** and 2-(2-methoxyethoxy)ethyl propionyl for the **PMDEGA** model **CTA5**. The spectroscopic data, summarized in Table 2.1, were collected in dichloromethane and acetonitrile for all CTAs and additionally in benzene for **CTA4** and **CTA5**. Note that the absorption coefficient of the bifunctional **CTA2**, bearing 2 trithiocarbonate moieties, must be divided by 2 for meaningful comparison.

Table 2.1: Molar absorptivities ϵ and maximum absorption wavelengths λ_{\max} of the studied trithiocarbonates in various solvents.

CTAs	ϵ [$\text{L}\cdot\text{mol}^{-1}\cdot\text{cm}^{-1}$]			λ_{\max} [nm]		
	C_6H_6	CH_2Cl_2	CH_3CN	C_6H_6	CH_2Cl_2	CH_3CN
 CTA1	- ^a	16800	16500	- ^a	308	307
 CTA2	- ^a	34000	- ^b	- ^a	309	- ^b
 CTA4	18000	16400	16200	312	312	308
 CTA5	15200	13900	14000	308	308	305

a) not determined; b) insufficient solubility; c) **CTA4** was additionally analysed in hexane ($\epsilon = 18600$, $\lambda_{\max} = 308$) and in butyl acetate ($\epsilon = 17500$, $\lambda_{\max} = 312$)

While for the 4 CTAs the values of λ_{\max} were roughly at the same wavelength (305 to 312 nm), the values of the molar absorptivities ϵ ranged between 13 900 and 18 600 $\text{L}\cdot\text{mol}^{-1}\cdot\text{cm}^{-1}$. The first reason of this variation was the substitution pattern: when the substitution was similar as in **CTA1**, **CTA2** and **CTA4** all bearing a benzyl or ethylbenzyl moieties, so were the values of ϵ ($\approx 16\,700$ $\text{L}\cdot\text{mol}^{-1}\cdot\text{cm}^{-1}$ as measured in dichloromethane). However in the case of **CTA5**, bearing an ester substitution, a notably lower ϵ value of about 13 900 $\text{L}\cdot\text{mol}^{-1}\cdot\text{cm}^{-1}$ was found. Additionally, the solvent had a strong influence on all absorption coefficient ϵ . For example in the case of **CTA4**, ϵ was as high as 18 000 and 18 600 $\text{L}\cdot\text{mol}^{-1}\cdot\text{cm}^{-1}$ in respectively benzene and hexane, and dropped to 16 400 and 16 200 $\text{L}\cdot\text{mol}^{-1}\cdot\text{cm}^{-1}$ in dichloromethane and acetonitrile. Unfortunately, no clear correlation could be observed between the variations of ϵ and the solvent polarity. Still, the results indicate the necessity to analyze the polymer in the same solvent as the one used for the determination of the coefficient ϵ . Additionally, since variations were also detected between the coefficients ϵ of the primary CTAs and the model **CTA5**, for a better UV-vis analysis, the use of the spectral data derived from a low mass molecular analog of the polymer's chain-end seems recommended. When having the same substitution pattern as the polymer to be analyzed, the model compound should exhibit, within the experimental error, a nearly identical molar absorptivity to the one of the polymer.

2.4.2. Analysis of homopolymers

To verify the validity of this hypothesis, molar masses derived from UV-vis end group analysis were compared, for a range of polymers, to values obtained from other methods such as SEC and $^1\text{H-NMR}$. Polystyrene served as a first model system by virtue of its easy characterization by SEC using polystyrene standards. As previously mentioned, the end-group conservation could be verified by $^1\text{H-NMR}$ analysis and within experimental precision, a complete preservation of end groups (ratio Z/R=1) was found.

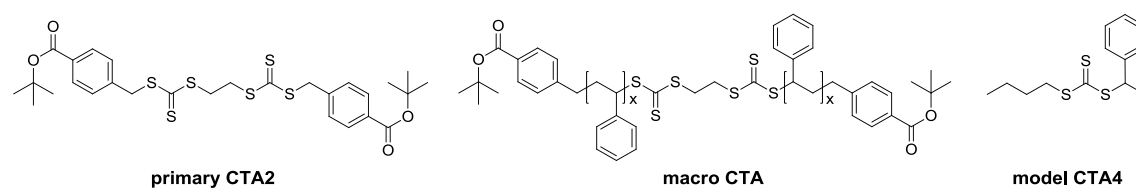


Figure 2.6: Structural comparison of the benzyltrithiocarbonate end groups in low molar mass RAFT agents **CTA2**, **CTA4**, and in a polystyrene macro CTA.

The molar masses derived from UV-vis analysis, using the molar absorptivity of the model RAFT agent **CTA4** (Figure 2.6.), match closely the values for the number average molar mass M_n obtained by $^1\text{H-NMR}$ and SEC. This demonstrates the general usefulness of the trithiocarbonate moiety as inherent polymer end-group label. In this particular example, the results in Table 2.1 are equally good if the molar absorptivity ϵ of the model RAFT agent, here **CTA4**, is used for the calculation, or the ϵ value of the RAFT agent originally engaged, here **CTA2**, as both values are very close (Cf Table 2.1).

Table 2.2: Analytical data of the **PS** homopolymers, made in presence of **CTA2**.

polystyrene ^a	molar mass M_n [g/mol], according to analysis via				
	λ_{\max} (nm)	UV-vis in CH_2Cl_2 ^b	$^1\text{H-NMR}$ ^c	SEC ^d	PDI ^d
PS16	315	2100	2200	2300	1.09
PS30	314	3900	3700	3500	1.17

a) numbers indicate the number average degree of polymerization DP_n according to c); b) by UV-vis analysis in CH_2Cl_2 using the absorption coefficient ϵ of $16400 \text{ L}\cdot\text{mol}^{-1}\cdot\text{cm}^{-1}$ of the model agent **CTA4**; c) by $^1\text{H-NMR}$ analysis in acetone d_6 , using the integrals of aromatic end-group signal and of the aryl signals of the constitutional repeat unit; d) in THF, RI detection, calibrated with polystyrene standards.

In the following, the importance of choosing the appropriate reference for the ϵ value to enable accurate end-group quantification is exemplified. Upon polymerization of methoxy diethylene glycol acrylate (MDEGA) in the presence of RAFT agents **CTA1** or **CTA2**, the substituent of the trithiocarbonate group changes from a primary to a secondary alkyl group, as the original benzyl R group is transformed into an acrylic chain end (Figure 2.7). **CTA5** is the model compound representing this transformation. According to Table 2.1, the molar absorptivities of the π - π^* -transition at λ_{\max} deviate by nearly 20%, with **CTA1** ($\epsilon = 16800 \text{ L}\cdot\text{mol}^{-1}\cdot\text{cm}^{-1}$) and **CTA2** ($\epsilon/2 = 17000 \text{ L}\cdot\text{mol}^{-1}\cdot\text{cm}^{-1}$) having a stronger absorbance band than **CTA5** ($\epsilon = 13900 \text{ L}\cdot\text{mol}^{-1}\cdot\text{cm}^{-1}$). Consequently, if the molar absorptivity of the engaged RAFT agent is used for determining the molar masses of PMDEGA, the concentration of end groups is underestimated, resulting in the overestimation of the true molar mass.

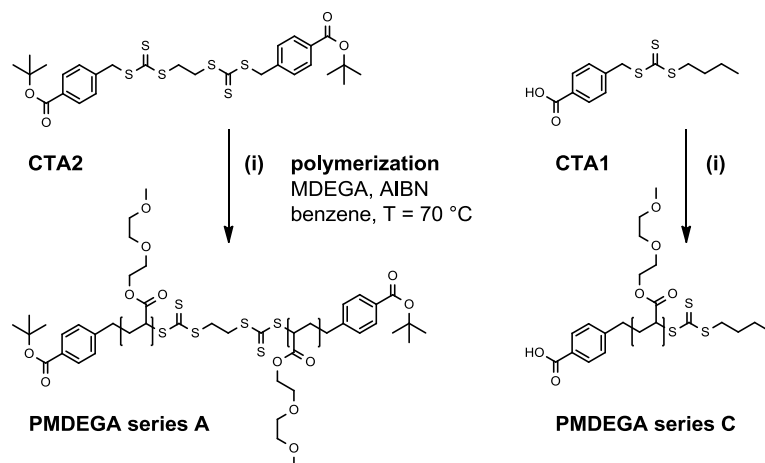


Figure 2.7: Synthesis of PMDEGA homopolymers of series A and C using functional RAFT agents.

To demonstrate this problem, Table 2.3 summarizes the characterization data of a range of poly(methoxy diethylene glycol acrylate)s **PMDEGA-a** made with **CTA2** and **PMDEGA-c** made with **CTA1** (Figure 2.7). For the series **PMDEGA-c**, the molar masses values resulting from UV-vis were determined in both acetonitrile and dichloromethane. Only acetonitrile was used for series **PMDEGA-a**. The values resulting from $^1\text{H-NMR}$, UV-vis and SEC characterizations were compared.

The excellent agreement between the values derived from $^1\text{H-NMR}$ data and UV-vis data using the molar absorptivity of the model **CTA5** demonstrates once again the sturdiness of the latter

characterization technique. Noteworthy, the M_n values derived from independent UV-vis measurements in dichloromethane and acetonitrile for the series **PMDEGA-c** were found identical within 6%. Thus, the experimental precision of UV-vis characterization under normal conditions was as good as the one generally observed in $^1\text{H-NMR}$. In contrast, M_n values calculated with the primary RAFT agent (**CTA1**) absorption coefficient ϵ , illustrate the apparent increase of M_n by using an inappropriate ϵ . The deviations are not catastrophic, still, there are notable. Therefore, precise end-group analysis through UV-vis, favorably requires the spectral data of a structurally closely related model compound. This may be possible by the generation a pool of data, providing the correct absorptivities for identical monomer-Z group combinations. In the work published by Skrabania, Miasnikova et al.,²⁷ the absorptivities of several model compounds suited for common polymers such as polystyrenes, poly(meth)acrylates, polyacrylates and polyacrylamides were already reported.

Table 2.3: Analytical data of the **PMDEGA** homopolymers prepared.

		molar mass M_n [g/mol], according to analysis via							
		UV-vis in CH_2Cl_2		UV-vis in CH_3CN		$^1\text{H-NMR}$	SEC		
CTAs	PMDEGA ^a	λ_{max}	ϵ CTA1 ^b	ϵ CTA5 ^c	ϵ CTA1 ^d	ϵ CTA5 ^e	M_n^f	$M_n^{\text{app g}}$	PDI ^g
CTA1	PMDEGA-24c		4900	4100	4950	4200	4500	2500	1.39
	PMDEGA-39c		7550	6250	7500	6500	7100	5100	1.25
	PMDEGA-87c		18600	15400	17300	14700	15400	9900	1.28
	PMDEGA-337c		64800	53600	67400	57200	59000	35200	1.44
CTA2	PMDEGA-53a				10400	8800	9900	9400	1.26
	PMDEGA-118a				21800	18500	21200	13400	1.32
	PMDEGA-153a				31100	26400	27300	14500	1.27
	PMDEGA-513a				100200	85000	90000	36400	1.31

a) numbers indicate the number average degree of polymerization DP_n according to f); b) by UV-vis analysis in CH_2Cl_2 using the absorption coefficient ϵ of $16500 \text{ L}\cdot\text{mol}^{-1}\cdot\text{cm}^{-1}$ of primary RAFT agent **CTA1**; c) by UV-vis analysis in CH_2Cl_2 using the absorption coefficient ϵ of $13900 \text{ L}\cdot\text{mol}^{-1}\cdot\text{cm}^{-1}$ of the model RAFT agent **CTA5**; d) by UV-vis analysis in CH_3CN using the absorption coefficient ϵ of $16800 \text{ L}\cdot\text{mol}^{-1}\cdot\text{cm}^{-1}$ of primary RAFT agent **CTA1**; e) by UV-vis analysis in CH_3CN using the absorption coefficient ϵ of $14000 \text{ L}\cdot\text{mol}^{-1}\cdot\text{cm}^{-1}$ of the model RAFT agent **CTA5**; f) by $^1\text{H-NMR}$ analysis in acetone d_6 , using the integrals of aromatic end-group signal and of the CH_3O - signal of the constitutional repeat unit; g) in DMF, RI detection, calibrated with polystyrene standards.

Additionally, apparent number average molar masses, M_n^{app} , were determined by SEC relative to polystyrene standards. Note, that those values were systematically lower than molar mass values measured by the other methods, the discrepancy increasing with M_n . The finding goes along with similar discrepancies observed for PMDEGA synthesized by nitroxide mediated polymerization ($M_n = 13600$ g/mol by $^1\text{H-NMR}$ but $M_n^{\text{app}} = 9200$ g/mol by SEC),⁵ as well as for poly(oligo (ethylene glycol) monomethyl ether methacrylate) polymers.²⁸ As the hydrodynamic volumes of linear and comb-like polymers can strongly diverge for identical molar masses,^{23, 29, 30} the differences of M_n^{app} obtained by SEC and M_n obtained by other methods are not surprising. Still, some comparisons of M_n^{app} of PMDEGA measured by SEC and M_n values derived from $^1\text{H-NMR}$ spectroscopy reported excellent agreement,²⁹ or only slight deviations.³¹ It is not clear for the moment, whether those matching values are due to better analytical equipment or are the result of a pure coincidence. In any case, SEC analysis was only employed to verify the monomodal molar mass distribution of the polymers, while the M_n values used in the following discussions were derived from $^1\text{H-NMR}$ end-group analysis.

2.4.3. Analysis of block copolymers

Finally the different characterization techniques were applied to the series of block copolymers, namely to diblock BA, triblock BAB and 3-arm star $(\text{AB})_3$. As already mentioned, a particular interest was taken in cross-checking the M_n values obtained from $^1\text{H-NMR}$ analysis, based on the R-groups, with the M_n values resulting from the end-group analysis via UV-vis spectroscopy, exploiting the thiocarbonyl chromophore of the Z-groups. Additionally, the values were compared with theoretically expected M_n derived from gravimetry. For diblock copolymers a good agreement was observed between the 3 methods. Still, for star and triblock copolymers, it was noted that M_n values derived from UV-vis analysis in dichloromethane were 10 to 20 % lower than the values derived from $^1\text{H-NMR}$ analysis. The UV-vis analysis was repeated on triblock polymers in different solvents such as acetonitrile and benzene, and gave the same underestimation. Any loss of trithiocarbonyl moieties during polymerization should, however, result in an overestimation of the molar mass. Therefore, these findings cannot be explained by a possible loss of trithiocarbonate Z groups. Also, neither $^1\text{H-NMR}$ nor SEC analysis gave any indication for a contamination by a low molar mass chromophore in the sample. Possibly, as the absorption coefficient ϵ of the thiocarbonyl group is known to vary notably with the environment,⁵ the specific triblock and star architecture with the Z-groups in the polymer center affects their local environment and thus the absorptivity of the chromophore in these particular polymer. However at the moment, no definitive explanation for these observations can be provided.

The molar mass of the block copolymers was also analyzed by SEC in the non-selective eluent dimethylformamide. All polymers showed a monomodal molar mass distribution and relatively low polymer dispersity ($M_w/M_n < 1.5$, Table 2). As in the case of the PMDEGA homopolymers, M_n^{app} values derived from SEC and M_n values determined by end-group analysis differ notably, for the reasons discussed above.

Table 2.4: Analytical data of the diblock, triblock and 3-arm star PS-PMDEGA block copolymers

architecture	polymers ^{a)}	molar mass [g·mol ⁻¹]				PDI ^{e)} M _w /M _n
		theoret. M _n ^{theo b)}	end-groups M _n ^{c)} M _n ^{d)}		SEC M _n ^{app e)}	
diblock	PS11		1500		1300	1.14
copolymer BA	PS11-PMDEGA101	16000	18900	16700	12100	1.27
	PS11-PMDEGA172	27000	31300	30400	14900	1.32
	PS11-PMDEGA275	36700	49100	47000	33200	1.29
	PS11-PMDEGA331	54800	59000	74700	42800	1.32
	PS11-PMDEGA513	74100	90700	84600	31300	1.48
triblock	PS16		2200		2300	1.09
copolymer BAB	PS8-PMDEGA41-PS8	11100	9800	7800	7900	1.17
	PS8-PMDEGA53-PS8	12300	11500	8700	8900	1.15
	PS8-PMDEGA93-PS8	18700	18500	16100	15600	1.17
	PS8-PMDEGA180-PS8	34900	33600	28400	23900	1.17
	PS8-PMDEGA337-PS8	61000	61300	48800	30000	1.30
	PS8-PMDEGA452-PS8	79900	81000	62400	40900	1.30
	PS8-PMDEGA659-PS8	118600	117000	107400	48800	1.42
3-arm star	PS23		3550		3300	1.19
copolymer (AB) ₃	(PMDEGA78-PS8)_{3X}	43600	44500	35400	23600	1.31
	(PMDEGA231-PS8)_{3X}	120800	123800	91600	51400	1.32

a) numbers indicate the number average degree of polymerization DP_n according to c); b) conversion determined by gravimetry; c) by ¹H-NMR analysis in acetone d₆, using the integrals of aromatic end-block signal and of the CH₃O- signal of the constitutional repeat unit ; d) by UV-vis analysis in CH₂Cl₂ using the absorption coefficient ϵ of 13900 L·mol⁻¹·cm⁻¹ of model RAFT agent: 2-(n-butylsulfanylthiocarbonylsulfanyl)-propionic acid 2-(2-methoxy-ethoxy)-ethyl ester **CTA5**; e) in DMF, RI detection, calibrated with polystyrene standards

2.5. Deprotection of *tert*-butyl end-groups

The cleavage of the *tert*-butyl ester end groups of the polymers was attempted by applying trifluoroacetic acid (TFA) in dry dichloromethane. This method has been well established for the selective deprotection of polymeric *tert*-butyl esters in the presence of primary ester groups, e.g. for making poly(acrylic acid) or poly(methacrylic acid) blocks.³² TFA catalyzed selective cleavage of the *tert*-butyl esters was also reported specifically in presence of poly(PEG acrylate)s synthesized by RAFT polymerization, and did not show any side reactions.³³⁻³⁵

The efficiency of the deprotection method was first tested on the low molar mass model **CTA2** bearing two *tert*-butyl ester termini. In this case, a 2-fold excess of TFA to *tert*-butyl ester group was sufficient to quantitatively deprotect the RAFT agent at room temperature overnight, without any loss of trithiocarbonate moiety.

Next, the same procedure was applied to bifunctional and trifunctional polystyrenes (**PS18** and **(PS9)_{3X}**) synthesized respectively in the presence of **CTA2** and **CTA3**. The reactions conditions were varied in order to determine a minimum amount of TFA needed to complete the deprotection. (Benítez-Montoya, Advanced Laboratory Report) This time, a 2-fold excess of TFA to *tert*-butyl ester group was not sufficient to quantitatively deprotect the polymers. However, when a 4-fold excess of TFA was applied in an overnight reaction, the ¹H-NMR analysis revealed the complete disappearance of the *tert*-butyl signals, and a small shift of the aromatic R-group signals (Figure 2.8.). Noteworthy, besides the transformation of *tert*-butyl ester groups to carboxylic acid groups, no other modifications of the polymer was detected by ¹H-NMR. The same was true for increased 8-fold amount of TFA and prolonged 3 days reaction; no cleavage of trithiocarbonate or of the star ester core was detected. The reaction was therefore found safe, for both linear and star architectures.

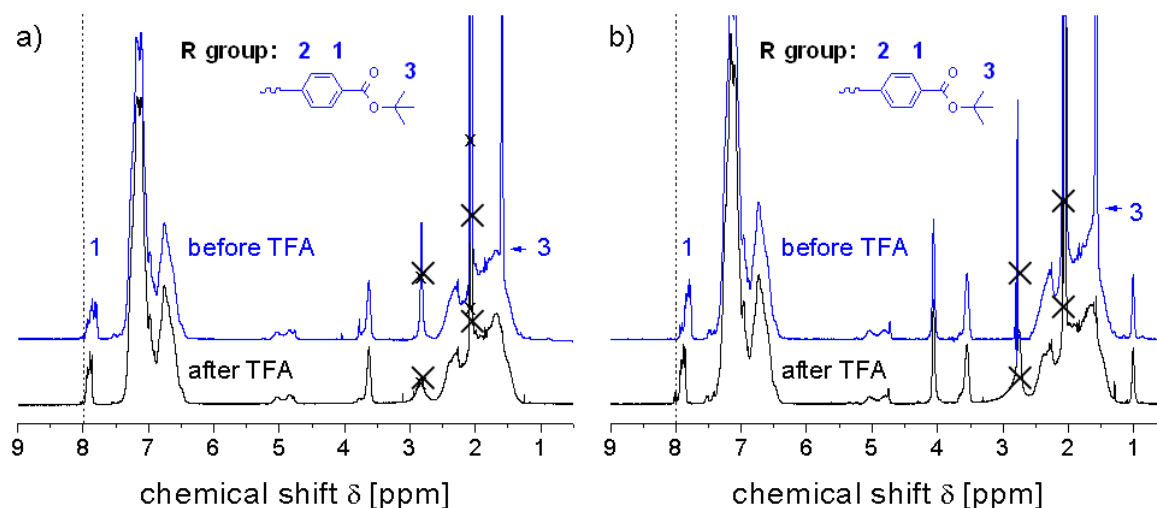


Figure 2.8: $^1\text{H-NMR}$ spectra in acetone d_6 of two polystyrenes before (blue line) and after (black line) deprotection by TFA; a) bifunctional **PS16** b) trifunctional (**PS8**) $_{3X}$. Signals marked by “x” originate from acetone and water.

When applied on the bifunctional **PMDEGA-371a**, the analogous deprotection procedure did not yield any free carboxylic groups up to a 10-fold excess of TFA over the *tert*-butyl ester end groups. Note that the $^1\text{H-NMR}$ signals of the aromatic protons in ortho-position to the carboxyl group are sensitive to esterification, as $-\text{COOH}$ substitution induced a chemical shift of 7.97 ppm compared to a shift of 7.89 ppm of the *tert*-butyl ester precursor. Accordingly, the evolution of these specific signals was used to verify the quantitative conversion at the end of the reaction. From ^1H analysis, a 130-fold excess of TFA resulted only in a 74 % of deprotection as determined by $^1\text{H-NMR}$, while a comparable stoichiometry sufficed to completely convert the shorter polymers **PMDEGA-28a**, **PMDEGA-53a**, and **PMDEGA-82a** to the benzoic acid end-capped products. Finally, a 400-fold excess was deliberately applied to achieve complete deprotection of the two carboxyl end-groups of **PMDEGA-371a**. Considering the fact that lower amounts of TFA were sufficient for complete deprotection of low molar mass **CTA2** and of the relatively small polymers, the degree of polymerization (DP_n) of PMDEGA seems to affect the deprotection efficiency. Importantly, neither $^1\text{H-NMR}$ nor UV-vis analysis gave any evidence for side reactions of the primary ester groups, or of the trithiocarbonate moieties after exposure to the TFA reaction mixtures, thus corroborating the selectivity of the deprotection method. Note in particular in Figure 2.9, that the small signal at 4.9 ppm, indicative of the $-\text{CH}(\text{COOR})-\text{S}-\text{C}(=\text{S})-\text{S}-$ methine moiety of the active chain ends is preserved.

The increasing quantities of TFA needed for efficient deprotection with increasing molar mass of the polymers might be explained by hydrogen bonding between the ether groups of the EG units and the carboxylic acid group of TFA. This would reduce the concentration of free protons in dichloromethane drastically, and render the catalytic cleavage of the *tert*-butyl ester end-groups ineffective. The strong interaction between carboxylic acid groups and PEG fragments units at low pH values has been described at several occasions.³⁶ In order to ensure the complete transformation of the *tert*-butyl ester groups, a large excess of TFA was added to the polymer solutions in CH₂Cl₂, and removed afterwards by freeze drying the TFA/polymer mixture in benzene.

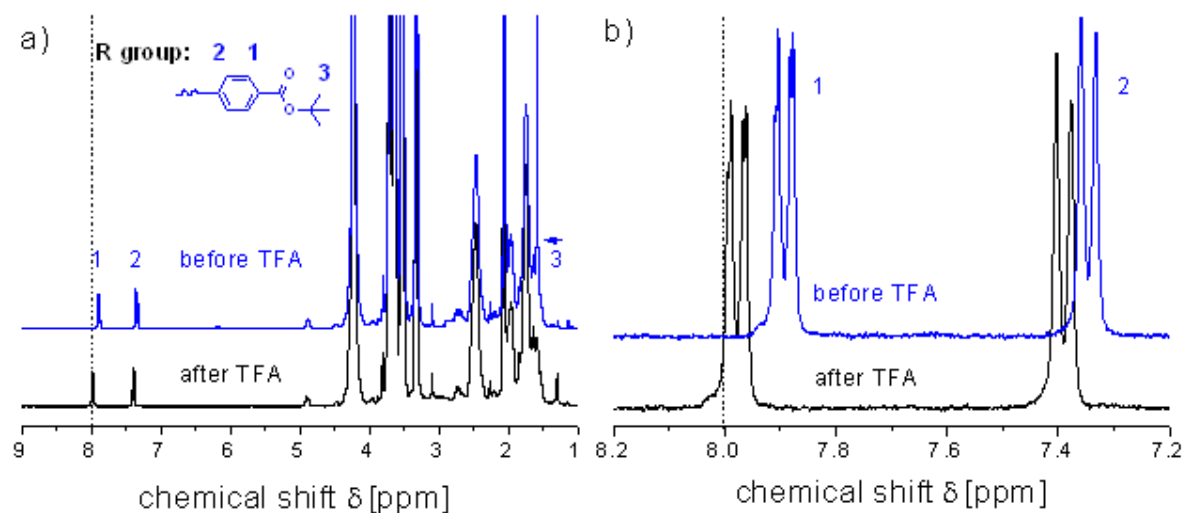


Figure 2.9: a) Exemplary ¹H-NMR spectra of polymer **PMDEGA-82a** before (blue line) and after (black line) the removal of the *tert*-butyl end groups. Note the disappearance in the series B of the *tert*-butyl singulet (3) and the shift of the aromatic R-group signals (1&2). b) Enlarged aromatic proton region of the same spectra, showing the resulting signal shift and indicating complete deprotection.

2.6. Functionalization of block copolymers with a rhodamine fluorophore

The telechelic block copolymers were next functionalized with a rhodamine fluorescent dye. The aim of the work was twofold, first to verify experimentally the possibility to further modify the benzoic acid end-group of PMDEGA polymers, second to produce fluorescent polymers suited for fluorescence correlation spectroscopy (FCS) analysis. Indeed, the technique should allow to determine the critical micelle concentration (CMC) and the micelle hydrodynamic radius of

amphiphilic block copolymers in water. Traditionally this information has been obtained by mixing the amphiphilic polymer with a hydrophobic dye such as pyrene.³⁷ As water insoluble dyes preferentially solubilize in the hydrophobic core, the diffusion coefficient of the trapped dye can be taken as equal to the diffusion coefficient of the micelle. The hydrodynamic radius is derived from the latter. However, it was recently reported, that hydrophobic dyes can exchange between the hydrophobic core and the aqueous medium. This leads to an overestimation of the micelle diffusion coefficient and to an underestimation of its hydrodynamic radius.³⁸⁻⁴⁰ Obviously, a covalent link between the dye and the polymer allows to avoid the problem.

An accurate use of FCS requires very low but constant concentration of fluorescent dye (1 μM), whereas the concentration of amphiphilic block copolymers has to be varied in a range of several orders of magnitude to investigate their complex phase behavior.⁴¹ Therefore in order to adjust the two concentrations, the labeled polymer has to be mixed with an identical non-labeled polymer in different proportions.⁴² The concentration of the labeled polymer, and therefore of the dye can thus be kept constant, while the overall polymer concentration, adjusted by the unlabeled polymer is allowed to vary. By introducing the dye in a post polymerization step, a pair of labeled and unlabeled, structurally identical block copolymers can be made.

In order to produce rhodamine functionalized block copolymers, the following synthetic pathway was chosen: the polystyrene macroCTA was synthesized using **CTA1**, **CTA2** or **CTA3**. In the case of polymers with *tert*-butyl termini, the deprotection reaction was conducted on the polystyrene in dichloromethane, then the macroCTA bearing benzoic acid termini was copolymerized with MDEGA. Finally, the resulting block copolymers were reacted for 2 days with an excess of rhodamine B piperazine amide^{43, 44} adduct in the presence of *N*-hydroxysuccinimide (NHS) and ethyl (dimethylaminopropyl) carbodiimide (EDC). Unreacted rhodamine dye was removed by dialysis in water for over a week. Noteworthy, a piperazine linker was chosen to bind the fluorophore to the polymer. Although primary amines are more efficient to react with carboxylic acid moieties, they are also known to cleave the trithiocarbonate moiety into thiols.⁴⁵⁻⁴⁷ As in the triblock and the star architectures synthesized here, the trithiocarbonate is placed in the middle of the molecule; the less reactive secondary amine was chosen, in order to insure the conservation of the polymer during the functionalization reaction.

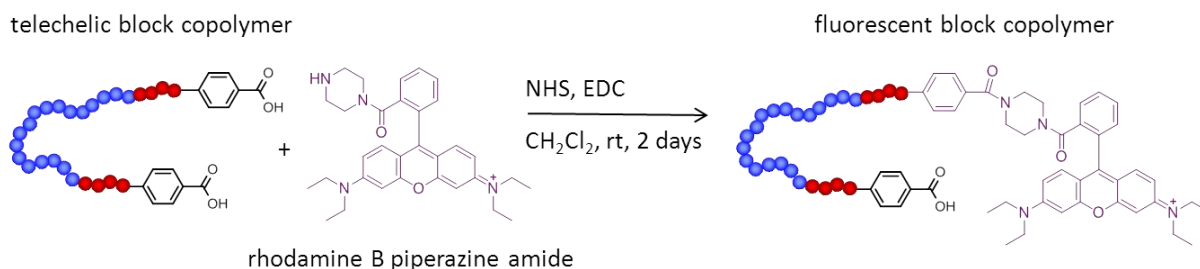


Figure 2.10: Synthesis of fluorescent block copolymers.

The characterization of the red fluorescent polymer was first conducted by GPC and thin layer chromatography to ensure the complete removal of unreacted rhodamine by dialysis from the polymer sample. No trace of low molar mass chromophore was detected by either of the methods, confirming the efficiency of work-up. Next, UV-vis analysis was used to determine the functionalization yield. The concentration of the trithiocarbonate chromophore in the solution, and thus the polymer concentration, can be calculated using the Lambert-Beer's law (eq.1). The concentration of rhodamine is given analogously by eq.4:

$$c_{\text{polymer}} = A_{\text{trithio}} / (l \times \epsilon_{\text{trithio}} \times f) \quad (\text{eq. 1})$$

$$c_{\text{rho}} = A_{\text{rho}} / (l \times \epsilon_{\text{rho}}) \quad (\text{eq.4})$$

Here, c is the molar concentration, A is the experimentally determined absorbance of the sample, l is the path length of the cell in cm, $\epsilon_{\text{trithio}}$ is the molar absorptivity of one trithiocarbonate moiety in $\text{L} \cdot \text{mol}^{-1} \cdot \text{cm}^{-1}$, ϵ_{rho} of the rhodamine chromophore and f the functionality of the polymer ($f = 1$ for a diblock, 2 for a triblock, 3 for a 3-arm star polymers). Since for every architecture, 100 % of end-groups functionalization correspond to $c_{\text{rho}} = f \times c_{\text{polymer}}$, the yield is given by eq. 5:

$$\text{functionalization yield} = c_{\text{rho}} / f \times c_{\text{polymer}} = (A_{\text{rho}} \times \epsilon_{\text{trithio}}) / (A_{\text{trithio}} \times \epsilon_{\text{rho}}) \quad (\text{eq. 5})$$

From previous investigations, $\epsilon_{\text{trithio}}$ was already determined as $13\,900 \text{ L} \cdot \text{mol}^{-1} \cdot \text{cm}^{-1}$ of the model RAFT agent **CTA5** in CH_2Cl_2 . The value of ϵ_{rho} was determined based on the low molar mass rhodamine B piperazine amide, and was found to be $76\,600 \text{ L} \cdot \text{mol}^{-1} \cdot \text{cm}^{-1}$ in CH_2Cl_2 with a λ_{max} of 562 nm. By using these two absorption coefficients in the equation 5, the yield of rhodamine functionalization could be determined. Figure 2.11 represents the exemplary UV-vis spectra of the rhodamine functionalized diblock polymer.

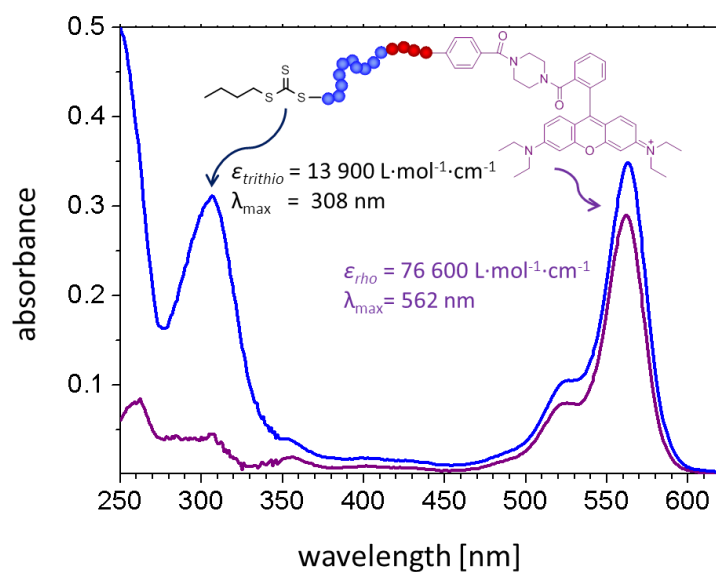


Figure 2.11: Exemplary UV-vis spectra in dichloromethane of the rhodamine B base piperazine (lilac line) and the rhodamine functionalized diblock PS10-PMDEGA167 (blue line).

The functionalization data of the diblock copolymer, the triblock copolymer **PS9-PMDEGA180-PS9** and the star copolymer **(PS9-PMDEGA219)₃** are given in Table 2.4. Different molar ratios of rhodamine B piperazine amide to benzoic acid end-group were used for the functionalization reaction. The reaction yield was always relatively low, with at best 20 % of functionalization achieved with a 10-fold excess of dye to end-groups. Thus, the reaction could not reach the click chemistry standards, however in all cases, the percentage of the functionalized chains was largely sufficient for FCS analysis.

Table 2.4: Rhodamine functionalization of telechelic block copolymers

polymers ^{a)}	n° of end-groups	[rho] _i / [-COOH] _i ^{b)}	[rho] _f / [-COOH] _f ^{c)}	average polymer ^{d)} functionalization
PS10-PMDEGA167	1	10.0	20.3	20.3
PS9-PMDEGA180-PS9	2	2.1	3.6	7.2
(PS9-PMDEGA219) ₃	3	3.1	5.3	16.0

a) numbers indicate the number average degree of polymerization DP_n according to $^1\text{H-NMR}$; b) initial molar ratio of rhodamine B base piperazine to polymer benzoic acid end-groups c) final molar ratio, or reaction yield, as determined by UV-vis analysis in CH_2Cl_2 using the absorption coefficient $\epsilon_{\text{trithio}}$ of 13900 $\text{L}\cdot\text{mol}^{-1}\cdot\text{cm}^{-1}$ of the model RAFT agent **CTAS** and the absorption coefficient ϵ_{rho} of 76600 $\text{L}\cdot\text{mol}^{-1}\cdot\text{cm}^{-1}$ of rhodamine B base piperazine; d) average degree of polymer chain functionalization derived from c)×number of end-groups.

2.7. Conclusion

In this chapter, the synthesis and characterization of benzoic acid and benzoic ester terminated polymers were described. The various **PMDEGA** based polymers were engineered by RAFT, with end-groups specifically chosen to improve polymer characterization by $^1\text{H-NMR}$ spectroscopy. Indeed, the aromatic protons of the benzoate moiety were found to provide characteristic signals in $^1\text{H-NMR}$ spectroscopy above 7 ppm, well-resolved from the typical signals of **PMDEGA**, and from the signals of **PS** to a certain extent. These enable the determination of number average molar masses M_n by comparing end-groups signals intensity with the intensity of characteristic **PMDEGA** signals. UV-vis spectroscopy was also performed on the homo- and block copolymers, based on the strong absorptivity of the inherent trithiocarbonate chromophore. Although the technique is well known, it is rarely used for the determination of M_n . For an optimal analysis, it was found most advisable to use the molar absorptivity values of low molar mass polymer analogues with a substitution pattern identical to the active polymer chain end, rather than the values of the primary RAFT agent employed for the polymerization. Furthermore, as the influence of the solvent on the trithiocarbonate absorptivity was found very strong, all measurements must be performed in the same solvent for meaningful analysis. If appropriate conditions are applied, and virtually full end group preservation is assured, the molar mass values obtained agree very well with the values determined by other methods.

Additionally, the potential of benzoic acid termini to undergo post-polymerization reaction was exploited. A straightforward approach to produce benzoic acid terminated polymers was successful for the synthesis of diblock copolymers using a benzoic acid terminated mono functional RAFT agent. A similar approach failed for the synthesis of symmetrical triblock and three arm star copolymers, due to a poor solubility of the bifunctional carboxylic acid terminated **CTA6** and an incompatible synthetic strategy for the trifunctional CTA. An indirect approach was developed for those polymers, using a protection-deprotection method. The telechelic block copolymers terminated by benzoic acid end-groups, were then functionalized with a rhodamine fluorophore, generating pairs of identical labeled and unlabeled polymers, most valuable for Fluorescence Correlation Spectroscopy analysis.

2.8. Acknowledgements

The experimental help of my internship students is gratefully acknowledged: Anne-Christin Stötzer for the first homopolymers synthesis and Carlos Adrián Benítez-Montoya for the deprotection of polystyrenes and the functionalization with rhodamine.

2.9. References

1. Theato, P. J. *Polym. Sci. Part A: Polym. Chem.* **2008**, 46, 6677-6687.
2. Barner-Kowollik, C.; ed., *Handbook of RAFT Polymerization*. Wiley-VCH: Weinheim (Germany), 2008.
3. Moad, G.; Rizzardo, E.; Thang, S. H. *Polym. Int.* **2011**, 60, 9-25.
4. Päch, M.; Zehm, D.; Lange, M.; Dambowsky, I.; Weiss, J.; Laschewsky, A. *J. Am. Chem. Soc.* **2010**, 132, 8757-8765.
5. Skrabania, K.; Miasnikova, A.; Bivigou-Koumba, A. M.; Zehm, D.; Laschewsky, A. *Polym. Chem.* **2011**, 2, 2074-2083.
6. Willcock, H.; O'Reilly, R. K. *Polym. Chem.* **2010**, 1, (2), 149-157.
7. Gregory, A.; Stenzel, M. H. *Prog. Polym. Sci.* **2012**, 37, 38-105.
8. Moad, G.; Rizzardo, E.; Thang, S. H. *Polymer* **2008**, 49, 1079-1131.
9. Legge, T. M.; Slark, A. T.; Perrier, S. *Macromolecules* **2007**, 40, 2318-2326.
10. Bivigou-Koumba, A. M.; Kristen, J.; Laschewsky, A.; Müller-Buschbaum, P.; Papadakis, C. M. *Macromol. Chem. Phys.* **2009**, 210, 565-578.
11. Gauthier, M. A.; Gibson, M. I.; Klok, H.-A. *Angew. Chem. Int. Ed.* **2009**, 48, (1), 48-58.
12. Binder, W. H.; Sachsenhofer, R. *Macromol. Rapid Commun.* **2008**, 29, (12-13), 952-981.
13. Gondi, S. R.; Vogt, A. P.; Sumerlin, B. S. *Macromolecules* **2007**, 40, (3), 474-481.
14. Duchateau, J.; Lutsen, L.; Guedens, W.; Cleij, T. J.; Vanderzande, D. *Polym. Chem.* **2010**, 1, (8), 1313-1322.
15. Inglis, A. J.; Sinnwell, S.; Stenzel, M. H.; Barner-Kowollik, C. *Angew. Chem.-Int. Edit.* **2009**, 48, (13), 2411-2414.
16. Jo, S.; Engel, P. S.; Mikos, A. G. *Polymer* **2000**, 41, (21), 7595-7604.
17. Lai, J. T.; Filla, D.; Shea, R. *Macromolecules* **2002**, 35, 6754-6756.
18. Wang, R.; McCormick, C. L.; Lowe, A. B. *Macromolecules* **2005**, 38, 9518-9525.
19. Wright, S. W.; Hageman, D. L.; Wright, A. S.; McClure, L. D. *Tetrahedron Lett.* **1997**, 38, (42), 7345-7348.
20. Strazzolini, P.; Misuri, N.; Polese, P. *Tetrahedron Lett.* **2005**, 46, (12), 2075-2078.
21. Subramanian, S.; Zaworotko, M. J. *Coord. Chem. Rev.* **1994**, 137, (0), 357-401.
22. Baussard, J.-F.; Habib-Jiwan, J.-L.; Laschewsky, A.; Mertoglu, M.; Storsberg, J. *Polymer* **2004**, 45, 3615-3626.
23. Mertoglu, M.; Laschewsky, A.; Skrabania, K.; Wieland, C. *Macromolecules* **2005**, 38, 3601-3614.
24. Kujawa, P.; Segui, F.; Shaban, S.; Diab, C.; Okada, Y.; Tanaka, F.; Winnik, F. M. *Macromolecules* **2006**, 39, 341-348.
25. Barner-Kowollik, C., In *Handbook of RAFT Polymerization*, Wiley-VCH Verlag GmbH & Co. KGaA: 2008.
26. Skrabania, K. The multifarious self-assembly of triblock copolymers: From multi-responsive polymers and multi-compartment micelles. Universität Potsdam, Potsdam, Germany, 2009.
27. Gruendling, T.; Pickford, R.; Guilhaus, M.; Barner-Kowollik, C. *J. Polym. Sci., Part A: Polym. Chem.* **2008**, 46, 7447-7461.
28. Hua, F.; Jiang, X.; Li, D.; Zhao, B. *J. Polym. Sci., Part A: Polym. Chem.* **2006**, 44, 2454-2467.
29. Holder, S. J.; Durand, G. G.; Yeoh, C.-T.; Illi, E.; Hardy, N. J.; Richardson, T. H. *J. Polym. Sci., Part A: Polym. Chem.* **2008**, 46, (23), 7739-7756.
30. Roth, P. J.; Jochum, F. D.; Forst, F. R.; Zentel, R.; Theato, P. *Macromolecules* **2010**, 43, 4638-4645.
31. Han, S.; Hagiwara, M.; Ishizone, T. *Macromolecules* **2003**, 36, 8312-8319.
32. Yamamoto, S.-I.; Pietrasik, J.; Matyjaszewski, K. *J. Polym. Sci., Part A: Polym. Chem.* **2008**, 46, 194-202.

33. Ritz, P.; Látalová, P.; Janata, M.; Toman, L.; Kríz, J.; Genzer, J.; Vlcek, P. *React. Funct. Polym.* **2007**, *67*, (10), 1027-1039.
34. Davis, K. A.; Matyjaszewski, K. *Macromolecules* **2000**, *33*, (11), 4039-4047.
35. Medel, S.; Manuel García, J.; Garrido, L.; Quijada-Garrido, I.; París, R. *J. Polym. Sci., Part A: Polym. Chem.* **2011**, *49*, (3), 690-700.
36. Jin, N.; Woodcock, J. W.; Xue, C.; O'Lenick, T. G.; Jiang, X.; Jin, S.; Dadmun, M. D.; Zhao, B. *Macromolecules* **2011**, *44*, 3556-3566.
37. Weberskirch, R.; Preuschen, J.; Spiess, H. W.; Nuyken, O. *Macromol. Chem. Phys.* **2000**, *201*, 995-1007.
38. Ohno, H.; Matsuda, H.; Tsuchida, E. *Makromol. Chem.* **1981**, *192*, 2267-.
39. Sukhishvili, S. A.; Granick, S. *J. Am. Chem. Soc.* **2000**, *122*, (39), 9550-9551.
40. Gohy, J.-F.; Willet, N.; Varshney, S.; Zhang, J.-X.; Jérôme, R. *Angew. Chem. Int. Ed.* **2001**, *40*, 3214-3216.
41. Bonné, T. B.; Papadakis, C. M.; Lüdtke, K.; Jordan, R. *Colloid Polym. Sci.* **2007**, *285*, 491-497.
42. Rutkaite, R.; Swanson, L.; Li, Y.; Armes, S. P. *Polymer* **2008**, *49*, (7), 1800-1811.
43. Nguyen, T.; Francis, M. B. *Org. Lett.* **2003**, *5*, 3245-3248.
44. Beija, M.; Afonso, C. A. M.; Farinha, J. P. S.; Charreyre, M.-T.; Martinho, J. M. G. *Polymer* **2011**, *52*, 5933-5946.
45. Shen, W.; Qiu, Q.; Wang, Y.; Miao, M.; Li, B.; Zhang, T.; Cao, A.; An, Z. *Macromol. Rapid Commun.* **2010**, *31*, (16), 1444-1448.
46. Qiu, X.-P.; Winnik, F. M. *Macromol. Rapid Commun.* **2006**, *27*, 1648-1653.
47. Roth, P. J.; Kessler, D.; Zentel, R.; Theato, P. *Macromolecules* **2008**, *41*, 8316-8319.

III Thermoresponsive behavior of PMDEGA polymers

Though the LCST of poly(methoxy diethylene glycol acrylate) PMDEGA is reported to be 37 °C¹ to 45 °C,² thus being close to body temperature range, PMDEGA has found surprisingly little interest so far, and reports on this polymer are rare.¹⁻⁵ Considering the discrepancy of the reported phase transition temperatures, it was interesting to look into the effect of various molecular parameters on the thermo-responsiveness of homopolymers as well as of block copolymers of MDEGA. First the influence of molar mass and hydrophilic or hydrophobic end groups on the thermo-responsive behavior of PMDEGA homopolymers was examined. Then, the influence of short hydrophobic polystyrene end-blocks (B blocks) was explored, in block copolymers of three different architectures, namely diblock AB, triblock BAB, and 3-arm star (BA)₃.

3.1. Thermoresponsive behavior of PMDEGA homopolymers

3.1.1. Synthetical strategy

The RAFT controlled polymerization was exploited to synthesize three series of well-defined PMDEGA homopolymers (in the following called series A, B and C), starting from two different CTAs, **CTA1** and **CTA2** as shown in Figure 3.1.

Polymer series A was prepared straightforward using the symmetrical bistrithiocarbonate as RAFT agent **CTA2**. The resulting polymers disposed of two identical *tert*-butyl benzoate end-groups and a central 1,2-bis(sulfanylthiocarbonyl sulfanyl) ethylene moiety (Figure 3.1). In order to vary the end-groups from hydrophilic to hydrophobic, a complementary set B was prepared via a post-polymerization step, transforming quantitatively the terminal *tert*-butyl ester groups into benzoic acid, i.e., carboxylic acid moieties. This strategy resulted in polymers series B with exactly the same molar mass and dispersity as polymers of series A, but with different, namely hydrophilic instead of hydrophobic, end-groups. **PMDEGA** homopolymers of series B were made by selective cleavage of the *tert*-butyl ester end groups of series A polymers, applying trifluoroacetic acid (TFA) in dichloromethane, as described in the Chapter 2.

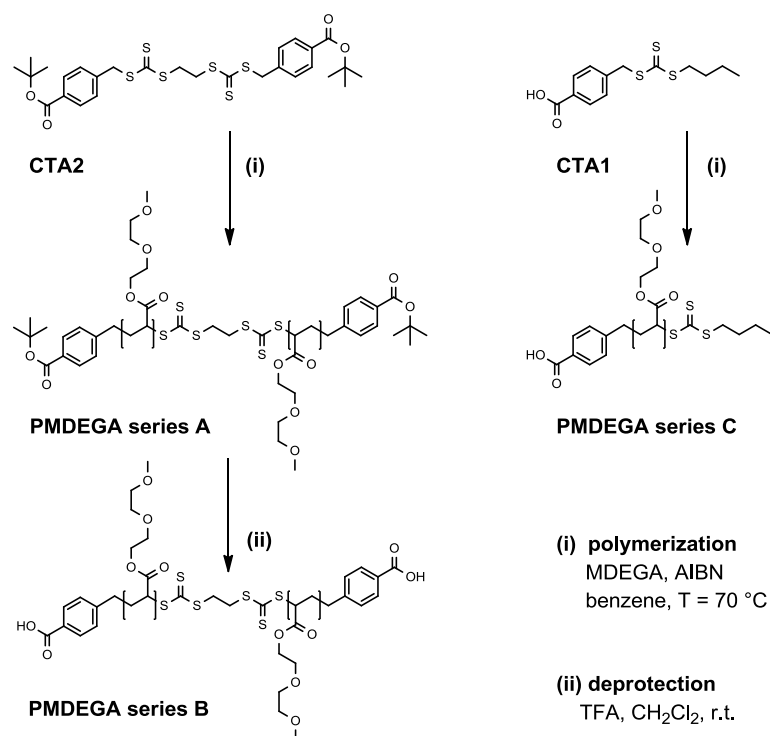


Figure 3.1: Synthesis of PMDEGA homopolymers of series A, B and C using functional RAFT agents.

To complete the library, polymer series C was made, by direct homopolymerization using the monofunctional non-symmetrical RAFT agent **CTA1**. Thus, polymers of series C bear a hydrophilic benzoic acid residue at one end, and a hydrophobic butylsulfanylthiocarbonylsulfanyl residue at the other end of the polymer chain. Table 3.1 lists the homopolymers produced.

Table 3.1: Analytical data of the **PMDEGA** homopolymers prepared.

CTAs used	polymers ^{a)}	molar mass [g·mol ⁻¹]				PDI ^{e)}	cloud point [°C] ^{f)}		
		theoret. M _n ^{theo b)}	end-groups M _n ^{c)}	SEC M _n ^{d)}	SEC M _n ^{app e)}		series A	series B	ΔCP ^{g)}
CTA2	series A								
	PMDEGA-28a	5500	5600	4900	4500	1.20	9.0	16.8	7.8
	PMDEGA-53a	9600	9900	8800	9400	1.26	24.5	30.5	6.0
	PMDEGA-82a	11500	14800	12400	9400	1.35	34.1	38.2	4.1
	PMDEGA-118a	18100	21200	18500	13400	1.32	37.0	40.4	3.4
	PMDEGA-153a	26200	27300	26400	14500	1.27	38.3	41.0	1.7
	PMDEGA-371a	61800	65300	56000	30400	1.47	40.8	41.0	0.2
PMDEGA-513a	91500	90000	85000	36400	1.31	41.2	42.0	0.8	

	polymers ^{a)}	$M_n^{\text{theo b)}}$	$M_n^{\text{c)}}$	$M_n^{\text{d)}}$	$M_n^{\text{app e)}}$	PDI ^{e)}	series C
CTA1	series C						
	PMDEGA-24c	4300	4500	4200	2500	1.39	18.0
	PMDEGA-39c	7000	7100	6500	5100	1.25	31.7
	PMDEGA-87c	14400	15400	14700	9900	1.28	41.8
	PMDEGA-123c	21900	22600	19100	14200	1.33	41.6
	PMDEGA-337c	65800	59000	57200	35200	1.44	41.8

a) numbers indicate the number average degree of polymerization DP_n according to c); b) conversion determined by gravimetry; c) by $^1\text{H-NMR}$ analysis in acetone d_6 , using the integrals of aromatic end-group signal and of the $\text{CH}_3\text{O-}$ signal of the constitutional repeat unit ; d) by UV-vis analysis in CH_3CN using the absorption coefficient ϵ of $14,000 \text{ L}\cdot\text{mol}^{-1}\cdot\text{cm}^{-1}$ of model RAFT agent **CTA5**: 2-(*n*-butylsulfanylthiocarbonylsulfanyl)-propionic acid 2-(2-methoxy-ethoxy)-ethyl ester; e) in DMF, RI detection, calibrated with polystyrene standards; f) by turbidimetry in water at concentration $3.0 \text{ g}\cdot\text{L}^{-1}$; g) difference between the cloud points of homologues of series A and B.

3.1.2. Behavior of the homopolymers in aqueous solution

To investigate the influence of molar mass on cloud points, a series of seven polymers with degrees of polymerization DP_n varying from 28 to 513 was prepared using **CTA2**, *i.e.*, all these polymers bear two hydrophobic *tert*-butyl benzoate end-groups (series A). Transmission versus temperature curves showed always a transition from clear solution to an opaque mixture upon heating (see Figure 3.2). The observed collapse transition of the polymers was fully reversible, exhibiting only a very small ($< 0.5 \text{ }^\circ\text{C}$) hysteresis in heating and cooling cycles (Figure 3.2). The cloud points (CP) of the various polymer samples showed a marked dependence on both molar mass, *i.e.* DP_n , and end-groups (Table 3.1, Figure 3.2). Also, it was noted that the temperature interval for the transition from clear to opaque ($< 1\%$ transmission) was relatively large for the smaller polymers, being $6 \text{ }^\circ\text{C}$ for **PMDEGA-28a** and $3 \text{ }^\circ\text{C}$ for **PMDEGA-53a**, but decreased to less than $1 \text{ }^\circ\text{C}$ for polymers with $DP_n > 100$ (Figure 3.2). This effect might be due to the polymers' dispersities: as the end-groups effect decreases with increasing molar mass, a given dispersity will affect the smallest polymers most, resulting in a broader collapse transition. Alternatively, the effect might be caused by a more cooperative collapse of bigger polymers with faster phase separation.⁶ The latter putative explanation is supported by previous similar observations on polymers, of which the cloud points were only weakly affected by the end-groups.^{7,8}

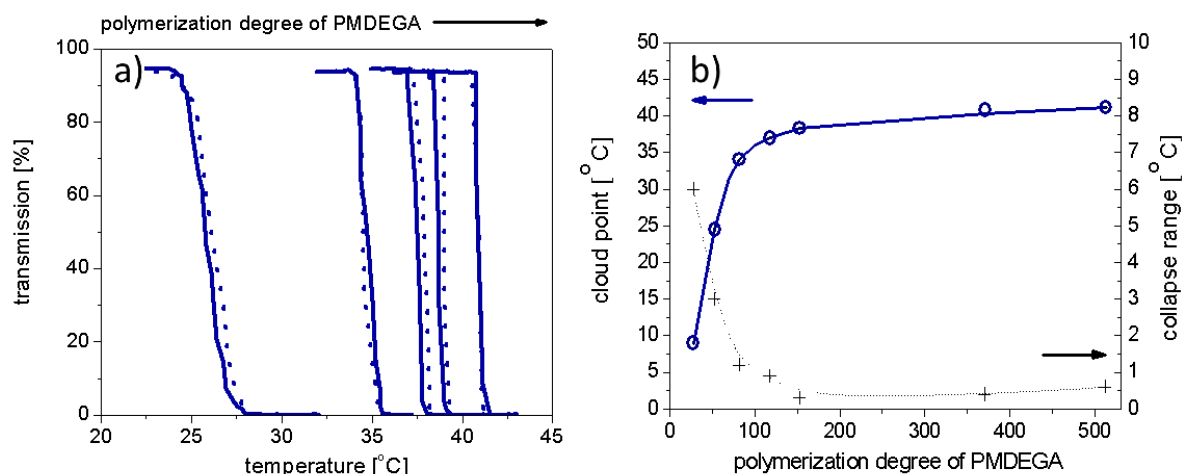


Figure 3.2: LCST-type behavior of PMDEGA series A ($3.0 \text{ g}\cdot\text{L}^{-1}$ polymer in water): a) transmittance as function of the temperature, heating (solid line) and cooling (dotted line) cycle at $1 \text{ }^\circ\text{C}\cdot\text{min}^{-1}$; b) corresponding cloud points and transition collapse range versus degree of polymerization DP_n . The lines are meant as guide to the eye.

Table 3.1 and Figure 3.2 demonstrate that the cloud points of all polymers of series A increase with DP_n . The evolution of the curve is particularly steep for low DP_n values; the cloud point being $9 \text{ }^\circ\text{C}$ for **PMDEGA-28a**, and $34 \text{ }^\circ\text{C}$ for **PMDEGA-82a**. For polymers exceeding $\text{DP}_n = 100$, the cloud point seems to approach asymptotically a maximum value, reaching a plateau value of $41\text{--}42 \text{ }^\circ\text{C}$.

Generally, the LCST of thermo-responsive polymers is expected to decrease with the molar mass, as the combinatorial entropy term of mixing becomes less favorable.^{9, 10} However, recent investigations draw a more complex picture and underline the important role of the hydrophobicity of end-groups in polymer-water interactions.^{9, 11-13} In fact, similar trends as observed here were reported for a series of PMDEGA terminated with hydrophobic 1-phenylethyl end-groups,¹ and for star branched PMDEGMA, terminated with the hydrophobic diphenylmethyl moiety.¹⁴ It is reasonable to expect that the hydrophobic *tert*-butyl benzoate end-group lowers the cloud point analogously, thus requiring high DP_n values to become negligible.

Still, to clarify possible end-group effects on the thermal phase transition, two additional series of PMDEGA were studied, replacing the hydrophobic *tert*-butyl benzoate end-groups by the hydrophilic benzoic acid group at both chain-ends in series B, or at one chain-end only in series C, which thus contains one hydrophobic and one hydrophilic end. Though specific reports on the effect of benzoate end groups are missing yet, polymers of 4-vinyl benzoic acid have been employed as pH-sensitive block for responsive block copolymers.¹⁵⁻¹⁷ While at the low pH of 3,

polymers were fully protonated and then behaved as hydrophobic blocks, at $\text{pH} > 5$, the carboxylic groups were sufficiently ionized to render the polymers water soluble.¹⁷ In deionized water equilibrated in air with naturally slightly acidic pH ($\text{pH} \approx 6$, as verified by pH test strip), the benzoic acid moiety of the PMDEGA of series B should therefore be mostly in the deprotonated, hydrophilic state, and significantly more polar than the bulky benzoic *tert*-butyl benzoate ester groups in series A. Therefore, it was not surprising to see the cloud points of polymer series B and series C markedly increase compared to series A. Again, turbidity transitions were broader for the smaller polymers than for the bigger ones (Figure 3.3), as discussed above. The difference in cloud points ΔCP between the homologous series A and B were 8 °C, 6 °C and 4 °C, respectively, for polymers **PMDEGA-28**, **PMDEGA-53**, and **PMDEGA-82** (Table 3.1), and hence, ΔCP decreases with DP_n as expected for an end-group effect.

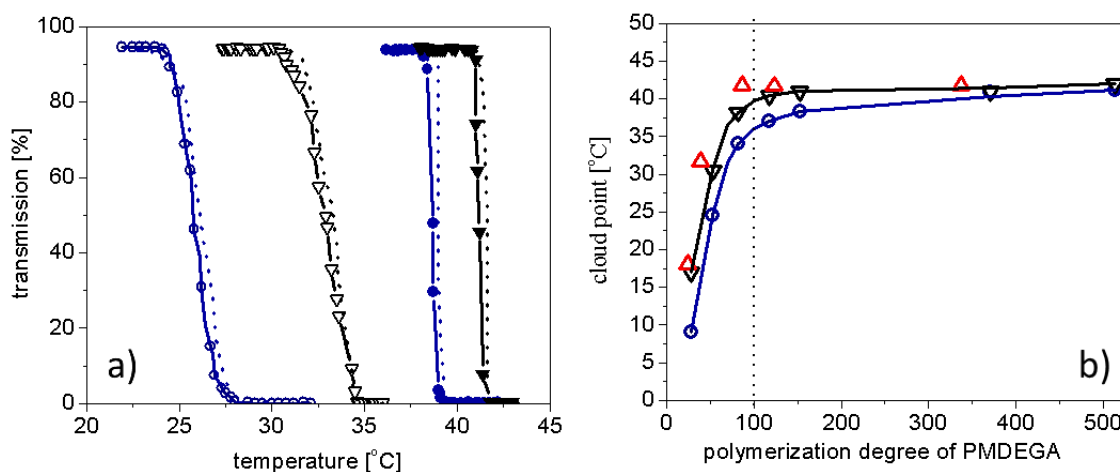


Figure 3.3: Comparison of the LCST-type behavior of PMDEGA of series A, B and C ($3.0 \text{ g}\cdot\text{L}^{-1}$ polymer in water). a) Transmission as function of the temperature, heating (solid line) and cooling (dotted line) cycle at $1 \text{ }^\circ\text{C}\cdot\text{min}^{-1}$: (\circ) = PMDEGA-53a, (∇) = PMDEGA-53b, (\bullet) = PMDEGA-153a, (\blacktriangledown) = PMDEGA-153b. b) Cloud point versus degree of polymerization DP_n : (\circ) = series A, (∇) = series B, (Δ) = series C. The lines are meant as guide to the eye.

Interestingly, PMDEGA series C, prepared with the non-symmetrical **CTA1**, and thus bearing one hydrophobic butyl trithiocarbonate and one hydrophilic benzoic acid end-group, exhibited slightly higher transition temperatures than the series B, which is terminated at both ends by benzoic acid (Table 3.1, Figure 3.3). For instance, the cloud point of **PMDEGA-123c** was $41.6 \text{ }^\circ\text{C}$, that is, $1.2 \text{ }^\circ\text{C}$ higher than the one of **PMDEGA-118b**. This finding is surprising, as with respect to the hydrophobicities and hydrophilicities of the end groups, the cloud points of

polymers of series C should be intermediate to series A and B. Obviously, this is not the case, and one can only speculate about the reasons. Possibly, the central hydrophobic bistrithiocarbonate segment characteristic for polymer series A and B, is responsible for an overall slightly reduced hydrophilicity of series B compared to series C. Alternatively, one may attribute the unexpected behavior to hydrogen bonding of the carboxylic acid end-groups with the PEG side chains, as discussed for the molar mass effects on deprotection efficiency of added trifluoroacetic acid in chapter 2. The presence of benzoic acid groups in the polymer could indeed favor additional polymer-polymer interactions through hydrogen bonding, leading to phase separation at lower temperature.^{18, 19} Similarly, lower cloud point values were observed in copolymers of PEG methacrylates and methacrylic acid in deionized water, which markedly increased in buffered neutral or basic solutions.^{18, 20, 21} The effect was attributed to an improved ionization of the carboxylic acid groups in buffer, which made the copolymers more hydrophilic.¹⁸

As for all three PMDEGA series, inverse dependence of the cloud point on DP_n was observed; it was important to verify if the nature of solvent, here the Millipore water with a slightly acidic pH of 6, had an influence of the unusual behavior. Therefore, PMDEGA of series C were exemplarily studied at pH = 7, in phosphate buffered solution.

3.1.3. Thermo-responsive behavior of PMDEGA series C in pH = 7 buffered solution

The cloud points of the unsymmetrical PMDEGA series C, bearing one hydrophobic butyl trithiocarbonate and one hydrophilic benzoic acid end-group, were measured again at concentration of $3.0 \text{ g}\cdot\text{L}^{-1}$ in buffered neutral solution. The new cloud point values, along with the values determined in Millipore water, are given in Figure 3.4. Interestingly, for short polymers, with $DP_n < 100$, the cloud points' values determined in buffer solution increased, confirming the improved ionization of the benzoic acid groups. However, the previously observed dependence of CP to DP_n persisted: the cloud point increased from $35.2 \text{ }^\circ\text{C}$ to $42.3 \text{ }^\circ\text{C}$, with increasing DP_n of the polymer (here respectively PMDEGA-24c and PMDEGA-123c).

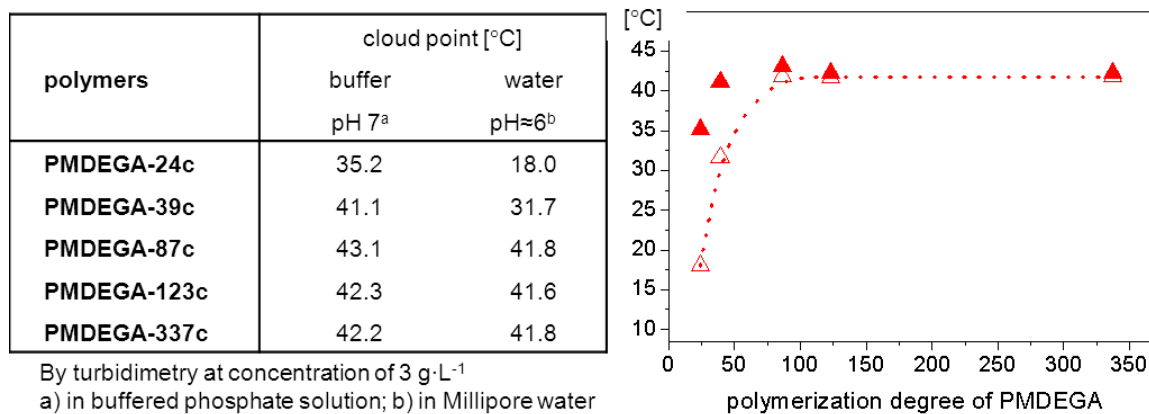


Figure 3.4: Comparison of the LCST-type behavior of series C PMDEGA at 1 °C·min⁻¹: (△) Cloud point versus degree of polymerization as determined in water at concentration of 3.0 g·L⁻¹; (▲) Cloud point versus degree of polymerization as determined in pH =7 phosphate buffered solution at concentration of 3.0 g·L⁻¹.

This trend cannot be understood by an inherent hydrophobic contribution of the end groups, as within this reasoning, the cloud points should not increase, but decrease with DP_n . It seems that PMDEGA exhibits an unusual inverse dependence of the LCST on the molar mass, possibly due to conformational effects of the polymer backbone, as may be invoked in the systematically increased LCSTs of substituted polymethacrylamides compared to the analogous polyacrylamides.²² A direct dependence of cloud points to DP_n was also most recently observed in a series of dendronized polymers carrying short EO peripheral chains.²³ The authors proposed as explanation that the side chains are not dense enough at low DP_n to shield the hydrophobic backbone from the surrounding water, thus lowering the cloud point of the polymer. Though more studies are necessary to clarify this question, the findings described in this work underline that specific end groups can be important for the thermo-responsive behavior of polymers up to relatively high M_n . Accordingly, possible end group effects should be always taken into account when designing thermo-responsive polymers, or when comparing their literature data.

3.2. Thermo-responsive behavior of PMDEGA block copolymers

3.2.1. Synthesis of poly(S-block-MDEGA) with different architectures

The logical extension of hydrophobically end-capped water-soluble polymers is amphiphilic block copolymers made of a hydrophilic inner block and hydrophobic outer blocks. As thermo-responsive amphiphilic block copolymers have found much interest in recent years,^{24, 25} in the following, the studies on the phase transition behavior of PMDEGA is complemented by looking

at the influence of the polymer architecture on the clouding of PMDEGA block copolymers solutions. In fact, while in some cases, architecture and topology did not affect markedly the LCST, for example in the case of high molar mass poly(*N*-isopropyl acrylamide),²⁶ in other cases strong effects on the LCST have been reported.^{14, 27} For example with poly(ethylene oxide) BAB block copolymers with hydrophobic poly(butylene oxide) end-blocks,^{27, 28} increasing the inner block length from 76 to 260 units, resulted in an increase of the cloud point from 12 to 25 °C.²⁷ Therefore, three series of polystyrene MDEGA block copolymers were prepared, bearing short end-blocks of the hydrophobic polystyrene, with three different architectures, namely diblock, triblock and 3-arm star copolymers (Scheme 2), in order to learn about the influences of the blocky structure as well as of the topology on the transition temperature. As described in the previous chapter, star architectures were realized via the "core-first" approach, and the RAFT synthesis of both the triblock and star block copolymers followed the so-called "Z-approach".

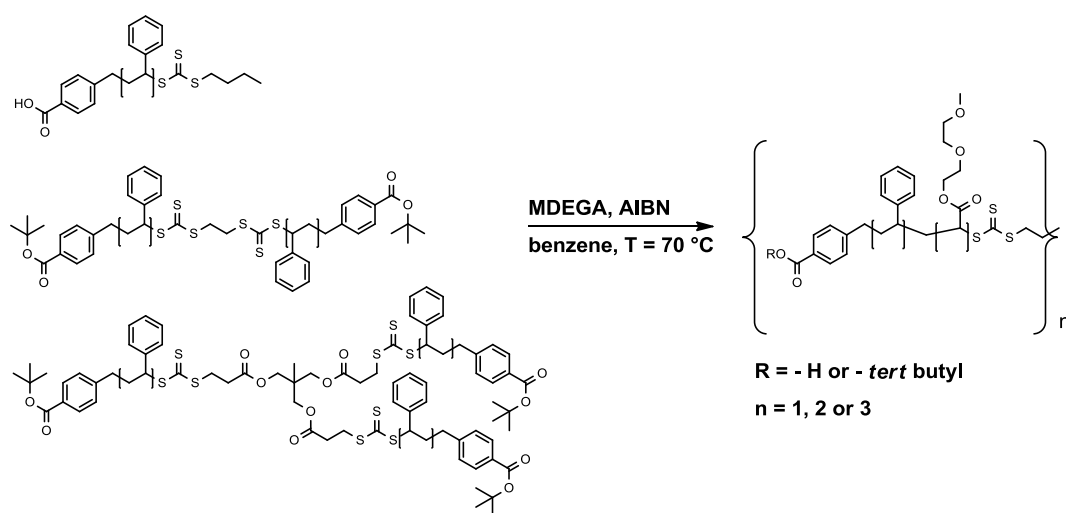


Figure 3.5: Synthesis of amphiphilic diblock, symmetrical triblock and 3-arm star PS-PMDEGA block copolymers, by using monofunctional, difunctional and trifunctional macro RAFT agents.

3.2.2. Behavior of the block copolymers in aqueous solution

The thermoresponsive and associative behavior of the triblock copolymers was first investigated in dilute aqueous solution of 3.0 g·L⁻¹. This concentration lies well above the critical micelle concentration for this type of polymers²⁹ (if existent at all), and small micelles with a monomodal distribution were observed by DLS. Temperature dependent DLS measurements (data shown in Chapter 5) revealed the sudden formation of large aggregates ($R_H > 400$ nm) above the

respective transition temperatures. The analytical data of the various block copolymers along with their respective cloud points are given in Table 3.2.

Table 3.2. Analytical data of the diblock, triblock and 3-arm star PS-PMDEGA block copolymers

architecture	polymers ^{f)}	molar mass [g·mol ⁻¹]				PDI ^{d)} (M _w /M _n)	cloud points [°C] ^{e)}
		theoret. M _n ^{theo a)}	end-groups M _n ^{b)} M _n ^{c)}		SEC M _n ^{app d)}		
diblock	PS11		1500		1300	1.14	---
copolymer BA	PS11-PMDEGA101	16000	18900	16700	12100	1.27	34.6
	PS11-PMDEGA172	27000	31300	30400	14900	1.32	38.0
	PS11-PMDEGA275	36700	49100	47000	33200	1.29	38.9
	PS11-PMDEGA331	54800	59000	74700	42800	1.32	40.0
	PS11-PMDEGA513	74100	90700	84600	31300	1.48	40.1
triblock	PS16		2200		2300	1.09	---
copolymer BAB	PS8-PMDEGA41-PS8	11100	9800	7800	7900	1.17	20.5
	PS8-PMDEGA53-PS8	12300	11500	8700	8900	1.15	22.1
	PS8-PMDEGA93-PS8	18700	18500	16100	15600	1.17	26.0
	PS8-PMDEGA180-PS8	34900	33600	28400	23900	1.17	30.1
	PS8-PMDEGA337-PS8	61000	61300	48800	30000	1.30	33.8
	PS8-PMDEGA452-PS8	79900	81000	62400	40900	1.30	35.4
	PS8-PMDEGA659-PS8	118600	117000	107400	48800	1.42	38.1
3-arm star	PS23		3550		3300	1.19	---
copolymer (AB) ₃	(PMDEGA78-PS8)_{3X}	43600	44500	35400	23600	1.31	27.2
	(PMDEGA231-PS8)_{3X}	120800	123800	91600	51400	1.32	34.1

a) conversion was determined by gravimetry; b) by ¹H-NMR analysis in acetone d₆, using the integrals of aromatic end-block signal and of the CH₃O- signal of the constitutional repeat unit; c) by UV-vis analysis in CH₂Cl₂ using the absorption coefficient ε of 13,900 L·mol⁻¹·cm⁻¹ of model RAFT agent: 2-(n-butylsulfanylthiocarbonylsulfanyl)-propionic acid 2-(2-methoxy-ethoxy)-ethyl ester **CTA5** ³⁰; d) in DMF, RI detection, calibrated with polystyrene standards; e) by turbidimetry in water at concentration 3.0 g·L⁻¹; f) numbers indicate the number average degree of polymerization DP_n according to b).

The clouding behavior of the various block copolymers is illustrated in Figures 3.6 and 3.7. While Figure 3.6 shows typical turbidity curves as function of the temperature, Figure 3.7 shows the evolution of the cloud points with increasing length of the PMDEGA blocks for the various architectures. The observed transitions, from clear to opaque for the block copolymers solutions, occurred at the same temperatures as the one observed by DLS. The transitions were

sharp and reversible upon heating (Figure 3.6), similar to the behavior of the PMDEGA homopolymers. Still, whereas solutions of the homopolymers and diblock copolymers showed hardly any hysteresis in the heating and cooling cycles, the cooling transition was systematically retarded for solutions of the linear triblock and 3-arm star block copolymers (compare Fig. 3.6.a with 3.6.b and 3.6.c). In this respect, these polymers show similarities to many poly(acrylamide)s such as *N*-isopropyl acrylamide PNIPAM,³¹⁻³⁵ for which the hysteresis was explained by intra- and inter-polymer attractive interactions requiring conformational rearrangements before redissolution of the resulting aggregates. In the case of PNIPAM, the attractive interactions were attributed to its simultaneous H-bonding donor and acceptor qualities.^{33, 36} Hysteresis effects have been also reported for some amphiphilic copolymers containing PEG and PEG analogues that are not intrinsic H-bond donors,^{37, 38} and were ascribed to hydrophobic effect driven aggregation.³⁸ In this study, an increasingly notable hysteresis and broadening of the cooling transition was indeed observed with decreasing block length of PMDEGA, i.e., with decreasing overall PMDEGA content, in the amphiphilic triblock and star systems, however it was never observed in the diblock system. Figure 3.6 illustrates exemplarily the transition curves at about 35 °C of three copolymers with different architectures. Note that triblock copolymer **PS8-PMDEGA452-P8** and 3-arm star block copolymer **(PS8-PMDEGA231)_{3X}** had very similar compositions, while diblock copolymer **PS10-PMDEGA101** has a shorter PMDEGA block and thus a higher hydrophobe content. The difference between the heating and the cooling runs was of 3 °C for the triblock and of 10 °C for the 3-arm star, when applying heating and cooling rates of 1°C·min⁻¹. Clearly in this case, it is the architecture and not the hydrophobe content, which primarily determines the presence or absence of a hysteresis in the collapse-redissolution process. Also, the hysteresis was strongly reduced for the star block copolymers (to below 1 °C) when slowing the rate of cooling down to 0.012 °C·min⁻¹. Possibly, the looping incorporation of the hydrophobic PS blocks within the individual aggregates results in more entanglements, which need more time to allow the copolymers' swelling and redissolution, when passing below the phase transition temperature.

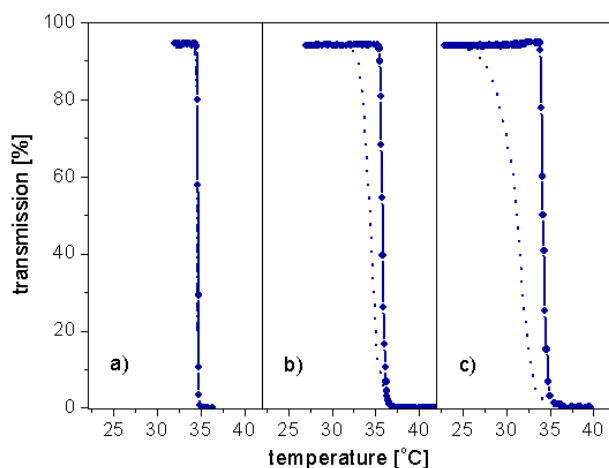


Figure 3.6. Evolution of the transmission of PS-PMDEGA block copolymers of various architecture (3.0 g/L polymer in water) with temperature; heating (solid line) and cooling (dotted line) cycle at 1°C/min of 3g/L polymer solutions: a) PS11-PMDEGA101; b) PS8-PMDEGA452-PS8 and c) (PS8-PMDEGA231)_{3X}.

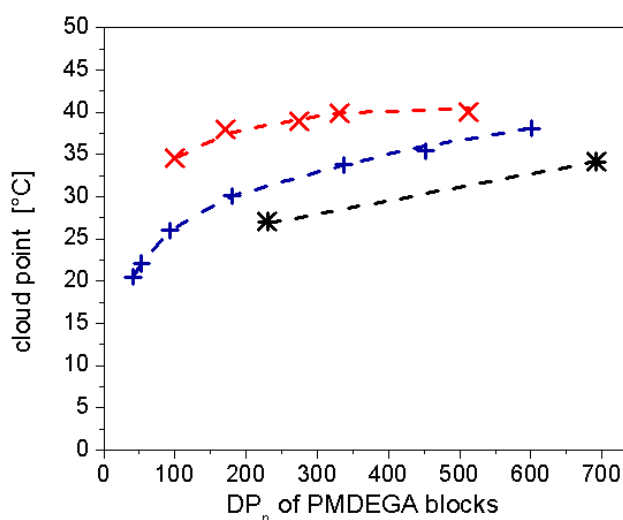


Figure 3.7. Comparison of the LCST-type behaviour of PS-PMDEGA block copolymers of different architectures. (3.0 g/L polymer in water, heating and cooling rates 1 °C/min): (X) = AB diblock series, (+) = BAB triblock series, (*) = (AB)₃ series. The lines are meant as guide to the eye.

Figure 3.7 shows that within a given polymer architecture, the cloud points of the block copolymers increase asymptotically with the length of the PMDEGA blocks. As a general feature, it was found that the presence of the hydrophobic PS end-blocks lowered the cloud points in comparison to those of PMDEGA homopolymers for a precise DP_n value (compare Tables 3.1 and 3.2). Amidst the different amphiphilic block copolymer architectures, the cloud points decrease in the order diblock < triblock < star block copolymer (Figure 3.7). Whereas for the linear block copolymers, the cloud points for very long PMDEGA blocks approach 40-41 °C, i.e., the same asymptotical value found for the homopolymer, the star block copolymers seem to stagnate at a value which is about 5 °C lower.

It is expected that for the same length of PMDEGA, an increased number of PS end-blocks lowers the CP, however the effect seen here goes beyond the influence of hydrophobic end-blocks. Indeed, if the number of hydrophobic end-blocks was the only influence on cloud points, polymers with the same composition but different architectures, namely **PS11-PMDEGA172**,

(PS8-PMDEGA226)₂ and **(PS8-PMDEGA231)₃** should have similar CP. Experimentally however the CPs were respectively 38.0 °C, 35.4 °C and 34.1 °C, and therefore decreased in the order diblock < triblock < star block copolymer. As mentioned before, the difference in cloud points may arise from the M_n effect (larger molecules present lower LCST), but it is tempting to see a topological effect in this tendency. Possibly, the reduction is due to the confinement of the PMDEGA blocks in the star and triblock looped geometry.¹⁴ In any case, these findings demonstrate that not only the presence of hydrophobic end-groups, but also the overall polymer architecture may be an effective parameter for controlling LCST-type phase transition temperatures in aqueous solution.

3.3. Conclusion

Temperature-responsive vinyl polymers based on methoxy diethylene glycol side chains can be easily engineered with the RAFT method, to implement defined end-groups of hydrophilic as well as hydrophobic character, and to produce different, also complex, architectures, such as triblock and star block copolymers. The various PMDEGA based polymers display a thermal collapse transition upon heating in the range of 20-40 °C, and thus, cover the physiological interesting range. Different from the widely used model polymer poly(*N*-isopropylacrylamide), end-groups and architecture affect the phase transition temperatures even at high molar masses still notably. This implies the need for a precise polymer structure on the one hand, and the option of a facile LCST variation on the other hand, for designing PMDEGA polymers with a particular LCST. Interestingly, all the studied polymers exhibit an unusual increase of the cloud point with increasing length of the PMDEGA blocks, equally for the hydrophobic as for the hydrophilic end groups studied in this work. No satisfactory explanation can be provided for this phenomenon at present. Possibly, increasingly improved steric shielding of the hydrophobic backbone with increasing degree of polymerization is responsible. It was also found that the architecture of amphiphilic block copolymers does not only affect the temperature, but also the kinetics of reswelling/redissolution when passing the phase transition. Star and tri-block copolymers seem to reduce not only the LCST, but also the rate of reswelling, thus causing a hysteresis effect. This may be a result of steric constraints imposed by their geometry. In any case, these findings underline that specific end-groups and the polymer architecture can be important for the thermo-responsive behavior of polymers up to relatively high molar masses. Therefore, as much as possible molecular parameters should be taken into account when designing thermo-responsive polymers with a precise transition temperature, or when comparing their literature data.

3.4. References

1. Hua, F.; Jiang, X.; Li, D.; Zhao, B. *J. Polym. Sci., Part A: Polym. Chem.* **2006**, *44*, 2454-2467.
2. Maeda, Y.; Yamauchi, H.; Kubota, T. *Langmuir* **2009**, *25*, 479-482.
3. Weiss, J.; Laschewsky, A. *Langmuir* **2011**, *27*, 4465-4473.
4. Lavigueur, C.; Garcia, J. G.; Hendriks, L.; Hoogenboom, R.; Cornelissen, J. J. L. M.; Nolte, R. J. M. *Polym. Chem.* **2011**, *2*, 333-340.
5. Zhong, Q.; Wang, W.; Adelsberger, J.; Golosova, A.; Koumba, A. M. B.; Laschewsky, A.; Funari, S. S.; Perlich, J.; Roth, S. V.; Papadakis, C. M.; Müller-Buschbaum, P. *Colloid Polymer Sci.* **2011**, *289*, 569-581.
6. Han, S.; Hagiwara, M.; Ishizone, T. *Macromolecules* **2003**, *36*, 8312-8319.
7. Lutz, J.-F.; Akdemir, Ö.; Hoth, A. *J. Am. Chem. Soc.* **2006**, *128*, 13046-13047.
8. Plummer, R.; Hill, D. J. T.; Whittaker, A. K. *Macromolecules* **2006**, *39*, 8379-8388.
9. Dormidontova, E. E. *Macromolecules* **2004**, *37*, 7747-7761.
10. Xia, Y.; Yin, X.; Burke, N. A. D.; Stöver, H. D. H. *Macromolecules* **2005**, *38*, 5937-5943.
11. Roth, P. J.; Jochum, F. D.; Forst, F. R.; Zentel, R.; Theato, P. *Macromolecules* **2010**, *43*, 4638-4645.
12. Xia, Y.; Burke, N. A. D.; Stöver, H. D. H. *Macromolecules* **2006**, *39*, 2275-2283.
13. Furyk, S.; Zhang, Y.; Ortiz-Acosta, D.; Cremer, P. S.; Bergbreiter, D. E. *J. Polym. Sci., Part A: Polym. Chem.* **2006**, *44*, 1492-1501.
14. Hirao, A.; Inushima, R.; Nakayama, T.; Watanabe, T.; Yoo, H.-S.; Ishizone, T.; Sugiyama, K.; Kakuchi, T.; Carlotti, S.; Deffieux, A. *Eur. Polym. J.* **2011**, *47*, 713-722.
15. Mitsukami, Y.; Donovan, M. S.; Lowe, A. B.; McCormick, C. L. *Macromolecules* **2001**, *34*, 2248-2256.
16. Lowe, A. B.; Torres, M.; Wang, R. *J. Polym. Sci., Part A: Polym. Chem.* **2007**, *45*, 5864-5871.
17. Mertoglu, M.; Garnier, S.; Laschewsky, A.; Skrabania, K.; Storsberg, J. *Polymer* **2005**, *46*, 7726-7740.
18. Yamamoto, S.-i.; Pietrasik, J.; Matyjaszewski, K. *Macromolecules* **2008**, *41*, 7013-7020.
19. Chen, G.; Hoffman, A. S. *Macromol. Chem. Phys.* **1995**, *196*, 1251-1259.
20. Medel, S.; Manuel García, J.; Garrido, L.; Quijada-Garrido, I.; París, R. *J. Polym. Sci., Part A: Polym. Chem.* **2011**, *49*, 690-700.
21. Longenecker, R.; Mu, T.; Hanna, M.; Burke, N. A. D.; Stöver, H. D. H. *Macromolecules* **2011**, *44*, 8962-8971.
22. Tang, Y.; Ding, Y.; Zhang, G. *J. Phys. Chem. B* **2008**, *112*, (29), 8447-8451.
23. Roeser, J.; Moingeon, F.; Heinrich, B.; Masson, P.; Arnaud-Neu, F.; Rawiso, M.; Méry, S. *Macromolecules* **2011**, *44*, 8925-8935.
24. Dimitrov, I.; Trzebicka, B.; Müller, A. H. E.; Dworak, A.; Tsvetanov, C. B. *Prog. Polym. Sci.* **2007**, *32*, 1275-1343.
25. Aseyev, V.; Tenhu, H.; Winnik, F. *Adv. Polym. Sci.* **2011**, *242*, 29-89.
26. Bivigou-Koumba, A.; Görnitz, E.; Laschewsky, A.; Müller-Buschbaum, P.; Papadakis, C. *Colloid. Polym. Sci.* **2010**, *288*, 499-517.
27. Liu, T.; Nace, V. M.; Chu, B. *J. Phys. Chem. B* **1997**, *101*, 8074-8078.
28. Kelarakis, A.; Havredaki, V.; Yuan, X.-F.; Chaibundit, C.; Booth, C. *Macromol. Chem. Phys.* **2006**, *207*, 903-909.
29. Hamley, I. W., In *Block Copolymers in Solution: Fundamentals and Applications*, Wiley-VCH Verlag GmbH & Co. KGaA: 2005.
30. Skrabania, K.; Miasnikova, A.; Bivigou-Koumba, A. M.; Zehm, D.; Laschewsky, A. *Polym. Chem.* **2011**, *2*, 2074-2083.
31. Ding, Y.; Ye, X.; Zhang, G. *Macromolecules* **2005**, *38*, 904-908.
32. Kujawa, P.; Aseyev, V.; Tenhu, H.; Winnik, F. M. *Macromolecules* **2006**, *39*, 7686-7693.
33. Cheng, H.; Shen, L.; Wu, C. *Macromolecules* **2006**, *39*, 2325-2329.

34. Berber, M. R.; Mori, H.; Hafez, I. H.; Minagawa, K.; Tanaka, M.; Niidome, T.; Katayama, Y.; Maruyama, A.; Hirano, T.; Maeda, Y.; Mori, T. *J. Phys. Chem. B* **2010**, *114*, 7784-7790.
35. Adelsberger, J.; Meier-Koll, A.; Bivigou-Koumba, A. M.; Busch, P.; Holderer, O.; Hellweg, T.; Laschewsky, A.; Müller-Buschbaum, P.; Papadakis, C. M. *Colloid Polym. Sci.* **2011**, *289*, 711-720.
36. Sun, S.; Wu, P. *J. Phys. Chem. B* **2011**, *115*, 11609-11618.
37. Qiao, Z.-Y.; Du, F.-S.; Zhang, R.; Liang, D.-H.; Li, Z.-C. *Macromolecules* **2010**, *43*, 6485-6494.
38. Cui, Q.; Wu, F.; Wang, E. *J. Phys. Chem. B* **2011**, *115*, 5913-5922.

IV Photoswitchable copolymers containing azobenzene moieties

A second responsivity, namely to light stimuli, can be added to a thermo-responsive system by incorporating, via copolymerization or by end-group modification, a light responsive moiety.¹ The azobenzene moiety is a classical candidate for this purpose, as it displays two isomers of different polarity. The transition from one isomer to the other is reversible and is easily achieved by (UV) light irradiation. While the azobenzene moiety is overall hydrophobic, the linear thermodynamically stable trans conformation is nearly apolar, whereas a dipole moment of about 3 Debye is induced by the bent geometry of the cis conformation.² Therefore, the presence of azobenzene in a thermo-responsive polymeric system is expected to globally lower the LCST, but to a greater extent for the apolar trans conformation than for the polar cis conformation. In other words, the difference between the transition temperatures of the cis copolymer and the trans copolymer, $\Delta T_{CP} \text{ cis-trans} = T_{CP} \text{ cis} - T_{CP} \text{ trans}$, is expected to be positive.²

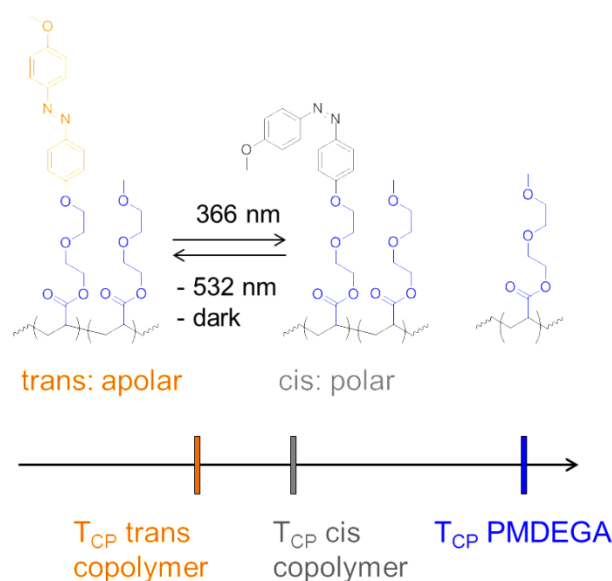


Figure 4.1: Expected cloud point variations upon copolymerization of MDEGA with an azobenzene containing monomer and photoisomerization of the resulting copolymer.

Interestingly, a literature survey revealed that this prediction is not always observed experimentally: In aqueous solution, the group of F. Winnik³ did not detect any change of cloud points upon irradiation of PNIPAM end-capped with azobenzene, while for a similar system, a difference of 10 °C between the CP of the cis polymer and the CP of the trans polymer, i.e. $\Delta T_{CP} \text{ trans-cis}$, was measured by Akiyama et al.⁴ $\Delta T_{CP} \text{ cis-trans}$ at about 4 °C was also found by

Jochum et al. with poly(PEG methacrylate)s functionalized by one or two azobenzene end-groups.¹ The observations become even more complex in the case of thermo-responsive polymers with azobenzene moieties incorporated in the side-chain. With increasing azobenzene content, ΔT_{CP} cis-trans was either found to increase up to a constant value,^{5,6} or to pass through a maximum with azobenzene content.^{2,7,8} Even more surprising, negative values of ΔT_{CP} cis-trans were reported on a few occasions.⁹⁻¹¹ In these cases, the transition from the apolar trans azobenzene to the polar cis, shifted the CP to lower temperatures.

Considering the diverse observations, it becomes evident that complex mechanisms take place in such thermo-responsive copolymers, depending eventually on the chemical structure of the chosen thermo-responsive and azobenzene-containing monomers, and on the distribution of the latter in the polymer. Keeping in mind these difficulties, the following chapter explores the effects of azobenzene moieties on the thermo-responsive behavior of PMDEGA. For this purpose, a series of copolymers was synthesized, containing **MDEGA** and various amount of azobenzene acrylate, 6-[4-(4-methoxyphenylazo)phenyl]diethylene glycol acrylate (**azoMDEGA**) and the temperature and light responsive behavior of the resulting series was studied.

4.1. Synthesis of copolymers of MDEGA and azoMDEGA

4.1.1. Synthetical strategy

As discussed in Chapter 3, molar mass and end-groups are two parameters that greatly influence the cloud point of PMDEGA based polymers. Beyond end-groups and molar masses, the type of copolymer also plays an important role on LCST, as block, gradient and random copolymers with the same chemical composition are known to display different transition temperatures.^{12,13} In an effort to produce a series of copolymers with as little variables as possible, a random distribution of the thermo-responsive and the light-responsive monomers within the copolymer chain was targeted. Although RAFT copolymerization allows to achieve a homogenous composition distribution at the molecular level,¹⁴ special care has to be taken in the choice of monomers, since a priori, co-monomers are consumed at different rates depending on steric and electronic substitution of the polymerizable double bond.¹⁵ Therefore the light responsive monomer used in this study was designed to be structurally similar to MDEGA, with an azobenzene moiety linked to acrylate functionality by a diethylene glycol spacer (see Figure 4.2). By varying the feed, i.e the ratio of the two monomers, it was expected to produce well defined polymers with a controlled molar mass and a random composition of the co-monomers, thus resulting in a homogeneous composition.

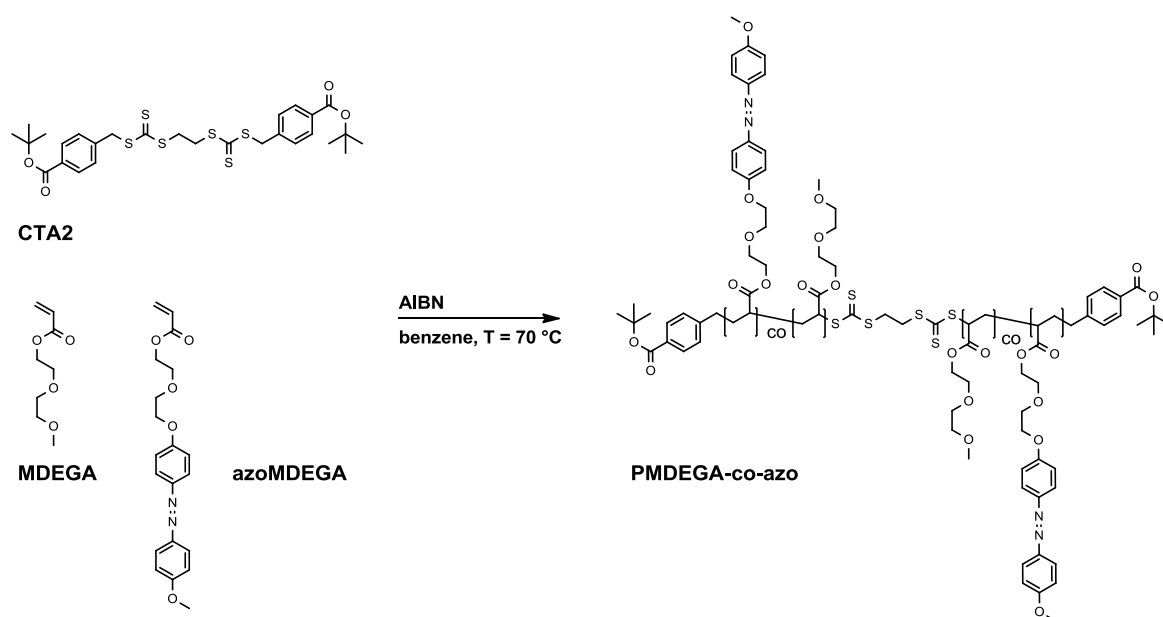


Figure 4.2: RAFT copolymerization of **MDEGA** (methoxy diethylene glycol acrylate) and **azoMDEGA** (6-[4-(4-methoxyphenylazo)phenyl]diethylene glycol acrylate).

4.1.2. Retardation in copolymerization reaction

A major difficulty when polymerizing an azobenzene functionalized monomer results from the retardation induced by the azobenzene moiety. In fact, the N=N double bond is thought to react with the propagating radical, leading to both retardation and low molar masses if the ratio of azobenzene moieties to initiator radicals is high.¹⁶ For a low ratio however, the polymerization can proceed and successful RAFT polymerizations of azobenzene containing homo- and copolymers were reported.^{13,17,18} Thus, although it seemed possible to obtain the aspired azobenzene containing polymer, experimental difficulties were expected. To determine the optimal reaction time in this particular system, two kinetic experiments were thus conducted. First, the conversion of MDEGA with polymerization time in absence of azoMDEGA was monitored. Second, the same reaction was studied in presence of 3 mol % of azoMDEGA in the initial feed. The conversion plots are presented in Figure 4.3. Experimentally, samples were taken at regular time intervals, cooled, stabilized with hydroquinone and analyzed by ¹H-NMR spectroscopy.

In the case of homopolymerization of MDEGA, the integral value (I_{total}) of the ¹H-NMR signals located in the range of 3.24-3.41 ppm, attributed to the terminal methoxy group (-CH₂-O-CH₃) in both the polymer and monomer were used as internal standard (see Figure 4.4). The consumption of the monomer was determined by using the summed values of the integrals

(I_{MDEGA}) at 5.86, 6.19 and 6.41 ppm, corresponding to the signals of the three acrylic protons.

The conversion τ of MDEGA was accordingly given by the ratio: $\tau = (I_{\text{total}} - I_{\text{MDEGA}}) / I_{\text{total}}$

The analogous procedure was used in monitoring MDEGA conversion during the copolymerization of MDEGA and azoMDEGA. Because azoMDEGA lacks the terminal methoxy group of MDEGA, no additional signals interfered with signals from MDEGA in the range of 3.24-3.41 ppm. I_{total} could be used again as internal standard. However, due to the identical substitution of the C=C bond in both monomers, their acrylic signals are superimposed. In order to calculate the conversion of MDEGA in this case, the hypothesis that the consumption of both monomers follows the same rate was made; i.e for this particular feed, that 97 % of each acrylic signal was due to MDEGA. Under this approximation τ was given as $(I_{\text{total}} - 0.97 \times I_{\text{MDEGA}}) / I_{\text{total}}$. Note, that even if the hypothesis is not confirmed, the error on MDEGA conversion will still be very small.

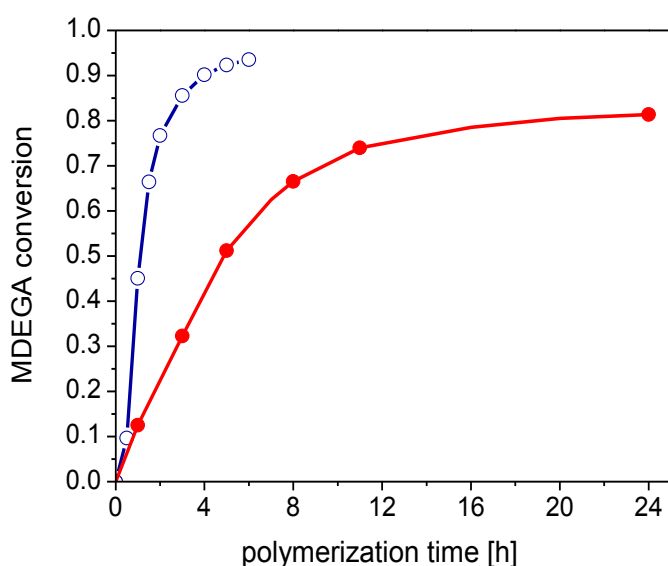


Figure 4.3: Conversion of MDEGA vs. polymerization time, as followed by $^1\text{H-NMR}$, for monomer concentration of 33 wt. % in benzene, and reaction temperature of 70°C . (○) homopolymerization of MDEGA. Feed: CTA/MDEGA/AIBN = 1/301/0.2; (●) copolymerization of MDEGA and 3 mol % of azoMDEGA. Feed CTA/MDEGA/azoMDEGA/AIBN = 1/280.2/8.6/0.2

In the absence of the azobenzene monomer, the polymerization of MDEGA was rapid and reached 50 % conversion within 1 h. 96 % yield were obtained after 6 h of polymerization. Under similar conditions, the copolymerization experiment with 3 mol % of azobenzene monomer revealed a much slower conversion: 5 h were needed to reach 50 % conversion, while after 24 h

the polymer was obtained with 81 % yield. The retardation effect was therefore noticeable even at only 3 mol % content of azobenzene, but did not compromise the synthesis of the polymer.

With the knowledge of the copolymerization kinetics, a series of copolymers of MDEGA and azoMDEGA was synthesized. The azobenzene content was varied between 1 mol % and 20 mol %. The polymerization kinetics was notably influenced by the azobenzene content, as expected. With low amounts of azoMDEGA, the reactions were fast and could reach high yields, whereas longer reaction times were needed when the azobenzene monomer/MDEGA ratios were increased, and much lower yields were obtained (see Table 4.1). For example, the copolymer containing 20 mol % of azoMDEGA was produced with only 13 % yield after a polymerization time of 84 h.

Noteworthy, Table 4.1 shows that at any conversion, the copolymer's final composition was, within analytical precision, always identical to the initial feed. This indicates that the two monomers were consumed at an identical rate, and therefore that the copolymerization presented an "ideal azeotropic" character.¹⁵ Thus the chosen design of the azobenzene containing monomer with a diethylene glycol spacer proved to be appropriate to obtain statistical copolymers of MDEGA and azoMDEGA.

Table 4.1: Analytical data of the copolymers P(MDEGA-co-azoMDEGA) prepared.

polymers ^{a)}	react. time [h]	composition				characterization		
		azo content [mol %]		conversion [%] ^{c)}		SEC ^{d)}		
		initial ^{b)}	final ^{c)}	azo	MDEGA	M _n ^{c)}	M _n ^{app}	PDI
PMDEGA-153	4	0	0	0		27300	14500	1.27
P(MDEGA158-azoMDEGA2)	14	1.0	1.0	95	99	28800	18000	1.29
P(MDEGA128-azoMDEGA3)	14	2.0	2.0	83	83	24000	14700	1.26
P(MDEGA228-azoMDEGA7)	24	3.0	3.0	81	82	43000	22700	1.37
P(MDEGA159-azoMDEGA9)	22	5.0	5.2	61	58	31600	20300	1.31
P(MDEGA81-azoMDEGA6)	22	7.0	7.2	57	55	17000	11290	1.33
P(MDEGA80-azoMDEGA9)	72	10.0	10.3	32	31	17900	10500	1.40
P(MDEGA29-azoMDEGA8)	84	20.0	22.1	14	13	8800	5400	1.41

a) numbers indicate the number average degree of polymerization DP_n according to ¹H-NMR; b) determined by gravimetry; c) by ¹H-NMR analysis in acetone d₆, using the integrals of aromatic end-group signal and of the CH₃O- signal of MDEGA or the aromatic azobenzene group signal; d) in DMF, RI detection, calibrated with polystyrene standards

For the study of light- and thermo-response of P(MDEGA-co-azoMDEGA) copolymers, it was important to reduce the number of variables within the series to a minimum, in order to minimize any additional effects on the polymers cloud points. Polymer molar mass is one of these variables. From the previous work on PMDEGA end-capped by two *tert*-butyl benzoate end-groups (Chapter 3), it was known that the cloud point does not vary much for polymers larger than DP_n 100. Therefore, it is preferable to work with a series of high molar mass copolymers, in order to reduce the influence of end-groups on CP. Yet, copolymers of high molar masses could not always be obtained, as increasing amounts of azobenzene monomer inhibit the polymerization reaction. In order to keep the molar mass of the different copolymers constant, DP_n between 130 and 160 were targeted, as a compromise. A series of 6 copolymers was studied: 4 copolymers, which had an azobenzene content between 1 to 5 mol % and were within the targeted polymer size, and 2 copolymers, which had about DP_n 80 and an azobenzene content of 7 and 10 mol %.

4.2. Characterization of the copolymers

4.2.1. Structural determination

The copolymers were characterized by $^1\text{H-NMR}$ and by size exclusion chromatography (SEC) in dimethylformamide. The results are summarized in Table 4.1. As discussed in Chapter 2, in the case of PMDEGA homopolymers, the values of M_n^{app} derived from SEC were always smaller than the M_n values derived from $^1\text{H-NMR}$. The polymers presented a monomodal distribution, although their polydispersity was slightly higher than typical values of PMDEGA homopolymers.

Figures 4.4.a and b present characteristic $^1\text{H-NMR}$ spectra of, respectively, PMDEGA and P(MDEGA-co-azoMDEGA). For PMDEGA, the two aromatic signals between 7 and 8 ppm of the end-groups could be used as internal standards. In the case of the copolymers of azoMDEGA, a partial overlap between the aromatic azobenzene and the end-groups signals was observed. Nevertheless, it was possible to integrate independently the reference signal (2) coming from the end-groups, the aromatic signal (8) of the azobenzene moiety and the methoxy group $-\text{CH}_2-\text{O}-\text{CH}_3$ of the MDEGA side chain (7), i.e. a molar mass and the composition of the polymer could be derived. The analytical data of the series are summarized in Table 4.1.

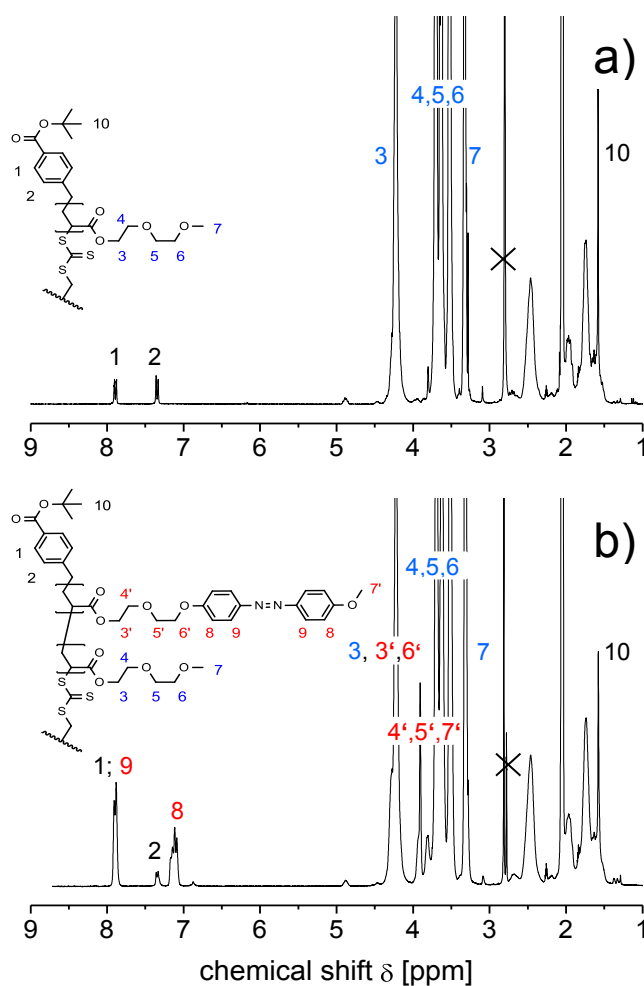


Figure 4.4: Exemplary $^1\text{H-NMR}$ spectra in acetone d_6 of a) the homopolymer **PMDEGA-82** and b) the copolymer **P(MDEGA81-co-azoMDEGA6)**. Note the appearance in b) of the signals 8, 9, 4', 5' and 7'.

4.2.2. Photochromism of P(MDEGA-co-azoMDEGA) in aqueous solution

The trans-cis photoisomerization and the thermal cis-trans isomerization of the azobenzene moieties in P(MDEGA-co-azoMDEGA) were investigated in dilute aqueous solution, at a concentration of $3.0 \text{ g}\cdot\text{L}^{-1}$. The polymers were always kept in the dark, and their aqueous solutions were also stored in the dark for at least 3 days prior to analysis. Thus, the azobenzene moieties could adopt the thermodynamically stable trans conformation. Alternatively, the trans polymer could be obtained from the cis conformation by laser light irradiation, for about a minute, at 532 nm. The resulting UV-vis spectra showed a characteristic intense signal corresponding to the $\pi \rightarrow \pi^*$ transition ($\lambda_{\text{max}} = 361 \text{ nm}$) of the trans azobenzene group. After UV-light irradiation at 366 nm, the trans azobenzene group was in majority isomerized to the cis

conformation. The transformation was characterized by a blue shift of the $\pi \rightarrow \pi^*$ transition to 312 nm and the increase in intensity of the signal corresponding to the $n \rightarrow \pi^*$ transition at 445 nm (Figure 4.5). Noteworthy, the UV-vis spectra of PMDEGA homopolymers also displays a strong signal at about 309 nm characteristic of the trithiocarbonate moiety, naturally present in all polymers synthesized by RAFT.¹⁹ This group is also present in the MDEGA/azoMDEGA copolymers and is responsible for the shoulder at about 310 nm, well visible in the spectra of the copolymer in trans conformation.

As shown in Figure 4.5, the absorbance bands of the cis and the trans conformation partially overlap, hence a full isomerization of the trans to the cis conformation is never possible. However, in order to simplify the discussion, this “photostationary state” will be referred to in the following, as the cis state of the azobenzene group.

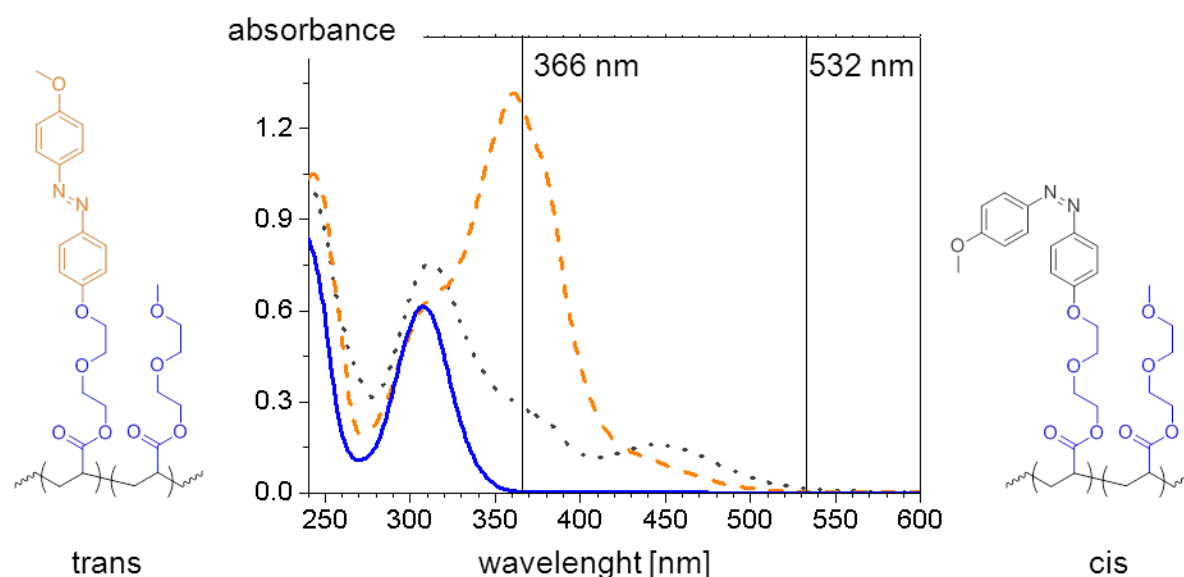


Figure 4.5: Representative UV-vis spectra of $3.0 \text{ g}\cdot\text{L}^{-1}$ polymers' solutions, recorded at $21 \text{ }^\circ\text{C}$ in a quartz cuvette of a light pathway of 0.1 cm : (---) trans conformation of **P(MDEGA130-azoMDEGA4)** recorded after storage in the dark; (···) cis conformation of the same sample after irradiation at 366 nm ; (—) **PMDEGA153a**. The vertical lines show the irradiation wavelengths of 366 nm and 532 nm .

From studying the thermal cis to trans isomerization in the dark at $21 \text{ }^\circ\text{C}$, a half-life time of 16 h was determined. Therefore, the cis conformation of the azoMDEGA containing copolymers had an advantageous stability: the thermal relaxation to the trans form was found slow enough to allow a convenient manipulation of the polymer with the azobenzene group mainly in cis

conformation, but fast enough to allow the sample to relax to trans conformation again in a few days.

4.3. Thermo-responsive behavior of P(MDEGA-co-azoMDEGA)

4.3.1. Solubility of the copolymers in water

Next the influence of azoMDEGA on cloud points of P(MDEGA-co-azoMDEGA) was investigated on polymers with the azobenzene groups in both trans and cis conformations. The trans conformation was obtained by storage of the solution in the dark for 3 days, and the majority of cis conformation by irradiation of the same solution for about 15 min by 366 nm UV-light. Note that longer irradiation times of about 40 min were necessary to complete the isomerization to cis conformation in copolymers with large azoMDEGA contents (7 and 10 mol %). UV-vis spectra were taken before the turbidity measurements of polymers in trans and in cis conformation, and additionally after the measurement, for polymers in cis conformation. Under the working conditions, the cis conformation was found stable during the cloud point measurements, thus the recorded transition temperature truly reflects the behavior of the cis polymer.

Table 4.2: Composition and cloud points of the copolymers P(MDEGA-co-azoMDEGA) studied.

Polymers ^{a)}	composition			cloud point [°C]		
	azo content ^{b)} (mol %)	MDEGA ^{a)} DP _n	n° of azoMDEGA per chain ^{a)}	T _{CP cis} ^{c)} [°C]	T _{CP trans} ^{c)} [°C]	ΔT _{CP cis-trans} ^{d)} [°C]
PMDEGA-153	0.0 %	153	0	38.3	38.3	0
P(MDEGA158-azoMDEGA2)	1.0 %	158	2	33.0	32.5	0.5
P(MDEGA128-azoMDEGA3)	2.0 %	128	3	27.2	27.4	-0.2
P(MDEGA130-azoMDEGA4)	3.1 %	130	4	25.5	25.9	-0.4
P(MDEGA159-azoMDEGA9)	5.2 %	159	9	20.6	21.8	-1.2
P(MDEGA81-azoMDEGA6)	7.2 %	81	6	13.7	15.2	-1.5
P(MDEGA80-azoMDEGA9)	10.3 %	80	9	8.2	10.0	-1.8

a) numbers indicate the number average degree of polymerization DP_n of MDEGA and the number average of azobenzene groups incorporated in the copolymer, according to ¹H-NMR; b) determined from ¹H-NMR, as the molar ratio of azoMDEGA and (azoMDEGA + MDEGA) units; c) by turbidimetry in water at concentration 3.0 g·L⁻¹. d) ΔT_{CP cis-trans} = T_{CP cis} - T_{CP trans}

The collapse transition of the copolymers was fully reversible, exhibiting virtually no hysteresis between the heating and cooling cycles (< 0.5 °C). The resulting CP values, presented in Table 4.2, showed a marked dependence of the azobenzene content. In the case of PMDEGA homopolymers with *tert*-butyl benzoate termini, CPs between 34 and 38 °C were observed for polymers' lengths of DP_n between 80 and 150 (Chapter 3). Compared to PMDEGA homopolymer, the copolymer P(MDEGA-co-azoMDEGA) with the same polymerization degree displayed a CP of almost 6 °C lower for azobenzene content of 1 mol % and of 24 °C lower for a content of 10 mol % in the copolymer. In the latter case, the cloud point temperature in the trans conformation was of only 10 °C. Thus, the hydrophobicity of P(MDEGA-co-azoMDEGA) strongly built-up with the azobenzene monomer content, making the copolymer aqueous solution difficult to handle.

4.3.2. Photocontrol of the cloud point temperatures

As the *cis* conformation of the azobenzene moiety is more polar than the *trans* conformation, the transition from *trans* to *cis* should confer a more hydrophilic character to the polymers, consequently increasing their LCST. The expected behavior was observed in **P(MDEGA158-co-azoMDEGA2)**, the copolymer with the lowest azobenzene content (1 mol %) of the series, where the transition from *trans* to *cis* increased the CP by 0.5 °C (Table 4.2). Similarly low values of ΔT_{CP} *cis-trans* were reported on several occasions for low amount of azobenzene. The difference then increased with the azobenzene content.^{1, 4, 6, 20} In the case of the P(MDEGA-co-azoMDEGA) copolymers studied here, no such increase of ΔT_{CP} *cis-trans* was observed. On the contrary, when the amount of azobenzene reached 2 mol %, the cloud points of the *cis* and the *trans* copolymers were found almost equal, T_{CP} of the *cis* copolymer being even slightly lower than T_{CP} *trans*. This trend further developed with increasing contents of azobenzene, reaching the largest "negative" temperature shift of -1.8 °C for **P(MDEGA80-azoMDEGA9)**, the copolymer with 10 mol % of azoMDEGA content (Figure 4.6).

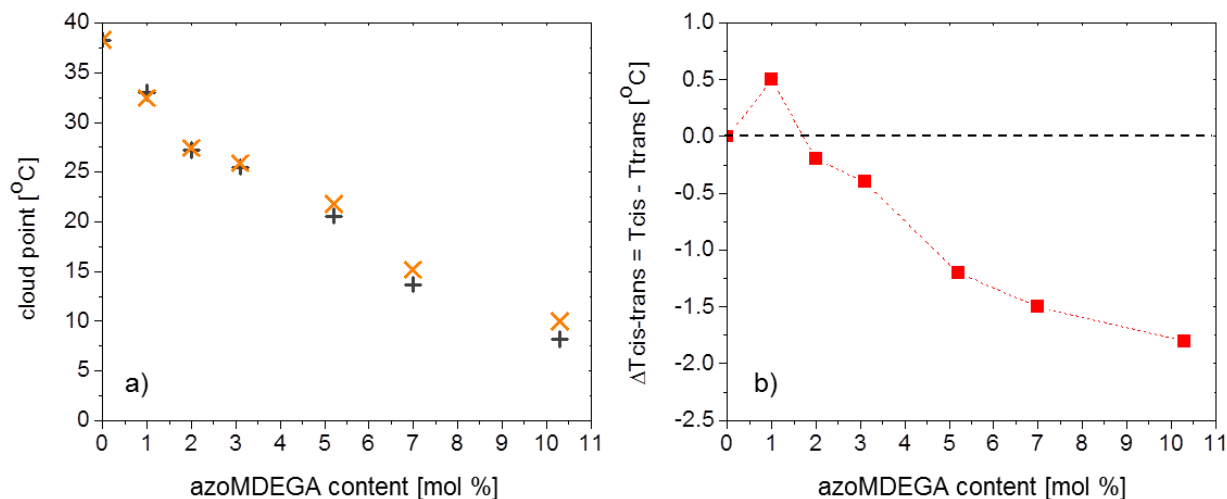


Figure 4.6: LCST-type behavior of the P(MDEGA-co-azoMDEGA) series ($3.0 \text{ g}\cdot\text{L}^{-1}$ polymer in water, heating rate $0.1 \text{ }^\circ\text{C}\cdot\text{min}^{-1}$): a) cloud points versus molar content of azoMDEGA, of copolymers with the azobenzene group in respectively (x) trans and (+) cis conformations; b) difference $\Delta T_{CP} \text{ cis-trans} = T_{CP} \text{ cis} - T_{CP} \text{ trans}$. The lines are meant as guide to the eye.

As already mentioned in the introduction, irregularities to the commonly expected trend have been previously reported in the literature.^{2, 3, 7, 8, 9-11} In most cases however, the cloud point temperatures of the cis polymers were always higher than the one of the trans.^{2, 7, 8} The irregularities then consisted in the fact that the difference between the two cloud points ($\Delta T_{CP} \text{ cis-trans}$) stopped increasing and eventually decreased or stagnated for polymers with an azobenzene content larger than 2 to 4 mol %.^{2, 7, 8} This peculiar behavior was explained by the double influence of azobenzene on polymer solubility: first, the introduction of large amount of azobenzene increases the difference of polarity between the cis and the trans-polymers. At the same time, however, the overall polymer hydrophobicity also increases. Thus, beyond a certain amount of azobenzene in the copolymer, the global hydrophobicity of the group suppresses the polarity gain of the cis conformation, and $\Delta T_{CP} \text{ cis-trans}$ tend to zero.^{2, 7} Although such an explanation fits well the “up and down” trend described in the literature, it clearly cannot account for the negative $\Delta T_{CP} \text{ cis-trans}$ values observed in the case of P(MDEGA-co-azoMDEGA), as the polarity of the cis conformation alone cannot render the polymer more hydrophobic than it is in the apolar trans conformation. Thus, one can only stipulate whether the behavior of P(MDEGA-co-azoMDEGA) reported here constitutes a counterexample for the above mentioned theory, or whether it is the effect of an entirely different mechanism.

Higher LCSTs than expected were described in thermo-responsive polymers on different occasions. For example, when hydrophobic end-groups or side chains of a polymer were large, they were shielded from water by aggregation and the overall hydrophilicity of the polymer was increased, as compared to polymers with hydrophobic groups unable to aggregate.²¹⁻²⁴

Additionally, topological effects such as the cyclization of polymer^{25, 26} or the formation of loops by intra-chain crosslinks, were reported to increase the cloud point temperature.²⁷ For example, a copolymer based on *N,N*-dimethylaminoethyl methacrylate showed a continuous increase of the cloud point with the number of inter-chain crosslinks. The shift of temperature between the non-crosslinked polymer and the identical crosslinked one accounted for up to 30 °C. The authors ascribed this increase of the cloud points to the fact, that loops reduce the inter-chain entanglement and generate a repulsive force between the polymers.^{27, 28} This retards chain aggregation upon the increase of temperature, and, consequently, increases the LCST.²⁷

At this point one must recall that the difference of geometry between the two isomers of an azobenzene group not only induces a change in polarity, but also a change in the group packing ability. Indeed, planar trans azobenzenes are capable to associate by strong aromatic-aromatic interactions,²⁹ but this packing is weaker and easily breakable for the bend cis conformation, and thus can be disrupted by UV-light irradiation.^{30, 31} Thus the unexpected behavior of P(MDEGA-co-azoMDEGA) could be explained by the partial protection of the hydrophobic azobenzene from water by aggregation when the group is in the trans conformation, and its exposure to water in the non-associated cis conformation. Additionally, the packing of trans-azobenzene group can generate intra-chain crosslinks at low, and inter-chain crosslinks at high concentrations, creating loops in the polymer chain. The number of loops will logically increase with the content of azobenzene groups, and enhance the stability of the polymer coil. Both “aggregation” and “loop” effects will be therefore more pronounced with increasing azobenzene content, leading to higher differences between the CPs of the polymers with the azobenzene group in cis and the trans conformations. Although no definitive arguments can be provided at this point, it is likely that the combination of these two effects accounts for the unusual photo-modulated thermo-responsive behavior of P(MDEGA-co-azoMDEGA). Figure 4.7 presents schematically the possible conformational change of the polymer chain upon irradiation.

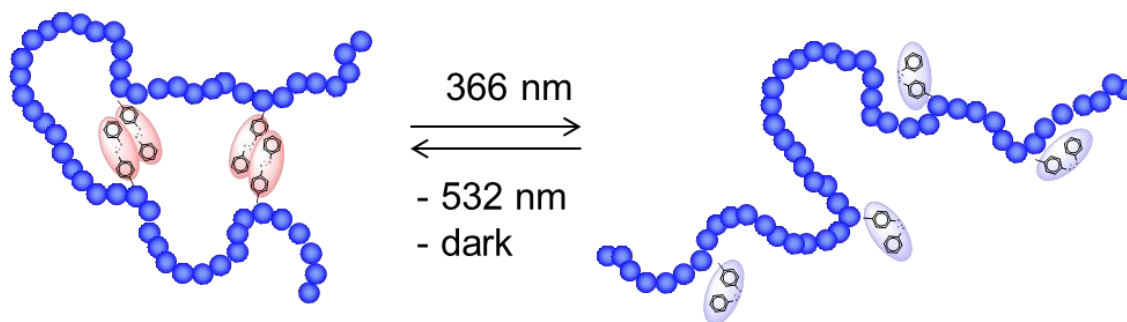


Figure 4.7: Possible conformational change of the polymer chain upon irradiation of the azobenzene containing copolymer in water. Azobenzene units in associated trans (●) and in dissociated cis (●) conformation.

It seems that only two comprehensive studies, by Menzel et al.⁵ and by Yu et al.,⁹ deal with a similar phenomenon as observed here. Both studies explain the higher CP value of copolymers with the trans-azobenzenes compared to copolymers with cis-azobenzenes by the argument of shielding aggregation. Interestingly, while working on large azobenzene-containing hyperbranched poly(ether amine)s, Yu et al.⁹ could detect by DLS a difference between the hydrodynamic diameters of the copolymers before and after UV-light irradiation. The nanoparticles formed by these polymers were at about 21 nm in diameter when the azobenzene group was in the cis form, shrinking to 18 nm when the azobenzene was switched to the trans form. This confirmed the closer packing of the polymer coil in the trans conformation.⁹

When analogous DLS experiments were conducted on a $3.0 \text{ g}\cdot\text{L}^{-1}$ solution of **P(MDEGA159-azoMDEGA9)**, a single chain coil of 3 nm in radius was observed, independently of the azobenzene group conformation. The detected dimensions were about the same as for PMDEGA homopolymers and the same as the values reported for isolated polymers in water by others.²¹ Therefore, no evidence of an inter-molecular association of the polymers before the LCST was found, as well as no evidence of intra-chain association, when the azobenzene group of the copolymer was in the trans form. Yet, it must be taken into account, that an intra-molecular association of azobenzene could have occurred, but the resulting contraction of the trans polymer in water was simply too small to be detected by the used equipment.

4.4. Conclusion

A series of random copolymers of methoxy diethylene glycol (MDEGA) and 6-[4-(4-methoxyphenylazo)phenyl]diethylene glycol acrylate (azoMDEGA) was synthesized by RAFT polymerization and their response to double stimuli of temperature and light analyzed.

Interestingly, ΔT_{CP} cis-trans, the difference between the cloud points of the cis and the trans copolymers, increased first with the azobenzene content, then continuously decreased. Thus, the thermo- and light-responsive behavior of P(MDEGA-co-azoMDEGA) differed from the common observations. To the best of my knowledge, the same peculiar behaviour was reported only twice in the past.^{5,9} The fact that for copolymers synthesized here, the LCST was higher, when the azobenzene group was in the hydrophobic trans conformation than when it was in the less hydrophobic cis, could be explained by the association of the trans azobenzene units. Such a stacking could partially shield the hydrophobic groups from water, increasing thus the apparent hydrophilicity of the copolymer with the trans-azobenzene. Alternatively, the polymer loops between two aggregated trans-azobenzene units could prevent the chain from collapsing with increasing temperature. However, no experimental proof of the azobenzene aggregation could be obtained by the analytical methods at disposal. In any case, the observations underline the complexity of the dissolution behavior of these polymers. Further investigations are needed to understand the influence of the different constituents of an azobenzene moiety, such as the nature and length of the flexible spacer, and the type of the substitution pattern of the azobenzene moiety, on its aggregation.

Apart from a fundamental interest in the system, the work with light responsive polymers was motivated by the possibility to build multi-responsive hydrogels. However for this purpose, the P(MDEGA-co-azoMDEGA) copolymers were found not suitable. The first difficulty consisted in the retardation of the polymerization kinetics, which increased with the initial amount of azobenzene, prohibiting the synthesis of long polymer with azobenzene content larger than 7 mol %. A second drawback was the strong hydrophobicity of azoMDEGA, which the hydrophilic diethylene-glycol spacer could not reduce sufficiently. Thus, for copolymers with an azobenzene content above 5 mol %, the CPs were below the room temperature, making the copolymers unpractical to work with. The last drawback of the system was the small difference of CP upon light irradiation, being at best of 1.8 °C. This seems not large enough to confer interesting light responsive properties to the copolymers.

4.5. Acknowledgments

This chapter would have been impossible without the practical help of my undergraduate student Carlos Adrián Benítez-Montoya, who performed most of the experimental work on azobenzene containing polymers. It was a pleasure to work with him on this project.

Jarosław Tomczyk is also greatly acknowledged for given us the access to the green laser and helping with the first irradiation experiments.

4.6. References

1. Jochum, F. D.; zur Borg, L.; Roth, P. J.; Theato, P. *Macromolecules* **2009**, *42*, 7854-7862.
2. Kungwachakun, D.; Irie, M. *Makromol. Chem., Rapid Commun.* **1988**, *9*, 243 -246.
3. Ishii, N.; Mamiya, J.-i.; Ikeda, T.; Winnik, F. M. *Chem. Commun.* **2011**, *47*, 1267-1269.
4. Akiyama, H.; Tamaoki, N. *Macromolecules* **2007**, *40*, 5129-5132.
5. Menzel, H.; Kröger, R.; Hallensleben, M. R. *Macromol. Rep.* **1995**, *32*, 779-787.
6. Luo, C.; Zuo, F.; Ding, X.; Zheng, Z.; Cheng, X.; Peng, Y. *J. Appl. Polym. Sci.* **2008**, *107*, 2118-2125.
7. Yoshida, T.; Kanaoka, S.; Aoshima, S. *J. Polym. Sci., Part A: Polym. Chem.* **2005**, *43*, 5337-5342.
8. Akiyama, H.; Tamaoki, N. *J. Polym. Sci., Part A: Polym. Chem.* **2004**, *42*, 5200-5214.
9. Yu, B.; Jiang, X.; Wang, R.; Yin, J. *Macromolecules* **2010**, *43*, 10457-10465.
10. Menzel, H.; Kröger, R.; Hallensleben, M. R. *Polym. Prepr. Am. Chem. Soc. Div. Polym. Chem.* **1998**, *39*, 330-331.
11. Desponds, A.; Freitag, R. *Langmuir* **2003**, *19*, 6261-6270.
12. Lee, H. I.; Pietrasik, J.; Matyjaszewski, K. *Macromolecules* **2006**, *39*, 3914-3920.
13. Ueki, T.; Nakamura, Y.; Yamaguchi, A.; Niitsuma, K.; Lodge, T. P.; Watanabe, M. *Macromolecules* **2011**, *44*, 6908-6914.
14. Barner-Kowollik, C., In *Handbook of RAFT Polymerization*, Wiley-VCH Verlag GmbH & Co. KGaA: 2008.
15. Odian, G. G., *Principles of polymerization*. 4th Edition ed.; John Wiley and Sons: Hoboken (USA), 2004; p 812.
16. Braun, D.; Arcache, G. *Makromol. Chem.* **1971**, *148*, 119-129.
17. Xiang, Y.; Xue, X.; Zhu, J.; Zhang, Z.; Zhang, W.; Zhou, N.; Zhu, X. *Polym. Chem.* **2010**, *1*, 1453-1458.
18. Li, Y.; Zhou, N.; Zhang, W.; Zhang, F.; Zhu, J.; Zhang, Z.; Cheng, Z.; Tu, Y.; Zhu, X. *J. Polym. Sci., Part A: Polym. Chem.* **2011**, *49*, 4911-4920.
19. Skrabania, K.; Miasnikova, A.; Bivigou-Koumba, A. M.; Zehm, D.; Laschewsky, A. *Polym. Chem.* **2011**, *2*, 2074-2083.
20. Kröger, R.; Menzel, H.; Hallensleben, M. L. *Macromol. Chem. Phys.* **1994**, *195*, 2291-2298.
21. Roth, P. J.; Jochum, F. D.; Forst, F. R.; Zentel, R.; Theato, P. *Macromolecules* **2010**, *43*, 4638-4645.
22. Huber, S.; Hutter, N.; Jordan, R. *Colloid. Polym. Sci.* **2008**, *286*, 1653-1661.
23. Qiao, Z.-Y.; Du, F.-S.; Zhang, R.; Liang, D.-H.; Li, Z.-C. *Macromolecules* **2010**, *43*, 6485-6494.
24. Jamróz-Piegza, M.; Utrata-Wesołek, A.; Trzebicka, B.; Dworak, A. *Eur. Polym. J.* **2006**, *42*, 2497-2506.
25. Honda, S.; Yamamoto, T.; Tezuka, Y. *J. Am. Chem. Soc.* **2010**, *132*, 10251-10253.
26. Qiu, X.-P.; Winnik, F. M. *Macromolecules* **2007**, *40*, 872-878.
27. Zhao, Y.; Tremblay, L.; Zhao, Y. *Macromolecules* **2011**, *44*, 4007-4011.
28. Boissiere, O.; Han, D.; Tremblay, L.; Zhao, Y. *Soft Matter* **2011**, *7*, 9410-9415.
29. Shimoboji, T.; Ding, Z. L.; Stayton, P. S.; Hoffman, A. S. *Bioconjugate Chem.* **2002**, *13*, 915-919.
30. Wang, G.; Tong, X.; Zhao, Y. *Macromolecules* **2004**, *37*, 8911-8917.
31. Tong, X.; Wang, G.; Soldera, A.; Zhao, Y. *J. Phys. Chem. B* **2005**, *109*, 20281-20287.

V Thermoresponsive hydrogels from symmetrical triblock copolymers

Amphiphilic block copolymers can form physical hydrogels under appropriate conditions.¹⁻³ Among them, symmetrical triblock copolymers BAB, with hydrophobic outer blocks B and a hydrophilic inner block A, are of particular interest in this context: The specific BAB architecture with two hydrophobic “stickers” at both ends of the polymer, induces two possibilities of chains arrangement in micelles. On the one hand, the inner block can form loops with the two hydrophobic extremities placed in the same micelle core, which at high concentration leads to gels of densely packed micelles, similar to gels of amphiphilic diblock copolymers.⁴ On the other hand, the outer blocks can be placed in two different micelle cores, while the inner block adopts a bridge conformation. Thus above a critical concentration, a gel of bridged micelles is formed. Whereas both types of organization coexist in a polymer solution, the mechanical properties result mainly from the proportion of active bridges.² This proportion depends on several molecular parameters such as the lengths of the inner and the outer blocks,⁵⁻⁷ and their respective chemical compositions.⁴ However, little is known about the influence of the latter parameter, and this adds to the difficulties to foresee, how a given polymer will behave in solution.

In this chapter, a series of BAB symmetrical triblock copolymers is described, namely polystyrene-*b*-poly(methoxy diethylene glycol acrylate)-*b*-polystyrene. These polymers are thermo-responsive by virtue of their switchable PMDEGA inner block, as reported in the Chapter 3. The focus here was set on the effects that PMDEGA inner block, and in particular the inner block length, will exert on the hydrogel mechanical properties. For better comparison, polystyrene (PS) was chosen as hydrophobic block, since BAB triblock copolymers with polystyrene outer blocks and poly(ethylene oxide),^{8, 9} poly(*N*-isopropylacrylamide),¹⁰⁻¹² or poly(acrylic acid)¹³ inner blocks have been investigated. Moreover, it was interesting to correlate the changes of the mechanical properties to the structural changes with temperature. For this purpose, temperature-resolved small-angle x-ray scattering experiments were carried out exemplarily on one of the block copolymers.

5.1. Concentration dependent thermoresponsive behavior

5.1.1. Synthesis and analysis of PS-PMDEGA-PS

Symmetrical BAB triblock copolymers were synthesized by a two steps RAFT polymerization technique using a bifunctional RAFT agent **CTA2** with the R groups placed at the extremities and the Z groups in the middle of the molecule. Styrene (S) was polymerized first, followed by MDEGA in a second step (Figure 5.1). As previously described in Chapter 2, this approach allows to keep an identical hydrophobic polystyrene block while varying the number average polymerization degree (DP_n) of the hydrophilic PMDEGA block.

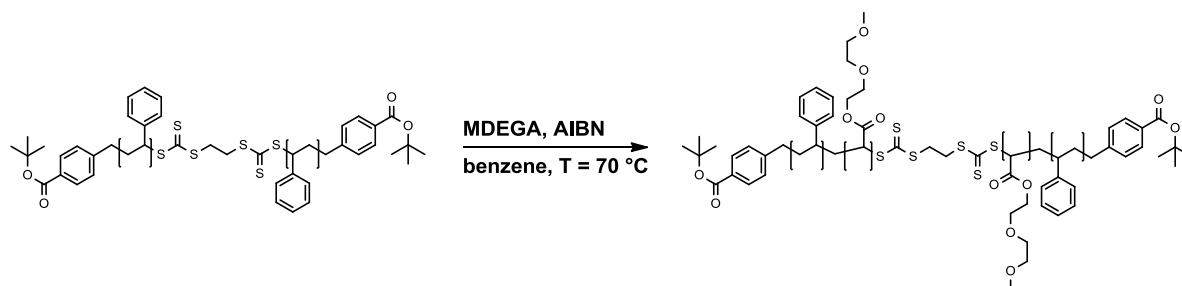


Figure 5.1: Synthesis of amphiphilic PS-PMDEGA-PS symmetrical triblock copolymers, by using a difunctional macro RAFT agents.

Five symmetrical triblock copolymers are described in following, bearing identical polystyrene end-blocks with a number average degree of polymerization $DP_n = 8$, and an inner block of PMDEGA varying from 17 to 452 DP_n . Their characteristics are summarized in Table 5.1. The analytical procedure was reported previously in Chapter 2.

All the triblock copolymers were soluble in various organic solvents such as acetone, dichloromethane, acetonitrile, benzene, toluene, dimethylformamide and tetrahydrofuran. Additionally, water was a solvent at temperatures below the respective cloud points (CP) of the polymers, with the exception of **PS8-PMDEGA17-PS8**, which was insoluble in water down to near 0 °C.

Table 5.1: Analytical data of the diblock, triblock and 3-arm star PS-PMDEGA block copolymers

polymers ^{a)}	molar mass [g·mol ⁻¹]				PDI ^{e)} (M _w /M _n)	characterization in dilute solution	
	theoret.	end-groups		SEC		R _H [nm] ^{f)}	CP [°C] ^{g)}
	M _n ^{theo b)}	M _n ^{c)}	M _n ^{d)}	M _n ^{app e)}			
PS16		2200		2300	1.09	--- ^{h)}	--- ^{h)}
PS8- PMDEGA17 -PS8	5200	5200	4000	4300	1.25	--- ^{h)}	--- ^{h)}
PS8- PMDEGA53 -PS8	12300	11500	8700	8900	1.15	5	22.1
PS8- PMDEGA93 -PS8	18700	18500	16100	15600	1.17	7	26.0
PS8- PMDEGA180 -PS8	34900	33600	28400	23900	1.17	10	30.1
PS8- PMDEGA452 -PS8	79900	81000	62400	40900	1.30	14	35.4

a) numbers indicate the number average degree of polymerization DP_n according to (c); b) conversion was determined by gravimetry; c) by ¹H-NMR analysis in acetone d₆, using the integrals of aromatic end-block signal and of the CH₃O- signal of the constitutional repeat unit; d) by UV-vis analysis in CH₂Cl₂ using the absorption coefficient ε = 13,900 L·mol⁻¹·cm⁻¹ of **CTA5**; e) in DMF, RI detection, calibrated with polystyrene standards; f) hydrodynamic radius in Millipore water, determined by DLS at concentration of 3.0 g·L⁻¹; g) cloud point determined by turbidimetry in water at concentration of 3.0 g·L⁻¹; h) samples not soluble in water

5.1.2. Collapse transition at various concentrations

The thermo-responsive and associative behavior of the triblock copolymers was first investigated in dilute aqueous solution of 3.0 g·L⁻¹. This concentration lies well above the critical micelle concentration for this type of polymers¹ (if existent at all). Small micelles with a monomodal distribution were observed by DLS. The volume average hydrodynamic radii of the micelles at ambient temperature increased from 5 to 14 nm with increasing length of the inner block (Table 5.1). These values are in the typical range found for hairy micelles of block copolymers with long hydrophilic and short hydrophobic blocks.^{14, 15} Temperature dependent DLS measurements revealed the sudden formation of large aggregates (R_H > 400 nm, volume average) above the respective transition temperatures (Figure 5.2a). Turbidimetry presented a sharp transition at the same temperature as the one observed by DLS, with a hysteresis between the cooling and the heating cycle. As described in details in Chapter 3, the cloud points increased with the length of the inner block (Figure 5.2b) due to overall hydrophilicity increase of the copolymers: for example the thermal transition was observed at 35 °C for **PS8-MDEGA452-PS8** and at 22 °C for **PS8-PMDEGA53-PS8**. This effect can be explained by the decreasing contribution of the hydrophobic end blocks and the resulting increase in the overall polymer hydrophilicity with an increase of the hydrophilic inner block. Similar results were reported with

PMDEGA homopolymers with hydrophobic end-groups¹⁶ and with poly(ethylene oxide) BAB block copolymers with hydrophobic poly(butylene oxide) end-blocks.^{17, 18} In the latter case, increasing the inner block length from 76 to 260 units, resulted in an increase of the cloud point from 12 to 25 °C.¹⁸

It was further noted that an increase in concentration from 0.3 to 30 wt. % induced a variation of cloud points, not necessarily in a monotonous way (see Figure 5.2b). For **PS8-PMDEGA53-PS8**, cloud point values decreased from 22 °C to 18 °C as the concentration increased from 0.3 to 20 wt. %, but increased at higher concentrations to reach 20 °C at 30 wt. %. **PS8-PMDEGA93-PS8** showed similar concentration dependence, but the minimum of the transition temperature was shifted to lower concentrations: the cloud point decreased first from 26 °C at 0.3 wt. % to 21 °C at 5 wt. %, above which concentration it continuously increased. In the cases of the copolymers with longer hydrophilic blocks, i.e. **PMDEGA180** and **PMDEGA452**, the cloud points steadily increased with concentration. However it cannot be excluded that a minimum occurs at a low concentration, which was not covered in this study.

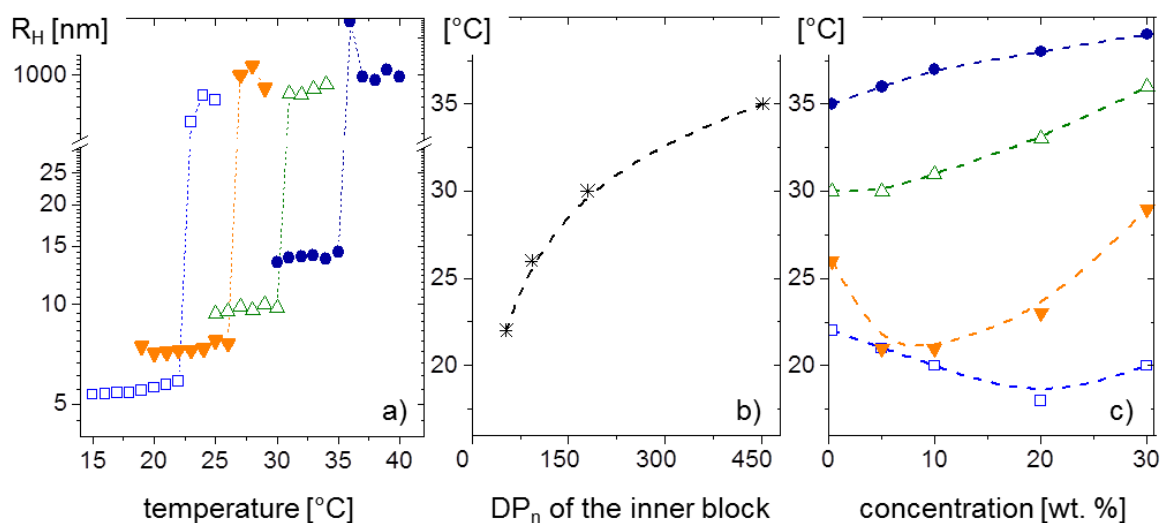


Figure 5.2: a) Hydrodynamic radii (R_H) as a function of temperature, as determined by DLS at concentration of $3.0 \text{ g}\cdot\text{L}^{-1}$, for (●) **PS8-PMDEGA452-PS8**, (Δ) **PS8-PMDEGA180-PS8**, (▼) **PS8-PMDEGA93-PS8** and (□) **PS8-PMDEGA53-PS8**. Cloud point temperatures of aqueous solutions of PS8-PMDEGA $_n$ -PS8 block copolymers b) as a function of DP_n of the inner PMDEGA block, at concentration of $3.0 \text{ g}\cdot\text{L}^{-1}$, and c) as a function of polymer concentration. Lines are guides to the eye.

Similar phase diagrams were observed or theoretically expected in other polymer solutions.¹⁹⁻²¹ However these results contrast with the very flat phase diagram of PNIPAM²² or the monotonous increase of the cloud points in PEO copolymers.^{17, 23} Possibly, the particular triblock architecture influences the evolution of the cloud point observed by us. On the one hand, the overall sensitivity of the cloud points to the length of the inner block is interesting, because different transition temperatures may be targeted via this molecular parameter. On the other hand, this behavior makes it more difficult to compare the mechanical properties of the polymers as a function of temperature, since for example, at 25 °C, not all polymers of this series are soluble in water.

5.1.3. Gel formation: a visual test

To elucidate the influence of the inner block A length on the gelation properties of the BAB copolymers, solutions of concentrations varying from 5 wt. % to 30 wt. % were prepared for each copolymer. Visual observation was possible at 21 °C for all samples with the exception of the samples **PS8-PMDEGA17-PS8** and **PS8-PMDEGA53-PS8**. Depending on the length of the inner block, different gelation concentrations were observed (Table 5.2).

Table 5.2: Gelation behavior of aqueous solution of triblock copolymers PS-PMDEGA-PS

copolymer	behavior at 5 °C ^{a)}				behavior at 21°C ^{b)}			
	polymer concentration				polymer concentration			
	5 wt%	10 wt%	20 wt%	30 wt%	5 wt%	10 wt%	20 wt%	30 wt%
PS8- PMDEGA53 -PS8	L	L	L	gel	← biphasic system →			
PS8- PMDEGA93 -PS8	L	gel	gel	gel	L	L	VL	soft gel
PS8- PMDEGA180 -PS8	L	gel	gel	gel	L	VL	soft gel	hard gel
PS8- PMDEGA452 -PS8	gel	gel	gel	gel	VL	soft gel	hard gel	hard gel

a) from rheological measurements at 5 °C, $f = 1\text{Hz}$, L = liquid when $G'' > G'$; gel when $G' > G''$

b) visually determined according to tube inversion test. L = freely flowing liquid, VL = viscous liquid (cf. experimental section for definitions).

In the case of the triblock copolymer with the longest PMDEGA block, the onset of gelation (indicated by a viscous behavior) was found at 5 wt. %, whereas for polymers with inner block

half the size and shorter, a viscous behavior was first observed at 10 wt. %. The samples gained strength with concentration, and at 30 wt. %, all soluble polymers formed a gel. To overcome the transition temperature boundaries and compare all the triblock copolymers, gelation behaviors at 5 °C are also described. The data were derived from rheological experiments and are discussed below in more details. In summary, the mechanical properties for all the viscous samples improved at 5 °C compared to observations at 21 °C. Table 5.2 shows that polymers characterized as viscous liquid at 21 °C by the visual test were found to form true gels at 5 °C by rheological experiments. At all temperatures, polymers with long inner blocks yielded gels at lower concentrations. This observation is in good agreement with theoretical expectation: loop formation of the inner block, leading to flower like micelles and competing with the bridge formation is known to be associated with an entropic penalty. This penalty increases with the length of the inner block.⁴ Long inner blocks are thus more hindered to fold back to the same micelle core and have a greater probability to bridge two different micelles.

5.2. Rheological analysis of PS-PMDEGA-PS polymers

5.2.1. Frequency sweep experiments

To further look into the gel characteristics, frequency sweeps were conducted at 20 °C and at concentration of 20 wt. % (see Figure 5.3; frequency sweep data at 10 °C for all polymers at the same concentration are given in the annex).

The dynamic oscillatory experiments provide a quantification of the elastic and the viscous components of the gel, namely of the storage modulus G' , and of the loss modulus G'' .^{24, 25} The slope of moduli values as a function of frequency allows to differentiate between liquid solutions, weak and strong gels and in a case of a gel, to determine the life time of the network junctions. For example, polymeric liquids are characterized by $G' < G''$, and scale as ω and ω^2 , respectively. Strong physically or chemically cross-linked gels are characterized by both $G' > G''$ and an almost infinite life time of their network. As a result, the frequency sweep exhibits an almost flat profile, with G' and G'' independent of the frequency.²⁴ Finally, for the intermediate case of weak gels, $G' > G''$ in the high frequency region, where the life time of the network junctions is superior to the measurement time, but this relation reverse in the low frequency region, i.e for long measurement times. The average relaxation time τ is then a key parameter to determine the life time of a network and can be taken as the inverse of the radial frequency ($\omega = 2\pi f$) at ω_c for which G' and G'' cross.²⁴

$$\tau = 1/\omega_c \text{ (s)} \quad (\text{eq. 1})$$

For all **PS8-PMDEGAN-PS8** polymers at all concentrations, G' and G'' were found frequency dependent. In the low frequency region, G'' was larger than G' , exhibiting a power law dependence of ω . G'' was scaling with ω^1 , and G' with $\omega^{1.8}$, i.e. the samples behave liquid-like. At higher frequencies, G' became larger than G'' with a much weaker frequency dependence, i.e., the samples showed a characteristic gel behavior (Figure 5.3).

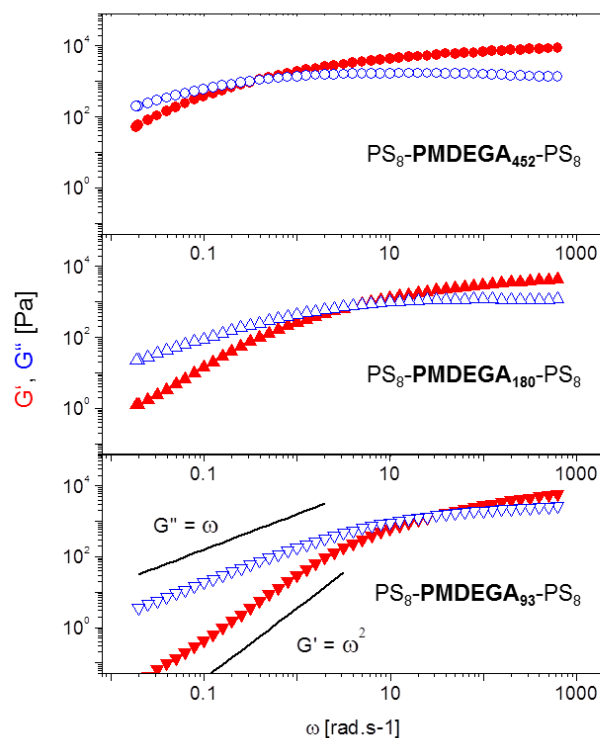


Figure 5.3: Frequency dependence of storage modulus G' (closed red symbol) and loss modulus G'' (open blue symbol) for 20 wt.% aqueous solution of copolymers at 20 °C: (●,○) **PS8-PMDEGA452-PS8**; (▲,△) **PS8-PMDEGA180-PS8**; and (▼,▽) **PS8-PMDEGA93-PS8**

Via equation (1) the relaxation time τ for the different copolymers was estimated. With increased inner block length, τ strongly increased from 0.03 s, to 0.25 s and to 1.45 s for respectively **PS8-PMDEGA93-PS8**, **PS8-PMDEGA180-PS8** and **PS8-PMDEGA452-PS8**.

Since the life time of the junctions determines the stability of a physical gel,² the influence of the inner blocks' length on the gel formation is evident. Presumably, these results reflect the enhanced possibility of polymers with long inner block to form inter-micellar bridges. A greater number of bridges increases the average life time of the network and lowers the frequency required to observe the network break down.²⁵

However, the frequency sweeps also revealed that all the gels studied are very dynamic, with a network average life time of about 1 s at best. Short average life times (\approx ms) are usually observed for BAB-like structures made of a hydrophilic inner block and low molecular mass

hydrophobic end caps, such as **C8F17** end-capped poly(ethylene oxide),²⁶ **C18** end-capped polyNIPAM²⁷ or **C12** end-capped poly(*N,N*-dimethylacrylamide).²⁸ On the one hand, the average life time τ determined here was 3 orders of magnitude higher than the one of polymers with classical low molar mass hydrophobic end-groups. On the other hand, the measured τ value was at least 3 orders of magnitude lower than the values observed for associating block polymers of the BAB type terminated with longer polystyrene end-blocks. For example, the group of Lodge examined the rheological behavior of poly(ethylene oxide) end-capped with short polystyrene block, **PS16-PEO-PS16**.^{8, 9} For a polymer concentration of 10 wt. % in an ionic liquid, no frequency dependence of G' and G'' was observed up to 40 °C, i.e., the life time of the junctions was too long to be determined experimentally. Only above 60 °C, the rheological profile presented a cross-over point and looked very similar to the one described in this work. Similar results were presented by Tsitsilianis and Iliopoulos for a 1 wt. % aqueous solution of **PS23-poly(acrylic acid)1134-PS23**.¹³

In the case of the **PS8-PMDEGAN-PS8** studied here, the polystyrene blocks have $DP_n = 8$, and are therefore 2 to 3 times shorter, than the ones in the examples cited above. The association strength of such short polystyrenes is probably weaker, thus enabling an enhanced mobility of the physical cross-links and eventually leading to bridge disruption with increasing temperature. This could be the reason why, the various gels analyzed in this work undergo a gel to sol transition even at relatively high concentration (20 wt. %) and low temperature (20 °C).

5.2.2. Temperature sweep experiments

Carrying on the thermo-responsive behavior found in dilute aqueous solution, dynamic shear moduli of the different polymers were measured during a temperature sweep from 5 °C to a temperature above the respective cloud point of the polymer solution, in a heating to cooling cycle (Figure 5.4). The rheological measurements were consistent with the previously conducted visual tests. At 20 °C and 20 wt. %, the gels identified as hard by the tube inversion test presented $G' > G''$, while for soft gels $G' \approx G''$ was found, and for viscous liquids $G' < G''$. The shortest polymer, **PS8-PMDEGA53-PS8**, exhibited a characteristic liquid-like behavior at all temperatures investigated. At 5 °C all gelling triblock copolymers had a similarly high storage modulus of around 10^4 Pa, but G' and G'' decreased significantly upon heating. This led eventually to cross points at different temperatures. The cross temperatures were taken as the gel-sol critical temperatures. They were for all the gel samples well below the cloud point, namely at 13 °C for **PS8-PMDEGA93-PS8**, at 21 °C for **PS8-PMDEGA180-PS8** and at 29 °C for **PS8-PMDEGA452-PS8**.

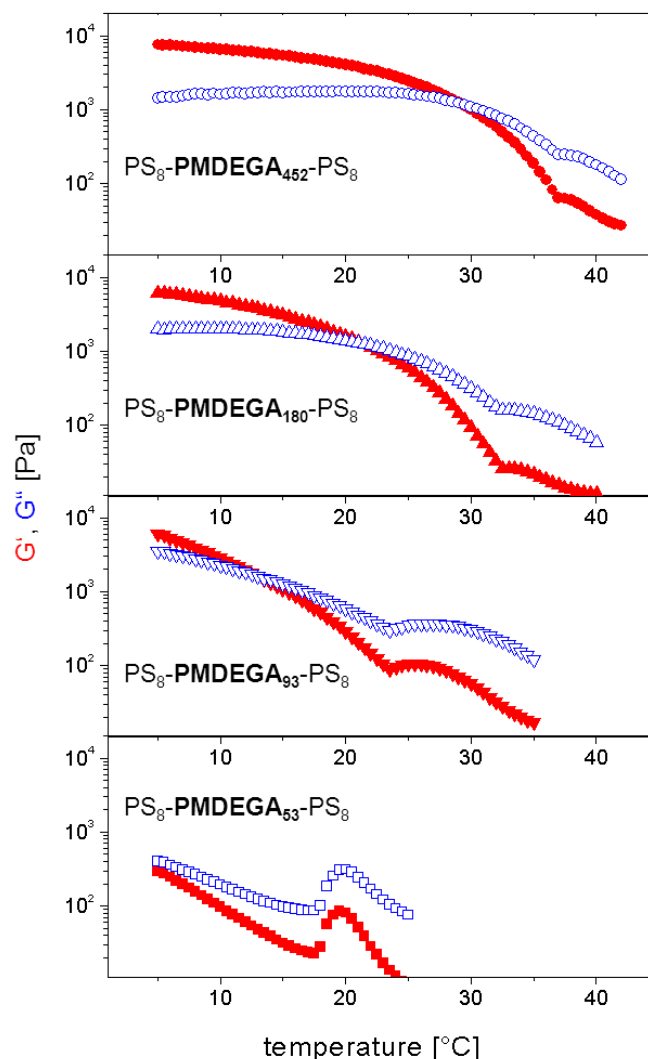


Figure 5.4: Temperature dependence of storage modulus G' (closed red symbol) and loss modulus G'' (open blue symbol) at 1 Hz frequency, for 20 wt. % aqueous solution of copolymers: (■, □) **PS8-PMDEGA53-PS8**, other symbols as in Figure 5.3.

For thermoresponsive hydrogels made of BAB triblock copolymers with switchable hydrophobic blocks, temperature induces a sharp transition from liquid to gel for LCST polymers²⁹ or from gel to liquid for UCST polymers,⁹ as the bridges get suddenly created or disrupted, respectively, upon heating. In the case of **PS8-PMDEGAN-PS8**, i.e. with a switchable hydrophilic block, one might intuitively expect a sudden transition from a gel to a freely flowing dispersion upon the collapse of the hydrophilic inner block. Instead, a smooth transition from gel to liquid developed, followed by a sudden change from a homogeneous liquid to dispersion at the cloud point. The transition from gel to sol might arise from two effects (Figure 5.5): first, the bridges between individual polymeric micelles disrupt progressively upon heating. This phenomenon has been

described for polymer solutions with permanently hydrophilic inner blocks.³⁰ The second effect might arise from the particular thermo-responsive nature of the PMDEGA inner block and lies in the gradual change in water-PMDEGA interactions with temperature (Figure 5.5).

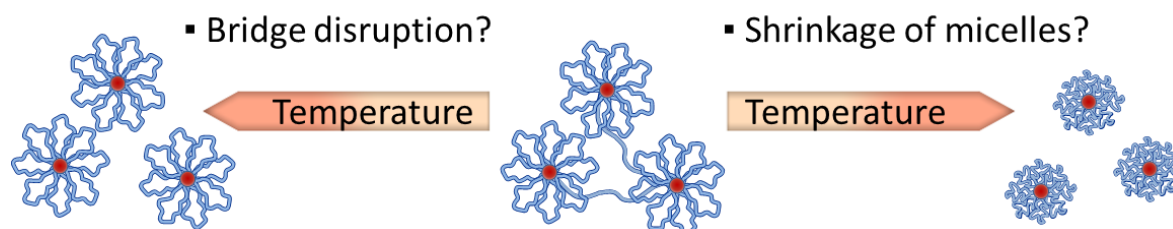


Figure 5.5: Possible mechanisms of gel-sol transition triggered by temperature

It is well known for poly(ethylene oxide) block copolymers, that with increasing temperature a progressive dehydration of the swollen polymers takes place, with a resulting contraction of the corona.^{17, 31} Considering the chemical similarity between poly(ethylene oxide) and the poly(oligo ethylene glycol acrylate), it is reasonable to expect a similar temperature dependence. The fast drop of storage modulus recorded at low temperatures for the polymers with shorter inner blocks, precisely those with the lowest LCST, might be a consequence of the progressive dehydration of their micelle shell. Figure 5.6 summarizes the phase boundaries for all four triblock copolymers. Noteworthy, the transition temperatures from gel to sol and from sol to dispersion all increased with the length of the inner block. It was thus interesting to investigate further the correlation between these two critical temperatures.

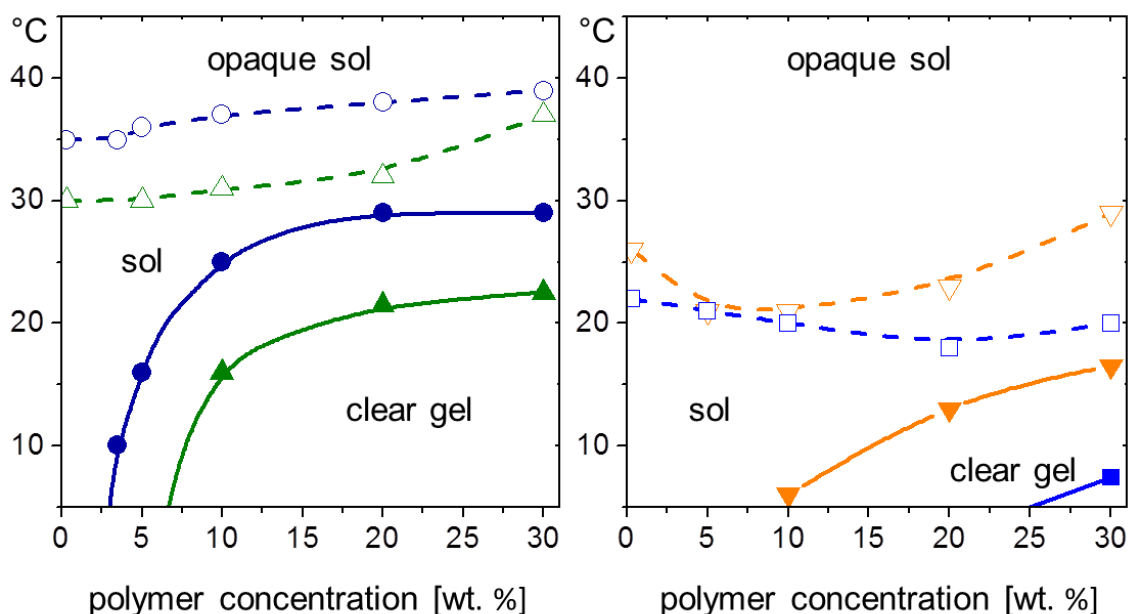


Figure 5.6: Gel-sol boundaries (closed symbols) for the polymers as function of the concentration and temperature, as determined from dynamic oscillatory experiments. Sol-dispersion boundaries (open symbols) were determined from visual test: a) (●) PS8-PMDEGA452-PS8, (▲) PS8-PMDEGA180-PS8; b) (▼) PS8-PMDEGA93-PS8 and (■) PS8-PMDEGA53-PS8. Lines are guides to the eye.

5.3. Structural characterization of the association as studied on PS8-PMDEGA452-PS8

5.3.1. Phase boundaries as determined by rheology

To learn more about the structural changes of the gels when passing the phase transitions, further analysis were done on the triblock copolymer with the longest inner block, **PS8-PMDEGA452-PS8**. Accordingly to the rheological studies, the polymer formed a gel for concentrations as low as 3.5 wt. % in the temperature range of 5 °C to 10 °C (see annex). Both the elastic and the storage moduli increased with concentration by one order of magnitude, as the concentration doubled from 5 to 10 wt. % and from 10 to 20 wt. % (Figure 5.7). This evolution is attributed to the decreasing inter-micellar distances in concentrated solutions, a fact that favors the probability of bridges between the micelles.

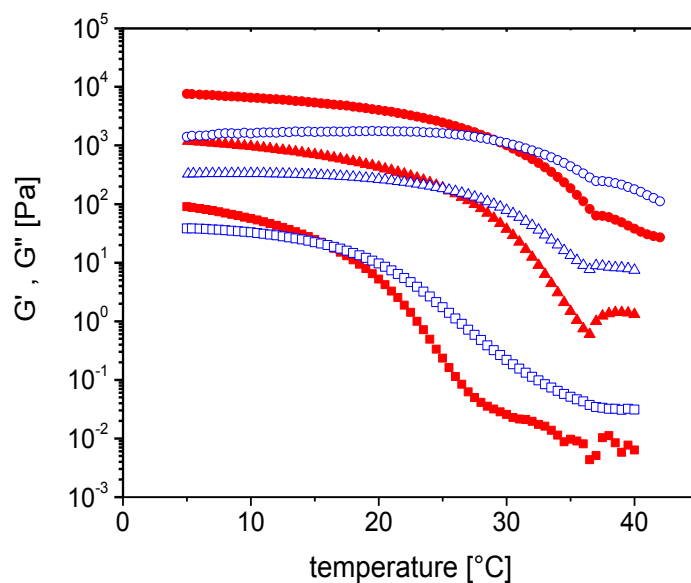


Figure 5.7: Temperature dependence of storage modulus G' (closed red symbol) and loss modulus G'' (open blue symbol) at 1Hz frequency, for aqueous solutions of **PS8-PMDEGA452-PS8** at (●, ○) 20 wt. %, (▲, △) 10 wt. %, (■, □) 5 wt. %.

Additionally, the gel-sol transition temperature increased with the concentration, namely from 16 °C to 25 °C and to 29 °C at 5 wt. %, 10 wt. % and 20 wt. %, respectively.

5.3.2. Dynamic Light Scattering in diluted solution

In order to verify whether or not in the case of PMDEGA block copolymers, shrinkage of the micelle shell takes place, the structure of **PS8-PMDEGA452-PS8** was next investigated by Dynamic Light Scattering (DLS) at concentration of $3.0 \text{ g}\cdot\text{L}^{-1}$.

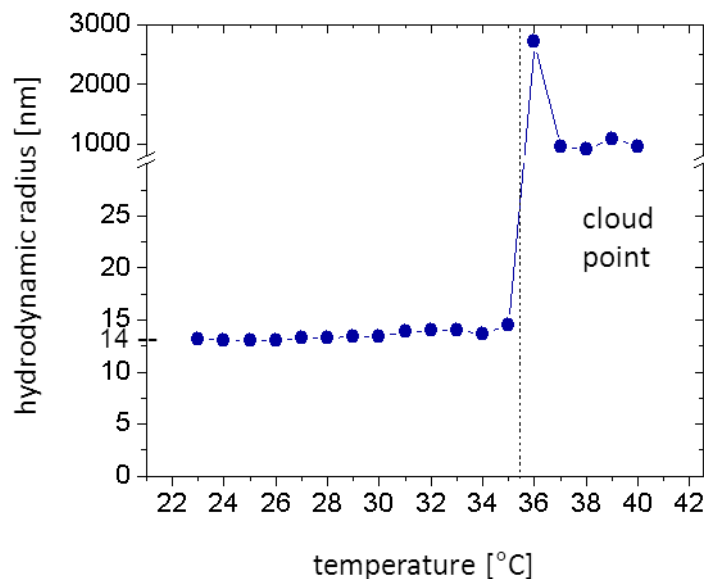


Figure 5.8: Hydrodynamic radii (R_H) as a function of temperature, as determined by DLS at concentration of $3.0 \text{ g}\cdot\text{L}^{-1}$ (0.3 wt. %) for (●) **PS8-PMDEGA452-PS8**.

The DLS data revealed that the temperature variation did not influence the value of the micelle hydrodynamic radius (R_H) below the cloud point (Figure 5.8.): micelles of about 14 nm of radius were constantly observed. At the cloud point, this value of R_H drastically increased, a transformation correlated to the formation of large aggregates of collapsed micelles. These findings did not corroborate the hypothesis of micelle dehydration and shrinkage well below the cloud point temperature. Still, to clarify if the same is true at high concentrations, temperature dependent SAXS measurements were conducted.

5.3.3. Temperature-resolved small-angle x-ray scattering (SAXS)

The temperature-resolved small-angle x-ray scattering experiments and their analysis were done by the group of Professor Christine M. Papadakis (Technische Universität München) on solutions of **PS8-PMDEGA452-PS8**, at three different concentrations, namely 5 wt. %, 10 wt. % and 20 wt. %. As the experiments were neither conducted nor analyzed by me, only the main results are reported here. The complete report is published elsewhere.³²

SAXS curves of **PS8-PMDEGA452-PS8** could be described by a model including spherical micelles with liquid-like correlation and a loose corona consisting of a solvent-swollen polymer matrix. With this model, good fits were obtained for all three concentrations and at all temperatures investigated.

In order to understand the structural changes in the polymer solution with temperature, a particular attention was given to the evolution of the micelle radius r_{mic} and to the evolution of

the volume fraction of correlated micelles ϕ . Indeed, while the first parameter can clarify the question whether or not the micelles are shrinking with temperature, the second parameter can give a hint of the bridges conservation.

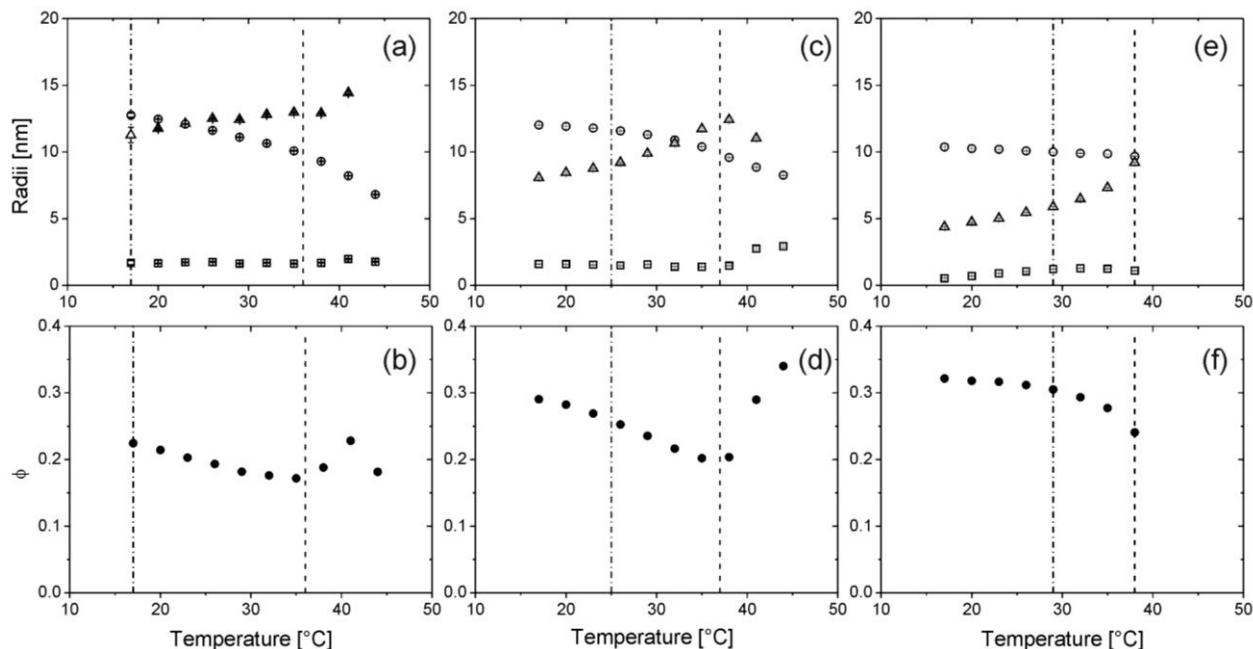


Figure 5.9: Temperature-dependent results from SAXS for 5 wt. % (a,b), 10 wt. % (c,d) and 20 wt. % (e,f). Open symbols for a), c), e): squares: correlation length ξ , triangles: r_{mic} , circles: r_{HS} . Closed symbols for b), d), f): circles. volume fraction of correlated micelles, ϕ . The dashed and dash-dotted lines mark the cloud point and the gel point from Figure 5.7.

Below the cloud point, the micelle radii r_{mic} as well as the volume fraction ϕ , were found to vary with concentration. Namely, the micelle radii decreased from an average value of 12 nm, to 10 nm and finally to a much smaller value of 6 nm, when the concentration increased from 5 wt. % to 10 wt. % and to 20 wt. % respectively. The evolution could be explained by a compression of the micelle shell with increasing amount of polymer in solution. At the same time, the volume fraction of correlated micelles ϕ became stronger with concentration reflecting, as expected from rheological measurements, a better bridging between the micelles. Interestingly, at all concentrations the values of r_{mic} did not decrease with temperature, corroborating therefore the observation done by DLS at low concentration. In the contrary, the values were found to increase. Additionally, the volume fraction of correlated micelles decreased with temperature well below the cloud point. Hence below the cloud point, the solution structure is prone to changes, namely an increase in micelle radii with a simultaneous decay of the micelle

correlation. Thus the results indicate that the gel-sol transition observed by rheology is not due to dehydration of the micelle shell but to a progressive disruption of bridges with temperature. In a previous study of analogously designed PS-PNIPAM-PS triblock copolymers, a clear correlation between mechanical properties and mesoscopic structure was observed.¹⁰ At the cloud point, important changes in the structure of the micellar network were found, with a strong and sharp decrease of the shell thickness. Interestingly here, at the cloud points, no discontinuities were observed: The distance between the micelles kept decreasing smoothly, and the correlation between micelles increased gradually. This makes an important difference of the thermo-responsive BAB triblock copolymer systems containing PMDEGA as switchable inner A block compared to the analogous system based on PNIPAM, which is widely used as model for thermo-responsive systems.

5.4. Conclusion

A series of new amphiphilic symmetrical triblock copolymers BAB was investigated, based on the thermo-responsive PMDEGA as inner block A of varying length, and bearing two short hydrophobic polystyrene outer blocks B, which allowed direct dissolution of the copolymer in water. Visual and rheological experiments of dilute and concentrated aqueous solutions were conducted to study the LCST-type phase separation, hydrogel formation and mechanical properties as function of temperature. Clearly, the behavior of the triblock copolymers is dominated by the length of the thermo-responsive inner block: At temperatures below 10 °C, the critical gelation concentration of the polymer with the longest inner block, **PS8-PMDEGA452-PS8**, was as low as 3.5 wt. %, whereas a concentration of 30 wt. % was necessary to obtain a gel from **PS8-PMDEGA53-PS8**. Noteworthy, the mechanical properties monotonously declined for all the gels with rising temperatures, leading eventually to two thermal transitions, namely from gel to liquid at temperatures well below the cloud point, and from sol to phase separated liquid at the cloud point.

SAXS data of a selected polymer were modeled successfully as micellar gel, and allowed relating the volume fraction of correlated micelles with the rheological profile. While the correlation between micelles becomes higher with concentration, it decreases already below the collapse temperature, thus indicating structural changes. As nor DLS measurements in diluted, neither SAXS in concentrated conditions, did provide evidence for progressive dehydration and shrinkage of the individual micelles with temperature, the unusual temperature dependence of the hydrogels seems to be due to a decreasing numbers of micelle bridging polymers. Though polystyrene is commonly believed to build kinetically frozen glassy micelle cores, the short PS8

blocks studied here seem to represent a good compromise for already providing sufficient hydrophobicity while still maintaining a certain mobility in aqueous self-organization.

5.5. Acknowledgements

Dr. Gabriele De Pauli and Prof. Christine Papadakis are acknowledged for the SAXS measurements of the triblock copolymer. In addition, Prof. Christine Papadakis and Prof. Peter Müller-Buschbaum are gratefully acknowledged for reviewing this chapter.

5.6. References

1. Hamley, I. W., *Block Copolymers in Solution: Fundamentals and Applications*. John Wiley & Sons Chichester (UK), 2005.
2. Chassenieux, C.; Nicolai, T.; Benyahia, L. *Curr. Opin. Colloid Interface Sci.* **2011**, *16*, 18-26.
3. Tsitsilianis, C. *Soft Matter* **2010**, *6*, 2372-2388.
4. Giacomelli, F. C.; Riegel, I. C.; Petzhold, C. L.; da Silveira, N. P.; Stepanek, P. *Langmuir* **2008**, *25*, 731-738.
5. Semenov, A. N.; Joanny, J. F.; Khokhlov, A. R. *Macromolecules* **1995**, *28*, 1066-1075.
6. Balsara, N. P.; Tirrell, M.; Lodge, T. P. *Macromolecules* **1991**, *24*, 1975-1986.
7. Nguyen-Misra, M.; Mattice, W. L. *Macromolecules* **1995**, *28*, 1444-1457.
8. He, Y.; Boswell, P. G.; Bühlmann, P.; Lodge, T. P. *J. Phys. Chem. B* **2006**, *111*, 4645-4652.
9. He, Y.; Lodge, T. P. *Macromolecules* **2007**, *41*, 167-174.
10. Bivigou-Koumba, A.; Görnitz, E.; Laschewsky, A.; Müller-Buschbaum, P.; Papadakis, C. *Colloid. Polym. Sci.* **2010**, *288*, 499-517.
11. Nykänen, A.; Nuopponen, M.; Laukkanen, A.; Hirvonen, S.-P.; Rytelä, M.; Turunen, O.; Tenhu, H.; Mezzenga, R.; Ikkala, O.; Ruokolainen, J. *Macromolecules* **2007**, *40*, 5827-5834.
12. Nykänen, A.; Nuopponen, M.; Hiekkataipale, P.; Hirvonen, S.-P.; Soininen, A.; Tenhu, H.; Ikkala, O.; Mezzenga, R.; Ruokolainen, J. *Macromolecules* **2008**, *41*, 3243-3249.
13. Tsitsilianis, C.; Iliopoulos, I. *Macromolecules* **2002**, *35*, 3662-3667.
14. Hamley, I. W., In *Block Copolymers in Solution: Fundamentals and Applications*, Wiley-VCH Verlag GmbH & Co. KGaA: 2005.
15. Riess, G. *Prog. Polym. Sci.* **2003**, *28*, 1107-1170.
16. Hua, F.; Jiang, X.; Li, D.; Zhao, B. *J. Polym. Sci., Part A: Polym. Chem.* **2006**, *44*, 2454-2467.
17. Kelarakis, A.; Havredaki, V.; Yuan, X.-F.; Chaibundit, C.; Booth, C. *Macromol. Chem. Phys.* **2006**, *207*, 903-909.
18. Liu, T.; Nace, V. M.; Chu, B. *J. Phys. Chem. B* **1997**, *101*, 8074-8078.
19. Kujawa, P.; Segui, F.; Shaban, S.; Diab, C.; Okada, Y.; Tanaka, F.; Winnik, F. M. *Macromolecules* **2006**, *39*, 341-348.
20. Lee, H.-N.; Lodge, T. P. *J. Phys. Chem. Lett.* **2010**, *1*, 1962-1966.
21. Jung, J. G.; Bae, Y. C. *J. Polym. Sci. Part B* **2010**, *48*, 162-167.
22. Aseyev, V.; Tenhu, H.; Winnik, F. *Adv. Polym. Sci.* **2006**, *196*, 1-85.
23. Rackaitis, M.; Strawhecker, K.; Manias, E. *J. Polym. Sci., Part B: Polym. Phys.* **2002**, *40*, 2339-2342.
24. Tadros, F. T., *Rheology of Dispersions: Principles and Applications*. Wiley-VCH Verlag Weinheim (Germany), 2010.
25. Rubinstein, M.; Colby, R. H., *Polymer Physics*. Oxford, 2003.
26. Xu, B.; Li, L.; Yekta, A.; Masoumi, Z.; Kanagalingam, S.; Winnik, M. A.; Zhang, K.; Macdonald, P. M.; Menchen, S. *Langmuir* **1997**, *13*, 2447-2456.
27. Kujawa, P.; Watanabe, H.; Tanaka, F.; Winnik, F. M. *Eur. Phys. J. E Soft Matter*. **2005**, *17*, 129-137.
28. Malo de Molina, P.; Herfurth, C.; Laschewsky, A.; Gradzielski, M. *Progr. Colloid Polym. Sci.* **2011**, *138*, 67-72.
29. Kirkland, S. E.; Hensarling, R. M.; McConaughy, S. D.; Guo, Y.; Jarrett, W. L.; McCormick, C. L. *Biomacromolecules* **2007**, *9*, 481-486.
30. Hietala, S.; Mononen, P.; Strandman, S.; Järvi, P.; Torkkeli, M.; Jankova, K.; Hvilsted, S.; Tenhu, H. *Polymer* **2007**, *48*, 4087-4096.
31. Lee, D. S.; Shim, M. S.; Kim, S. W.; Lee, H.; Park, I.; Chang, T. *Macromol. Rapid Commun.* **2001**, *22*, 587-592.
32. Miasnikova, A.; Laschewsky, A.; De Paoli, G.; Papadakis, C. M.; Müller-Buschbaum, P.; Funari, S. S. *Langmuir* **2012**, accepted.

VI Making gels stronger: influence of the length and the number of end-blocks

In the previous chapter, the length of the inner block was shown to influence notably the gelation of symmetrical PS-PMDEGA-PS triblock copolymers. In particular, when the inner block was long, a lower minimal amount of polymer was needed to induce gelation, and these gels could better withstand variations of temperature. However, even the strongest gel made of **PS8-PMDEGA452-PS8**, exhibits a gel-to-sol transition below 30 °C. In order to improve the resistance of the gels to temperature, the architecture of the polymers was therefore modified, following two different approaches (see Figure 6.1).

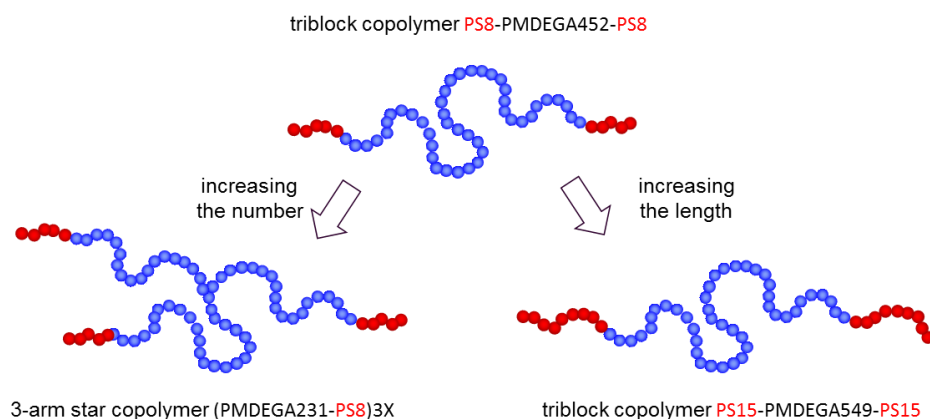


Figure 6.1: Schematical representation of two strategies to strengthen the mechanical stability of hydrogels of symmetrical triblock **PS8-PMDEGA452-PS8**.

Hypothesizing that the high mobility of the short PS8 hydrophobic outer blocks is responsible for the gel to sol transition, the number of end blocks was increased in a first approach, by synthesizing a 3-arm star copolymer of PS and PMDEGA. Compared to linear triblock copolymers, the 3-arm star topology presents an additional hydrophobic end-block functionality, and should promote a more efficient network building. Indeed, studies of the self-assembly of star copolymers into hydrogels systematically reported low critical gel concentrations.¹⁻⁴ However, reports dealing with the architecture's influence on gelation are rare⁵⁻⁹ and even more so on gelation of polymers with small hydrophobic end-blocks.^{8,9} In this context, it was interesting to find out to which extent an additional end-block can improve the mechanical integrity of the gels made of the copolymers of PS and PMDEGA. Moreover, to complete the topological

investigation, the rheological behavior of the triblock and the 3-arm star block copolymers was compared to the behavior of a diblock copolymer of the same composition.

As the rheological behavior of the transient network depends on both the amount and the lifetime of the bridges,¹⁰ a second strategy to act upon the gels' stability was increasing the length of the hydrophobic outer blocks within the triblock architecture. By doing so, the strength of the hydrophobic interactions is increased, which in turn should decrease the mobility of the hydrophobic junctions. The targeted improved stability towards thermal stress should therefore be easily gained.^{1,8} However, by increasing the length of the outer blocks, a frozen system might be formed so that the dynamic character of the gels gets lost. Furthermore, when the strength of the hydrophobic interactions is very high, the amphiphilic system is expected to phase separate, leading to heterogeneous dispersions.¹¹

Keeping in mind these difficulties, a new triblock copolymer **PS15-PMDEGA549-PS15** was synthesized, in which the length of the hydrophobic PS block was nearly doubled in comparison to the reference triblock copolymer **PS8-PMDEGA452-PS8**. The synthesis and analysis of **PS15-PMDEGA549-PS15** followed the procedures and experimental setups described in Chapter 2. The rheological behavior of these two polymers and of the 3-arm star analogue as well as of the "parent" diblock copolymer was compared. Thus, a set of four amphiphilic block copolymers was studied in the following. Their characteristics are compiled Table 6.1.

Table 6.1: Analytical data of the diblock, triblock and 3-arm star PS-PMDEGA block copolymers

polymers ^{a)}	molar mass [g·mol ⁻¹]				PDI ^{e)} (M _w /M _n)	cloud points in dilute solution [°C] ^{f)}
	theoret. M _n ^{theo b)}	end-groups M _n ^{c)} M _n ^{d)}		SEC M _n ^{app e)}		
diblock BA PS11-PMDEGA275	36700	49100	47000	33200	1.29	39
triblock BAB PS8-PMDEGA452-PS8	79900	81000	62400	40900	1.30	35
PS15-PMDEGA549-PS15	96900	99200	88100	49300	1.32	37
3-arm star block (AB) ₃ (PMDEGA231-PS8)_{3x}	120800	123800	91600	51400	1.32	34

a) numbers indicate the number average degree of polymerization DP_n according to (c); b) conversion was determined by gravimetry; c) by ¹H-NMR analysis in acetone d₆, using the integrals of aromatic end-block signal and of the CH₃O- signal of the constitutional repeat unit; d) by UV-vis analysis in CH₂Cl₂ using the absorption coefficient ε = 13,900 L·mol⁻¹·cm⁻¹ of **CTA5**; e) in DMF, RI detection, calibrated with polystyrene standards; f) cloud point determined by turbidimetry in water at concentration of 3.0 g·L⁻¹

6.1. Influence of polymer topology on gelation

6.1.1. Comparison of triblock and diblock copolymers

As previously mentioned, the gelation of triblock copolymers with hydrophobic outer blocks occurs by bridging of separate micelles, but can also be due to the jamming of micelles, or to a combination of both effects.¹² Differently, the gelation of diblock copolymers is due to jamming only, and occurs usually at higher concentrations of about 30 wt. %.¹³⁻¹⁵ However, much lower critical gelation concentrations are sometimes reported,¹¹ with viscosity build-up at already 10 to 14 wt. %, ^{16, 17} which is explained by the formation of worm-like aggregates capable of more efficient jamming than spherical micelles.¹⁷ Thus jamming can have a significant contribution to the viscosity of a micelles solution and it was interesting to see whether or not it is the case for **PS-PMDEGA** diblock copolymers. Moreover, a comparison between the gelation behavior of diblock and the triblock copolymers allows to determine to which extent jamming contributes to the gelation behavior of the latter. For these reasons, the rheological analysis of **PS8-PMDEGA452-PS8** triblock was compared with the analysis of a diblock copolymer of similar composition, namely **PS11-PMDEGA275**.

Carrying on the temperature dependent rheological measurements conducted on **PS8-PMDEGA452-PS8**, dynamic shear moduli were measured for the diblock copolymer solutions during a temperature sweep from 5 °C to 46 °C, at concentrations of 20 and 40 wt. % (Figure 6.2). At all temperatures and both concentrations investigated, the values of the storage modulus G' were lower than the values of the loss modulus G'' . Therefore **PS11-PMDEGA275** exhibited a characteristic liquid-like behavior.¹⁸ This behavior was clearly different from **PS8-PMDEGA452-PS8**, which at concentration of 20 wt.% self-assembled into a hard gel (Figure 5.4). Additionally, at 5 °C and 20 wt. %, the storage modulus G' of **PS8-PMDEGA452-PS8** was of about 10^4 Pa, while under the same conditions, the storage modulus of **PS11-PMDEGA275** was of only 10 Pa. Thus, the gelling ability of the diblock copolymer **PS11-PMDEGA275** was found significantly poorer than the one of any symmetrical triblock copolymer studied here.

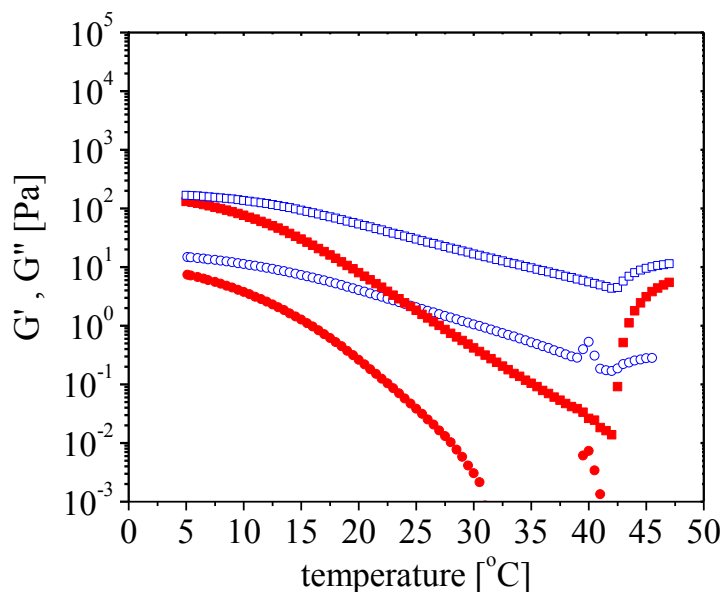


Figure 6.2: Temperature dependence of storage modulus G' (closed red symbols) and loss modulus G'' (open blue symbols) at 1 Hz frequency, for aqueous solutions of the diblock copolymer **PS11-PMDEGA275** at (■, □) 40 wt. %; (●, ○) 20 wt. %.

The rheology of concentrated micellar solutions is based on the repulsion between the hydrophilic coronas, which depends on the aggregation number^{13, 19} and the strength of repulsion between the hydrophilic polymer chains.¹¹ This in turn depends on the length and the nature of the hydrophobic and hydrophilic blocks. With DP_n 11, the hydrophobic block of **PS11-PMDEGA275** is small, and consequently the aggregation number of the polymer is expected to be low.²⁰ Therefore, the fact that **PS11-PMDEGA275** was unable to build gel up to high concentrations, can be explained by the low repulsion between the micelles, due to the low aggregation number or alternatively, to the chemical nature of PMDEGA. This poor gelation ability is not an isolated case. Analogous results have been reported on solutions of diblock copolymers with even bigger hydrophobic blocks, and probably larger aggregation numbers.^{21, 22} By comparison, it becomes evident that the gelation in PS/PMDEGA block copolymers with more than one hydrophobic PS end-block, is not due to jamming to any extent, but exclusively to bridging between the aggregates.

Note that several diblock copolymers were synthesized during this thesis, all bearing identical short polystyrene block and PMDEGA blocks of various lengths. The molecular characteristics of 5 diblocks, including **PS11-PMDEGA275** are reported in Chapter 3 (Table 3.2). Analogously to **PS11-PMDEGA275**, temperature dependent rheological measurements were carried out for all the polymers, in the hope to detect any influence of the length of PMDEGA block on their

gelation ability. An identical behavior to the one reported here was usually observed: independently of the PMDEGA block length, the diblock copolymers were found unable to build gel. However, for two diblock copolymers, namely **PS11-PMDEGA101** and **PS11-PMDEGA331**, irregularities were detected, consisting in gel formation at respectively 30 wt. % and 10 wt. %. This behavior seemed somehow accidental, as solutions of shorter and longer polymers were consistently able to flow. Hence, it is possible that the abnormal behavior of the two polymers was due to a poorer quality of the samples. Indeed, even during controlled RAFT polymerization, termination reactions by chain coupling may occur.²³ When the hydrophobic block is polymerized first and the hydrophilic second, as it is the case here, the coupling results in the formation of symmetrical triblock copolymers, bearing two polystyrene outer blocks. Yet, a small percentage of triblock copolymers is sufficient to bridge micelles of diblock copolymers, so that their presence can lead to gelation.²⁴ Therefore, it is assumed that the gelation of **PS11-PMDEGA101** and **PS11-PMDEGA331** probably results from contaminations, too small to be detected by analytical methods, of these two particular samples by symmetrical triblock copolymers.

It is possible to avoid this type of contamination by polymerizing the hydrophilic block first and the hydrophobic block last. Again in this case, the eventual radical coupling will result in the formation of a triblock copolymer, but this time the hydrophobic block will be placed in the middle of the macromolecule. The self-assembly and gelation behavior of this triblock copolymer are very similar to regular diblock copolymers and should therefore hardly influence the gelation of the whole sample.²⁵

6.1.2. Comparison of triblock and 3-arm star copolymers

The topological effect on gelation was investigated next by comparing the rheology of a 3-arm star block copolymer with the rheology of the linear triblock copolymer **PS8-PMDEGA452-PS8**. The motivation for this work originated from the results published by Hietala et al.,²⁶ on the rheology of a 4-arm star copolymer of polystyrene and poly(acrylic acid). For a 3 wt. % sample of **(PAA54-PS6)_{4x}**, the gel to sol transition was observed at 38 °C,²⁶ thus significantly higher than for a 3.5 wt. % gel of **PS8-PMDEGA452-PS8**, where the transition took place at 10 °C. Hence, despite a shorter polystyrene block, the 4-arm star architecture seemed to confer a better stability to the gel. Although copolymers made of a polyelectrolyte build stronger elastic gels and at lower concentration than neutral amphiphiles, because the charged inner block inhibit the loop formation of the inner block,²⁷ it was interesting to find out if comparable improvements can be

achieved with a star copolymer made of PS and PMDEGA. For this purpose, a 3-arm star copolymer, **(PMDEGA231-PS8)_{3X}**, was synthesized, with a comparable composition to the previously studied triblock **PS8-PMDEGA452-PS8**.

Similar to the triblock copolymer **PS8-PMDEGA452-PS8**, the new star copolymer was easily dispersible in water at room temperature and in the cold. Also similar, the 2 wt. % sample exhibited a liquid-like behavior, while gel formation was observed first at the concentration of 3.5 wt. %. Thus, although the exact value was not determined, the star architecture seemed to have a reduced effect, if any, on the minimal concentration required for the gelation.

To find out whether or not the number of arms improved the mechanical stability of the gels, solutions of **(PMDEGA231-PS8)_{3X}** were prepared with concentrations varying from 3.5 wt. % to 20 wt. % and the dynamic shear moduli of the different samples measured. Depending on the concentration, divergences from the rheological behavior of the symmetrical triblock were observed (Figure 6.3).

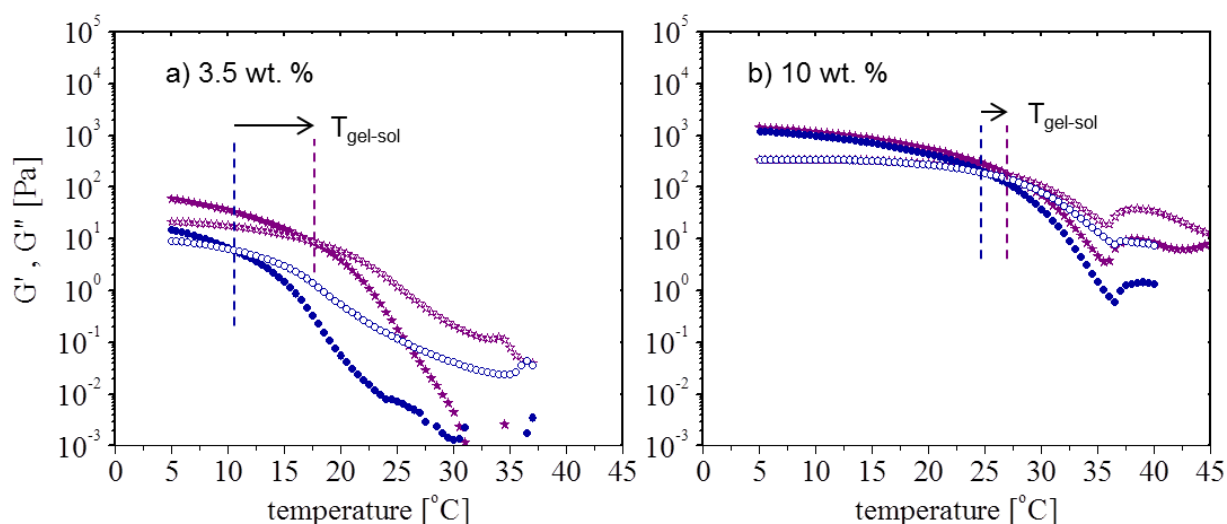


Figure 6.3: Temperature dependence of storage modulus G' (closed symbol) and loss modulus G'' (open symbol) at 1 Hz frequency, for aqueous solutions of (●,○) **PS8-PMDEGA452-PS8** and (★,★) **(PMDEGA231-PS8)_{3X}**. a) at concentration of 3.5 wt. %; b) at concentration of 10 wt. %.

At the concentration of 3.5 wt. %, the values of both storage and loss moduli were significantly higher for the gel made of the star polymer than for the gel of the linear triblock. For example at 5 °C, G' was 14 Pa for **PS8-PMDEGA452-PS8**, and 60 Pa for **(PMDEGA231-PS8)_{3X}**. Moreover, although hydrogels made from the star polymer melted with temperature, compared to analogous gel of triblock copolymer, the melting temperatures were notably displaced to higher values, at low concentrations. Thus, for gels built by the star polymer, the stability gain was of 7 °C and 5 °C at concentrations of 3.5 wt. % and 5 wt. %, respectively (Figure 6.3a and

Figure 6.4). However, when the concentration was increased, the differences between the gelation behaviors of the two copolymers became marginal. Already at 10 wt. %, neither the strength of the moduli, nor the melting temperature (with a difference of only 2 °C) was changed much between the triblock and star topology. Figure 6.4 summarizes the phase boundaries of **PS8-PMDEGA452-PS8** and **(PMDEGA231-PS8)_{3X}** block copolymers. Considering the data, it becomes clear that the topological effect was significant at concentrations below 5 wt. % and became reduced and nonexistent for concentrations of 10 wt. % and above.

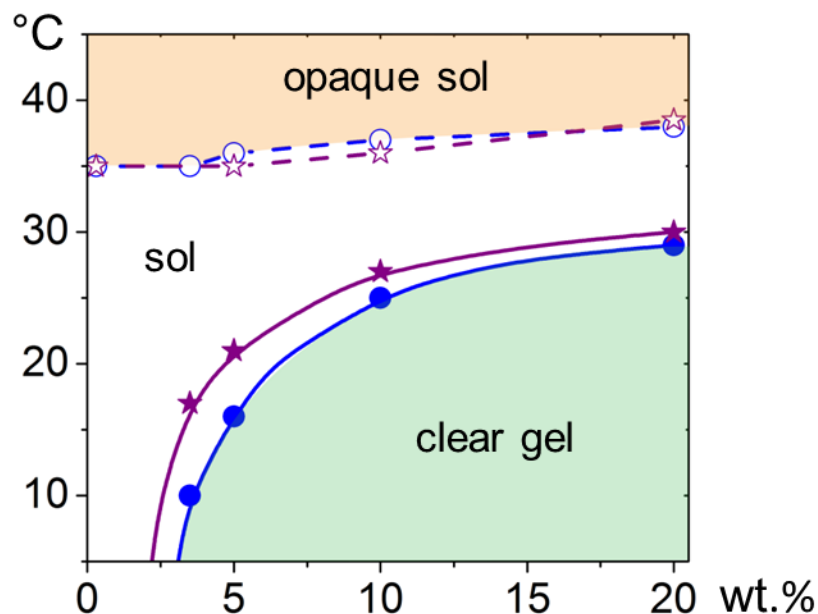


Figure 6.4: Gel-sol boundaries (closed symbols) for the polymers as function of the concentration and temperature, as determined from dynamic oscillatory experiments. Sol-dispersion boundaries (open symbols) were determined from visual test: (●,○) **PS8-PMDEGA452-PS8**, (★,☆) **(PMDEGA231-PS8)_{3X}**. Lines are guides to the eye.

These findings can be explained by the different ability of the two polymers to build intermicelles bridges. At low concentration, the 3-arm star topology favors the formation of bridges, whereas for the linear triblock copolymer, the loop conformation of the chains is predominant. The supplementary number of junctions in the network of the star **(PMDEGA231-PS8)_{3X}**, leads to stronger gels with a notably better resistance to temperature. When the concentration is increased, so is the fraction of elastically active bridges in both gels of star and triblock copolymers, and the network is rapidly saturated. Thus, any further increase of concentration, as well as any increase of the number of arms, seems to barely influence the rheological behavior of the gels. Although significant at low concentration, the effect of architecture is negligible at high, and the gel of star polymer **(PMDEGA231-PS8)_{3X}**, analogously to the gel of the triblock

polymer **PS8-PMDEGA452-PS8**, melt at the same temperature, when the association strength of the short polystyrenes blocks becomes weaker. Thus, 30 °C seems to be the highest temperature that the physical cross-links made of short PS8 end-blocks can withstand, regardless of the topology of the polymer. To further improve the stability of the gel, the length of the hydrophobic block was therefore increased.

6.2. Influence of the hydrophobic block length

6.2.1. Triblock copolymers design

In a telechelic architecture, longer hydrophobic blocks confer a greater strength to the associative interactions.^{1, 8} However, most of such polymers reported so far are kinetically frozen, i.e. unable to rearrange in the experimental time frame and to self-assemble into homogeneous micelles or homogeneous gels at room temperature.²⁸ To overcome the dissolution barrier, samples of amphiphilic block copolymers bearing long hydrophobic blocks are usually prepared by equilibration at about 80 °C.^{8, 29, 30} However, in the case of polymers made of the thermo-responsive PMDEGA, this procedure cannot be applied, as heating at such high temperatures will result in unwanted phase separation. Thus, increasing the polystyrene block length for PMDEGA copolymers is not without difficulties and the blocks were purposely kept small throughout this thesis, in order to achieve spontaneous dissolution in water. Ideally, the hydrophobic PS blocks of the new triblock copolymer should be small enough to allow a spontaneous dissolution, but long enough to give the polymer the targeted thermal stability. In previous investigations on triblock copolymers, **PS11** was found too short to significantly increase the gel-sol transition temperature³¹, while **PS23** was too long for the polymer to be dissolved.³⁰ Thus, **PS15**, a block of intermediate length, was chosen, and incorporated in the triblock copolymer **PS15-PMDEGA549-PS15**. Its rheological behavior is compared in the following with the behavior of the reference polymer **PS8-PMDEGA452-PS8**.

6.2.2. Frequency sweep experiments

Unfortunately, when **PS15-PMDEGA549-PS15** was dispersed in water at the concentration of 3.0 g.L⁻¹, an inhomogeneous solution of swollen aggregates was obtained that persisted after 2 days of heating at 30 °C. Therefore, acetone was used as co-solvent to prepare the various solutions of the copolymer, and was subsequently removed by evaporation at room temperature. Although more cumbersome, this procedure yielded homogeneous samples.

In analogy to the reference triblock **PS8-PMDEGA452-PS8** and to the star block copolymer **(PMDEGA231-PS8)_{3X}**, solutions of **PS15-PMDEGA549-PS15** were prepared with concentrations varying from 2 wt. % to 20 wt. %. Again, gel formation was first observed for concentrations above 3.5 wt. %.

At first, frequency sweeps were conducted at 20 °C and at the concentration of 3.5 wt. % for the three block copolymers **PS15-PMDEGA549-PS15**, **(PMDEGA231-PS8)_{3X}** and **PS8-PMDEGA452-PS8**. Under these conditions, all the polymers were capable to self-assemble into micelles, but not necessarily yet into hydrogels. Indeed, notable differences in their response to shearing were observed. The data are presented in Figure 6.5.

The two **PS8** end-capped polymers behaved analogously, as for both, G' and G'' markedly varied with frequency, exhibiting a power law dependence of ω in the low to intermediate frequencies regions. Whereas at all frequencies, G'' was larger than G' in the case of the triblock copolymer, G' became larger than G'' at higher frequencies in the case of the star block copolymer. As a consequence, at 20 °C and concentrations of 3.5 wt.%, the triblock copolymer **PS8-PMDEGA452-PS8** presented a liquid-like behavior, whereas the star copolymer **(PMDEGA231-PS8)_{3X}** behaved as a weak gel. Following the discussion of chapter 5, a relaxation time τ of 80 ms was determined from the crossover frequency.

Differently, in the case of the triblock **PS15-PMDEGA549-PS15**, G' was larger than G'' , and both G' and G'' showed a much weaker frequency dependence. Accordingly, the polymer end-capped by the larger PS15 blocks formed a strong gel, behaving similar to gels made by chemical crosslinking. However, the frequency dependence of both moduli was not parallel, indicating some residual mobility of the cross-links at 20 °C. By linear extrapolation, a crossover frequency of $1.75 \cdot 10^{-6} \text{ rad} \cdot \text{s}^{-1}$ was calculated, which corresponds to a relaxation time τ of more than 6 d.

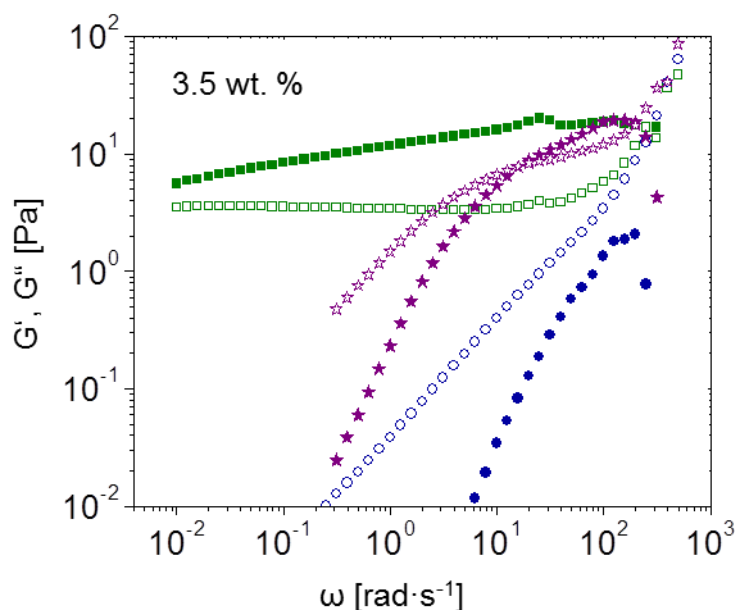


Figure 6.5: Frequency dependence of storage modulus G' (closed symbol) and loss modulus G'' (open symbol) for 3.5 wt. % aqueous solution of copolymers at 20 °C: (■, □) PS15-PMDEGA549-PS15; (★, ★) (PMDEGA231-PS8)_{3x} and (●, ○) PS8-PMDEGA452-PS8.

Thus, compared to the linear PS8-PMDEGA452-PS8, the star architecture could generate enough cross-links at 3.5 wt. %, to allow the structure to hold at 20 °C. However due to the high mobility of PS8 end-blocks, the cross-links were easily broken by shearing. In the case of the linear PS15-PMDEGA549-PS15 at the same concentration, the structure could withstand even high frequencies. This can be explained by the strong associations of the PS15 outer blocks, as indicated by their strongly increased average relaxation time of over 6 days.

6.2.3. Investigation in concentrated solution

Carrying on the comparison, dynamic shear moduli of PS15-PMDEGA549-PS15 at two concentrations were measured during a temperature sweep from 5 °C to 42 °C (Figures 6.6 and 6.7). The behavior of the triblock copolymer differed notably from the one of the copolymers bearing shorter hydrophobic blocks.

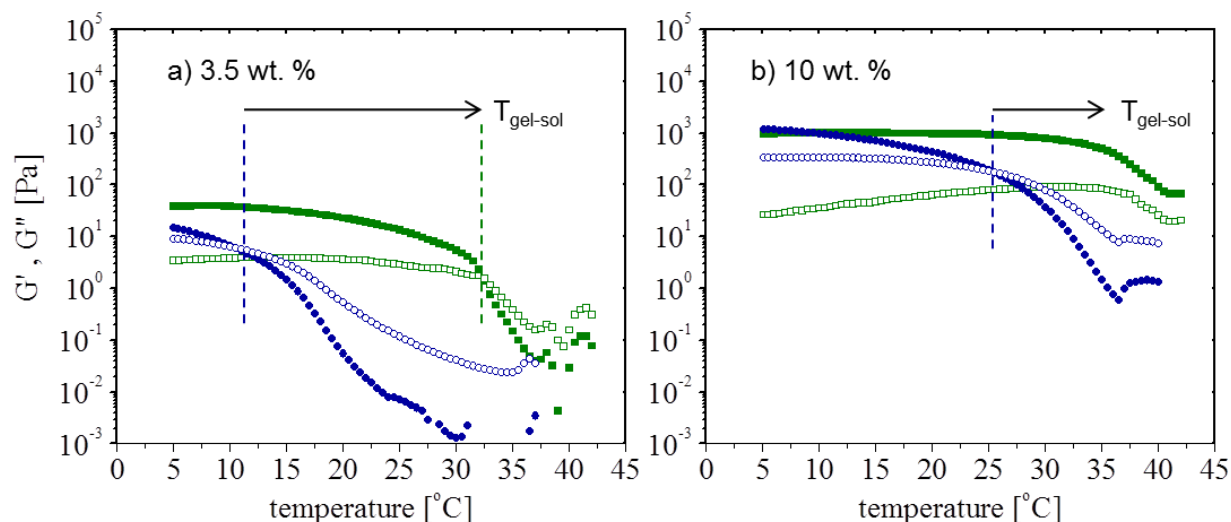


Figure 6.6: Temperature dependence of storage modulus G' (closed symbol) and loss modulus G'' (open symbol) at 1 Hz frequency, for aqueous solution of (●,○) **PS8-PMDEGA452-PS8** and (■,□) **PS15-PMDEGA549-PS15**. a) at concentration of 3.5 wt. %; b) at concentration of 10 wt. %.

Whereas hydrogels made of polymers bearing short PS8 blocks always melted at temperatures below 30 $^{\circ}\text{C}$, the storage modulus G' remained largely constant for the gel made of **PS15-PMDEGA549-PS15** (Figure 6.5). Transitions from gel to sol were only observed at low concentrations of 3.5 wt. % and 5 wt. %, and occurred at much higher temperatures than in the case of the triblock or the star block copolymers with the short end caps, namely at 32 $^{\circ}\text{C}$ and 36 $^{\circ}\text{C}$ (Figure 6.6). For concentrations above 5 wt. %, the gel-to-sol transition disappeared. Instead, G' barely decayed with temperature below 35 $^{\circ}\text{C}$, and its value decreased only at temperatures close to the cloud point of the sample. Noteworthy, at concentrations above 5 wt. %, solutions of **PS15-PMDEGA549-PS15** remained viscoelastic even in the collapse state. This was never observed with copolymers of PMDEGA bearing shorter hydrophobic blocks, and can presumably be correlated to the formation of more hydrophobic, compact aggregates.

Thus, compared to the analogous polymer bearing PS8 termini, PS15 blocks did in fact confer a greater stability to the hydrogels of **PS15-PMDEGA549-PS15**. From frequency sweep and temperature sweep experiments, it becomes obvious that tighter association takes place, and that the blocks are less prone to exchange even at elevated temperatures. At concentrations above 5 wt. %, the sample remained in a gel state throughout the collapse transition, i.e. the mechanical properties of the gel were no more responsive to the thermal collapse of the inner block. Noteworthy, subsequent cooling of the samples (at 2, 3.5 and 5 wt. %) below the cloud point resulted in transparent gels with higher moduli than observed during the heating cycle and in turbid solution at 3.0 $\text{g}\cdot\text{L}^{-1}$ (see annex). Thus, the structural rearrangement after switching was

markedly slowed down compared to the behavior of **PS8-PMDEGAn-PS8** polymers. Presumably, in diluted and semi-diluted conditions, the hydrophobic associations can rearrange to some extent, when the sample is heated in the collapsed state, and the new structure is fixed by the decrease of temperature.

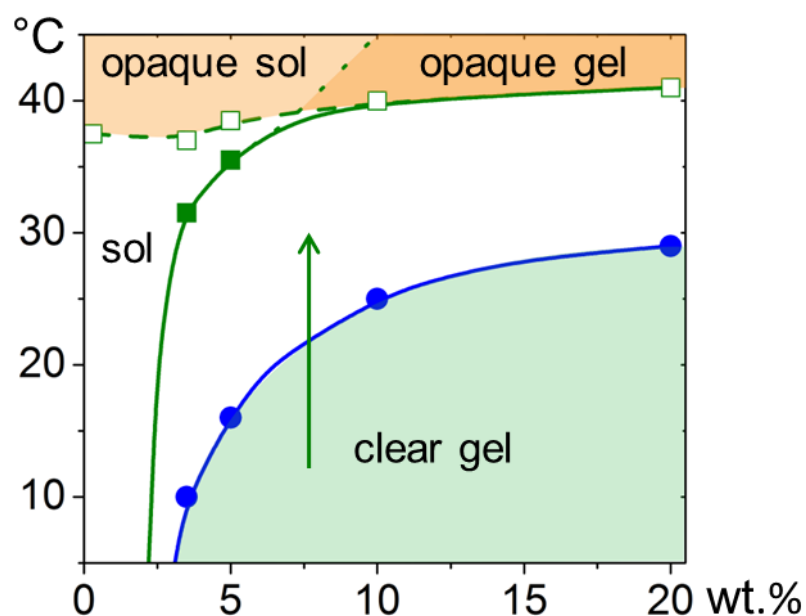


Figure 6.7: Gel-sol boundaries (closed symbols) for the polymers as function of the concentration and temperature, as determined from dynamic oscillatory experiments. Sol-dispersion boundaries (open symbols) were determined from visual test: (■, □) **PS15-PMDEGA549-PS15** and (●, ○) **PS8-PMDEGA452-PS8**. Lines are guides to the eye.

6.3. Conclusion

The rheology of a series of new amphiphilic block copolymers based on PMDEGA as hydrophilic, thermo-responsive inner block A and polystyrene as permanently hydrophobic outer block B, was investigated in semi-concentrated aqueous solution. Keeping the average composition identical but varying the topology of the polymers, the rheological behavior of diblock BA, triblock BAB and 3-arm star block copolymers (AB)₃ were compared. While solutions made of **PS11-PMDEGA275** were freely flowing even at concentration of 40 wt. %, their gelation ability was highly increased by the addition of a second and a third hydrophobic block. At concentrations between 3.5 and 5 wt. %, gels were formed for BAB as well as (AB)₃ architectures. The gels produced by the star copolymer showed higher storage moduli and were

less prone to melting. The comparison elucidated that gels of associative PMDEGA end-capped by short **PS8** blocks result from the bridging of the micelles, but not from their jamming, and further, that the number of arms enhance the bridging ability. However, at concentrations above 10 wt. %, the bridging ability of the gels is saturated, and neither the topology nor the concentration variations could improve their mechanical stability. When heated these gels underwent a gel-sol transition at temperatures below 30 °C, attributed to the decreasing strength of the hydrophobic associations with increasing temperature.

Due to longer hydrophobic PS15 blocks, hydrogels produced by triblock copolymer **PS15-PMDEGA549-PS15** are much more resistant to temperature variations. The transition from gel to sol is shifted to over 30 °C at low concentrations, and disappears even at higher concentrations. While enhancing the mechanical stability, the larger outer polystyrene blocks conferred a “frozen” behavior to this polymer. The polymer could not be brought into solution without a co-solvent, and re-equilibration of the hydrogel structure once collapsed was slow. Thus when aiming at "smart" hydrogels of further increased mechanical and thermal stability, it is recommended to explore a star polymer with even more than three end-blocks and with a PS length of DP_n 11-13.

6.4. References

1. Calucci, L.; Forte, C.; Buwalda, S. J.; Dijkstra, P. J.; Feijen, J. *Langmuir* **2010**, *26*, 12890-12896.
2. Fehler, N.; Badi, N.; Schade, K.; Pfeifer, S.; Lutz, J.-F. o. *Macromolecules* **2008**, *42*, 33-36.
3. Zhu, W.; Nese, A.; Matyjaszewski, K. *Journal of Polymer Science Part A: Polymer Chemistry* **2011**, *49*, 1942-1952.
4. Velthoen, I. W.; van Beek, J.; Dijkstra, P. J.; Feijen, J. *React. Funct. Polym.* **2011**, *71*, 245-253.
5. Li, Y.; Tang, Y.; Narain, R.; Lewis, A. L.; Armes, S. P. *Langmuir* **2005**, *21*, 9946-9954.
6. Hiemstra, C.; Zhong, Z.; Dijkstra, P. J.; Feijen, J. *Macromol. Symp.* **2005**, *224*, 119-132.
7. Lafilèche, F.; Nicolai, T.; Durand, D.; Gnanou, Y.; Taton, D. *Macromolecules* **2003**, *36*, 1341-1348.
8. Hietala, S.; Strandman, S.; Järvi, P.; Torkkeli, M.; Jankova, K.; Hvilsted, S. r.; Tenhu, H. *Macromolecules* **2009**, *42*, 1726-1732.
9. Lee, S. J.; Han, B. R.; Park, S. Y.; Han, D. K.; Kim, S. C. *J. Polym. Sci., Part A: Polym. Chem.* **2006**, *44*, 888-899.
10. Charbonneau, C. I.; Chassenieux, C.; Colombani, O.; Nicolai, T. *Macromolecules* **2011**, *44*, 4487-4495.
11. Chassenieux, C.; Nicolai, T.; Benyahia, L. *Curr. Opin. Colloid Interface Sci.* **2011**, *16*, 18-26.
12. Giacomelli, F. C.; Riegel, I. C.; Petzhold, C. L.; da Silveira, N. P.; Stepanek, P. *Langmuir* **2008**, *25*, 731-738.
13. Bhatia, S. R.; Murchid, A.; Joanicot, M. *Curr. Opin. Colloid Interface Sci.* **2001**, *6*, 471-478.
14. Chen, C. F.; Lin, C. T. Y.; Chu, I. M. *Polym. Int.* **2010**, *59*, 1428-1435.
15. Ogura, M.; Tokuda, H.; Imabayashi, S.-i.; Watanabe, M. *Langmuir* **2007**, *23*, 9429-9434.
16. Reinicke, S.; Schmelz, J.; Lapp, A.; Karg, M.; Hellweg, T.; Schmalz, H. *Soft Matter* **2009**, *5*.
17. Mortensen, K.; Brown, W.; Almdal, K.; Alami, E.; Jada, A. *Langmuir* **1997**, *13*, 3635-3645.
18. Tadros, F. T., *Rheology of Dispersions: Principles and Applications*. Wiley-VCH Verlag Weinheim (Germany), 2010.
19. Buitenhuis, J.; Forster, S. *J. Chem. Phys.* **1997**, *107*, 262-272.
20. Hamley, I. W., *Block Copolymers in Solution: Fundamentals and Applications*. John Wiley & Sons Chichester (UK), 2005.
21. Vogt, A. P.; Sumerlin, B. S. *Soft Matter* **2009**, *5*, 2347-2351.
22. Liu, J.; Chen, G.; Guo, M.; Jiang, M. *Macromolecules* **2010**, *43*, 8086-8093.
23. Favier, A.; Charreyre, M.-T.; Pichot, C. *Polymer* **2004**, *45*, 8661-8674.
24. Kelarakis, A.; Havredaki, V.; Yuan, X.-F.; Yang, Y.-W.; Booth, C. *J. Mater. Chem.* **2003**, *13*, 2779-2784.
25. Li, F.; Li, S.; El Ghzaoui, A.; Nouailhas, H.; Zhuo, R. *Langmuir* **2007**, *23*, 2778-2783.
26. Hietala, S.; Mononen, P.; Strandman, S.; Järvi, P.; Torkkeli, M.; Jankova, K.; Hvilsted, S.; Tenhu, H. *Polymer* **2007**, *48*, 4087-4096.
27. Kimerling, A. S.; Rochefort, W. E.; Bhatia, S. R. *Ind. Eng. Chem. Res.* **2006**, *45*, 6885-6889.
28. Lejeune, E.; Drechsler, M.; Jestin, J.; Müller, A. H. E.; Chassenieux, C.; Colombani, O. *Macromolecules* **2010**, *43*, 2667-2671.
29. Agrawal, S. K.; Sanabria-DeLong, N.; Tew, G. N.; Bhatia, S. R. *Macromolecules* **2008**, *41*, 1774-1784.
30. Tsitsilianis, C.; Iliopoulos, I. *Macromolecules* **2002**, *35*, 3662-3667.
31. Zhong, Q.; Wang, W.; Adelsberger, J.; Golosova, A.; Koumba, A. M. B.; Laschewsky, A.; Funari, S. S.; Perlich, J.; Roth, S. V.; Papadakis, C. M.; Müller-Buschbaum, P. *Colloid Polymer Sci.* **2011**, *289*, 569-581.

VII Conclusion

The goal of this thesis was to design synthetic block copolymers capable of self-assembly into stimuli-responsive hydrogels. For this purpose the hitherto virtually overlooked, thermo-responsive poly(methoxy diethylene glycol acrylate) **PMDEGA** was chosen as water-soluble, non-ionic starting system, and extended by hydrophobic polystyrene **PS** termini. Three different architectures were targeted, namely diblock, symmetrical triblock and 3-arm star block copolymers, in order to improve control over mechanical properties.

In a first step, the complex, well-defined polymers were successfully synthesized via the RAFT polymerization method. Furthermore, by appropriate choice of RAFT chain transfer agents, specific end-groups could be introduced to the polymers, enabling an efficient macromolecular characterization by routine $^1\text{H-NMR}$ and UV-vis spectroscopies. For the amphiphilic, complex polymers made, such characterization would have been difficult to achieve by other analytical methods.

In a second step, the thermo-responsive behavior of **PMDEGA** was investigated regarding the influence of molar mass, end-groups and architecture. The various polymers underwent a reversible and fast collapse transition upon heating within the physiological interesting range of 20 to 40 °C. Their cloud points (CP) proved to be sensitive to all the molecular variables studied even at high molar masses. This implies the need for a precise polymer structure on the one hand, but the option of a facile LCST variation on the other hand, when designing **PMDEGA** polymers with a specific LCST. The observed unusual increase of the cloud point with increasing molar mass of **PMDEGA**, independently of the nature of the end-groups studied, is attributed to improved steric shielding of the hydrophobic backbone with increasing polymer size.

Additional responsivity of the system to light was explored, by random copolymerization of **MDEGA** with a specifically designed photo-switchable azobenzene acrylate. Although the CP could be modified by UV-light irradiation, i.e depending on the polymers' content of azobenzenes in trans or in cis conformation, respectively, the difference was small and seemed insufficient to confer useful light responsiveness to these copolymers.

Finally, the self-assembly of various block copolymers in water was investigated. As commonly expected, a polystyrene block containing 15 units conferred a kinetically frozen state to the polymer, which could not be brought into solution without a co-solvent and could not spontaneously recover after the thermo-responsive collapse. However, polystyrenes containing

up to 11 units could maintain the system sufficiently dynamic to allow spontaneous self-assembly of the polymers into “hairy” micelles even in cold water.

The polymers viscosifying and gelling properties were studied and were found to increase from diblock (incapable to produce gels), to triblock and to star block copolymers. Thus, the more complex **PMDEGA** polymers end-capped by short **PS** blocks formed gels by bridging of micelles, while this ability was enhanced by the number of arms. The stronger gels obtained from star polymers were also less sensitive to hydrophobic blocks dissociation with temperature. Indeed, all gels underwent a gel-sol transition when heated at temperatures below the cloud point, but the transition was retarded in the gels made from the star copolymers.

In summary, this work demonstrates that **PMDEGA** block copolymers with complex architecture can be easily fabricated by RAFT polymerization. With appropriate molecular characteristics, the amphiphilic copolymers are able to efficiently build hydrogels at room temperature. These could be reversibly switched to fluid dispersions at the cloud point of **PMDEGA**. Considering the results of this thesis, it is recommended to use star polymers with 3 or more arms and **PS** end-blocks of 11 to 13 units, to generate "smart" hydrogels presenting optimized mechanical and thermal stability.

VIII Experimental part

8.1. Analytical instruments

¹H-NMR spectroscopy: The spectra were taken with an apparatus Bruker Avance 300 (300 MHz). The polymers were always dissolved in acetone-d₆ and the low molar mass molecules usually in chloroform-d.

UV-vis spectroscopy: The spectra were recorded on a spectrophotometer Cary-1 (Varian) equipped with temperature controller (Julabo F-10). Quartz cuvettes (Suprasil, Hellma, Germany) with an optical path length of 10 mm were used.

Size-exclusion chromatography (SEC) was run at 50 °C in DMF (flow rate 1mL/ min) using a Spectra Physics Instruments apparatus equipped with a UV-detector SEC-3010 and a refractive index detector SEC 3010 from WGE Dr. Bures (Columns: Guard (7.5 x 75 mm), PolarGel-M (7.5 x 300 mm)), calibration with linear polystyrene standards (PSS, Germany).

Turbidity measurements: For dilute solutions (3.0 g·L⁻¹), cloud points were determined using a temperature controlled turbidimeter (model TP1, E. Tepper, Germany) with heating and cooling rates of 1.0 °C /min, respectively and in a Cary 50 UV-vis spectrometer (Varian) equipped with a single cell Peltier thermostated cell holder. Temperatures were precise within 0.5 °C.

Dynamic light scattering (DLS) was employed to study the association of the block copolymers, using a high-performance particle sizer (HPPS-ET, Malvern Instruments, UK) equipped with a He-Ne laser ($\lambda=633$ nm) and a thermoelectric Peltier temperature controller. The measurements were made at the scattering angle of $\theta=173^\circ$ ("backscattering detection") and the autocorrelation functions were analyzed with the CONTIN method.

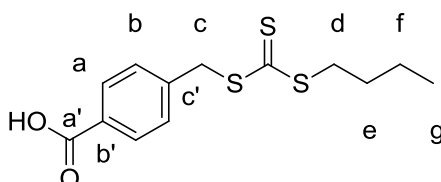
Rheological experiments were performed with an ARG2 rheometer (TA Instruments) equipped with cone-plate geometry and a Peltier plate for temperature control. The cone diameter was 40 mm, cone angle 1°, and the truncation gap 30 μ m. A water-filled solvent trap was used to minimize solvent evaporation during the measurements.

8.2. Synthesis of Chain Transfer Agents CTAs

8.2.1. Monofunctional CTA1: 4-Butylsulfanylthiocarbonylsulfanylmethyl-benzoic acid

A solution of 40 mL 1,2-dimethoxyethane, potassium hydroxide (1.5 g, 26.7 mmol) and 1-butanethiol (1.3 g, 14.4 mmol) was stirred under nitrogen flow at 60 °C for 40 min, before 1.0 mL (16.6 mmol) of carbon disulphide was added dropwise and the reaction allowed to proceed for

an additional 15 min. To the bright yellow solution 3.0 g (13.9 mmol) of 4-bromomethylbenzoic acid, dissolved in 40 mL of 1,2-dimethoxyethane were added and the mixture stirred for 2 h at 60 °C, then left over night at room temperature. The organic phase was then mixed with 150 mL of 0.1 M HCl solution and the precipitated solid filtered off. The cake was washed several times with deionized water, prior being dried under vacuo. Recrystallization from *n*-hexane/THF: 4v/1v afforded a bright yellow crystalline product.



4-Butylsulfanylthiocarbonylsulfanylmethyl-benzoic acid (CTA1)

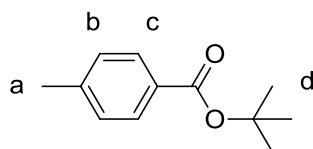
Yield:	62 % (2.6 g)
¹H-NMR [ppm]: (300 MHz, CDCl ₃)	0.94 (t, 3H, H-g), 1.38-1.50 (m, 2H, H-f), 1.74-1.64 (m, 2H, H-e), 3.40 (t, 2H, H-d), 4.67 (s, 2H, H-c), 7.44 (d, 2H, H-b), 8.05 (d, 2H, H-a)
¹³C-NMR [ppm]: (75 MHz, CDCl ₃)	13.6 (CH ₃ , g), 22.0 (CH ₂ , f), 30.0 (CH ₂ , e), 37.0 (CH ₂ , d), 40.5 (CH ₂ , c), 128.6 (C aryl, c'), 129.3 (CH aryl, b), 130.5 (CH aryl, a), 141.8 (C aryl, b'), 171.7 (C, a')
MS (EI, negative ions):	m/z = 300
Elemental analysis:	C ₁₃ H ₁₆ O ₂ S ₃ M _w = 300.46 Calculated: C 51.97, H 5.37, S 32.02 Found: C 51.88, H 5.22, S 31.76

8.2.2. Bifunctional chain transfer agent CTA2

(i) *tert*-butyl 4-methylbenzoate from Wright S.W. et al. ¹

Concentrated sulfuric acid (7.8 mL, 148 mmol) was added to a vigorously stirred suspension of anhydrous magnesium sulfate (73.0 g, 606 mmol) in 400 mL of dry dichloromethane. The mixture was stirred for 15 minutes, after which 4-methylbenzoic acid (20.2 g, 148 mmol) was added. *Tert*-butanol (70 mL, 746 mmol) was added last. The mixture was stoppered tightly in a pressure resistant flask and stirred at room temperature. After 19 h, the reaction vessel was cooled in a dry/ice isopropanol bath to reduce any pressure that might have been generated

during the reaction. The flask was opened, the content poured into 1 L of saturated sodium bicarbonate solution and stirred until all magnesium sulfate had dissolved. The organic phase was washed with brine, dried over MgSO_4 and concentrated, to afford yellowish oil. The crude product was finally purified by distillation in a Kugelrohr apparatus (110 °C, 2 mbar) to give colorless liquid.

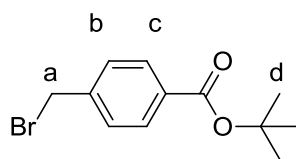


tert-butyl 4-methylbenzoate

Yield:	72 % (20.4g)
$^1\text{H-NMR}$ [ppm]:	1.59 (s, 9H, H-d), 2.39 (s, 3H, H-a), 7.21 (d, 2H, H-b), (300 MHz, CDCl_3) 7.88 (d, 2H, H-c)

(ii) *tert*-butyl 4-(bromomethyl) benzoate

A suspension of the previously synthesized *tert*-butyl 4-methylbenzoate (20.0 g, 0.104 mol), *N*-bromosuccinimide (18.9 g, 0.106 mol), and azobisisobutyronitrile (0.068 g, 0.417 mmol) in CCl_4 (140 mL) was heated to 95 °C. After the beginning of the reaction, indicated by a strong boiling, the mixture was allowed to reflux for 1 h. The suspension was then cooled to room temperature and the precipitated *N*-succinimide filtered. The organic layer was washed with saturated aqueous NaHCO_3 solution (2 x 75 mL) and distilled water (1 x 75 mL), dried over anhydrous MgSO_4 , filtered and evaporated to give a slightly yellow oil. The oil crystallized at room temperature to form a white solid. TLC analysis of the crude product (Silica, hexane/toluene: 3/1) indicated the presence of 4-methyl-benzoic acid *tert*-butyl ester. From $^1\text{H-NMR}$ analysis, the crude product contained 86.4 mol% of *tert*-butyl 4-(bromomethyl) benzoate, 8.8 mol% of *tert*-butyl 4-methylbenzoate and 4.8 mol% of *tert*-butyl 4-(dibromomethyl) benzoate. It was used without further purification for the synthesis of **CTA2**.



tert-butyl 4-(bromomethyl) benzoate

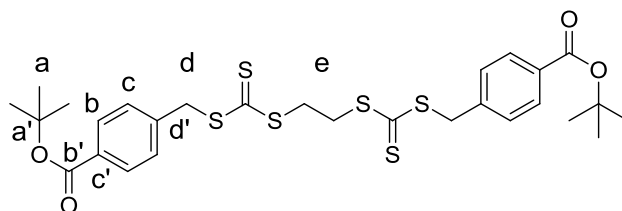
Yield: crude 20.4 g (corrected yield 62 %)

¹H-NMR [ppm]: 1.59 (s, 9H, H-d), 4.49 (s, 2H, H-a), 7.43 (d, 2H, H-b),
(300 MHz, CDCl₃) 7.96 (d, 2H, H-c)

(iii) 1,2 bis (4-(*t*-butoxycarbonyl)benzyl sulfanylthiocarbonyl sulfanyl) ethane

Adapted from Sugawara et al. ²

6 mL deionized water, potassium hydroxide (0.88 g, 15.7 mmol), Aliquat[®] 336 (0.44 g, 1.1 mmol) and 1,2-ethanedithiol (0.45 mL, 6.6 mmol) were stirred at room temperature for 30 min, before 1.0 mL (16.5 mmol) of carbon disulphide was added dropwise. After an additional 1h30 of stirring, 4.0 g (15.5 mmol) of *tert*-butyl 4-(bromomethyl) benzoate, dissolved in 18 mL benzene were added and the bright yellow mixture stirred over night at room temperature. The organic layer turned progressively orange and the aqueous phase became colorless. After the completion of the reaction the benzene layer was washed with three portions of 25 mL deionized water, dried over MgSO₄ and concentrated. The solid product was recrystallized from THF/hexane to yield bright yellow crystals.



1,2 bis (4-(*t*-butoxycarbonyl)benzyl sulfanylthiocarbonyl sulfanyl) ethane (**CTA2**)

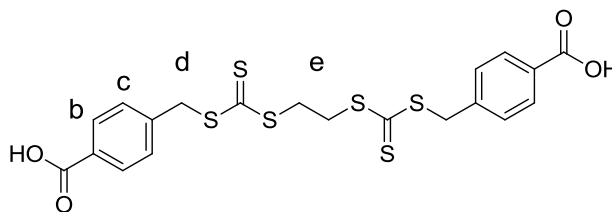
Yield: 86 % (3.8 g)

¹H-NMR [ppm]: (300 MHz, CDCl ₃)	1.58 (s, 18H, H-a), 3.69 (s, 4H, H-e), 4.63 (s, 4H, H-d), 7.37 (d, 4H, H-c), 7.93 (d, 4H, H-b)
¹³C-NMR [ppm]: (75 MHz, CDCl ₃)	28.1 (CH ₃ , a), 34.8 (CH ₂ , e), 41.0 (CH ₂ , d), 81.1 (C, a'), 129.0 (CH aryl, c), 129.8 (CH aryl, b), 131.5 (C aryl, c'), 139.6 (C aryl, d'), 165.2 (C, b')
MS (EI, negative ions):	m/z = 626
Elemental analysis:	C ₁₃ H ₁₆ O ₂ S ₃ M _w = 626.96 Calculated: C 53.64, H 5.47, S 30.69 Found: C 53.72, H 5.18, S 30.48

8.2.3. Bifunctional chain transfer agent CTA6

Adapted from Sugawara et al. ²

A solution of 10 mL deionized water, potassium hydroxide (1.1 g, 19.6 mmol), Aliquat[®] 336 (0.25 g, 0.6 mmol) and 1,2-ethanedithiol (0.3 mL, 3.6 mmol) was stirred at room temperature for 20 min, before 0.6 mL (9.9 mmol) of carbon disulfide were added dropwise. The reaction was then allowed to proceed for an additional 1h. To the bright yellow solution 2.0 g (9.3 mmol) of 4-bromomethylbenzoic acid, dissolved in 20 mL benzene and 5 mL DMF were added and the mixture stirred over night at room temperature. During the reaction, a thick yellow suspension formed. As additional 20 mL of DMF were not sufficient to yield a clear solution, the organic mixture was mixed with 150 mL of deionized water and the precipitated solid filtered off. The solid was found soluble only in DMSO, thus every attempt of recrystallization failed. The dull yellow product was analyzed by ¹H-NMR without further purification.



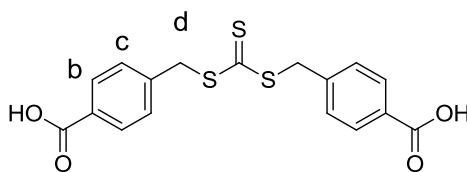
1,2 bis (4-carboxybenzyl sulfanylthiocarbonyl sulfanyl) ethane (CTA6)

¹H-NMR [ppm]: (300 MHz, DMSO)	4.09 (s, 4H, H-e), 4.75 (s, 4H, H-d), 7.49 (d, 4H, H-c), 7.89 (d, 4H, H-b)
--	--

8.2.4. Bifunctional CTA7

Adapted from Charleux et al.³

In a first step carbon disulfide (0.3 mL, 5.0 mmol) was slowly added to a mixture of nonahydrated sodium sulfide (1.2 g, 5.0 mmol), tetrabutylammonium bromide (0.085 g, 0.3 mmol) and 7 mL of water. The yellow solution progressively turned red indicating the formation of disodium trithiocarbonate. The reaction was allowed to proceed for 5h at room temperature. In a second step, a solution of α -bromo-p-toluic acid (2.0 g, 9.3 mmol) and triethylamine (2.0 mL, 14.3 mmol) in 25 mL of DMF and 25 mL of CH_2Cl_2 was introduced. The mixture was stirred at 50 °C for 20h. A yellow solid precipitated during the reaction. Next, the organic phase was poured in 200mL of 0.1 M HCl aqueous solution and the precipitated product was collected by filtration. As in the case of CTA6, every attempt of recrystallization failed, and the yellow dull solid was dried under vacuo without further purification.



bis (4-carboxybenzyl) trithiocarbonate (CTA7)

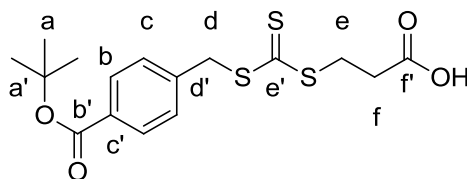
¹H-NMR [ppm]: 4.75 (s, 4H, H-d), 7.49 (d, 4H, H-c), 7.89 (d, 4H, H-b)
(300 MHz, DMSO)

8.2.5. Trifunctional Chain Transfer Agent CTA3

(i) 3-(4-(tert-butoxycarbonyl)benzylthiocarbonothioylthio) propanoic acid

In analogy to a procedure from O'Reilly et al.,⁴ 1-mercapto propionic acid (4.1 mL, 47 mmol, $d = 1.22 \text{ g/cm}^3$) was added to a suspension of K_3PO_4 (10.9 g, 47 mmol) in dry acetone (200 mL) and stirred for 15 min at room temperature. Then, CS_2 (8.0 mL, 133 mmol, $d = 1.262 \text{ g/cm}^3$) was added, followed, after 10 min of stirring, by *tert*-butyl 4-(bromomethyl) benzoate (11.0 g, 43 mmol). The reaction was allowed to proceed for additional 30 min, then the suspension was filtered and the filter cake washed with acetone (3 x 50 mL). The organic filtrate was concentrated under reduced pressure to yield a yellow solid. For recrystallization, the yellow

solid was suspended in hexane, the mixture was brought to reflux, and small amounts of THF were added until the boiling solution became clear. The product was dried under vacuo to yield 11.4 g (71 %) of yellow powder.

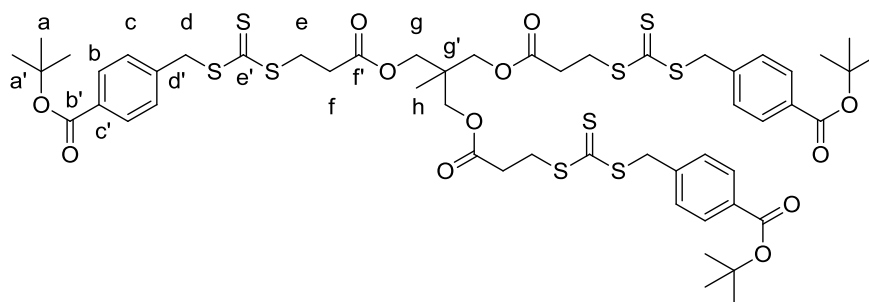


3-(4-(tert-butoxycarbonyl)benzylthiocarbonothioylthio) propanoic acid

Yield:	71 % (11.4 g)
¹H-NMR [ppm]: (300 MHz, CDCl ₃)	1.58 (s, 9H, H-a), 2.83 (t, 2H, H-f), 3.61 (t, 2H, H-e), 4.62 (s, 2H, H-d), 7.37 (d, 2H, H-c), 7.93 (d, 2H, H-b), 10.71 (s broad, 1H, COOH)
¹³C-NMR [ppm]: (75 MHz, CDCl ₃)	28.1 (CH ₃ , a), 31.0 (CH ₂ , f), 32.8 (CH ₂ , e), 40.8 (CH ₂ , d), 81.1 (C, a'), 129.0 (CH aryl, c), 129.7 (CH aryl, b), 131.3 (C aryl, c'), 139.7 (C aryl, d'), 165.3 (C, b'), 177.1 (C, f'), 222.1 (C=S, e')

(ii) 1,1,1 tris(3-(4-(tert-butoxycarbonyl)benzylthiocarbonothioylthio)propanoyloxy)ethane

In analogy to a procedure from O'Reilly et al.,⁵ 3-(4-(tert-butoxycarbonyl)-benzylthiocarbonothioylthio) propanoic acid (4.080 g, 11.0 mmol), 1,1,1-tris(hydroxymethyl)-ethane (0.314 g, 2.6 mmol) and 4-(dimethylamino)pyridine (0.351 g, 2.9 mmol) dissolved in dry dichloromethane (200 mL) were placed in an ice bath. EDC×HCl (4.515 g, 29.1 mmol) in dichloromethane (200 mL) was added dropwise. The reaction was allowed to proceed at room temperature overnight. The reaction mixture was washed with 1M HCl (3 x 150 ml), the organic phase dried over MgSO₄ and concentrated by rotary evaporation. The crude product was purified by column chromatography (silicagel 60, Merck, 0.040-0.063 mm, eluent: ethyl acetate/hexane: 2/1) to give a dark orange glassy solid.



1,1,1 tris (3-(4-(tert-butoxycarbonyl)benzylthiocarbonothioylthio) propanoyloxy) ethane (**CTA3**)

Yield: 42 % (1.3 g)

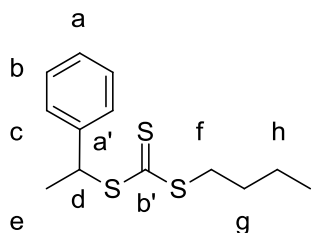
¹H-NMR [ppm]: 1.01 (s, 3H, H-h), 1.57 (s, 27H, H-a), 2.78 (t, 6H, H-f), 3.61 (t, 6H, H-e), 4.02 (s, 6H, H-g), 4.62 (s, 6H, H-d), 7.36 (d, 6H, H-c), 7.92 (d, 6H, H-b)

¹³C-NMR [ppm]: 17.2 (CH₃, h), 28.1 (CH₃, a), 31.3 (CH₂, f), 33.0 (CH₂, e), 38.4 (C, g'), 40.9 (CH₂, d), 66.0 (CH₂, g), 81.1 (C, a'), 129.0 (CH aryl, c), 129.7 (CH aryl, b), 131.5 (CH aryl, c'), 139.7 (C aryl, d'), 165.2 (C, b'), 170.9 (C, f'), 222.0 (C=S, e')

Elemental analysis: C₅₃H₆₆O₁₂S₉ M_w = 1183.67
Calculated: C 53.78, H 5.62, S 24.38 Found: C 54.78, H 5.32, S 22.45

8.2.6. Butyl-1-phenylethyltrithiocarbonate (CTA4)

Triethylamine (5.4 g, 31.6 mmol) and 1-butanethiol (1.9 mL, 17.7 mmol) were stirred with 15 mL of chloroform at room temperature for 30 min, before 2.7 mL (44.8 mmol) of carbon disulphide were added dropwise. After an additional 15 min, 2.2 mL (15.5 mmol) of (1-bromoethyl)benzene were slowly added and the mixture stirred overnight. The organic phase was then washed with four portions of 15 mL deionized water, dried over MgSO₄, and concentrated at high vacuo to yield 3.9 g (89 %) of deep orange oil.



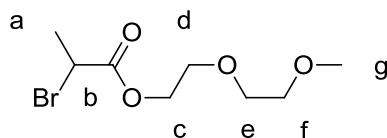
butyl-1-phenylethyltrithiocarbonate (CTA4)

Yield:	89 % (3.9 g)
¹H-NMR [ppm]: (300 MHz, CDCl ₃)	0.92 (t, 3H, H-i), 1.41 (sext, 2H, H-h), 1.66 (quint, 2H, H-g), 1.75 (d, 3H, H-e), 3.34 (t, 2H, H-f), 5.33 (q, 1H, H-d), 7.22-7.40 (m, 5H, H-a, H-b, H-c)
¹³C-NMR [ppm]: (75 MHz, CDCl ₃)	13.5 (CH ₃ , i), 21.3 (CH ₃ , e), 22.0 (CH ₂ , h), 30.0 (CH ₂ , g), 36.5 (CH ₂ , f), 50.0 (CH, d), 127.60 (CH aryl, a), 127.63 (CH aryl, c), 128.6 (CH aryl, b), 141.1 (C aryl, a'), 223.0 (C=S, b')
MS (EI, negative ions):	m/z = 270
Elemental analysis:	C ₁₃ H ₁₈ S ₃ M _w = 270.48 Calculated: C 57.73, H 6.71, S 35.56 Found: C 57.67, H 6.53, S 35.15

8.2.7. 2-Butylsulfanylthiocarbonylsulfanyl-propionic acid 2-(2-methoxy-ethoxy)-ethyl ester (CTA5)

(i) 2-Bromo-propionic acid 2-(2-methoxy-ethoxy)-ethyl ester

Triethylamine (2.4 g, 24 mmol) and diethylene glycol monomethylether (3.4 g, 28 mmol) were mixed with 25 mL of dry dichloromethane and cooled to 0 °C. 2.4 mL (23 mmol) of 2-bromopropionyl bromide were added dropwise. The reaction mixture was maintained at 0 °C for 30 min, then stirred at ambient temperature overnight. The precipitated triethylammonium bromide was filtered off and the cake washed with CH₂Cl₂. The collected organic phases were washed with molar HCl solution and brine. After drying over MgSO₄ and evaporation of the solvent, the crude product was obtained as light yellow oil. Vacuum distillation at 150°C (≈2 mbar) gave 4.3 g (73%) of colorless liquid.



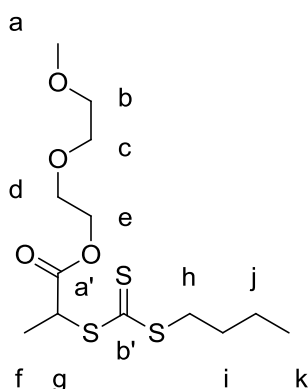
2-Bromo-propionic acid 2-(2-methoxy-ethoxy)-ethyl ester

Yield: 73 % (4.3 g)

¹H-NMR [ppm]: 1.82 (d, 3H, H-a), 3.38 (s, 3H, H-g), 3.53-3.56 (m, 2H, H-f), 3.64-3.67 (300 MHz, CDCl₃) (m, 2H, H-e), 3.73 (t, 2H, H-d), 4.33 (t, 2H, H-c), 4.40 (q, 1H, H-b)

(ii) 2-Butylsulfanylthiocarbonylsulfanyl-propionic acid 2-(2-methoxy-ethoxy)-ethyl ester

Triethylamine (1.2 mL, 8.5 mmol) and 1-butandithiol (0.7 mL, 6.5 mmol) were mixed with 10 mL of methyl *tert*-butyl ether and purged with nitrogen for 15 min. The dropwise addition of 0.5 mL (8.8 mmol) of CS₂ at room temperature, gave a clear, bright yellow solution. After 30 min of stirring, 1.5 g (5.9 mmol) of 2-bromo-propionic acid 2-(2-methoxy ethoxy)-ethyl ester were added dropwise and the mixture allowed to react overnight. 20 mL of water were added and the mixture was extracted two times with 20 mL of *n*-hexane. The combined *n*-hexane phases were dried over anhydrous MgSO₄ and concentrated. According to TLC (Kiesel gel, *n*-hexane/ethyl acetate: 1/1), the crude product contained by-products and was therefore purified by column chromatography (silicagel 60, Merck, 0.040-0.063 mm, eluent: *n*-hexane/ethyl acetate: 1/1) to give a dark orange oil.



2-(butylsulfanylthiocarbonylsulfanyl)-propionic acid 2-(2-methoxy-ethoxy)-ethyl ester (CTA5)

Yield:	55 % (1.1 g)
¹H-NMR [ppm]: (300 MHz, CDCl ₃)	0.92 (t, 3H, H-k), 1.36-1.48 (m, 2H, H-j), 1.59 (d, 3H, H-f), 1.62-1.72 (m, 2H, H-i), 3.35 (t, 2H, H-h), 3.37 (s, 3H, H-a), 3.52-3.55 (m, 2H, H-b), 3.60-3.64 (m, 2H, H-c), 3.69 (t, 2H, H-d), 4.29 (t, 2H, H-e), 4.83 (q, 1H, H-g)
¹³C-NMR [ppm]: (75 MHz, CDCl ₃)	13.4 (CH ₃ , k), 16.8 (CH ₃ , f), 21.9 (CH ₂ , j), 29.8 (CH ₂ , i), 36.8 (CH ₂ , h), 47.8 (CH, g), 58.9 (CH ₃ , a), 64.8 (CH ₂ , e), 68.8 (CH ₂ , d), 70.4 (CH ₂ , c), 71.8 (CH ₂ , b), 170.9 (C, a'), 221.9 (C=S, b')
MS (EI, negative ions):	m/z = 340
Elemental analysis:	C ₁₃ H ₂₄ O ₄ S ₃ M _w = 340.52 Calculated: C 45.85, H 7.10, S 28.25 Found: C 46.06, H 7.14, S 27.24

8.3. Synthesis of monomers

8.3.1. Methoxy diethylene glycol acrylate (MDEGA)

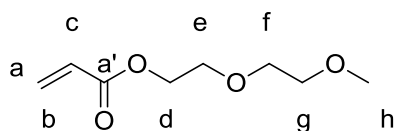
MDEGA was synthesized by 2 different methods, first by acylation reaction, using acryloyl chloride as reactant, second by trans-esterification reaction, using the less expensive ethyl acrylate as reactant.

(i) Synthesis by acylation

Diethylene glycol monomethyl ether (40.0 g, 0.33 mol), triethylamine (37.0 g, 0.37 mol) and 250 mL of dry dichloromethane were added to a 1L three-necked round bottom flask, placed in an isopropanol/dry ice bath and purged with N₂ for 30 min. Acryloyl chloride (30.0 mL, 0.37 mol) and hydroquinone (0.3 g, 27 mmol) dissolved in 190 mL of dichloromethane were added drop wise under nitrogen atmosphere. The reaction was maintained in the ice bath for 1h, and then left overnight at room temperature. The precipitated ammonium salts were filtered off and the organic phase washed two times with 250 mL of saturated sodium bicarbonate solution and two times with 250 mL of deionized water. The collected organic phases were dried over MgSO₄ and concentrated by rotary evaporation at ambient temperature to give an orange viscous liquid. Further distillation in Kugelrohr apparatus (p < 3 mbar, 85-100°C) gave a colorless viscous liquid. Yield: 43.1 g, 75 %.

(ii) Synthesis by trans-esterification:

The previously described synthesis of **MDEGA** using acryloyl chloride as reactant was improved by applying trans-esterification of the inexpensive ethyl acrylate with diethylene glycol monomethyl ether, and by replacing the inhibitor hydroquinone by phenothiazine, since traces of benzoquinone were found by TLC in the final product after distillation. Thus ethyl acrylate (400 mL, 3.68 mol, 0.92 g/cm³), diethylene glycol monomethyl ether (150 g, 1.25 mol) and phenothiazine (0.75 g, 4.0×10⁻³ mol) were placed in a three necked round bottom flask equipped with a fractionating column. The mixture was brought to boiling and as the vapor reached 100°C, titanium (IV) iso-propoxide (2.0 mL, 6.7×10⁻³ mol, d = 0.955 g/cm³) was added. The reaction was stopped after 6 h, as no more condensate was produced. The brown liquid residue was dissolved in dichloromethane and washed once with a saturated solution of NaHCO₃, and twice with brine, in order to remove unreacted diethylene glycol monomethyl ether. The organic phase was dried over MgSO₄ and distilled (p < 3 mbar, ≈ 85°C) to yield 131.2 g (60.4%) of colorless liquid.

methoxy diethylene glycol acrylate (**MDEGA**)

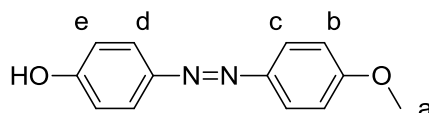
Yield:	(i) 75 % (43.1 g) (ii) 60 % (131.2 g)
¹H-NMR [ppm]: (300 MHz, CDCl ₃)	3.36 (s, 3H, H-h), 3.52-3.55 (m, 2H, H-g), 3.62-3.65 (m, 2H, H-f), 3.72 (t, 2H, H-e), 4.30 (t, 2H, H-d), 5.82 (dd, 1H, H-a), 6.13 (dd, 1H, H-c), 6.41 (dd, 1H, H-b).
¹³C-NMR [ppm]: (75 MHz, CDCl ₃)	58.9 (CH ₃ , h), 63.5 (CH ₂ , d), 69.0 (CH ₂ , e), 70.4 (CH ₂ , f), 71.8 (CH ₂ , g), 128.2 (CH, c), 130.7 (CH ₂ , a), 166.0 (C=O, a').
MS (EI, negative ions):	m/z = 173
Elemental analysis:	C ₈ H ₁₄ O ₄ M _w = 174.19 Calculated: C 55.16, H 8.10 Found: C 54.31, H 7.72

8.3.2. 6-(4-[4-methoxyphenylazo]phenyl) diethylene glycol acrylate (azoMDEGA)

The synthesis followed a classic procedure, including a diazotization and coupling reaction to generate the azobenzene moiety, followed by an alkylation reaction to introduce a diethylene glycol spacer, and finished by an acylation reaction with acryloyl chloride to introduce the vinyl function.

(i) 4-((4-methoxyphenyl)diazenyl)phenol^{6,7}

For the diazotization reaction, *p*-methoxy aniline (17.0 g 138 mmol) was dissolved in 250 mL of HCl 1.0 M and the solution placed in an ice bath. Throughout the reaction, special care was taken to keep the temperature below 5 °C. Next, a solution of sodium nitrite (10.6 g, 154 mmol) in 100 mL of distilled water was slowly added. At the end of the addition, a starch-iodide indicator was used to verify the excess of sodium nitrite. For the coupling reaction, phenol (13.0 g, 138 mmol) was dissolved in 31 mL of NaOH 15 M and the solution cooled in an ice bath. The solution of diazonium salt previously synthesized was slowly added to the solution of sodium phenolate under vigorous stirring keeping both vessels in an ice bath. At the end of the addition, the mixture was acidified with HCl 1.0 M to reach pH < 2. The precipitated red ochre solid was filtered, recrystallized in water/ethanol mixture (1:1 in volume) and dried under vacuo.



4-((4-methoxyphenyl)diazenyl)phenol

Yield: 87.9 % (27.7 g)

¹H-NMR [ppm]: 3.89 (s, 3H, H-a), 6.97 (m, 4H, H-b and H-e), 7.86 (m, 4H, H-c and H-d)
(300 MHz, CDCl₃)

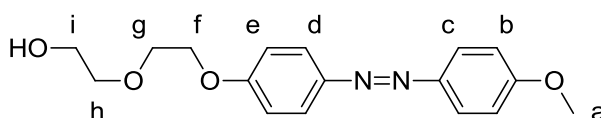
TLC (hexane/EtOAc = 1/1): R_f = 0.7

(ii) 2-(2-(4-((4-methoxyphenyl)diazenyl)phenoxy)ethoxy)ethanol

The diethylene glycol spacer was added next, in analogy to a procedure by Angeloni et al.⁸

4-((4-methoxyphenyl)diazenyl)phenol (30.00 g, 131.4 mmol), dry potassium carbonate (72.67 g, 525.8 mmol) together with a small amount of KI were dissolved in dry acetone (150 mL) under inert atmosphere. The reaction mixture was heated at 30°C and 21.5 mL (393 mmol) of 2-(2-

chloroethoxy)ethanol were added drop wise. After finishing the addition, the reaction mixture was heated at 70°C and left under reflux for 7.5 h. As large amounts of unreacted 4-((4-methoxyphenyl)diazenyl)phenol were detected by TLC in the reaction mixture, a further 20.0 mL (189 mmol) of 2-(2-chloroethoxy)ethanol were added and the reaction allowed to proceed for additional 15 h. The mixture was then cooled to room temperature and filtered. The filtrate cake was dispersed into a saturated solution of NaHCO₃ and filtered again. The procedure was repeated twice with distilled water. The resulting yellow solid was then dried under vacuo, recrystallized in acetone and dried under vacuo again, to yield 16.74 g (40.3 %) of golden crystals.



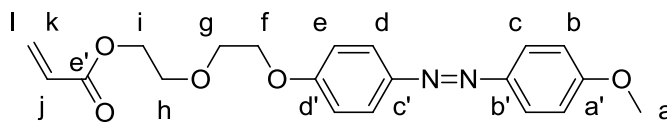
2-(2-(4-((4-methoxyphenyl)diazenyl)phenoxy)ethoxy)ethanol

Yield:	40.3 % (16.74 g)
¹H-NMR [ppm]: (300 MHz, CDCl ₃)	3.75 (m, 4H, H-i and H-h), 3.91 (m, 5H, H-a and H-g), 4.22 (m, 2H, H-f), 7.02 (m, 4H, H-b and H-e), 7.88 (m, 4H, H-c and H-d)
Elemental analysis:	C ₈ H ₁₄ O ₄ M _w = 316.35 Calculated: C 64.54, H 6.37, N 8.86 Found: C 62.92, H 6.24, N 7.31
TLC (hexane/EtOAc = 1/1)	R _f = 0.3

(iii) 6-(4-[4-methoxyphenylazo]phenyl) diethylene glycol acrylate (azoMDEGA)

A mixture of 2-(2-(4-((4-methoxyphenyl)diazenyl)phenoxy)ethoxy)ethanol (12.11 g, 38.3 mmol), triethylamine (6.5 mL, 46 mmol), hydroquinone (0.045 g, 4 mmol) and 100 mL of dry dichloromethane was cooled in a isopropanol/dry ice bath. Acryloyl chloride (3.7 mL, 45 mmol) was then added drop wise. At the end of the addition, the reaction was allowed to proceed for 5h at room temperature. As TLC revealed traces of unreacted azobenzene alcohol, another 2.5 mL (31 mmol) of acryloyl chloride were added. The reaction was allowed to proceed for additional 16 h. The obtained red solution was washed two times with a saturated solution of NaHCO₃ and two times with distilled water. The organic phase was dried over MgSO₄ and

concentrated by rotary evaporation to yield a yellow solid. Further recrystallization in methanol gave 6.7g (47 %) of yellow powder.



6-(4-[4-methoxyphenylazo]phenyl) diethylene glycol acrylate (**azoMDEGA**)

Yield:	47 % (6.7 g)
¹H-NMR [ppm]: (300 MHz, CDCl ₃)	3.82-3.92 (m, 7H, H-h, H-a and H-g), 4.21 (m, 2H, H-f), 4.36 (m, 2H, H-i), 5.82 (dd, 1H, H-k), 6.13 (dd, 1H, H-j), 6.41 (dd, 1H, H-l), 7.01 (m, 4H, H-b and H-e), 7.87 (m, 4H, H-c and H-d)
¹³C-NMR [ppm]: (75 MHz, CDCl ₃)	55.5 (CH ₃ , a), 63.5 (CH ₂ , i), 67.7 (CH ₂ , g), 69.3 (CH ₂ , h), 69.6 (CH ₂ , f), 114.1 (CH, e), 114.8 (CH, b), 124.25 (CH, d), 124.3 (CH, c), 128.2 (CH, j), 130.1 (CH ₂ , l), 147.0 (C, c'), 147.2 (C, b'), 160.6 (C, d'), 161.6 (C, a'), 166.0 (C=O, e').
Elemental analysis:	C ₈ H ₁₄ O ₄ M _w = 370.40 Calculated: C 64.85, H 5.99, N 7.56 Found: C 62.96, H 5.94, N 7.29
TLC (hexane/EtOAc = 1/1)	R _f = 0.7 (trans), 0.55 (cis)

8.4. Synthesis of rhodamine B piperazine amide

Rhodamine B piperazine amide was synthesized according to a procedure of Nguyen and Francis.⁹ Note that the reaction took place under inert atmosphere (N₂), in freshly dried glassware and using dry distilled dichloromethane as solvent, as trimethyl aluminium is a pyrophoric compound.

Piperazine (2.0 g, 23 mmol) was dissolved in 10 mL of dry dichloromethane under nitrogen flow, and a 2.0 M solution of trimethyl aluminium in toluene (5.5 mL, 11 mmol) was added dropwise at room temperature. After one hour of stirring, a solution of rhodamine B base (2.5 g, 5.7 mmol) in dry dichloromethane (6mL) was slowly added. The mixture was then brought to

reflux and the reaction allowed to proceed for 24 h. As TLC revealed large amount of unreacted rhodamine B base, the mixture was cooled to room temperature and additional 2 mL (4 mmol) of trimethyl aluminium in toluene were slowly added. The mixture was kept under reflux overnight, after which time only traces of rhodamine B base were observed by TLC. Next a 0.1 M aqueous solution of HCl was added dropwise, until gas evolution ceased. The dark dispersion was filtered and the filter cake rinsed first with CH₂Cl₂, then with a 4v/1v CH₂Cl₂/MeOH solution. The filtrate was concentrated and the dark violet residue was dissolved in small amount of CH₂Cl₂, filtered to remove insoluble salts and concentrated again. The violet foamy solid was dissolved in saturated NaHCO₃ solution and washed 3 times with ethyl acetate. The aqueous phase was saturated with NaCl, acidified with 1M HCl aqueous solution and extracted several times with 2v/1v isopropanol/dichloromethane solution until the red color almost disappeared. The organic phase was dried over MgSO₄ and concentrated under reduced pressure. The violet solid was dissolved in a small amount of methanol and precipitated by dropwise addition to a large volume of diethyl ether. Finally the precipitated solid was filtered and dry under vacuo to yield 49 % of dark violet solid.

8.5. Synthesis of polymers

8.5.1. Synthesis of polystyrene PS₁₆

In a typical procedure, styrene (11.0 mL, 96 mmol, $d = 0.916 \text{ g/cm}^3$) and **CTA2** (1.5 g, 2.4 mmol) were mixed in a round bottom flask. The flask was sealed with a rubber septum and purged with nitrogen for 15 min. Polymerization was conducted for 18 h at 110 °C. The obtained yellow viscous liquid was diluted with acetone and precipitated 3 times into methanol. The collected polymer was dried in vacuo at room temperature for over 2 days to give 5.1 g (44 %) of yellow powder.

¹H-NMR (300 MHz in acetone d₆, δ in ppm): $\delta = 1.57$ (br, 18H, -(CH₃)₃), 3.61 (s, 4H, -S-(CH₂)₂-S-), 4.75–5.13 (br, 2H, -S-CH(phenyl)-), 6.41–7.42 (br, 4H aromatic R group and 5H×DPn polystyrene), 7.74–7.94 (m, 4H, aromatic R group).

8.5.2. Synthesis of PMDEGA-371a

In a typical procedure, **MDEGA** (3.5919 g, 20.6 mmol), **CTA2** (0.0295 g, 4.7×10^{-2} mmol), AIBN (0.0013 g, 7.9×10^{-3} mmol) and benzene (12 mL) were mixed in a round bottom flask. The flask was sealed with a rubber septum and purged with nitrogen for 15 min. The polymerization took place for 4 h at 70 °C. The obtained yellow viscous liquid was diluted with acetone and precipitated 3 times into hexane. The collected polymer was dried in vacuo at room temperature

for over 3 days to give 2.9 g (80.1 %) of yellow viscous oil.

$^1\text{H-NMR}$ (300 MHz in acetone d_6 , δ in ppm): δ = 1.58 (br, 18H, $-(\text{CH}_3)_3$), 3.33 (br s, 3H \times DPn, $-\text{O}-\text{CH}_3$), 4.23 (br s, 2H \times DPn, $-\text{C}(=\text{O})\text{O}-\text{CH}_2-\text{CH}_2-\text{O}-$), 4.85–4.93 (br s, 2H, $-\text{S}-\text{CH}(\text{COOR})-$), 7.35 (br d, 4H, 2 \times 2H aromatic R group), 7.89 (dd, 4H, 2 \times 2H aromatic R group).

8.5.3. Synthesis of $\text{PS}_8\text{-PMDEGA}_{452}\text{-PS}_8$

In a typical procedure, MDEGA (6.88 g, 39 mmol), polystyrene macroRAFT agent (0.0596 g, 0.066 mmol) and AIBN (0.0017 g, 0.010 mmol) were mixed with benzene (20 mL) and purged with N_2 for 15 min at room temperature. After 5 h at 70 °C, the polymerization was quenched by placing the flask into liquid nitrogen. The obtained yellow liquid was precipitated three times into hexane and dried in vacuo at room temperature over 3d to give 5.2 g (74 %) of viscous yellow oil.

$^1\text{H-NMR}$ (300 MHz in acetone d_6 , δ in ppm): δ = 1.57 (br, 18H, $-(\text{CH}_3)_3$), 3.33 (br s, 3H \times DPn, $-\text{O}-\text{CH}_3$), 4.23 (br s, 2H \times DPn, $-\text{C}(=\text{O})\text{O}-\text{CH}_2-\text{CH}_2-\text{O}-$), 4.84–4.93 (br s, 2H, $-\text{S}-\text{CH}(\text{COOR})-$), 6.40–7.36 (br, 4H aromatic R group and 5H \times DPn polystyrene), 7.75–7.89 (br, 4H, aromatic R group).

8.5.4. Synthesis of PMDEGA-co-azoMDEGA

In a typical procedure, **CTA2** (0.0341 g, 0.054 mmol), **AIBN** (0.0018 g, 0.011 mmol), **azoMDEGA** (0.17 g, 0.468 mmol) and **MDEGA** (2.63 g, 15.12 mmol) were mixed in a round bottom flask together with 9.5 mL of benzene. The flask was sealed with a rubber septum and the mixture purged with N_2 for 20 min. The reaction was allowed to proceed for 14 h at 70 °C. The polymer was purified by precipitation. Noteworthy, the solubility of azoMDEGA was found poor in hexane and average in diethyl ether. On the other hand, PMDEGA polymers of about 100 DP_n precipitate very well in hexane and poorly in diethyl ether. Thus, the polymer-monomer mixture was precipitated in a 1v/1v solution of hexane/diethyl ether and the resulting dispersion centrifuged, to collect the entire suspended polymer. After 5 cycles of precipitation and centrifugation, the polymer was dried in vacuo at room temperature over 3d to give 1.22 g (42 %) of viscous dark orange oil.

$^1\text{H-NMR}$ (300 MHz in acetone d_6 , δ in ppm): δ = 3.33 (s, 3H \times DPMDEGA, $-\text{OCH}_3$), 3.52 (dd, 2H \times DPMDEGA, $\text{CH}_3\text{OCH}_2\text{CH}_2\text{O}-$), 3.62–3.64 (dd, 2H \times DPMDEGA, $\text{CH}_3\text{OCH}_2\text{CH}_2\text{O}-$), 3.7 (dd, 2H \times DPMDEGA, $-\text{OCH}_2\text{CH}_2\text{OAr}-$), 3.79–3.96 (m, 7H \times DPazoMDEGA, $-\text{CH}_2\text{OCH}_2-$ and $-\text{OCH}_3$), 4.05–4.42 (m, 2H \times DPMDEGA + 4H \times DPazoMDEGA, mixture), 7.06–7.20 (m, 4H \times DPazoMDEGA, signal d Figure 3.3), 7.29–7.40 (dd, 4H, signal c Figure 3.3), 7.83–7.97 (m, 4H + 4H \times DPazoMDEGA, mixture)

8.6. Polymers functionalization

8.6.1. Cleavage of the *tert*-butyl ester group

In a typical procedure, **PS** (1.14 g, 5.1×10^{-4} mol, $M_n = 2400$ g/mol) bearing two *tert*-butyl benzoate end-groups was dissolved in 2.3 mL of dry dichloromethane, and a 4-fold excess of trifluoroacetic acid (TFA) to end-groups was added (0.3 mL, 3.89×10^{-3} mol, $d = 1.49$ g/cm³). The small vial was tightly sealed and the reaction was set under continuous stirring at room temperature. After 24h, the mixture was precipitated 3 times in methanol. The resulting yellow powder was dried under vacuo for 3 days.

¹H-NMR (300 MHz in acetone d₆, δ in ppm): $\delta = 3.61$ (s, 4H, -S-(CH₂)₂-S-), 4.75–5.13 (br, 2H, -S-CH(phenyl)-), 6.41–7.42 (br, 4H aromatic R group and 5H×DPn polystyrene), 7.74–7.94 (m, 4H, aromatic R group).

In a typical procedure, polymer **PMDEGA-371a** (1.01 g, 3.6×10^{-2} mmol of *tert*-butyl ester end-groups) was dissolved in dry dichloromethane (2 mL) and trifluoroacetic acid (1.1 mL, 14 mmol, $d = 1.49$ g/cm³) was added. The vial was sealed, and the solution left at room temperature under continuous stirring for 24 h. Volatiles were then removed under reduced pressure and the polymer freeze dried twice from benzene (2 x 5 mL) to completely eliminate the excess of trifluoroacetic acid.

¹H-NMR (300 MHz in acetone d₆, δ in ppm): $\delta = 3.33$ (br s, 3H×DPn, -O-CH₃), 4.23 (br s, 2H×DPn, -C(=O)O-CH₂-CH₂-O-), 4.85–4.93 (br s, 2H, -S-CH(COOR)-), 7.37 (br d, 4H, 2x2H aromatic R group), 7.97 (dd, 4H, 2x2H aromatic R group).

8.6.2. Functionalization with rhodamine B base piperazine

In a typical functionalization experiment, **PS10-PMDEGA167** (0.5033 g, 0.0078 mmol, $M_n = 30400$ g·mol⁻¹), rhodamine B base piperazine (16.4 mg, 0.0321 mmol), *N*-hydroxysuccinimide **NHS** (8.6 mg, 0.0747 mmol) and ethyl(dimethylaminopropyl) carbodiimide **EDC** (12.4 mg, 0.080 mmol) were dissolved in 2 mL of dry dichloromethane. The reaction was allowed to proceed for 24 h under continuous stirring at room temperature. After which, the product was precipitated in an equivolume mixture of hexane and diethyl ether, then dialyzed against water for over a week using a cellulose membrane (4000 – 6000 cutoff). After lyophilization, a pink, viscous product was obtained.

8.7. Methods

Sample preparation

With the exception of PS15-PMDEGA549-PS15, all the polymers were directly soluble in water, at any concentrations and without the need of organic co-solvents. Polymers and “Millipore” water were mixed in the desired proportions and left to equilibrate at 10 °C in a tightly screw-capped vial for 1 d to 4 d depending on the concentration. The procedure yielded clear, homogeneous samples.

In the case of PS15-PMDEGA549-PS15, the polymer was dispersed in water at the desired proportions, and the level of the liquid was marked. Then acetone was added to the mixture. Usually, acetone/water ratios of 2/10 in volume were sufficient to yield homogeneous solutions. The mixture was left to equilibrate under stirring or shaking, depending on the viscosity of the sample for 1 to 2 d. The vial was then opened and acetone left to evaporate at room temperature for 2 to 3 d. Every 24 h, the liquid level was controlled and water added if necessary. At last, the concentration of the sample was verified by determination of the solid content.

Characterization in dilute aqueous solution

For dilute solutions (3.0 g·L⁻¹), cloud points were determined using a temperature controlled turbidimeter with heating and cooling rates of 1.0 °C·min⁻¹, respectively. Temperatures were precise within 0.5 °C.

Characterization in concentrated aqueous solution

For concentrated solutions (5 wt. % to 30 wt. %), cloud points were determined by visual observation, as the turbidimetry set-up could not be used because of the high viscosity. The samples were placed in a thermostated bath, and the temperature was raised by 1 °C·min⁻¹ until the samples became turbid. Concentration dependent sol-gel transitions were evaluated by the tube inversion test. We distinguished on the one hand between liquid and viscous liquid samples, able respectively to flow freely or slowly upon tube inversion, and on the other hand between soft and hard gels. Samples considered as gels were not flowing upon tube inversion for at least 30 min, however soft gels presented a visible surface deformation whereas hard gel did not.

For each measurement, the sample was first heated to temperatures about 2° to 3 °C below its transition temperature and left to equilibrate under gentle oscillations for at least 20 min. The temperature was then set to the desired value for the measurement, and the sample left to

equilibrate for 5 more min. For frequency sweeps, the samples were subjected to frequencies ranging from 0.002 to 100 Hz and oscillatory stress of 5 Pa, at both 10 °C and 20 °C.

Temperature-dependent experiments were conducted in the temperature range between 5 °C and 45 °C with a heating/cooling rate of 1 °C·min⁻¹, applying an oscillatory stress of 5 Pa at a frequency of 1 Hz. Based on the ratio of the values for the storage modulus G' and the loss modulus G'' , a system was considered as viscous liquid for $G' < G''$, as soft-gel for G' equal to G'' , and as hard gel for $G' > G''$.¹⁰

8.8. References

1. Wright, S. W.; Hageman, D. L.; Wright, A. S.; McClure, L. D. *Tetrahedron Lett.* **1997**, 38, 7345-7348.
2. Sugawara, A.; Hasegawa, K.; Suzuki, K.-i.; Takahashi, Y.; Sato, R. *Bull. Chem. Soc. Jpn.* **1987**, 60, 435-437.
3. Houillot, L.; Bui, C.; Save, M.; Charleux, B.; Farcet, C.; Moire, C.; Raust, J.-A.; Rodriguez, I. *Macromolecules* **2007**, 40, 6500-6509.
4. Skey, J.; O'Reilly, R. K. *Chem. Commun.* **2008**, 4183-4185.
5. O'Reilly, R. K.; Hansell, C. *Polymers* **2009**, 1, 3-15.
6. Zhang, Q.; Bazuin, C. G. *Macromolecules* **2009**, 42, 4775-4786.
7. Kim, J.; Novak, B. M.; Waddon, A. J. *Macromolecules* **2004**, 37, 8286-8292.
8. Angeloni, A. S.; Campagnari, I.; Caretti, D.; Carlini, C.; Altomare, A.; Chiellini, E.; Galli, G.; Solaro, R.; Laus, M. *Gazz. Chim. Ital.* **1990**, 120, 171-178.
9. Nguyen, T.; Francis, M. B. *Org. Lett.* **2003**, 5, 3245-3248.
10. Hamley, I. W.; Mai, S.-M.; Ryan, A. J.; Fairclough, J. P. A.; Booth, C. *Phys. Chem. Chem. Phys.* **2001**, 3, 2972-2980.

IX Annex

9.1. Supplementary information to Chapter 5

Table A5.1: Gel-sol transition temperatures and cloud point temperatures of aqueous solutions of PS₈-PMDEGA_n-PS₈ block copolymers:

copolymer	a) gel-sol transition [°C]				b) cloud point [°C]			
	5 wt%	10 wt%	20 wt%	30 wt%	5 wt%	10 wt%	20 wt%	30 wt%
PS ₈ -PMDEGA ₅₃ -PS ₈	L	L	L	7.5	21	20	18	20
PS ₈ -PMDEGA ₉₃ -PS ₈	L	6	13	16.5	21	21	23	29
PS ₈ -PMDEGA ₁₈₀ -PS ₈	L	16	21.5	22.5	30	31	32	37
PS ₈ -PMDEGA ₄₅₂ -PS ₈	16	25	29	29	36	37	38	39

a) from rheological measurements at $f = 1\text{Hz}$, as temperature for which $G' = G''$
b) visual determination, as temperature for which the solution becomes cloudy

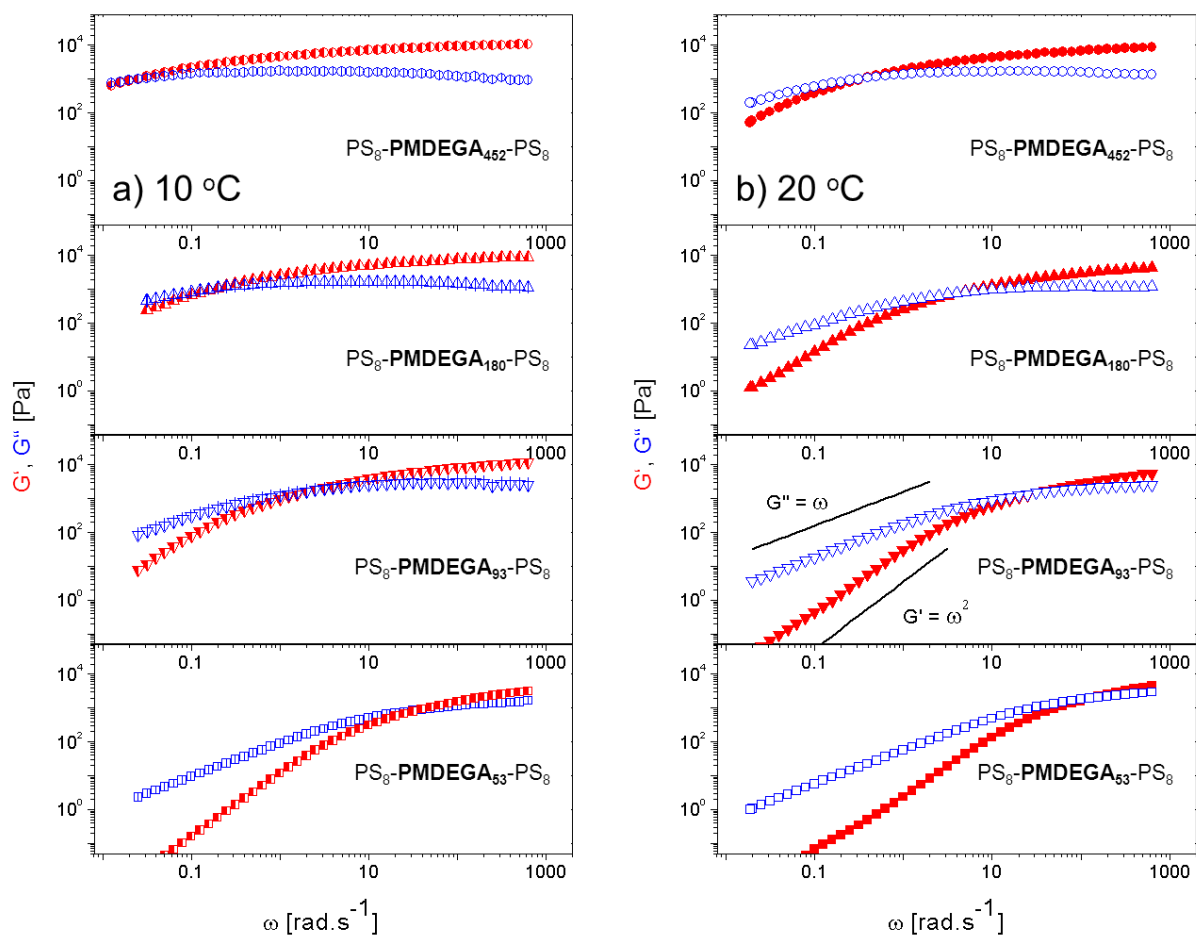


Figure A5.1: Frequency dependence of storage modulus G' (closed red symbols) and loss modulus G'' (open blue symbols) at 10 °C and 20 °C for 20 wt.% aqueous solution of copolymers: (●,○) $\text{PS}_8\text{-PMDEGA}_{452}\text{-PS}_8$; (▲,△) $\text{PS}_8\text{-PMDEGA}_{180}\text{-PS}_8$; (▼,▽) $\text{PS}_8\text{-PMDEGA}_{93}\text{-PS}_8$; and (■,□) $\text{PS}_8\text{-PMDEGA}_{53}\text{-PS}_8$.

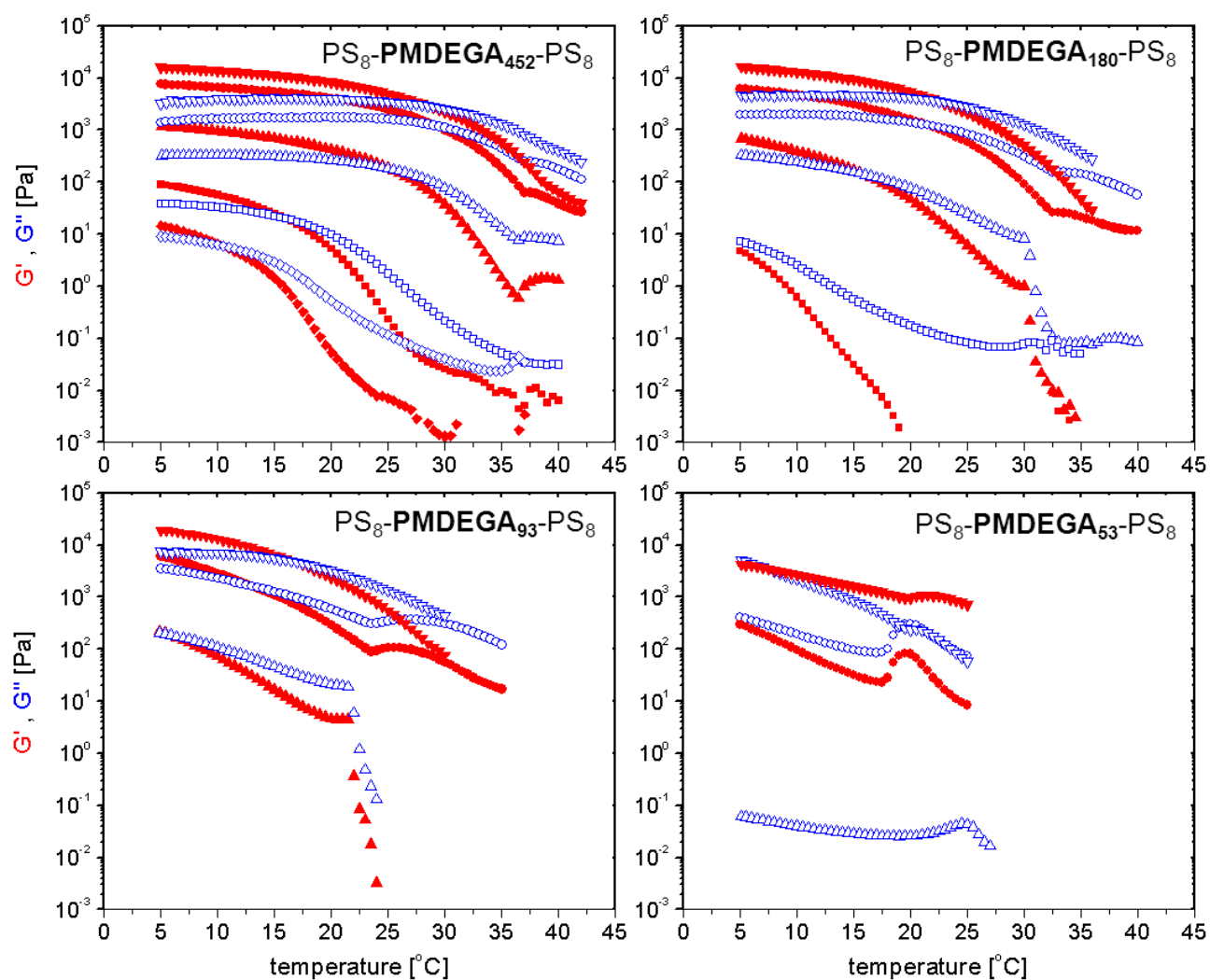


Figure A5.2: Temperature dependence of storage modulus G' (closed red symbols) and loss modulus G'' (open blue symbols) at 1 Hz frequency, for aqueous solutions of the block copolymers at (\blacktriangledown , \triangledown) 30 wt. %, (\bullet , \circ) 20 wt. %, (\blacktriangle , \triangle) 10 wt. %, (\blacksquare , \square) 5 wt. %, and (\blacklozenge , \lozenge) 3.5 wt. % (only for $\text{PS}_8\text{-PMDEGA}_{452}\text{-PS}_8$)

9.2. Supplementary information to Chapter 6

Table A6.1: Gel-sol transition temperatures and cloud point temperatures of aqueous solutions of block copolymers:

copolymer	a) gel-sol transition [°C]				b) cloud point [°C]			
	3.5 wt%	5 wt%	10 wt%	20 wt%	3.5 wt%	5 wt%	10 wt%	20 wt%
PS8-PMDEGA452-PS8	10	16	25	29	35	36	37	38
(PMDEGA231-PS8) _{3X}	17	21	27	30	35	35	36	38
PS15-PMDEGA549-PS15	32	36	gel	gel	37	38	40	41

a) from rheological measurements at $f = 1\text{Hz}$, as temperature for which $G' = G''$
b) visual determination, as temperature for which the solution becomes cloudy

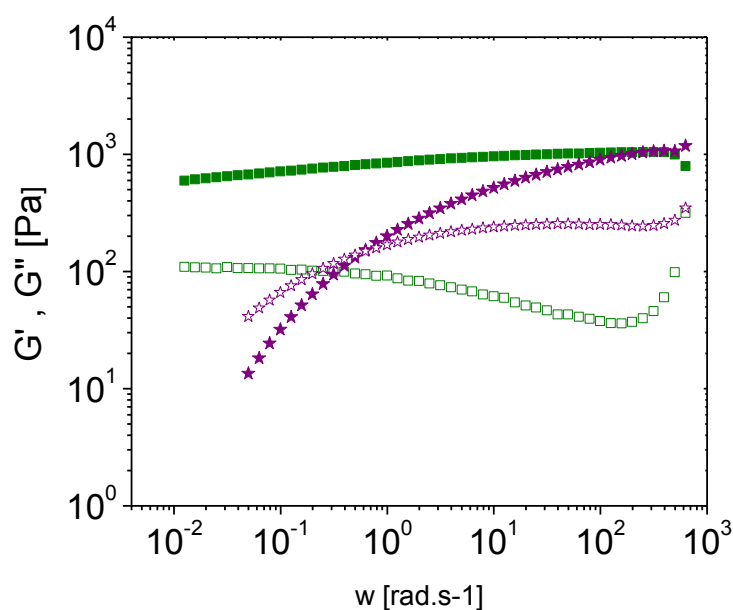


Figure A6.1: Frequency dependence of storage modulus G' (closed symbol) and loss modulus G'' (open symbol) for 10 wt.% aqueous solution of copolymers at 20 °C: (■, □) PS15-PMDEGA549-PS15; (★, ★) (PMDEGA231-PS8)_{3X}.

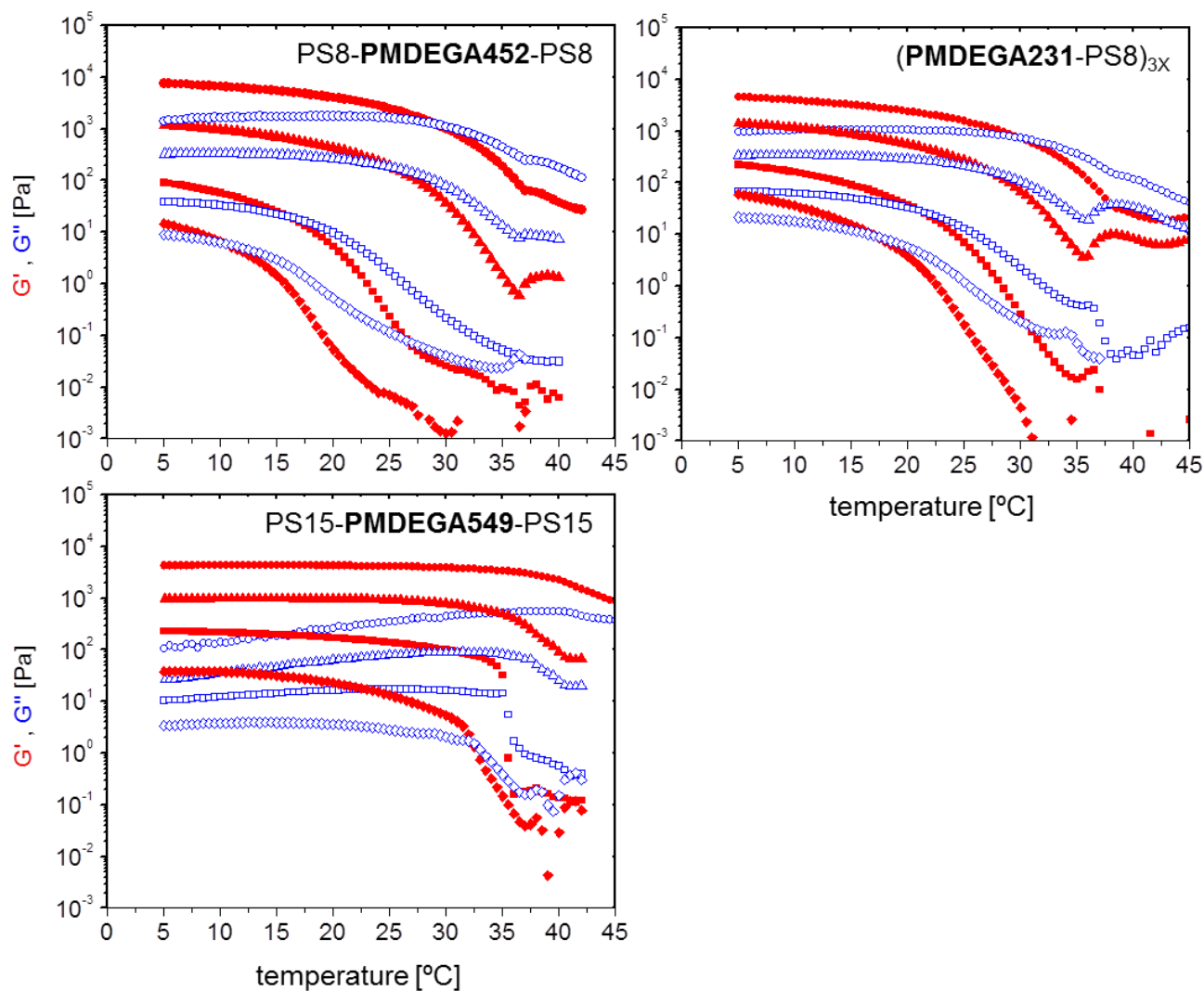


Figure A6.2: Temperature dependence of storage modulus G' (closed red symbols) and loss modulus G'' (open blue symbols) at 1 Hz frequency, for aqueous solutions of the block copolymers at (●, ○) 20 wt. %, (▲, △) 10 wt. %, (■, □) 5 wt. %, and (◆, ◇) 3.5 wt. %

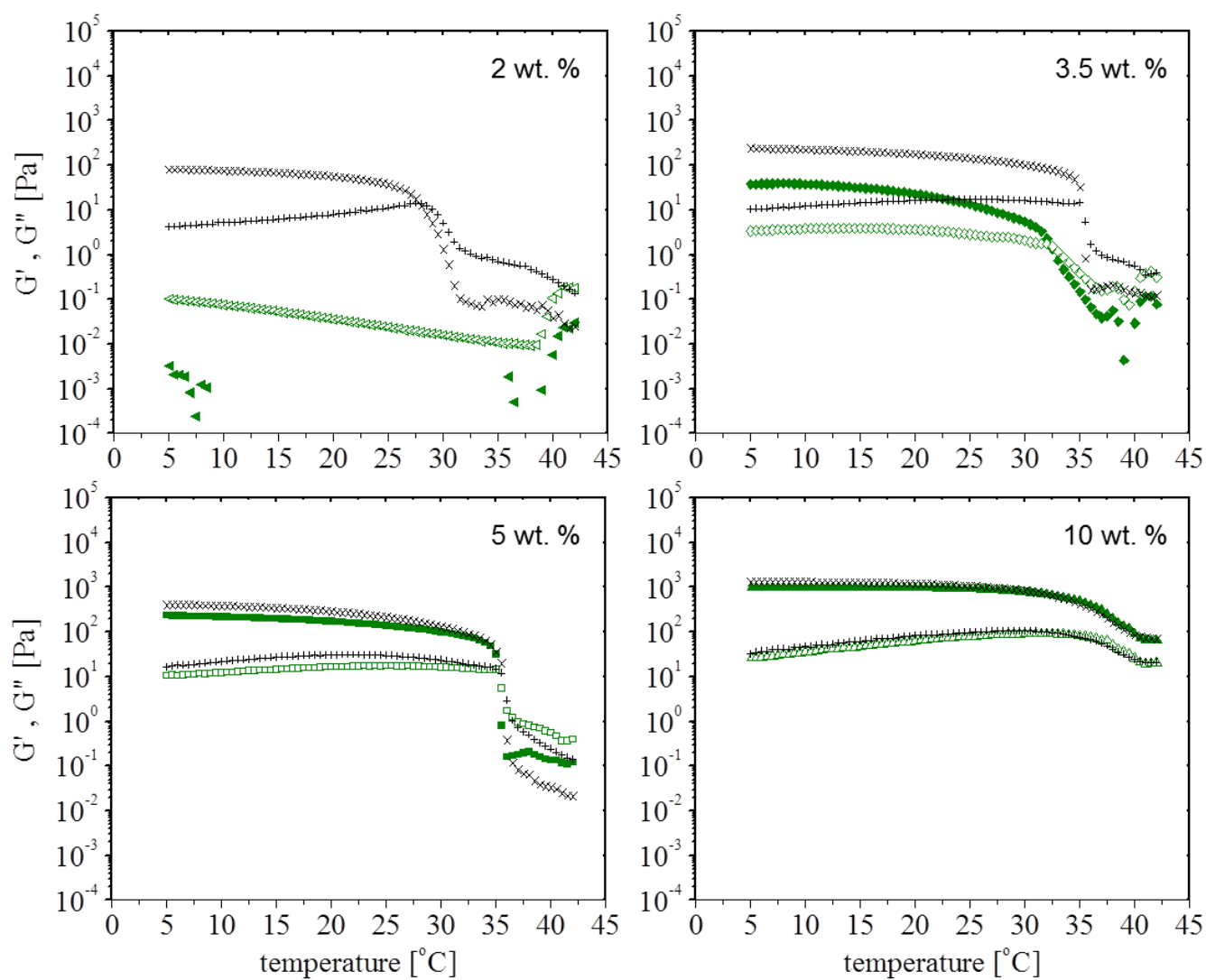
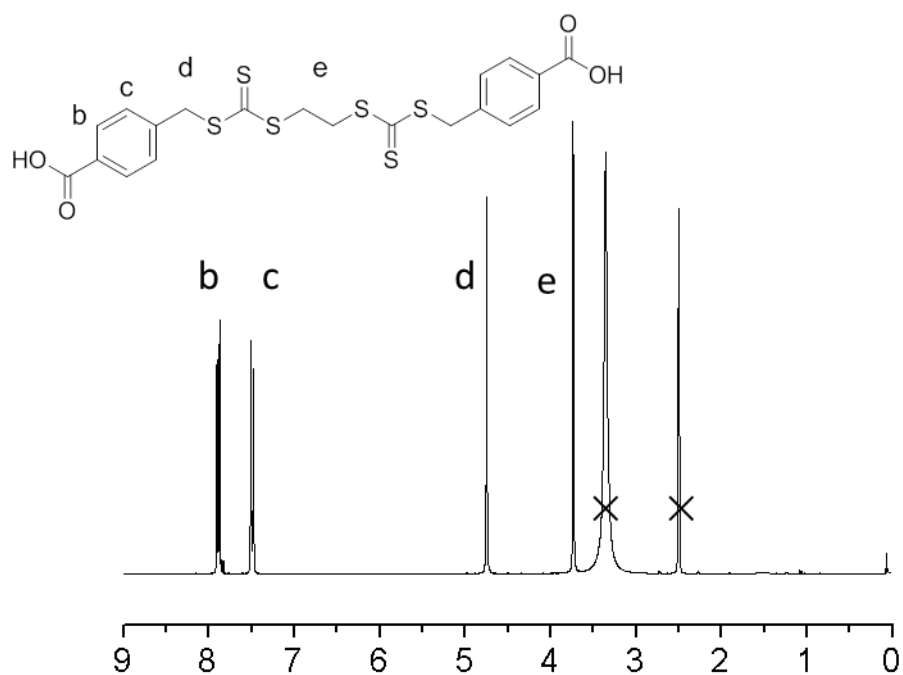


Figure A6.3: Temperature dependence of storage modulus G' (■,×) and loss modulus G'' (□,+), at 1 Hz frequency, for aqueous solutions of PS15-PMDEGA549-PS15 triblock copolymer in a heating (■,□) and cooling (×,+) cycle.

9.3. Supplementary information to Chapter 8

1,2 bis (4-carboxybenzyl sulfanylthiocarbonyl sulfanyl) ethane (**CTA6**)



bis (4-carboxybenzyl) trithiocarbonate (**CTA7**)

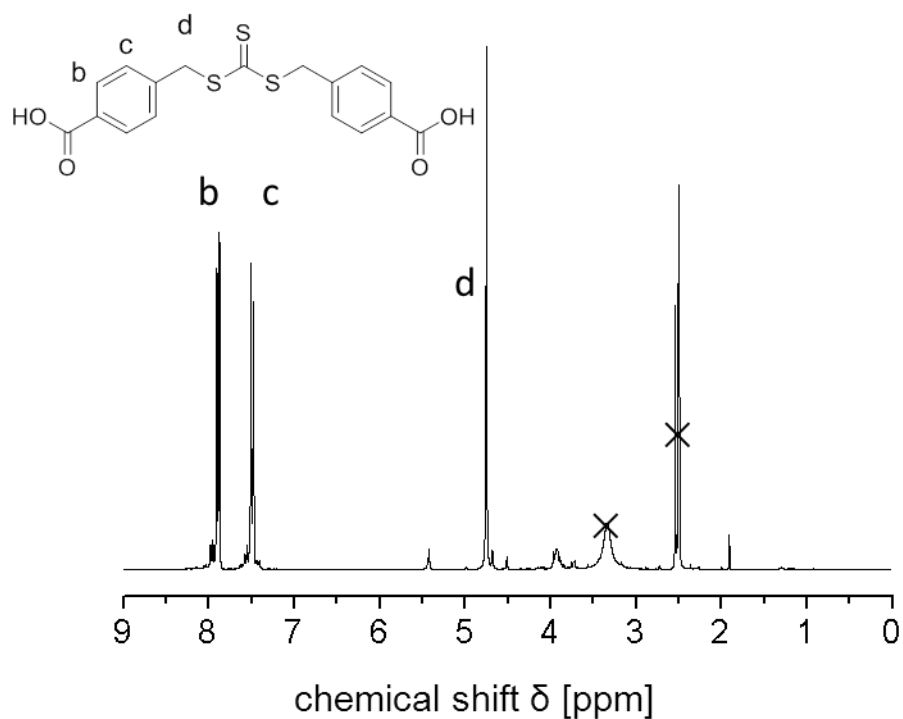
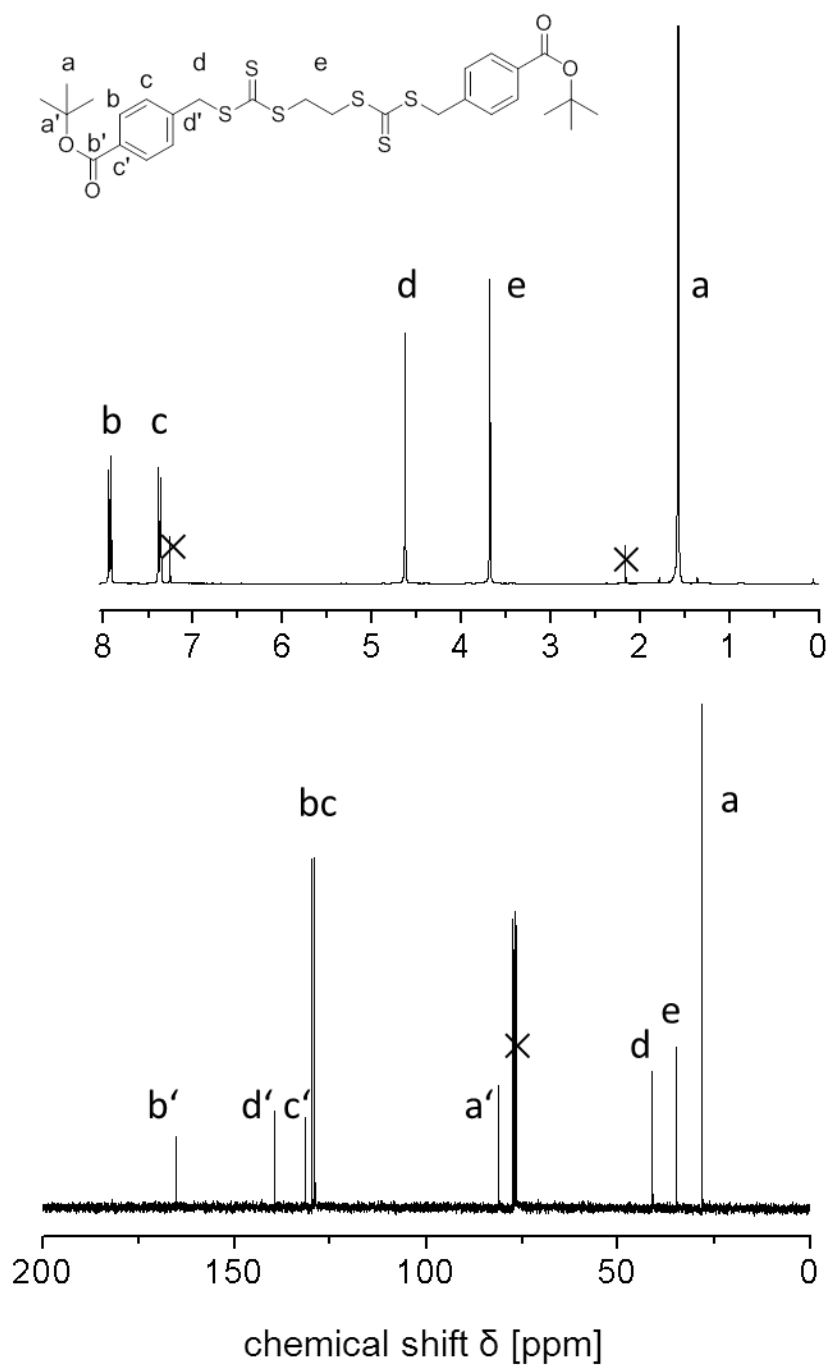
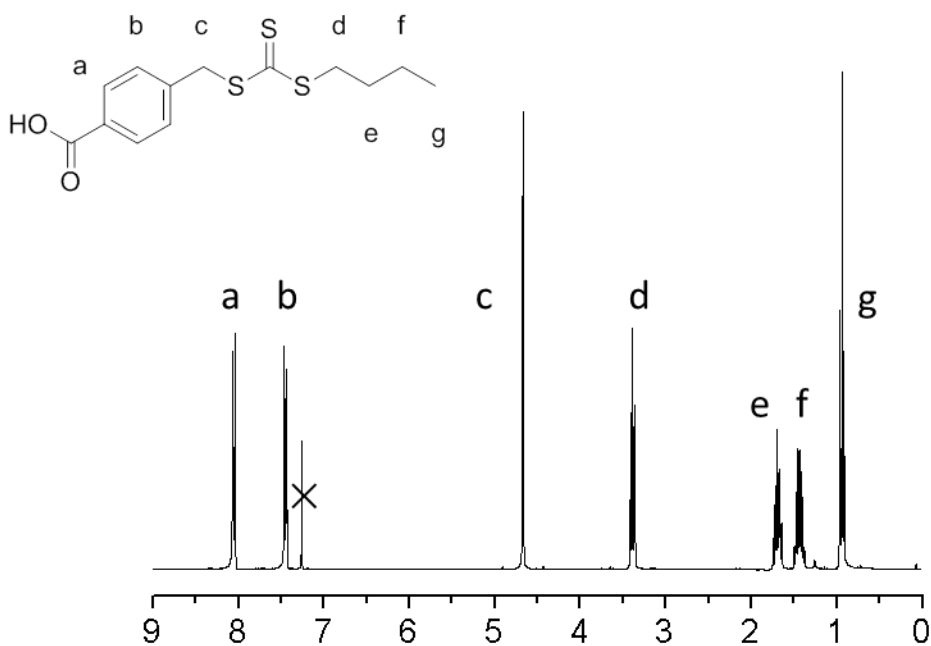


Figure A8.1: ¹H-NMR of CTA6 and CTA7 in DMSO

1,2 bis (4-(*t*-butoxycarbonyl)benzyl sulfanylthiocarbonyl sulfanyl) ethane (**CTA2**)**Figure A8.2:** ^1H - and ^{13}C -NMR of **CTA2** in CDCl_3

4-Butylsulfanylthiocarbonylsulfanylmethyl-benzoic acid (**CTA1**)

3-(4-(tert-butoxycarbonyl)benzylthiocarbonothioylthio) propanoic acid

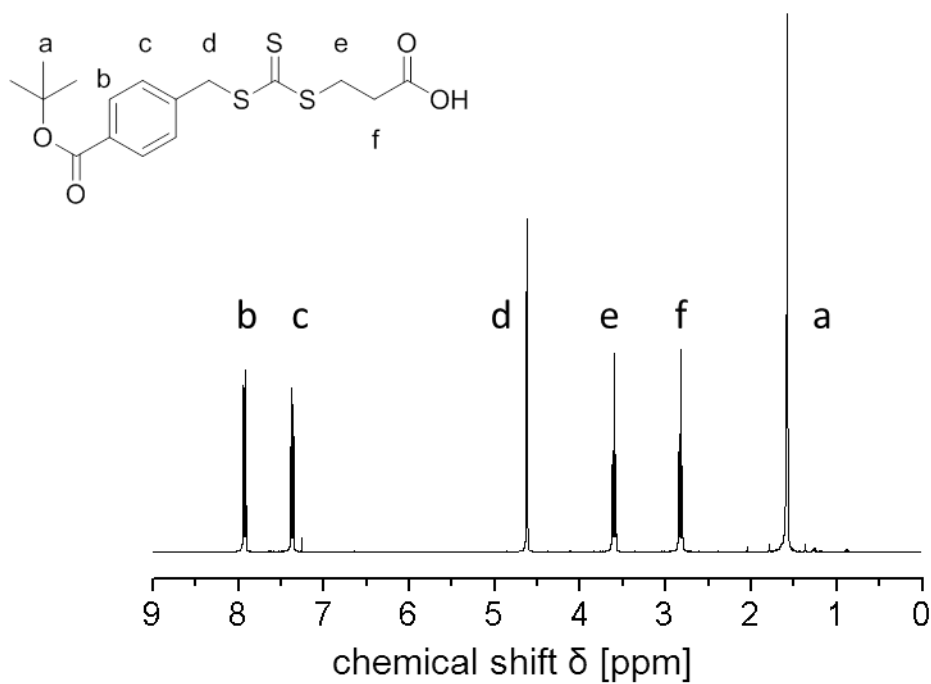
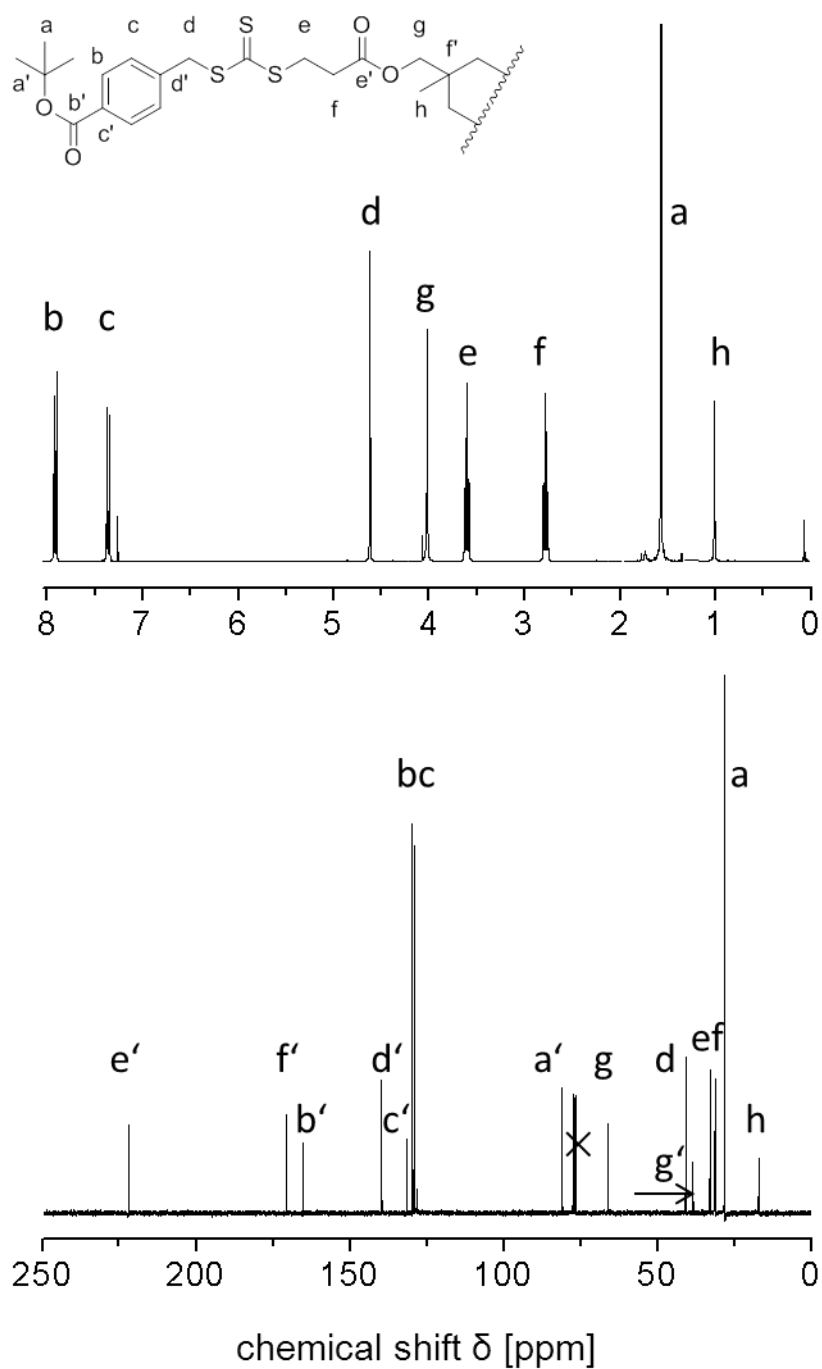


Figure A8.3: $^1\text{H-NMR}$ of **CTA1** and 3-(4-(tert-butoxycarbonyl)benzylthiocarbonothioylthio)propanoic acid in CDCl_3

1,1,1 tris (3-(4-(tert-butoxycarbonyl)benzylthiocarbonothioylthio)propanoyloxy) ethane (**CTA3**)**Figure A8.4:** ^1H - and ^{13}C -NMR of **CTA3** in CDCl_3

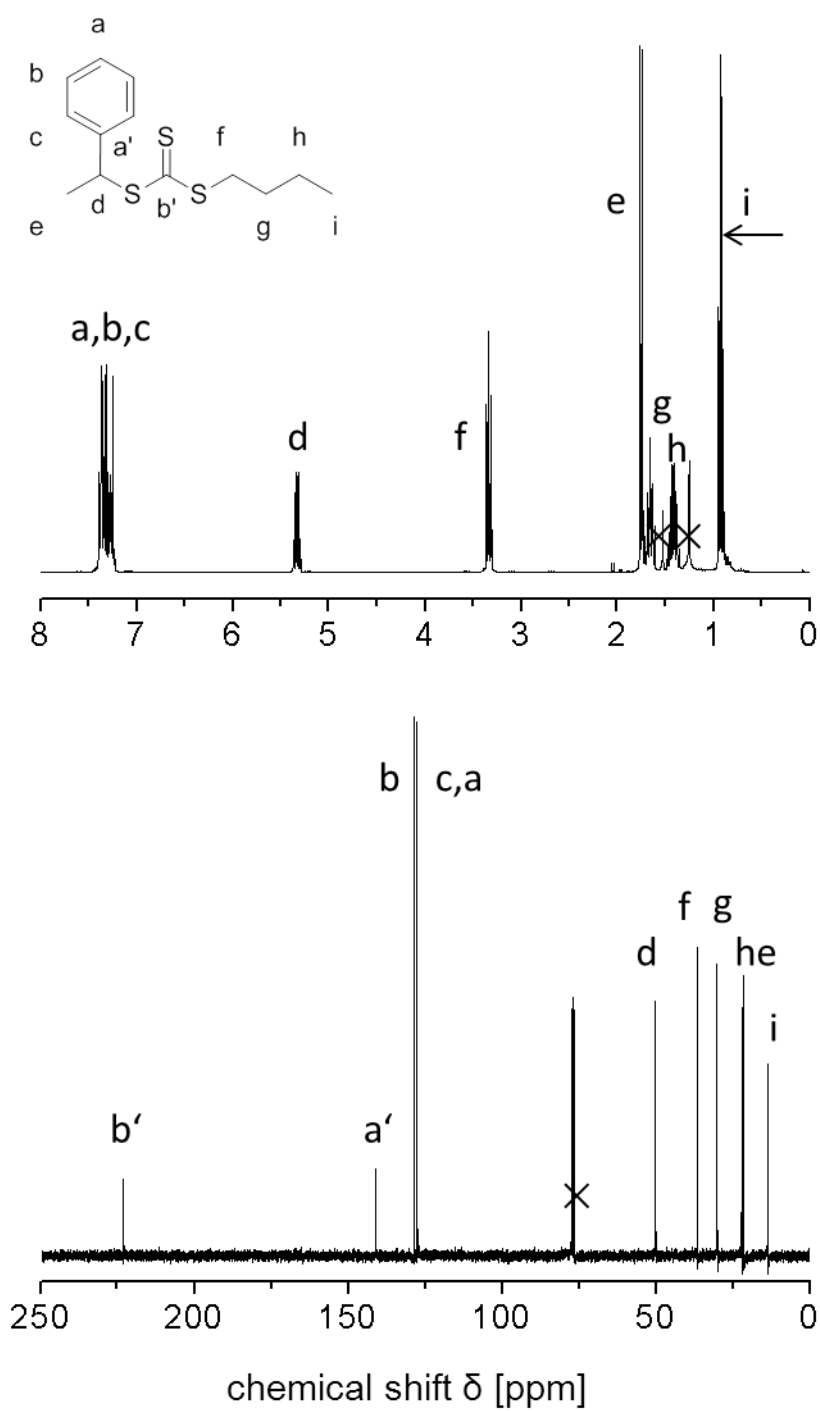
butyl-1-phenylethyltrithiocarbonate (**CTA4**)

Figure A8.5: ^1H - and ^{13}C -NMR of **CTA4** in CDCl_3

2-(butylsulfanylthiocarbonylsulfanyl)-propionic acid
2-(2-methoxy-ethoxy)-ethyl ester (**CTA5**)

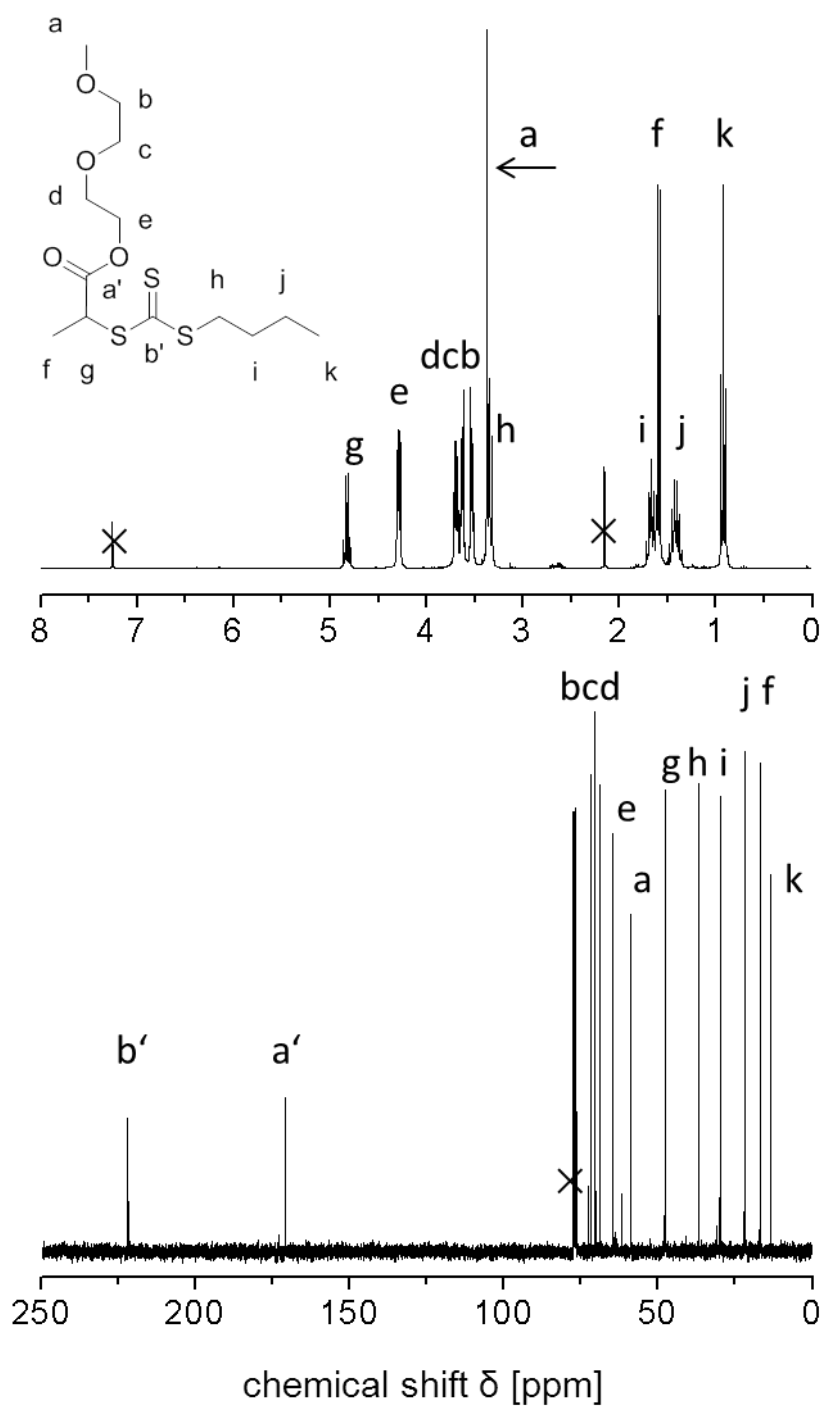


Figure A8.6: ^1H - and ^{13}C -NMR of **CTA5** in CDCl_3

methoxy diethylene glycol acrylate (MDEGA)

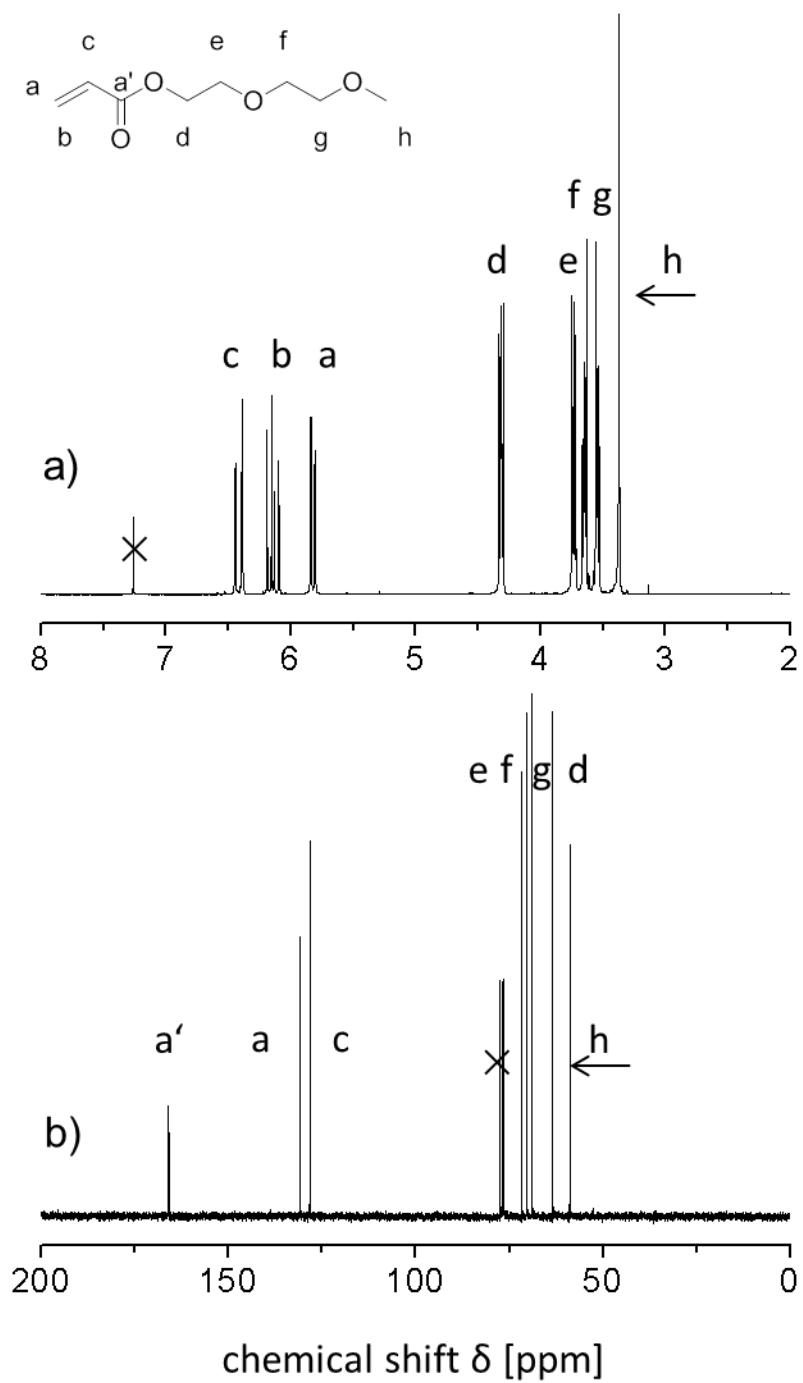


Figure A8.7: ¹H- and ¹³C-NMR of MDEGA in CDCl₃

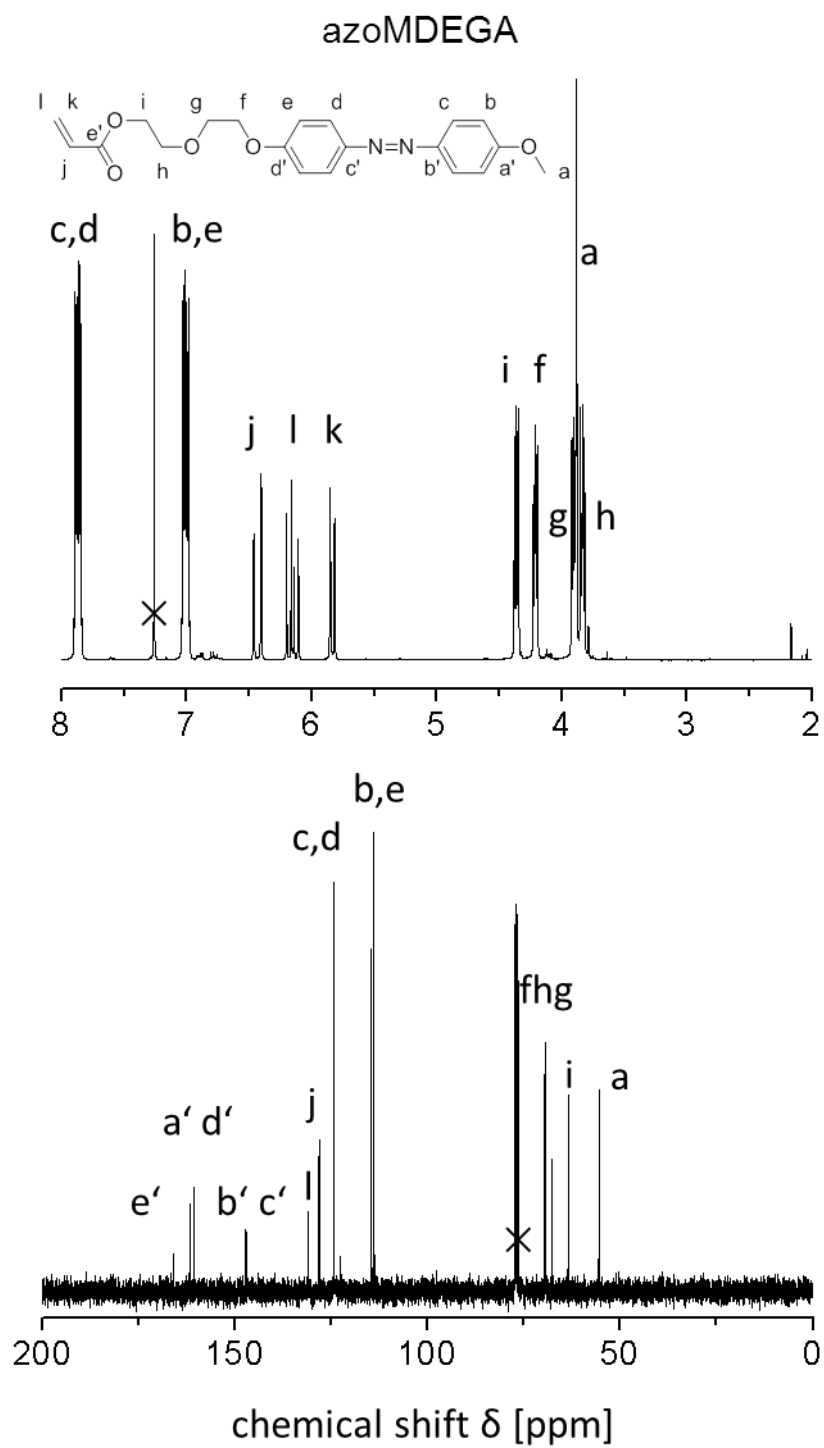


Figure A8.8: ^1H - and ^{13}C -NMR of azoMDEGA in CDCl_3